Lecture Notes
in Geoinformation and Cartography

LNG&C

Igor Ivan · Itzhak Benenson
Bin Jiang · Jiří Horák
James Haworth · Tomáš Inspektor *Editors*

Geoinformatics for Intelligent Transportation

Springer

Lecture Notes in Geoinformation and Cartography

About the Series

The Lecture Notes in Geoinformation and Cartography series provides a contemporary view of current research and development in Geoinformation and Cartography, including GIS and Geographic Information Science. Publications with associated electronic media examine areas of development and current technology. Editors from multiple continents, in association with national and international organizations and societies bring together the most comprehensive forum for Geoinformation and Cartography.

The scope of Lecture Notes in Geoinformation and Cartography spans the range of interdisciplinary topics in a variety of research and application fields. The type of material published traditionally includes:

- proceedings that are peer-reviewed and published in association with a conference;
- post-proceedings consisting of thoroughly revised final papers; and
- research monographs that may be based on individual research projects.

The Lecture Notes in Geoinformation and Cartography series also includes various other publications, including:

- tutorials or collections of lectures for advanced courses;
- contemporary surveys that offer an objective summary of a current topic of interest; and
- emerging areas of research directed at a broad community of practitioners.

More information about this series at http://www.springer.com/series/7418

Igor Ivan · Itzhak Benenson
Bin Jiang · Jiří Horák · James Haworth
Tomáš Inspektor
Editors

Geoinformatics for Intelligent Transportation

January 27th–29th 2014

Springer

Editors
Igor Ivan
Institute of Geoinformatics
VŠB—Technical University of Ostrava
Ostrava
Czech Republic

Jiří Horák
Institute of Geoinformatics
VŠB—Technical University of Ostrava
Ostrava
Czech Republic

Itzhak Benenson
Department of Geography
Tel Aviv University
Tel Aviv
Israel

James Haworth
SpaceTimeLab
University College London
London
UK

Bin Jiang
Department of Technology and Built Environment
University of Gävle
Gävle
Sweden

Tomáš Inspektor
Institute of Geoinformatics
VŠB—Technical University of Ostrava
Ostrava
Czech Republic

ISSN 1863-2246 ISSN 1863-2351 (electronic)
Lecture Notes in Geoinformation and Cartography
ISBN 978-3-319-11462-0 ISBN 978-3-319-11463-7 (eBook)
DOI 10.1007/978-3-319-11463-7

Library of Congress Control Number: 2014956481

Springer Cham Heidelberg New York Dordrecht London

Printed on acid-free paper

Springer International Publishing AG Switzerland is part of Springer Science+Business Media (www.springer.com)

Auspices

AGILE—Association of Geographic Information Laboratories for Europe
EuroSDR—European Spatial Data Research Organisation
ITS&S—Intelligent Transport Systems & Services
CAGI—Czech Association for Geoinformation
SAGI—Slovak Association for Geoinformatics
Miroslav Novák, President of the Moravian-Silesian Region
Ing. Petr Kajnar, Mayor of the City of Ostrava
Prof. Ing. Ivo Vondrák, CSc., Rector of VŠB—Technical University of Ostrava

Programme Committee

Igor Ivan (VŠB-Technical University of Ostrava, CZ)-Chairman
Tao Cheng (University College London, GB)
Hrvoje Gold (University of Zagreb, HR)
Jiří Horák (VŠB-Technical University of Ostrava, CZ)
Marcel Horňák (Comenius University in Bratislava, SK)
Pavel Hrubeš (Czech Technical University of Prague and ITS&S, CZ)
Ľudmila Jánošíková (University of Žilina, SK)
Bin Jiang (University of Gävle, SE)
Dagmar Kusendová (Comenius University in Bratislava, SK)
Miroslav Marada (Charles University in Prague, CZ)
Harvey J. Miller (Ohio State University, US)
Peter Nijkamp (VU University Amsterdam, NL)
David O'Sullivan (University of Auckland, NZ)
Soora Rasouli (Technische Universiteit Eindhoven, NL)
Martin Raubal (ETH Zurich, CH)
Marcin Stępniak (Polish Academy of Sciences, PL)
Zbigniew Taylor (Polish Academy of Sciences, PL)
Harry J.P. Timmermans (Technische Universiteit Eindhoven, NL)
Bert Van Wee (Delft University of Technology, NL)
Stephan Winter (University of Melbourne, AU)
Frank Witlox (Ghent University, BE)

Preface

The title *Geoinformatics for Intelligent Transportation* defines the focus of the 11th Symposium GIS Ostrava 2014. Shorter or longer movements inevitably accompany everyday people's activities including commuting to work and school, shopping, leisure time, etc. Transportation developments have a significant impact on the evolution of human society. The demand for the fastest, cheapest, safest and ecologically friendly means of transport attracts professionals from various disciplines with one mutual goal, to increase the efficiency and effectiveness of transportation, and increase its intelligence. The impact of geoinformatics in the attainment of this goal is clearly evident.

The aim of the conference is to present and discuss new methods, issues and challenges of the geoinformatics contributing to make transportation more intelligent, efficient and human friendly. More than 300 attendees from 11 countries discussed current research directions and applications of Geoinformatics, with the objective of intelligent transportation.

The papers collected in these Proceedings cover a wide range of topics related to transportation and geoinformatics and are divided into four thematic groups, including: Transport modelling, Sensor data and services, Intelligent transport system, and finally Transport planning and accessibility. All papers underwent rigorous double-blind peer-review process of journal scientific standards.

Acknowledgments

The publication is supported by the project OP VK CZ.1.07/2.4.00/31.0162 "Practical competence and professional qualifications improvement in the area of technical education," which is co-financed by the European Social Fund and the state budget of the Czech Republic.

Papers Selection

Number of registered papers: 34
Number of papers published in the proceedings: 19

Home countries of the authors of the papers published in these proceedings are Belgium, Czech Republic, Lithuania, Netherlands, Poland, Portugal, Slovakia and United States of America.

Contents

Investigation of Sonar Stabilisation Method for Improved Seafloor Image Quality 1
Arūnas Andziulis, Tomas Lenkauskas, Tomas Eglynas, Miroslav Vozňák and Sergej Jakovlev

Global Land Cover Classification Based on Microwave Polarization and Gradient Ratio (MPGR) 17
Mukesh Boori and Ralph Ferraro

Optimal Path Problem with Possibilistic Weights 39
Jan Caha and Jiří Dvorský

Optimal Placement of the Bike Rental Stations and Their Capacities in Olomouc 51
Zdena Dobešová and Radek Hýbner

Detecting Spatial and Temporal Route Information of GPS Traces . . . 61
Tao Feng and Harry J.P. Timmermans

Impact of Particular Indicators of Urban Development of Cities in the Czech Republic on Average Road Traffic Intensity 77
Vladimír Holubec and Lena Halounová

Time of Day Dependency of Public Transport Accessibility in the Czech Republic 93
Jiří Horák, Igor Ivan and David Fojtík

Automatic Generation of 3D Building Models from Point Clouds 109
Vojtěch Hron and Lena Halounová

Towards a Solution for the Public Web-Based GIS Monitoring and Alerting System 121
Jitka Hübnerová

Demand and Supply of Transport Connections for Commuting in the Czech Republic 137
Igor Ivan and Jiří Horák

Train Platforming Problem 149
Ľudmila Jánošíková and Michal Krempl

Examples of the Implementation of Fuzzy Models in Tourism in the South Moravian Region 161
Pavel Kolisko

Photovoltaics as an Element of Intelligent Transport System Development 187
Krystyna Kurowska, Hubert Kryszk and Ewa Kietlińska

Urban Heartbeats (Daily Cycle of Public Transport Intensity) 201
Ivica Paulovičová, Slavomír Ondoš, Lukáš Belušák and Dagmar Kusendová

Improving Geolocation by Combining GPS with Image Analysis 213
Fábio Pinho, Alexandre Carvalho and Rui Carreira

The Impact of Data Aggregation on Potential Accessibility Values 227
Marcin Stępniak and Piotr Rosik

The Accuracy of Digital Models for Road Design 241
Václav Šafář and Zdeněk Šmejkal

GPS Data and Car Drivers' Parking Search Behavior in the City of Turnhout, Belgium 247
Peter van der Waerden, Harry Timmermans and Lies Van Hove

Mobile Application for Acquiring Geodata on Public Transport Network 257
Lenka Zajíčková

Author Index 271

Contributors

Arūnas Andziulis Informatics Engineering Department, Klaipeda University, Klaipeda, Lithuania

Lukáš Belušák Faculty of Natural Sciences, Department of Human Geography and Demography, Comenius University in Bratislava, Bratislava, Slovakia

Mukesh Boori National Research Council (NRC), College Park, USA; NOAA/NESDIS/STAR/Satellite Climate Studies Branch and Cooperative Institute for Climate and Satellites (CICS), ESSIC, University of Maryland, College Park, MD, USA

Jan Caha Faculty of Science, Department of Geoinformatics, Palacký University, Olomouc, Czech Republic

Rui Carreira Departamento de Engenharia Electrotécnica e de Computadores, Faculdade de Engenharia da Universidade do Porto, Porto, Portugal

Alexandre Carvalho INESC Porto, Porto, Portugal

Zdena Dobešová Department of Geoinformatics, Palacký University, Olomouc, Czech Republic

Jiří Dvorský Faculty of Science, Department of Geoinformatics, Palacký University, Olomouc, Czech Republic

Tomas Eglynas Informatics Engineering Department, Klaipeda University, Klaipeda, Lithuania

Tao Feng Urban Planning Group, Department of the Built Environment, Eindhoven University of Technology, Eindhoven, The Netherlands

Ralph Ferraro NOAA/NESDIS/STAR/Satellite Climate Studies Branch and Cooperative Institute for Climate and Satellites (CICS), ESSIC, University of Maryland, College Park, MD, USA

David Fojtík Faculty of Mechanical Engineering, Department of Control Systems and Instrumentation, VSB-Technical University of Ostrava, Ostrava, Czech Republic

Lena Halounová Faculty of Civil Engineering, Department of Mapping and Cartography, Czech Technical University in Prague, Praha 6, Czech Republic; Faculty of Civil Engineering, Department of Geomatics, Czech Technical University in Prague, Prague 6, Czech Republic

Vladimír Holubec Faculty of Civil Engineering, Department of Mapping and Cartography, Czech Technical University in Prague, Praha 6, Czech Republic

Jiří Horák Institute of Geoinformatics, VSB-Technical University of Ostrava, Ostrava, Czech Republic

Vojtěch Hron Faculty of Civil Engineering, Department of Geomatics, Czech Technical University in Prague, Prague 6, Czech Republic

Jitka Hübnerová Faculty of Mechatronics, Informatics and Interdisciplinary Studies, Institute of Novel Technologies and Applied Informatics, Technical University of Liberec, Liberec, Czech Republic

Radek Hýbner Department of Geoinformatics, Palacký University, Olomouc, Czech Republic

Igor Ivan Institute of Geoinformatics, VSB-Technical University of Ostrava, Ostrava, Czech Republic

Sergej Jakovlev Informatics Engineering Department, Klaipeda University, Klaipeda, Lithuania

Ľudmila Jánošíková Faculty of Management Science and Informatics, Department of Mathematical Methods and Operations Research, University of Žilina, Žilina, Slovak Republic

Ewa Kietlińska IMAGIS S.A, Warsaw, Poland

Pavel Kolisko Faculty of Science, Department of Geography, Masaryk University, Brno, Czech Republic

Michal Krempl Faculty of Mechanical Engineering, Institute of Transport, VŠB Technical University of Ostrava, Ostrava, Poruba, Czech Republic

Hubert Kryszk Faculty of Geodesy and Land Management, Department of Planning and Spatial Engineering, University of Warmia and Mazury in Olsztyn, Olsztyn, Poland

Krystyna Kurowska Faculty of Geodesy and Land Management, Department of Planning and Spatial Engineering, University of Warmia and Mazury in Olsztyn, Olsztyn, Poland

Dagmar Kusendová Faculty of Natural Sciences, Department of Human Geography and Demography, Comenius University in Bratislava, Bratislava, Slovakia

Tomas Lenkauskas Informatics Engineering Department, Klaipeda University, Klaipeda, Lithuania

Slavomír Ondoš Faculty of Natural Sciences, Department of Human Geography and Demography, Comenius University in Bratislava, Bratislava, Slovakia

Ivica Paulovičová Faculty of Natural Sciences, Department of Human Geography and Demography, Comenius University in Bratislava, Bratislava, Slovakia

Fábio Pinho Associação Fraunhofer Portugal Research, Porto, Portugal

Piotr Rosik Polish Academy of Sciences, Institute of Geography and Spatial Organization, Warsaw, Poland

Marcin Stępniak Polish Academy of Sciences, Institute of Geography and Spatial Organization, Warsaw, Poland

Václav Šafář Výzkumný ústav geodetický, topografický a kartografický v.v.i., Zdiby, Czech Republic

Zdeněk Šmejkal Znalecká a realitní kancelář - Ing. Zdeněk Šmejkal, Pardubice I, Czech Republic

Harry J.P. Timmermans Urban Planning Group, Department of the Built Environment, Eindhoven University of Technology, Eindhoven, The Netherlands; Urban Planning Group, Faculty of the Built Environment, Eindhoven University of Technology, Eindhoven, The Netherlands

Peter Van der Waerden Urban Planning Group, Faculty of the Built Environment, Eindhoven University of Technology, Eindhoven, The Netherlands

Lies Van Hove Transport Research Group, Hasselt University, Hasselt, Belgium

Miroslav Vozňák Telecommunications Department, VSB-Technical University of Ostrava, Poruba, Ostrava, Czech Republic

Lenka Zajíčková Faculty of Science, Department of Geoinformatics, Palacky University in Olomouc, Olomouc, Czech Republic

Abbreviations

A-GPS	Assisted GPS
ALS	Airborne Laser Scanning
AMSR-E	Advanced Microwave Scanning Radiometer
API	Application Programming Interface
BBN	Bayesian Belief Networks
BT	Brightness Temperatures
CCI	Correctly Classified Instances
CIS JŘ	National Information System on Timetables
CORS	Cross-Origin Resource Sharing
COSMOC	Czech Office of Survey, Mapping and Cadastre
CR	Czech Republic
CSP	Concentrating Solar Power
CTU	Czech Technical University
CV	Computer Vision
DSM	Digital Surface Model
DTM	Digital Terrain Model
EASE	Equal Area Scalable Earth
EDA	Event-Driven Architecture
EIA	Environmental Impact Assessment
EOS	Earth Observing Systém
GDDKiA	General Directorate of National Roads and Motorways
GIS	Geographic Information Systems
GPS	Global Positioning System
GR	Gradient Ratio
GSD	Ground Sampling Distances
HDOP	Horizontal Dilution of Precision
HOG	Histogram of Oriented Gradients
HTTP	Hypertext Transfer Protocol
HTTPS	Hypertext Transfer Protocol Secure

HTML	HyperText Markup Language
ICI	Incorrectly Classified Instances
IDS	Integrovaný dopravní systém (integrated transport systems)
IGBP	International Geosphere Biosphere Programme
ITS	Intelligent Transport System
KIDSOK	Coordinator of the Integrated Transport System in the Olomouc Region
LAN	Local Area Network
LAU	Local Administrative Unit
LiDAR	Light Detection and Ranging
MAUP	Modified Areal Unit Problem
MHP	Multiple Hypothesis Probability
MLR	Multiple Linear Regression
MODIS	Moderate Resolution Imaging Spectro Radiometer
MPGR	Microwave Polarization and Gradient Ratio
NASA	National Aeronautics and Space Administration
NDVI	Normalized Difference Vegetation Index
NSATS	Number of Satellites
NSIDC	National Snow and Ice Data Center
NUTS	Nomenclature of Units for Territorial Statistics
ODBC	Open Database Connectivity
ODM	Observations Data Model
OGC	Open Geospatial Consortium
PDOP	Position Dilution of Precision
POI	Point of Interest
PT	Public Transport
RA	Rate of Accessible Municipalities
RANSAC	RANdom SAmple Consensus
REST	Representational State Transfer
RMSE	Root-Mean-Square-Error
RMRC	Rate of Missing Return Connection
ROV	Remotely Operated Underwater Vehicle
RBWA	Rate of Both-way Accessible Municipalities
SES	Sensor Event Service
SIRI	Service Interface for Real-time Information
SOAP	Simple Object Access Protocol
SOS	Sensor Observation Service
SPSS	Statistical Package for the Social Sciences
SQL	Structured Query Language
SSM/I	Special Sensor Microwave/Imager
SURF	Speeded-up Robust Features
TCP	Transmission Control Protocol
UV	Unit Vehicle
VDOP	Vertical Dilution of Precision

WFS	Web Feature Services
WIFI	Wireless Fidelity
WMS	Web Map Service
XML	Extensible Markup Language
XMPP	Extensible Messaging and Presence Protocol
ZABAGED	Fundamental Base of Geographic Data of the Czech Republic

Investigation of Sonar Stabilisation Method for Improved Seafloor Image Quality

Arūnas Andziulis, Tomas Lenkauskas, Tomas Eglynas, Miroslav Vozňák and Sergej Jakovlev

Abstract Constant monitoring of sea floor in harbours is an essential part of economy development of every sea country. Exact estimation of the sea floor relief parameters is very important not only for port development but also for scientists. Sonar image corrections are constantly made with a high margin of error, using GIS. New correction methods are developed. They include: mechanical correction of the cables of the side-scan sonar, programmable correction of the ship navigation and steering system, other software tolls with developed correction and control algorithms. Most commonly sea floor images are made using side scan sonar. It is used for rapid seafloor imaging. The quality of the captured images is strongly influenced by the sonar towing consistency. Even small sonar disturbances caused by the vessels' towing motion can affect the quality of the images. Therefore, to reduce the influence of the ship motion new methods are being developed. In some cases heave motion compensation can prove to be effective. In this paper an efficient heave motion detecting system was proposed and briefly analysed. Sonar and the ship motion were taken into account during the development and testing of the heave motion compensation system prototype.

Keywords Side scan sonar · Heave motion compensation · Ship movement · GIS

A. Andziulis (✉) · T. Lenkauskas · T. Eglynas · S. Jakovlev
Informatics Engineering Department, Klaipeda University, Bijunu Str. 17,
91225 Klaipeda, Lithuania
e-mail: arunas.ik.ku@gmail.com

T. Lenkauskas
e-mail: tomas.lenkauskas@gmail.com

T. Eglynas
e-mail: tmse@inbox.lt

S. Jakovlev
e-mail: s.jakovlev.86@gmail.com

M. Vozňák
Telecommunications Department, VSB-Technical University of Ostrava,
17. Listopadu 15, 70833 Poruba, Ostrava, Czech Republic
e-mail: miroslav.voznak@vsb.cz

I. Ivan et al. (eds.), *Geoinformatics for Intelligent Transportation*,
Lecture Notes in Geoinformation and Cartography,
DOI 10.1007/978-3-319-11463-7_1

1 Introduction

In 2012–2020 the Republic of Lithuania will build two major sea transport objects. These objects are: the liquefied natural gas terminal in the Klaipeda seaport and the outer deep seaport near Butinge. Examination of the seabed in the waterfront of Klaipeda and Butinge seaports and under the major sea lanes is very important (CORPI data funds, www.portofklaipeda.lt). Sea floor exploration is important topic in Baltic region and globally. Kuchler et al. [1, 2] are working on sea crane stabilization. This system reduces motions caused by rough sea waters. Wenlin et al. [3] created system that reduces ship motion influence to remotely operated vehicles. Sarker et al. [4] made comparison of several systems for heave motion compensation on ocean drilling ship. Adamson [5] created efficient heave motion compensation. Huster et al. [6] designed and tested passive heave compensation for ROV. Other scientists work with software solutions, such as Trucco and Garofalo [7], with their image merging from twin sonar system solution and Teixeira et al. [8] with their nonlinear adaptive control of an underwater towed vehicle. Yet–Chung et al. [9] presented side scan sonar image correction algorithms, for correcting brightness variation and patching gaps. New, improved methods are developed, how to produce the best quality sea floor maps and extract objects of interest, using GIS applications [10, 11]. Also our team was working on object detection in images produced by side scan sonar [12].

In the coming years the Republic of Lithuania will build two major sea transport objects. These objects are liquefied natural gas terminal in Klaipeda seaport, and outer deep-sea port near Būtingė. Both projects require good preparation. One of most important preparation part is to explore big areas of Baltic Sea and Curonian Bay floor in great detail. Lithuanian territorial waters in Baltic Sea are shallow, deepest places in sea are just over 100 m deep, in Curonian Bay, where the Klaipeda sea port is and liquefied natural gas terminal will be located, waters are just 1–16.5 m deep. For sea-floor imaging in shallow waters Klaipeda University Coastal Research and Planning Institute use ship with small draught and side scan sonar system. This system performs well only at perfect or nearly perfect sea conditions. Image quality produced by side scan sonar depends on how smoothly the side scan sonar is towed. Most of towed device distortions come from uneven towing vessel movement. At rough waters small ship heaves a lot, and images generated by towed sonar are disturbed and not usable. Using current system, seafloor images produced by side scan sonar are good quality when sea waves are up to 0.5 m high. When height of waves is between 0.5 and 1 m, images produced by side sonar system are distorted, but still usable quality. In Figs. 1 and 2 are samples of such images with objects on sea floor. It is much harder to use automatic object detection using distorted messages, because wavy pattern and big colour variations. If waves are over 1 m high, sonar images are very distorted and unusable. Few methods were designed to improve image captured by the side scan sonar quality. To reduce vessel heave motion effect to seafloor images we designed system that can detect and mechanically reduce motions of side scan sonar.

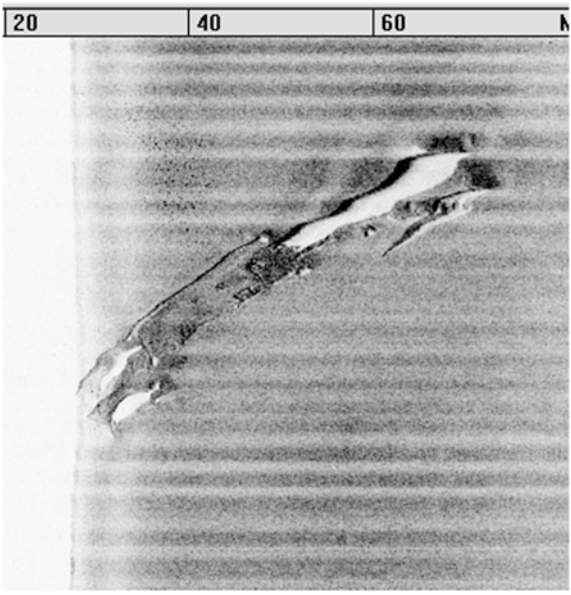

Fig. 1 Fragment of old and rotten ship wreck

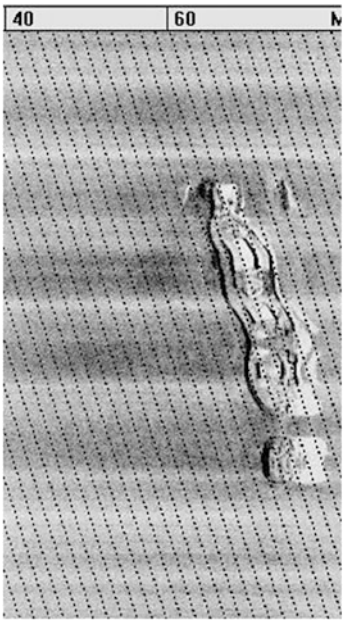

Fig. 2 Recent small ship wreck

2 Heave Compensation Method

The essence of the mechanical side scan sonar stabilization is to physically remove intrusive sonar and towing vessel movements and imaging noises that cause poor quality sonar image [13]. These movements are mostly caused by the sea waves, sudden manoeuvring of the towing vessel sonar and underwater currents. The biggest and the most common issue addressed on side scan sonar systems is the poor quality of the seafloor images, obtained by the side scan sonars, due to heaving of the ship caused by the rough sea waves. There are several methods to cope with this problem. The easiest way to avoid the swinging of the ship is to plan the seafloor-scanning expeditions at the time when sea waves at their minimum. Even though this method is effective, it limits the number of days per year for expeditions. Another method is to choose the preferable swimming route. When the ship swims lengthwise but not perpendicular to the waves to reduce the impact of rebounding waves.

The depth of the Baltic Sea in Lithuania's territorial waters is up to 100 m. However there are shallow areas, which also need to be researched. The optimum operating height of the sonar is about 12 m above the seabed. But when scanning shallow areas near coast, the sonar has to be towed just 3–4 m above the seabed. It can be done by using a short cable (from 2 to 5 m) which connects the ship and the sonar. Because of the turbulence caused by the ship, the sonar towed with a short cable is more disturbed. It happens because a short cable does not absorb the imbalances of tension. Exploring seabed in the deeper waters long cable is used and the sonar is towed far from the ship. This reduces the impact of the turbulence caused by the ship. Also Long cables absorb shock caused by the ship. Scanning the seabed in deeper waters it is faced with a problem of maintaining the sonar in a constant depth. Towed sonar tends to rise to the surface. It moves away from the optimal 12 m height above the seabed. As a result, the quality of images is worse than needed.

3 Current System Parameters

The standard Current system uses Side Scan Sonar. Its main parameters are presented in Table 1. For our tests we used standard a typical side scan sonar system (see Figs. 3 and 4). It consists of dual frequency (100/500 kHz) sonar "Edgetech 272–TD", "Edgetech 560P" controller and a portable computer with sonar and GIS software, for real time map producing.

This system is mounted on Klaipeda University ship. Sonar cable is mounted on the cable drum, which helps to adjust sonar immersion depth. At end of ship sonar cable goes through pulley, it is the last point in ship where sonar and ship are connected. All further measurements of ship movement will be captured at this point.

Table 1 Side scan sonar parameters

Parameter		Value
Frequency kHz		100/500
Horizontal beam width, °	100 kHz	1.2
	500 kHz	0.5
Maximal imaging area width, m	100 kHz	500
	500 kHz	200
Diameter, cm		11.4
Length, cm		140
Weight, kg		25
Submerged weight, kg		12
Maximum operating depth, m		1,000

Fig. 3 Side scan sonar system Edgetech 4100

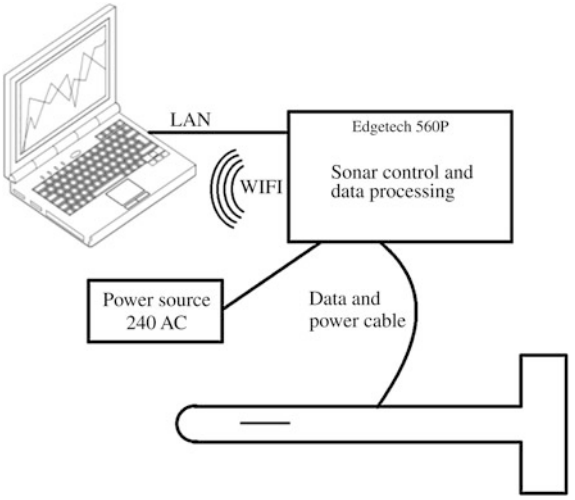

Fig. 4 Sonar connection scheme

3.1 Operating Conditions

In the Baltic Sea there are no strong underwater currents. Image disturbances occur due to uneven movement of the vessel that tows the sonar. While scanning in the rough sea, sonar heaves together with the vessel. If the sonar rises higher above the sea floor, the scanned sea floor path widens. If the sonar goes down, the image captured by sonar becomes narrower and distorted. The fluctuations of the ship and the sonar are not completely identical due to the flexible cable that connects the sonar and the ship [14, 15]. Using current vessel without any additional stabilization system, the seafloor scanning surveys can be done only when the sea waves are not higher than 0.5 m. In order to ensure stable side scan sonar towing, a system that could accurately capture heave motions of the towing vessel and the side scan sonar was designed (Figs. 5 and 6). The initial system operating conditions have to be determined in order to calculate the engine parameters that ensure the minimization of sonar fluctuation in the sea waters [1]. According to the ship crew, the maximum height of the waves that still enables the ship to maintain constant speed and trajectory is 2 m. We have calculated the maximum speed of the vertical (axis Z) movement of the starting point, while ship is swimming on h = 1 m waves.

It is assumed that the ship runs perpendicularly to the direction of waves. The vertical fluctuation of the ship coincides with the wave's fluctuation in the axis Z. Fluctuation of the keel aboard is not taken into account. The simplified equation of the wave motion is presented as (1):

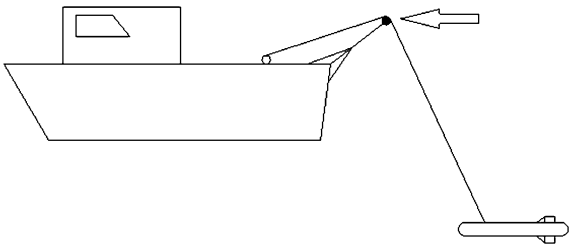

Fig. 5 Chosen start point

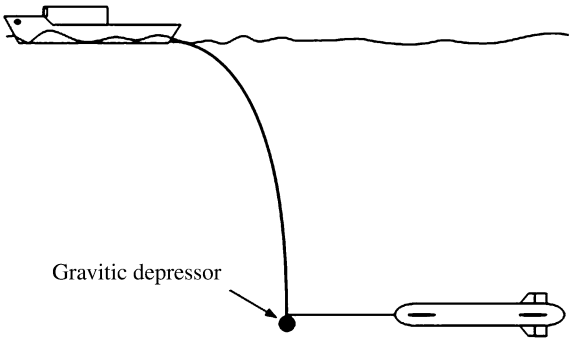

Fig. 6 System with a gravitic depressor

$$Z_b = r_0 \cos\frac{2\pi t}{\tau} \tag{1}$$

The equation: of ship vertical velocity while swimming on wave (2):

$$v_z = -\frac{2\pi}{\tau} r_0 \sin\frac{2\pi t}{\tau} \tag{2}$$

here, v_z—speed, m/s, τ—the wave length, m, r_0—wave radius, m, The radius r_0 is equal to the half of the wave height (3):

$$r_0 = \frac{h_b}{2} = 1\text{m} \tag{3}$$

Here h_b—the wave height, m, then:

$$\upsilon_{max} = \left|\frac{2\pi}{\tau} r_0\right| = 1.52\,\text{m/s} \tag{4}$$

v_{max}—maximum velocity on vertical axis, m/s.

Real waves can mismatch the waves being described with the equations of the motion. That is why we will use the maximum speed $\upsilon_{max} = 2\,\text{m/s}$, which is higher than counted value. The maintenance of height above the seabed that is required by the side view sonar is also a very important aspect to be addressed. If sonar is towed not in optimal depth, image quality drops drastically. It is complicated to reach the necessary depth. The scientists of CORPI cope with this issue by running the ship slower than is required by the manufacturer. Decreasing the speed means that the quality of the images would be worse. Avoiding sonar hitting the seabed is also very important, as sonar can be damaged. Several scientists like Teixeira et al. [8] proposed a standard system of seabed scanning. This system includes a ship and a side scan sonar with the stabilizer of weight. Their system is used to explore the seabed of the deep ocean. The length of the cable used in the system reached 900 m. The mass of the stabilizing weight reached 200 kg and the weight of the sonar was 113 kg. To implement this method the following components are proposed to be used: ship's motion sensors, data processing system and the weight of the stabilization of the sonar. Similar system was used by Teixeira et al. [8].

The purpose of weight is the stabilisation of sonar depth and steady movement of the sonar. In our system case we are planning to use gravitic depressor that will be scaled down to 50 kg weight, but system will operate on same basic method. The total weight of modified sonar system with gravitic depressor is 90 kg, it consists of the sonar, 50 kg of stabilization weight and connecting cables. This does not include cable drum motor and its controllers weight, because they are considered as a part of ship, not sonar, weight. For modifying our system we will leave same basic sonar lifting mechanism, only motor and its controller will be changed. Cable

connecting ship and sonar is wrapped around the drum, whose maximum angular velocity ω is calculated according to this formula described by [14]:

$$\omega = \frac{v}{r_b} = \frac{2}{0.15} = 13.33\frac{1}{s} \tag{5}$$

ω—the cable drum angular velocity, 1/s, r_b – radius of the cable drum, m. The rpm of the drum is calculated according to this formula:

$$n = \frac{30\omega}{\pi} = 127.36\,\text{aps/min} \tag{6}$$

The moment of the inertia of the load:

$$J_m = m\left(\frac{v_{max}^2}{\omega^2}\right) = 90\left(\frac{2^2}{13.33^2}\right) = 2.02\,\text{kg}\,\text{m}^2. \tag{7}$$

The coefficient of reduction for cable drum is described (8):

$$i = \frac{n_{mot}}{n} \approx 20 \tag{8}$$

i—the reduction coefficient, n_{mot}—the cable drum motor rpm. The torque that is needed to lift the weight (9):

$$M_s = mgr = 90 \cdot 9.81 \cdot 0.15 = 132.44\text{Nm} \tag{9}$$

M_s—the system torque, Nm. The angular velocity of the engine rotor:

$$\omega_{mot} = \frac{n_{mot}\pi}{30} = \frac{2400\pi}{30} = 251.2\frac{1}{s} \tag{10}$$

ω_{mot}—angular velocity of cable drum motor, 1/s. The engine reach the maximum speed during the time period $\Delta t = 0.5$ s. We assumed that the moment of the engine inertia is equal to the reduced moment of the inertia of the load is described as:

$$J = J_{mot} + \frac{J_m}{i^2} = 0.01\,\text{kgm}^2 \tag{11}$$

J_{mot}—the motor inertia moment, kgm^2, The general moment of inertia of the motor rotor is (12):

$$J = J_{mot} + \frac{J_m}{i^2} = 0.01\,\text{kgm}^2 \tag{12}$$

Resistance to the axis of the engine torque presented as (12):

$$M_{sv} = \frac{M_s}{i\eta} = \frac{132.44}{20 \cdot 0.95} = 6.97\,\text{Nm} \tag{13}$$

M_{sv}— the resistance moment, Nm, η—the reducer efficiency coefficient. The torque which is required to start the engine is (14):

$$M = M_{sv} + J\frac{\omega_{mot}}{\Delta t} = 11.99\,\text{Nm} \tag{14}$$

The power of the engine is (15):

$$P = \omega_{mot} M = 3011.88\,\text{W} \tag{15}$$

The reserve coefficient of 1.25 is applied to the engine power PR is calculated as follows (16).

$$P_R = P \cdot 1.25 \approx 4000\,\text{W} \tag{16}$$

Therefore, the parameters of the engine are obtained:

- Power P = 4000 W;
- The maximum speed is 2400 rpm;
- Gear box ratio 1:20.

4 The New Software Creation of the Measurement System

The designed motion measuring system prototype consists of a laptop, controller and some sensors. Accelerometers and gyroscopes that are used in the system make the appropriate measurements, calculate the difference in the motion of towing vessel and sonar. Sensors are connected to the Arduino Duemilanove controller. This controller performs collects data. We used paired sensors in the prototype. Pair consists of accelerometer and gyroscope. Both sensors are mounted on the same chip. The developed system data reliability is estimated as high, because the angles between the sensors axis are fixed. Due to the low number of the connecting wires, this system is more compact and easier to use than the conventional systems with one-sensor-per-chip. For capturing vessel motions the sensor unit is mounted to the vessel (Fig. 5).

The main system works with the SerialChart and Arduino 1.0 software. Such interconnection between SerialChart and the Arduino's functions of data scanning allows not only to see the digital values of sensors in real time, but also depict data in real time with updated diagrams. The maximum operating frequency of the accelerometer ADXL 345 is 200 Hz, ITG-3200—400 Hz. System sensors frequency can be up to 150 Hz only if just accelerometers are connected. If the

gyroscope is connected to the system, frequency drops to 20 Hz. The differences between the maximum operating frequency of sensors and the frequency of the measurement systems occur since the system performance is limited by the controller Arduino Duemilanove computing power. The gyroscope "ITG-3200" sends the data to the controller which converts signals into degrees, additional processing of the signal is not required. The data from the accelerometer is sent by signals in which 1 g (9.81 m/s^2) is 256 bytes. If the accelerometer is not moved, the value of axis Z is—256 bites. That is because the accelerometer senses earth gravitation pull. In order to properly provide the axis Z accelerations it adds 256 to the value of the received signal. The result is to be divided by 256 and multiplied by 9.81. The resulting units of acceleration are m/s^2. Accelerometer data is converted in the same way.

The main parts of the algorithm that were used/programmed within the controller are shown in Fig. 7. The first step was to integrate drivers for all sensors, including calibration. Reading the data from the sensors is the first part of the actual program. Here it is very important to get 'smooth' data. The first part is to combine the data form the g-sensor and the accelerometer. The second part is to use a virtual filter proposed by Koseeyaporn and Koseeyaporn [16]. For system testing we used the mentioned virtual filter with some simple adjustment modifications for our case study. Vessel heave motion was calculated using the acquired raw data. Calculations were done to determine how the speed of the electric motor and the direction of spinning affected the heave motion compensation. Finally, we examined the sending signal to the electric motor. On our small scale testing model we used a low power stepper motor. Our model was functioning properly and efficiently compensated the heave motion. Also alternative data collection system is now being prepared, using the same sensors and the new National Instruments (NI) software and hardware components in Klaipeda University research laboratories.

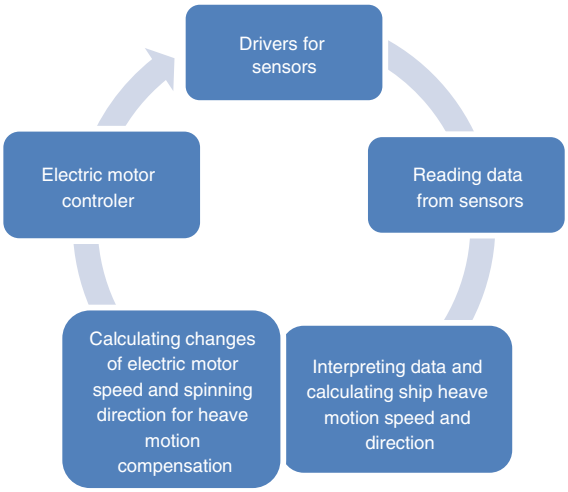

Fig. 7 Algorithm scheme

5 Experimental Research

The designed system prototype was installed and used in the Klaipeda university ship. The measurement was carried out when the weather conditions were favourable for working at sea. The direction of wind was variable from 1 to 2 m/s, the height of the waves was from 0.3 to 0.5 m and the sip used an "Edgetech 4100" side view sonar system. For a proper research of the seabed the ship movement has to be at least 4 knots (about 2.06 m/s) (the data foundation of CORPI). During the research, the speed of the ship was 10 knots (about 5.14 m/s).

5.1 Experimental Results

The results of the first experimental measurements are presented in Figs. 8, 9, 10 and 11. Figure 8 provides the data collected with the three-axis gyroscope. It can be seen that parameters vary very slightly. The data collected with the three-axis accelerometer is presented in Fig. 9. There appear vibrations of the vessel engine

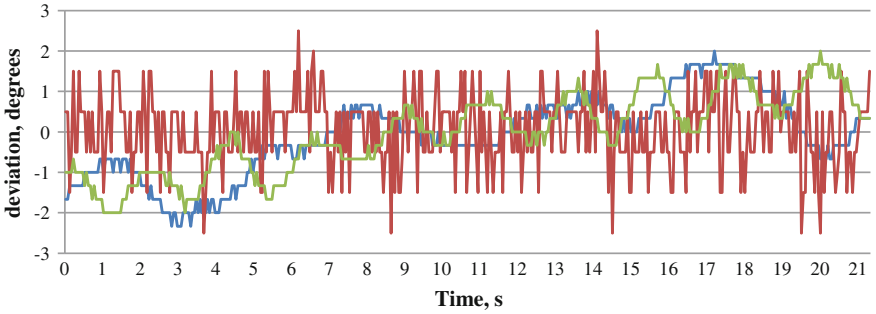

Fig. 8 First test results, data from the 3 axis gyroscope

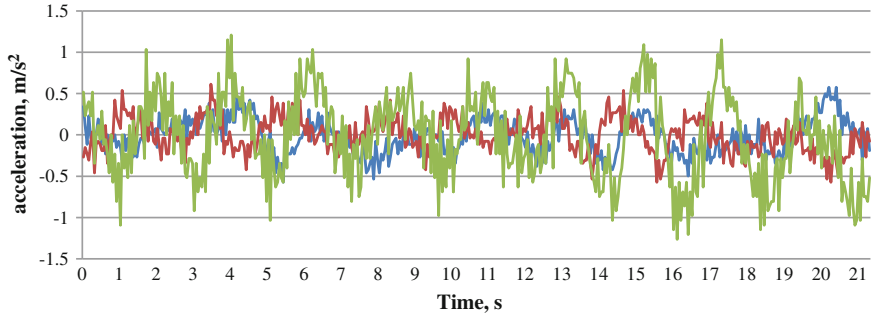

Fig. 9 First test results, data from the 3 axis accelerometer

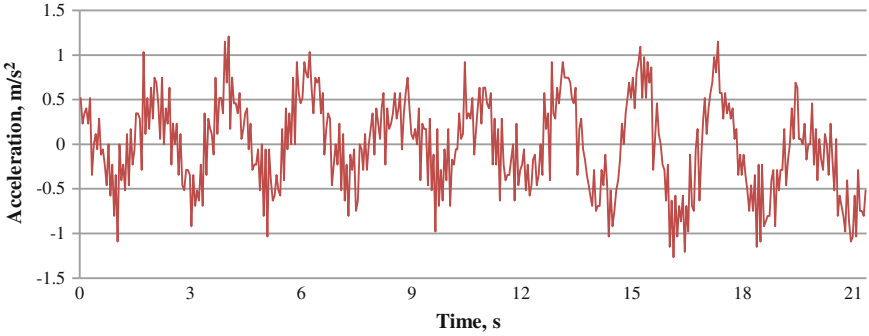

Fig. 10 First test results, data from the Z axis accelerometer

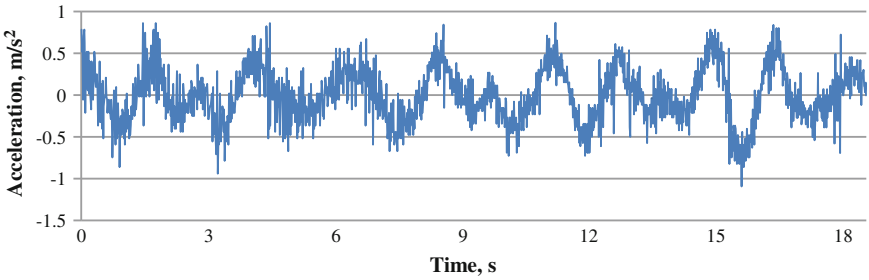

Fig. 11 Second test results, data from the Z axis accelerometer

and other disturbances the collected data of accelerometer. On the other hand, the parameters of ship movement can be clearly seen. The heaving motion of the ship rise when the ship swims through the waves is clearly visible. The acceleration of the ship fixed with axis Z is presented in Fig. 10.

The second measurement was performed on the same day. The data acquisition system worked at 80 Hz frequency and only accelerometer was enables. In this case, the values scanned with Z axis accelerometer are only relevant. Collected data is presented in Fig. 11. It can be seen that the values between each measurement vary. The collected data was adjusted with a virtual filter proposed by Koseeyaporn and Koseeyaporn [16]. The processed data is presented in Fig. 12.

6 Calculations Using the Collected Data

Further calculations were made using the data from the second measurement. This data was not processed with any filters. Measurements started with the speed of the vertical fluctuation of the starting point when its value was 0. Then the modulus of acceleration was the biggest.

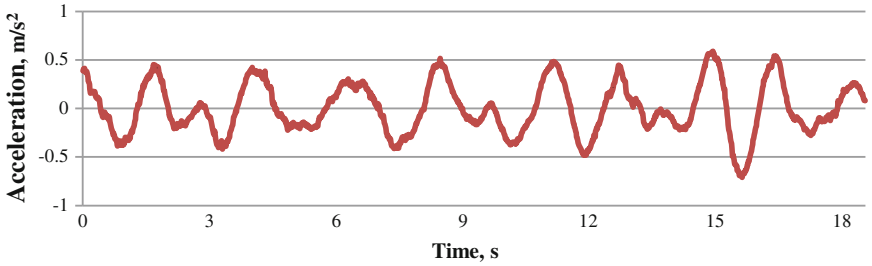

Fig. 12 Filtered accelerometer parameters. Second test, Z axis

To calculate the speed the following equation was used:

$$v_{n+1} = \frac{(a_n + a_{n+1})}{2}\Delta t + v_n \tag{17}$$

Here: v_{n+1}—is the current speed; a_{n+1}—is the current acceleration; a_n—is the acceleration, measured during the previous measurement; Δt—is the measurements frequency, 0.05 s; V_n—is the speed, during the previous measurement. Accelerations of the axis Z and the calculated speed of the heaving are presented in the Fig. 13.

The researcher operating the system, determines the required length of the cable h. Taking into account the heaving of the ship, the provided stabilization system can change the length of the cable. However, the length of the cable must remain at similar approximate value (±0.5–2 m). The operator can set the maximal allowable change of the cable's length. In the calculations the cable's length is marked as h_n. The starting settings of the system are: $\Delta t = 0.0125$ s; $h_n = 0$ m

To calculate the general change of the cable's length h_{n+1} the following equation was used (18):

$$h_{n+1} = h_n + \Delta t \cdot v_n + (a_n + a_{n+1})\Delta t^2 \tag{18}$$

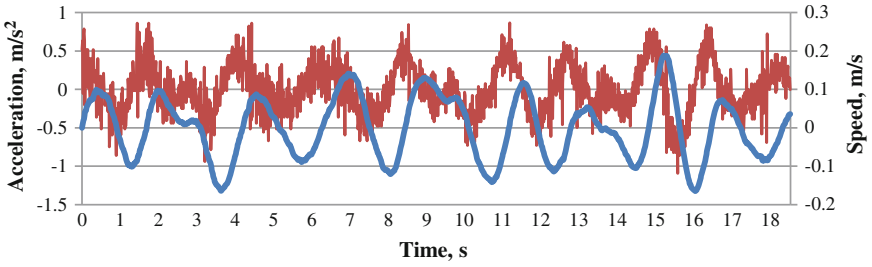

Fig. 13 Ship accelerations and speed

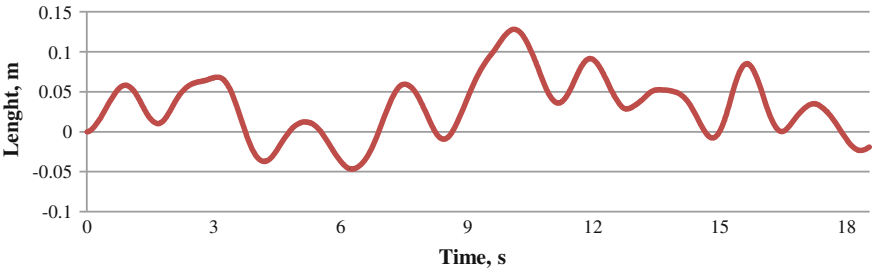

Fig. 14 Calculated sonar cable length

Here: h_{n+1}—is the current difference of cable's length from the starting point, h_n—is the difference of cable's length from starting point that was fixed before the time period Δt. Results are shown in Fig. 14. The instant changes of the cable's length Δh are calculated according to this Eq. (19)

$$\Delta h = \Delta t \cdot v_n + (a_n + a_{n+1}) \cdot \Delta t^2 \tag{19}$$

For more accurate data collection we can use two or three identical sensors mounted in the same place. Then some average values can be calculated for a better accuracy. In order to get better results, different types of sensors could be combined as well. For constantly changing angle between the axis Z of accelerometer and g-sensor subtraction the accelerometers can be mounted on the stable sleeve.

7 Conclusion

The biggest influence to the side scan sonar high quality images is done by towing vessel motion disturbances, caused by rough sea waves. Other less important factors are towing vessel turbulence, sonar distortions during U turns and underwater currents [17]. In this paper a successfully designed and manufactured motion detection measurement system that detects towing vessel and side scan sonar motions was tested in real life operations. The side scan sonar prototype control parameters were estimated and calculations were made. A side scan sonar system prototype that is suitable for seafloor imaging in shallow waters was designed. It uses mechanical stabilization using DC motor and the motion measurement system. In the future, more experimental data will be collected and additional research will be conducted to further improve the presented system. Also full a scale heave motion compensation system with gravitic depressor will be manufactured and mounted on the research ship. These improvements will increase number of days per year that sonar system can be used.

Acknowledgments This work was supported by several projects, including the European Regional Development Fund in the IT4Innovations Centre of Excellence project (CZ.1.05/1.1.00/02. 0070), Development of human resources in research and development of latest soft computing methods and their application in practice project (CZ.1.07/2.3.00/20.0072) funded by Operational Programme Education for Competitiveness, co-financed by ESF and state budget of the Czech Republic, the European Community's Seventh Framework Programme (FP7/2007–2013) under grant agreement no. 218086 and the Latvia-Lithuania cross border cooperation programme project Cross-border DISCOS (JRTC Extension in Area of Development of Distributed Real-Time Signal Processing and Control Systems, code: LLIV-215).

References

1. Kuchler S, Mahl T, Neupert J, Schneider K, Sawodny O (2010) Active control for an offshore crane using prediction of the vessel's motion. Trans Mechatron 16(2):297–309
2. Sawodny O, Kuchler S (2010) Nonlinear control of an active heave compensation system with time-delay. In: International conference on control applications, pp 1313–1318
3. Wenlin Y, Zhuying Z, Aiqun Z (2008) Research on an active heave compensation system for remotely operated vehicle. In: International conference on intelligent computation technology and automation, pp 407–410
4. Sarker G, Myers G, Williams T, Goldberg D (2006) Comparison of heave-motion compensation systems on scientific ocean drilling ship and their effects on wireline logging data. In: Proceeding of offshore technology conference
5. Adamson JE (2003) Efficient heave motion compensation for cable-suspended systems. In: Underwater Intervention
6. Huster A, Bergstrom H, Gosior J, White D (2009) Design and operational performance of a standalone passive heave compensation system for a work class ROV. In: Proceeding of oceans, MTS/IEEE Biloxi—Marine technology for our future global and local challenges
7. Trucco A, Garofalo M (2009) Processing and analysis of underwater acoustic images generated by mechanically scanned sonar systems. IEEE Trans Instrum Meas 58(7):2061–2071
8. Teixeira FC, Aguiar AP, Pascoal A (2010) Nonlinear adaptive control of an underwater towed vehicle. Ocean Eng 37:1193–1220
9. Chang Y-C, Hsu S-K, Tsai C-H (2010) Sidescan sonar image processing: correcting brightness variation and patching gaps. J Mar Sci Technol 18(6):785–789
10. Brown CJ, Sameoto JA, Smith SJ (2012) Multiple methods, maps, and management applications: purpose made seafloor maps in support of ocean management. J Sea Res 72:1–13
11. Masetti G, Calder B (2012) Remote identification of a shipwreck site from MBES backscatter. J Environ Manag 111:44–52
12. Andziulis A, Gaigals G, Lenkauskas T, Visakavičius E, Jakovlev S, Eglynas T, Beniušis V (2011) Comparison of two image processing techniques for objects detection on the sea floor. In: Proceedings of the 15th international conference. Transport means, pp. 62–64. ISSN:1822-296X
13. Peterson RS, Nguyen TC, Rodriguez RR (1994) Motion minimization of AUVs for improved imaging sensor performance beneath a seaway. In: Autonomous underwater vehicle technology, pp 247–254
14. Barrass B (2001) Ship stability notes and examples. Butterworth-Heinemann, London
15. Buckham B, Nahon M, Seto M, Zhao X, Lambert C (2003) Dynamics and control of a towed underwater vehicle system, part I: model development. Ocean Eng 30:453–470

16. Koseeyaporn J, Koseeyaporn P (2005) Kalman filtering adaptive stabilization of robot manipulator under sea wave interference. In: Proceedings of international symposium on intelligent signal processing and communication systems, pp 689–692
17. Lambert C, Nahon M, Buckham B, Seto M (2003) Dynamics and control of towed underwater vehicle system, part II: model validation and turn maneuver optimization. Ocean Eng 30:471–485

Global Land Cover Classification Based on Microwave Polarization and Gradient Ratio (MPGR)

Mukesh Boori and Ralph Ferraro

Abstract Microwave polarization and gradient ratio (MPGR) is an effective indicator for characterizing the land surface from sensors like EOS Advanced Microwave Scanning Radiometer (AMSR-E). Satellite-generated brightness temperatures (BT) are largely influenced by soil moisture and vegetation cover. The MPGR combines the microwave gradient ratio with polarization ratio to determine surface characteristics (i.e., bare soil/developed, ice, and water) and under cloud covered conditions when this information cannot be obtained using optical remote sensing data. This investigation uses the HDF Explorer, Matlab, and ArcGIS software to process the pixel latitude, longitude, and BT information from the AMSR-E imagery. This paper uses the polarization and gradient ratio from AMSR-E BT for 6.9, 10.7, 18.7, 23.8, 36.5, and 89.0 GHz to identify seventeen land cover types. A smaller MPGR indicates dense vegetation, with the MPGR increasing progressively for mixed vegetation, degraded vegetation, bare soil/developed, and ice and water. This information can help improve the characterization of land surface phenology for use in weather forecasting applications, even during cloudy and precipitation conditions which often interferes with other sensors.

Keywords AMSR-E · MODIS · MPGR · Microwave remote sensing · GIS · Climate change · CHAPTER

M. Boori (✉)
National Research Council (NRC), College Park, USA
e-mail: msboori@gmail.com

M. Boori · R. Ferraro
NOAA/NESDIS/STAR/Satellite Climate Studies Branch and Cooperative Institute for Climate and Satellites (CICS), ESSIC, University of Maryland, College Park, MD, USA
e-mail: ralph.r.ferraro@noaa.gov

I. Ivan et al. (eds.), *Geoinformatics for Intelligent Transportation*,
Lecture Notes in Geoinformation and Cartography,
DOI 10.1007/978-3-319-11463-7_2

1 Introduction

Timely monitoring of natural disasters is important for minimizing economic losses caused by floods, drought, etc. Access to large-scale regional land surface information is critical to emergency management during natural disasters. Remote sensing of land cover classification and surface temperature has become an important research subject globally. Many methodologies use optical remote sensing data (e.g. Moderate Resolution Imaging Spectro Radiometer—MODIS) and thermal infrared satellite data to retrieve land cover classification and surface temperature. However, optical and thermal remote sensing data is greatly influenced by cloud cover, atmospheric water content, and precipitation, making it difficult to combine with microwave remote sensing data [1]. Thus, optical or thermal remote sensing data cannot be used to retrieve surface temperature during active weather conditions. However, microwave remote sensing can overcome these disadvantages. Passive microwave emission penetrates non-precipitating clouds, providing a better representation of land surface conditions under nearly all weather conditions. Global data are available daily from microwave radiometers, whereas optical sensors (e.g., Landsat TM, ASTER, and MODIS) are typically available globally only as weekly products due to clouds. The coarse spatial resolution of passive microwave sensors is not a problem for large scale studies of recent climate change [2]. For example McFarland et al. [3] showed that surface temperature for crop/range, moist soils, and dry soils can be retrieved using linear regression models from the Special Sensor Microwave/Imager (SSM/I) BT.

Microwave polarization ratio (PR; the difference between of the first two stokes parameters (H- and V-polarization) divided by their sum) and gradient ratio (GR; the difference of two Stokes Parameters either H or V with different frequency divided by their sum) correspond with seasonal changes in vegetation water content and leaf area index [4–6]. The possibility of simultaneously retrieving "effective surface temperature" with two additional parameters, vegetation characteristics and soil moisture, has been demonstrated, mainly using simulated datasets [7–9]. The MPGR is sensitive to the NDVI [4, 10], as well as open water, soil moisture, and surface roughness [11]. Paloscia and Pampaloni [12] used microwave radiometer to monitor vegetation and demonstrate that the MPGR is very sensitive to vegetation types (especially for water content in vegetation), and that microwave polarization index increases exponential with increasing water stress index. The polarization index also increases with vegetation growth [13]. Since microwave instruments can obtain accurate surface measurements in conditions where other measurements are less effective, MPGR has great potential for observing soil moisture, biological inversion, ground temperature, water content in vegetation, and other surface parameters [1]. This paper derives MPGR and uses it to discriminate different land surface cover types, which is turn will help improve monitoring of weather, climate, and natural disasters.

Table 1 MODIS land cover classes with their code

0 Water	09 Savannas
1 Evergreen needle leaf forest	10 Grasslands
2 Evergreen broad leaf forest	11 Permanent wetlands
3 Deciduous need leaf forest	12 Croplands
4 Deciduous broad leaf forest	13 Urban built-up
5 Mixed forest	14 Cropland natural vegetation mosaic
6 Closed shrub lands	15 Snow Ice
7 Open shrub lands	16 Barren Sparsely Vegetated
8 Woody savannas	

2 Data Used

The Advanced Microwave Scanning Radiometer (AMSR-E) was deployed on the NASA Earth Observing System (EOS) polar-orbiting Aqua satellite platform. The AMSR-E sensor measures vertically (V) and horizontally (H) polarized BT at six frequencies (6.9, 10.7, 18.7, 23.8, 36.5, and 89.0 GHz) at a constant Earth incidence angle of 55° from nadir. In this study, we use AMSR-E level 2A product (AE_L2A), and the daily 25 km resolution global Equal Area Scalable Earth (EASE) Grid BT provided by the National Snow and Ice Data Center (NSIDC). AMSR-E is a successor to the Scanning Multi-channel Microwave Radiometer (SMMR) and SSM/I instruments, first launched in 1978 and 1987, respectively. AMSR-E provides global passive microwave measurements of terrestrial, oceanic, and atmospheric variables for investigation of the global water and energy cycles. MODIS land cover data (MCD12Q1) was acquired from the NSIDC and used to determine land cover information. The MODIS land cover type product contains classification schemes, which describe land cover properties derived from observations spanning a year's input of Terra data. The primary land cover scheme identifies 17 land cover classes defined by the international Geosphere Biosphere Programme (IGBP), including 11 natural vegetation classes, 3 developed and mosaicked land classes, and 3 non-vegetation classes (Table 1).

3 Methodology

The derivation of microwave polarization ratio (PR) and gradient ratio (GR) is based on the radiance transfer theory as follows:

$$B_f(T) = 2hf^3/c^2\left(e^{hf/kT} - 1\right) \tag{1}$$

$$B_f(T) = 2kT/\lambda^2 1/1 + (hf/kT) + (hf/kT)^2 + \cdots + (hf/kT)^n \tag{2}$$

Planck's function (Eq. 1) describes the relationship between spectral radiance emitted by a black body and real temperature, where T is the temperature in Kelvin, $B_f(T)$ is the spectral radiance of the blackbody at T Kelvin, h is the Planck constant, f is the frequency of the wave band, c is the light speed, and k is Boltzman constant. On the basis of the Taylor series expansion equation, Planck's function can be written as Eq. 2.

$$B_f(T) = 2kT/\lambda^2 \tag{3}$$

$$T_f = \tau_f \varepsilon_f T_{soil} + \left(1 - \tau_f\right)\left(1 - \varepsilon_f\right)\tau_f T_a^{\downarrow} + (1 - \tau_i)T_a^{\uparrow} \tag{4}$$

In most passive microwave applications, the value of the term hf/kT can be assumed to be zero. Hence Planck's function can be simplified as Eq. (3). For land cover surface temperature ground emissivity and atmospheric effects are considered in the general radiance transfer equations for passive microwave remote sensing [14, 15] so Eq. 3 can be rewrite as Eq. (4), where Tf is the BT in frequency f, Tsoil is the average soil temperature, Ta is the average atmosphere temperature, Bf (Tsoil) is the ground radiance, Bf (Ta↓) and Bf (Ta↑) are the down-welling and up-welling path radiance, respectively, τf(θ) is the atmosphere transmittance in frequency f at viewing direction θ (zenith angle from nadir), and εf is the ground emissivity. From Eq. (4), a linear relationship is evident between remotely sensed BT and land surface temperature.

Furthermore, we assume that a vegetation layer can be considered a plane, parallel, absorbing, and scattering medium at a constant temperature Tc upon the soil surface. The brightness temperature Tp(τ, μ) of the radiation emitted by vegetation canopy at an angle θ from the zenith can be written as follows [13]:

$$T_p(\tau, \mu) = (1 - w)\left(1 - e^{-\tau/\mu}\right)T_c + \varepsilon_p T_{soil}\, e^{-\tau/\mu} \tag{5}$$

where p stands for horizontal (H) or vertical (V) polarization, μ = cosθ. τ is the equivalent optical depth, w is the single scattering albedo. The two parameters (background and atmospheric effect) can characterize the absorbing and scattering properties of vegetation, respectively. ε_p is the soil emissivity for the p polarization.

MPGR Eq. (6a) and (6b) is an effective indicator for characterizing the land surface vegetation cover density. The polarization ratio used in the study can be described as Eq. (6a)

$$PR\left(_f\right) = [BT(_fV) - BT(_fH)]/[BT(_fV) + BT(_fH)] \tag{6a}$$

And the gradient ratio as Eq. (6b)

$$\left[GR\left(_f1p_f2p\right) = BT\left(_f1p\right) - BT\left(_f2p\right)\right]/\left[BT\left(_f1p\right) + BT\left(_f2p\right)\right] \tag{6b}$$

where BT is the brightness temperature at frequency $_f$ for the polarized component p. When there is little vegetation cover over the land surface, the value of τ can be defined as zero. So the MPGR of bare ground can be written as Eq. (7a) for polarization and Eq. (7b) for gradient ratio.

$$\mathrm{PR}(_f) = \left[\varepsilon(_f\mathrm{V}) - \varepsilon(_f\mathrm{H})\right] / \left[\varepsilon(_f\mathrm{V}) + \varepsilon(_f\mathrm{H})\right] \tag{7a}$$

$$\left[\mathrm{GR}(_f1\mathrm{p}_f2\mathrm{p}) = \varepsilon(_f1\mathrm{p}) - \varepsilon(_f2\mathrm{p})\right] / \left[\varepsilon(_f1\mathrm{p}) + \varepsilon(_f2\mathrm{p})\right] \tag{7b}$$

According to Paloscia and Pampaloni [13], we can assume $\varepsilon_{soil}(\varepsilon_\mathrm{V} + \varepsilon_\mathrm{H})/2$, and $\mathrm{T_c} = \mathrm{T_{soil}}$. Then Eq. (7a, 7b) can be further simplified as

$$\mathrm{MPGR}(\tau, \mu) \approx \mathrm{MPGR}(0, \mu)\mathrm{e}^{-\tau/\mu} \tag{8}$$

Since microwave radiation is polarized, it can be used to depict the condition of vegetation if the vegetation-soil is made a pattern. Equation (8) shows that MPGR mainly depends on μ and τ, and MPGR values fall as vegetation becomes thicker. Therefore, MPGR indicates the density of land surface vegetation cover. Vegetation cover also greatly influences the land surface temperature. Thus, we classify the land surface vegetation cover conditions into several types based on values of MPGR (Fig. 1).

4 Result and Discussion

To identify the behavior of each land cover class, we first selected/determined sample sites in all 17 land cover classes through the use of the ArcGIS system. Then their maximum, minimum, mean, and standard deviation were derived all horizontal and vertical AMSR-E frequencies to determine which combination of MPGR are best suited for land cover classification. We find (Fig. 2) that vertical and higher frequency are closer to actual physical land surface condition/type compared with horizontal and lower frequency. Low frequencies of AMSR-E are hardly influenced by atmospheric effects during bad weather, but they are affected by surrounding (near features) and background surface effects since they absorb less and scatter more by soil. Frequencies of 89 GHz and above are more likely to be influenced by the atmosphere than other AMSR-E bands, especially during bad weather conditions [16, 17]. Our approach makes use of the 89 GHz channels, because the 89 GHz data are influenced less by surface effects than the lower frequencies, and the 89 GHz channels have successfully been used in water and sea ice concentration retrievals under clear atmospheric conditions [18]. Lower frequencies help to distinguish the land surfaces' vegetation cover conditions. However, the BT differences between

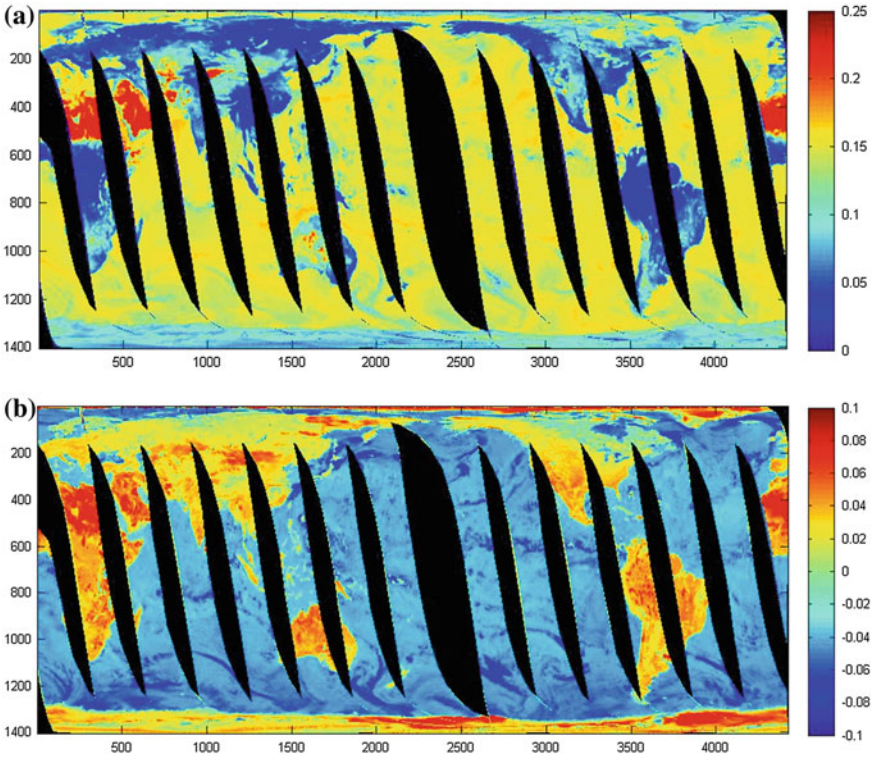

Fig. 1 AMSR-E image with MPGR value range for **a** polarization ratio (PR 36.5) and **b** gradient ratio GR-V (36.5–18.7). In *panel a*, the *dark red* areas indicate deserts, *dark blue* represents dense vegetation, and the color in between correspond to mixed vegetation. In *panel b*, *dark red* highlights desert regions, and *light red* showing vegetation condition, *yellow* and *sky blue* showing mixed vegetation (30/09/2011). Both images clearly differentiate land and water on earth after polarization or gradient ratio

high frequencies also can be used to evaluate the influence of soil moisture and barren sparsely vegetation/bare soil.

In Fig. 2 evergreen needle leaf and broad leaf forest have higher temperatures than deciduous forest, but both forest types have lower temperatures than shrub land and savanna. Mixed forest has a much smaller range of standard deviations and always falls between evergreen and deciduous forest (Fig. 2). Close shrub has lower temperature and a smaller standard deviation than open shrub. Wetland has lower temperature than grassland and cropland due to water content. Built-up area has higher standard deviation than other land cover classes except for water and ice (Fig. 2). But in Fig. 2 it is hard to find a clear set of parameters that can uniquely identify all of the 17 land surface type. Thus, we utilize MPGR which combines much of the information and may potentially separate the 17 land surface type.

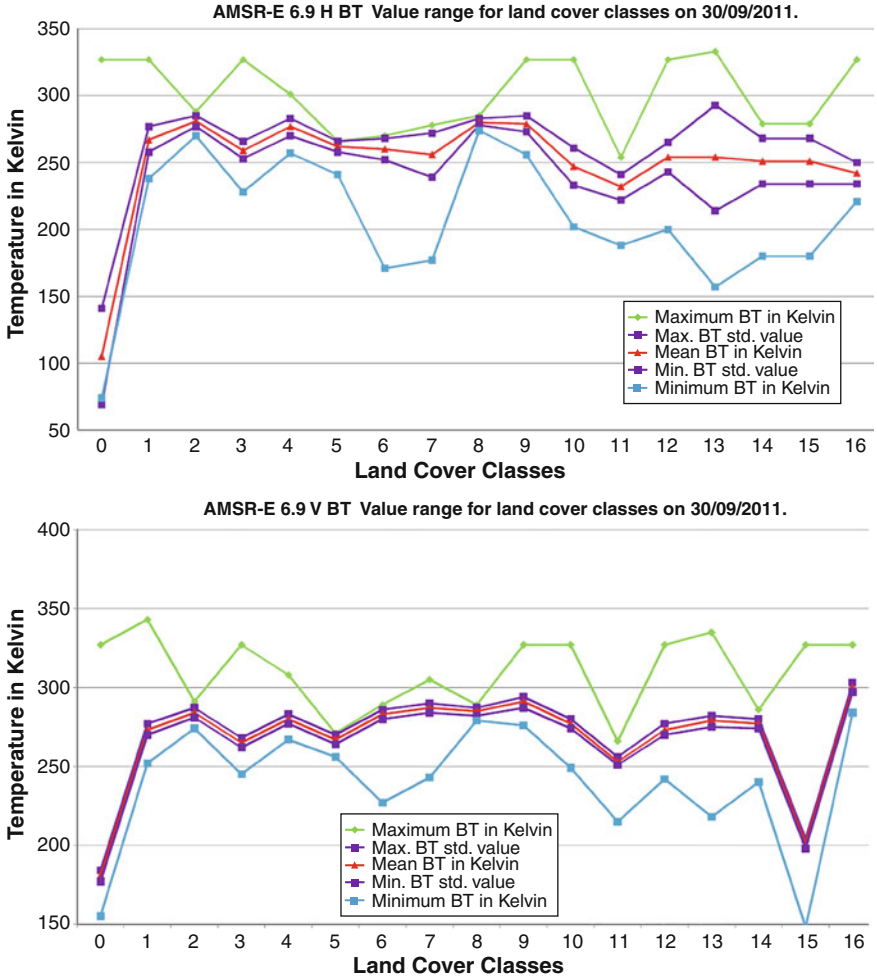

Fig. 2 Seventeen land cover classes maximum, minimum, mean and standard deviation temperature in kelvin for 6.9, 10.7, 18.7, 23.8, 36.5 and 89.0 Ghz AMSR-E frequency

Using AMSR-E frequencies and MPGR is an effective way to derive surface type based on the land surface vegetation cover classification. We used two lower frequencies (10, 18 GHz), and two higher frequencies (36, 89 GHz) for further analysis. For land cover classification on the basis of MPGR, we focused on three combinations of PR-PR, PR-GR and GR-GR, and plot two graphs for each combination (Fig. 3). The scatterplots identify all 17 land cover classes (as shown in Fig. 3). Water pixels are located at highest value in the graph, then ice, bare soil, built-up area, and grasslands, savanna, mixed vegetation, degraded vegetation and dense/evergreen vegetation, respectively.

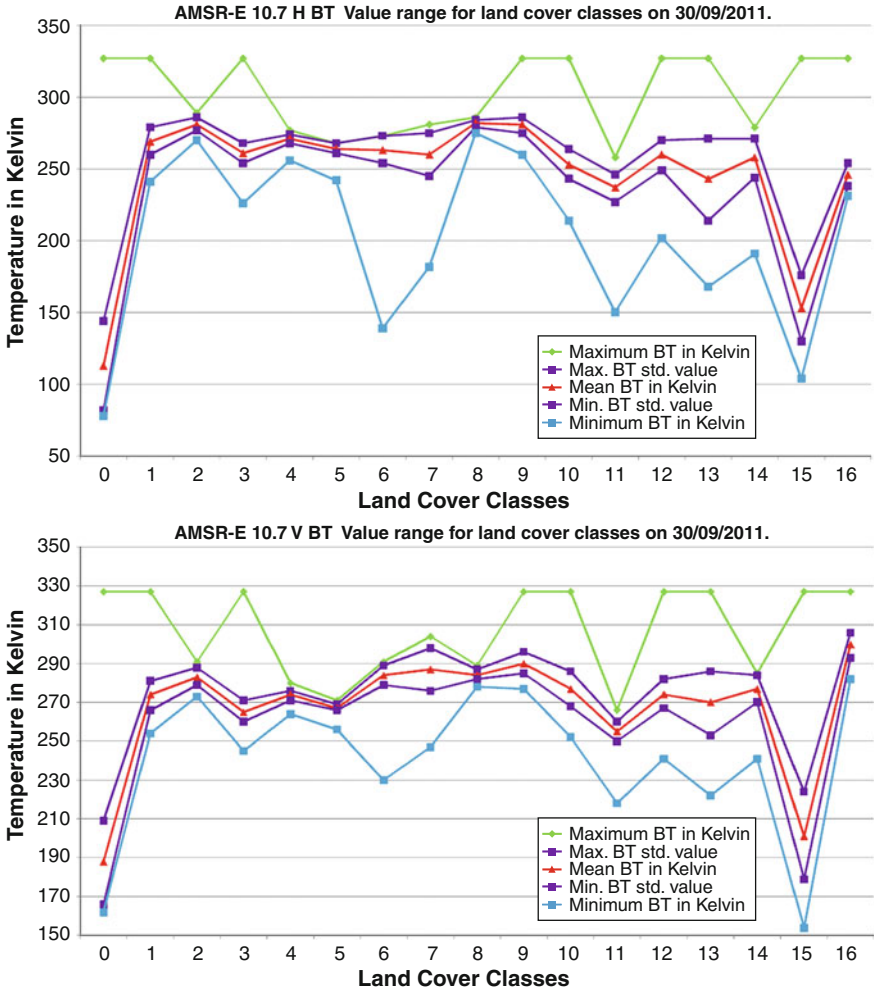

Fig. 2 continued

Table 2 shows all 17 land cover classes based on the MPGR graphs. For the PR–PR (36–18, 10–89 GHz) combination, vegetation is present from 0.0 to 0.06, and then barren/sparse vegetation or bare soil from 0.06 to 0.09, with ice between 0.09 and 0.012 and then water. For the PR–GR [18—(18–89), 10—(10–18)] combination, vegetation is from 0.0 to 0.04, bare soil from 0.06 to 0.08, and ice 0.09 to 0.12 followed by water. For the GR–GR (89–18, 36–10) combination, dense vegetation is present between −0.03 and 0.0, then normal vegetation, bare soil between 0.04 and 0.05, then snow/ice from 0.05 to 0.06, and again followed by water.

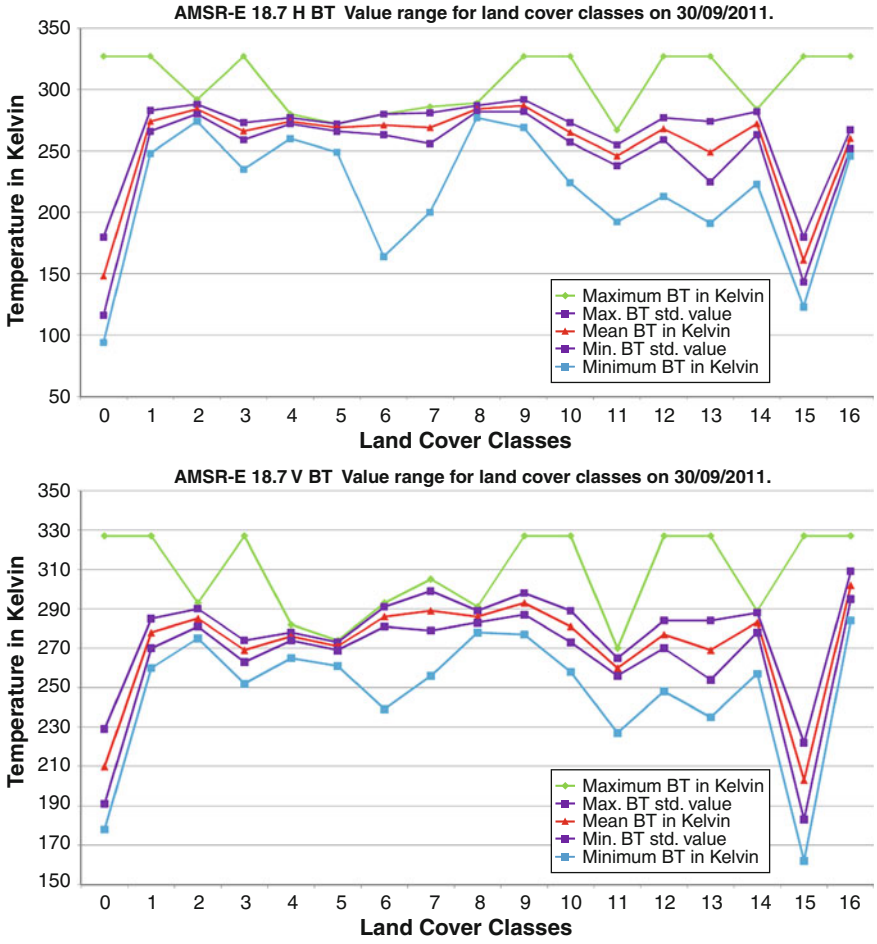

Fig. 2 continued

Table 3 and Fig. 3 identify the location and behavior of all 17 land cover classes. Now we can say MPGR-based classification is dependent upon dielectric constant or water content because water class is always have higher value in graph, and with greater values than ice, bare soil, and built-up areas. In terms of vegetation, dense or healthy vegetation is present near 0 and mixed, low, or degraded vegetation follows healthy vegetation (near 0.5). High values of PR-PR, PR-GR, and GR-GR indicate open water; the range of this value is larger because of the greater dynamic range in vegetation, soil, built-up, ice, and water. Although the use of the 89 GHz data requires a correction for atmospheric effects, it provides additional information to

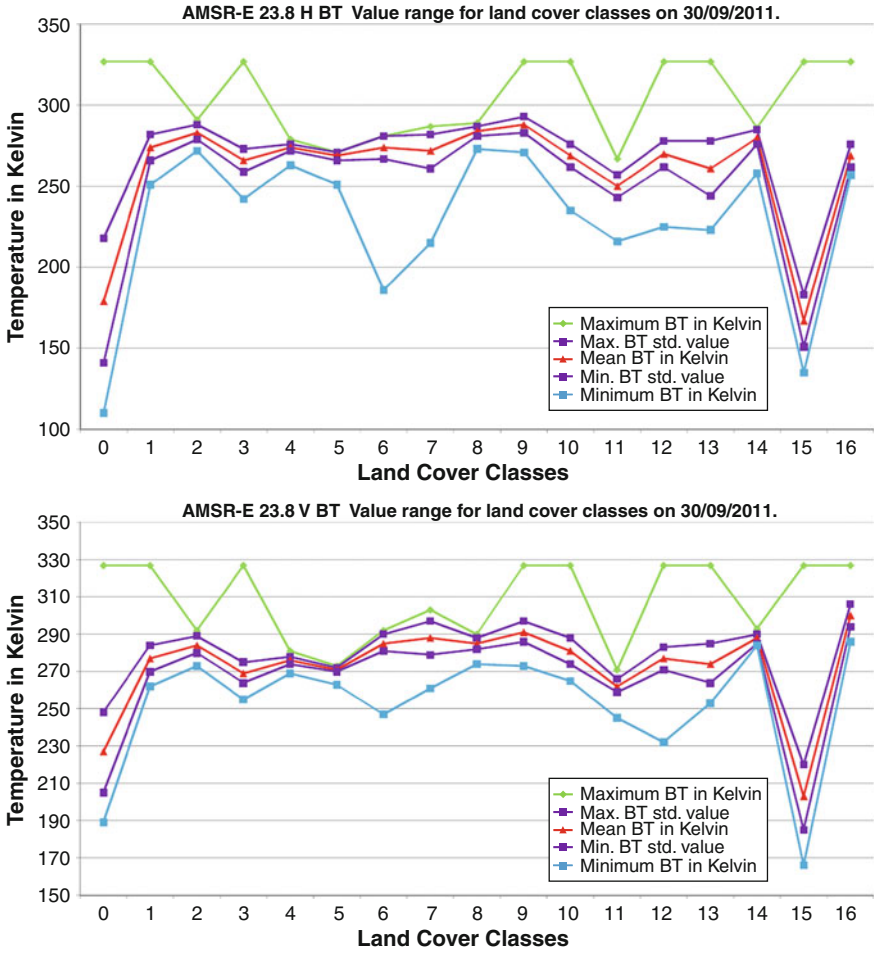

Fig. 2 continued

unambiguously distinguish weather effects from changes in land cover features. These results are similar with previous research results by Chen et al. [19] with land cover classification over China.

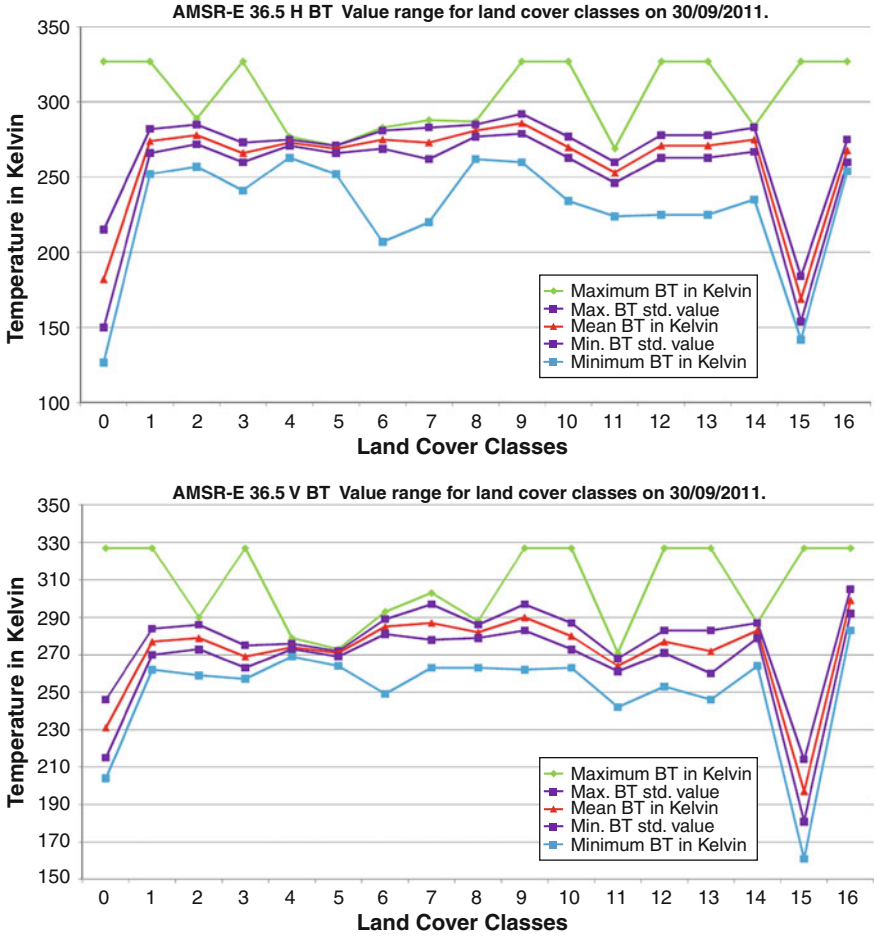

Fig. 2 continued

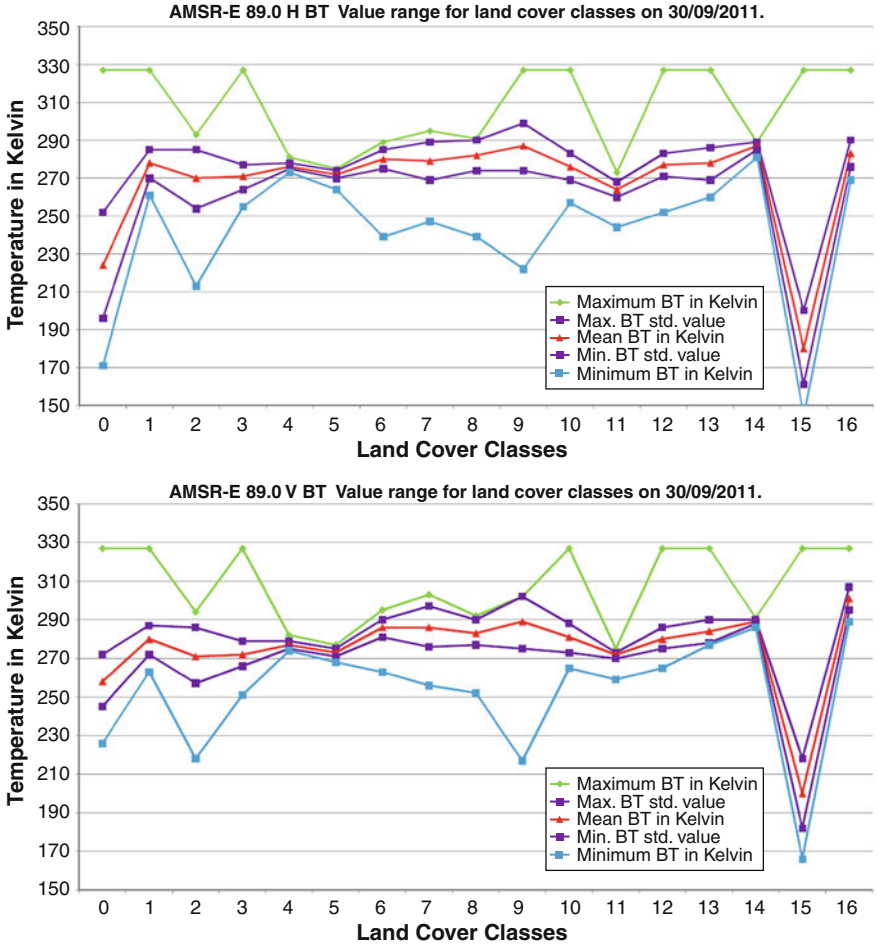

Fig. 2 continued

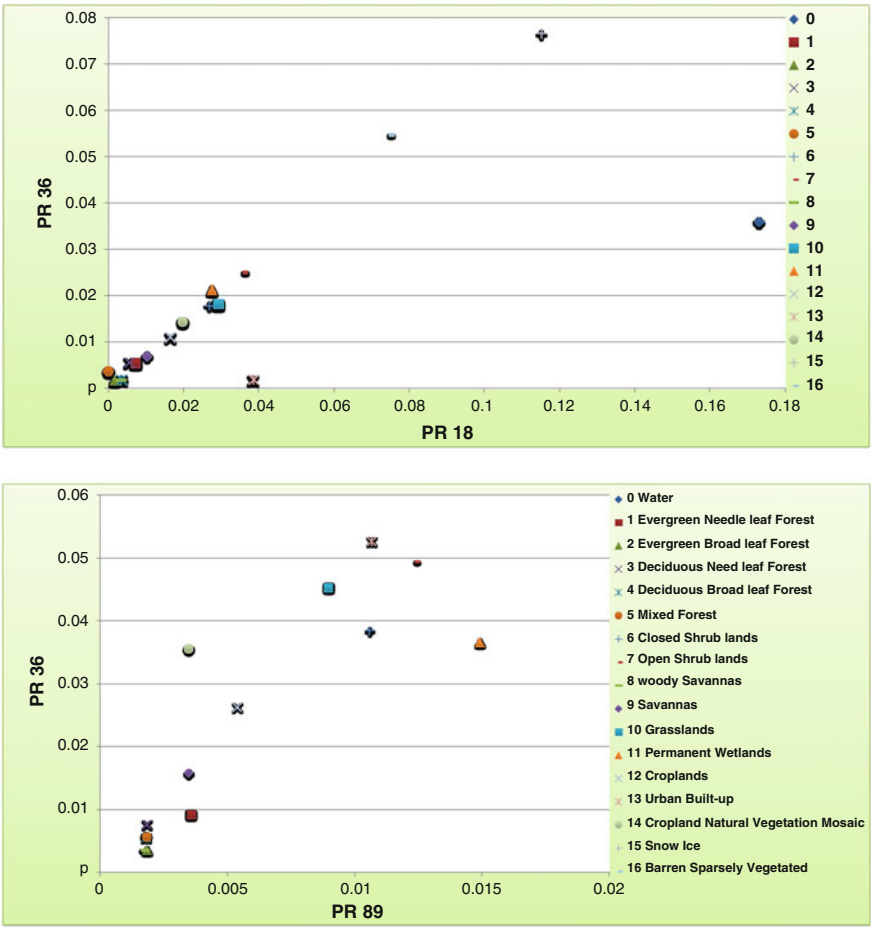

Fig. 3 Seventeen land cover classes mean PR-PR (Fig A and B), PR-GR (Fig C and D) and GR-GR (Fig E and F) relation ratio with 10.7, 18.7, 36.5 and 89.0 Ghz H–V AMSR-E frequency

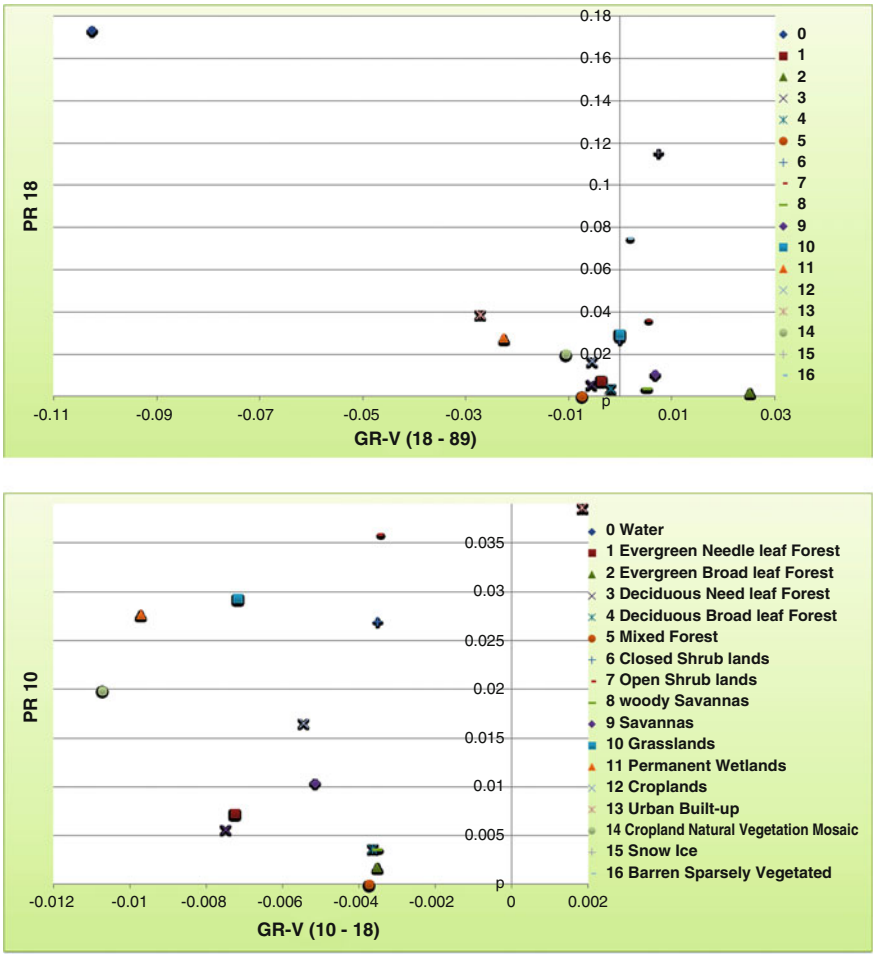

Fig. 3 continued

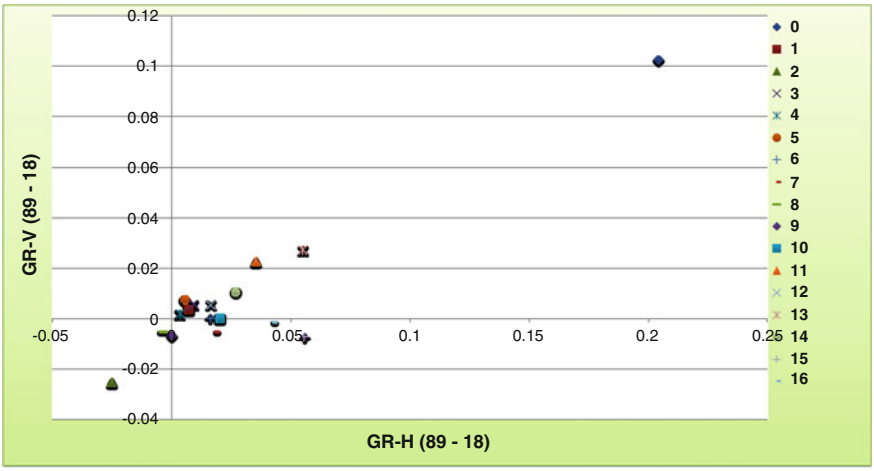

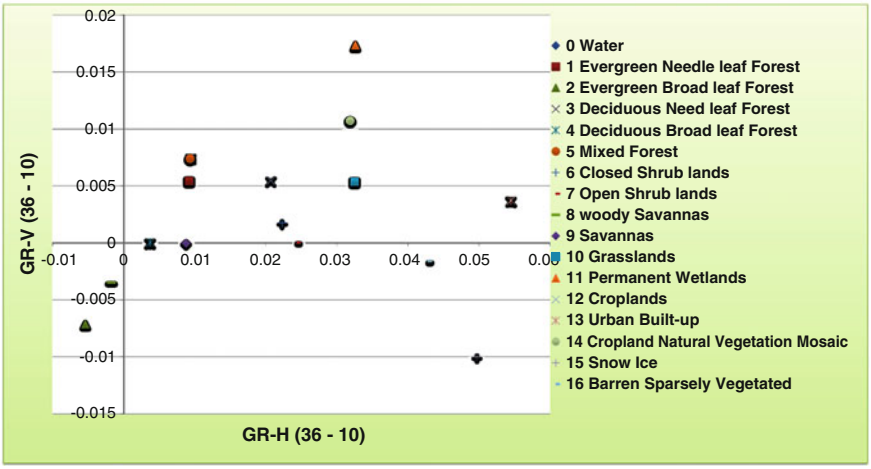

Fig. 3 continued

Table 2 Land cover classes and there MPGR value

Land cover classes	PR-10	PR-18	PR-36	PR-89	GR-V (89–18)	GR-H (89–18)	GR-V (36–10)	GR-H (36–10)
Water	0.20–0.25	0.17–0.18	0.035–0.04	0.06–0.07	0.10–0.11	0.20–0.25	0.10–0.11	0.30–0.4
Evergreen Needle leaf Forest	0.005–0.01	0.005–0.01	0.005–0.01	0.00–0.005	0.00–0.005	0.005–0.01	0.005–0.01	0.005–0.01
Evergreen broad leaf forest	0.00–0.005	0.00–0.005	0.00–0.005	0.00–0.005	-0.02 to −0.03	−0.02 to −0.03	−0.01 to -0.005	−0.01 to −0.005
Deciduous needle leaf forest	0.005–0.01	0.005–0.01	0.005–0.01	0.00–0.005	0.005–0.01	0.005–0.01	0.005–0.01	0.005–0.01
Deciduous broad leaf forest	0.005–0.01	0.00–0.005	0.00–0.005	0.00–0.005	0.00–0.005	0.00–0.005	−0.005–0.0	0.00–0.005
Mixed forest	0.005–0.01	0.00–0.005	0.00–0.005	0.00–0.005	0.005–0.01	0.005–0.01	0.005–0.01	0.005–0.01
Closed shrub lands	0.035–0.04	0.025–0.03	0.015–0.02	0.01–0.015	−0.005–0.0	0.015–0.02	0.00–0.005	0.02–0.025
Open shrub lands	0.04–0.05	0.035–0.04	0.025–0.03	0.01–0.015	−0.01 to −0.005	0.015–0.02	−0.005–0.0	0.025–0.03
Woody savannas	0.00–0.005	0.00–0.005	0.00–0.005	0.00–0.005	−0.01 to −0.005	−0.005–0.0	−0.005–0.0	−0.005–0.0
Savannas	0.015–0.02	0.01–0.015	0.005–0.01	0.00–0.005	−0.01 to −0.005	0.00–0.005	−0.005–0.0	0.005–0.01
Grasslands	0.04–0.05	0.025–0.03	0.015–0.02	0.005–0.01	−0.005–0.0	0.02–0.025	0.005–0.01	0.03–0.035
Permanent wetlands	0.035–0.04	0.025–0.03	0.02–0.025	0.015–0.02	0.02–0.025	0.035–0.04	0.015–0.02	0.03–0.035
Croplands	0.025–0.03	0.015–0.02	0.01–0.015	0.005–0.01	0.005–0.01	0.015–0.02	0.005–0.01	0.02–0.025
Urban built-up	0.05–0.06	0.035–0.04	0.00–0.005	0.01–0.015	0.025–0.03	0.05–0.06	0.00–0.005	0.05–0.06
Cropland natural vegetation mosaic	0.03–0.035	0.02–0.025	0.01–0.015	0.00–0.005	0.01–0.015	0.025–0.03	0.01–0.015	0.03–0.035
Snow ice	0.13–0.14	0.11–0.12	0.07–0.08	0.05–0.06	−0.01 to –0.005	0.05 to –0.06	−0.02 to −0.01	0.05–0.06
Barren sparsely vegetated	0.09–0.10	0.07–0.08	0.05–0.06	0.035–0.04	−0.005–0.0	0.04–0.05	−0.005–0.0	0.04–0.05

Table 3 MPGR based Land cover classification

MPGR range	PR-10	PR-18	PR-36	PR-89	GR-V (89–18)	GR-H (89–18)	GR-V (36–10)	GR-H (89–18)
−0.02 to -0.03					Evergreen broad leaf forest	Evergreen broad leaf forest		
−0.02 to −0.01							Snow ice	
−0.01 to −0.005					Savannas, snow ice, woody savannas, open shrub lands		Evergreen broad leaf forest	Evergreen broad leaf forest
−0.005 to –0.00					Barren sparsely vegetated/ bare soil, closed shrub lands, grasslands	Woody savannas	Woody savannas, barren sparsely vegetated/bare soil, deciduous broad leaf forest, savannas, open shrub lands	Woody savannas
0.00–0.005	Evergreen broad leaf forest, woody savannas	Mixed forest, evergreen broad leaf forest, woody savannas, deciduous broad leaf forest	Evergreen broad leaf forest, woody savannas, deciduous broad leaf forest, urban built-up, mixed forest	Evergreen broad leaf forest, woody savannas, deciduous broad leaf forest, mixed Forest, deciduous need leaf forest, evergreen needle leaf forest, savannas, cropland natural vegetation mosaic	deciduous broad leaf forest, evergreen needle leaf forest	Savannas, deciduous broad leaf forest	Closed shrub lands, urban built-up	Deciduous broad leaf forest
0.005–0.01	Deciduous broad leaf forest, mixed forest, deciduous need leaf forest, evergreen needle leaf forest	Deciduous need leaf forest, evergreen needle leaf forest	Evergreen needle leaf forest, deciduous need leaf forest, savannas	Croplands, grasslands	Deciduous need leaf forest, croplands, mixed forest	Mixed forest, evergreen needle leaf forest, deciduous need leaf forest	Evergreen needle leaf forest, croplands, grasslands, deciduous need leaf forest, mixed forest	Savannas, evergreen needle leaf forest, deciduous need leaf forest, mixed forest
0.01–0.015		Savannas	Croplands, cropland natural vegetation mosaic	Closed shrub lands, open shrub lands, urban built-up	Cropland natural vegetation mosaic		Cropland natural vegetation mosaic	

(continued)

Table 3 (continued)

MPGR range	PR-10	PR-18	PR-36	PR-89	GR-V (89–18)	GR-H (89–18)	GR-V (36–10)	GR-H (89–18)
0.015–0.02	Savannas	Croplands	Closed shrub lands, grasslands	Permanent wetlands		Closed shrub lands, open shrub lands, croplands	Permanent wetlands	
0.02–0.025		Cropland natural vegetation mosaic	Permanent wetlands		Permanent wetlands	Grasslands		Croplands, closed shrub lands
0.025–0.03	Croplands	Closed shrub lands, grasslands, permanent wetlands	Open shrub lands		Urban built-up	Cropland natural vegetation mosaic		Open shrub lands
0.03–0.035	Cropland natural vegetation mosaic							Grasslands, cropland natural vegetation mosaic, permanent wetlands
0.035–0.04	Permanent wetlands, closed shrub lands	Open shrub lands, urban built-up	Water	Barren sparsely vegetated/bare soil		Permanent wetlands		
0.04–0.05	Grasslands, open shrub lands					Barren sparsely vegetated		Barren sparsely vegetated
0.05–0.06	Urban built-up		Barren sparsely vegetated	Snow ice		Snow ice, urban built-up		Snow ice, urban built-up
0.06–0.07				Water				
0.07–0.08		Barren sparsely vegetated	Snow ice					
0.08–0.09								

(continued)

Table 3 (continued)

MPGR range	PR-10	PR-18	PR-36	PR-89	GR-V (89–18)	GR-H (89–18)	GR-V (36–10)	GR-H (89–18)
0.09–0.10	Barren sparsely vegetated							
0.10–0.11					Water		Water	
0.11–0.12		Snow ice						
0.12–0.13								
0.13–0.14	Snow ice							
0.14–0.15								
0.15–0.16								
0.17–0.18		Water						
0.18–0.19								
0.19–0.20								
0.20–0.25	Water					Water		
0.25–0.30								
0.30–0.40								Water

5 Conclusion

This study is an attempt to use AMSR-E BT data for retrieving land cover classes. AMSR-E frequencies have relationship between land cover and MPGR values. Results confirm that the simplified land cover classification based on MPGR has the potential to reveal more precise land surface features from AMSR-E remote sensing data. Using a single day data, we classified the land surface into 17 types based on their MPGR values. Where all green/healthy vegetation comes near to 0.0 in polarization ratio and bellow then 0.0 in gradient ratio. Normal vegetation falls till 0.05 and then higher values for degraded or low vegetation/bare soil and built up. Highest values above 0.12 are for ice/water. This method can be used to target specific locations based on ground observations, but needs additional investigation, using data from different times of the year where the surface characteristics change. In addition, applying these relationships to independent data to learn about their stability also needs to be performed. Building an improved monitoring system for meteorological applications should be a subject of further research.

References

1. Mao KB, Tang HJ, Zhang LX, Li MC, Guo Y, Zhao DZ (2008) A Method for retrieving soil moisture in Tibet region by utilizing microwave index from TRMM/TMI Data. Int J Remote Sens 29:2903–2923
2. Fily M, Royer A, Goitab K, Prigentc C (2003) A simple retrieval method for land surface temperature and fraction of water surface determination from satellite microwave brightness temperatures in sub-arctic areas. Remote Sens Environ 85:328–338
3. McFarland MJ, Miller RL, Neale CMU (1990) Land surface temperature derived from the SSM/I passive microwave brightness temperatures. IEEE Trans Geosci Remote Sens 28 (5):839–845
4. Becker F, Choudhury BJ (1988) Relative sensitivity of normalized difference vegetation index (NDVI) and microwave polarization difference index (MPDI) for vegetation and desertification monitoring. Remote Sens Environ 24:297–311
5. Boori MS, Vozenilek V (2014) Assessing land cover change trajectories in Olomouc, Czech Republic. Int J Environ Ecol Geol Min Eng 8(8):540–546
6. Jackson TJ, Schmugge TJ (1991) Vegetation effects on the microwave emission of soils. Remote Sens Environ 36:203–212
7. Calvet JC, Wigneron JP, Mougin E, Kerr YH, Brito LS (1994) Plant water content and temperature of the Amazon forest from satellite microwave radiometry. IEEE Trans Geosci Remote Sens 32:397–408
8. Felde GW (1998) The effect of soil moisture on the 37 GHz microwave polarization difference index (MPDI). Int J Remote Sens 19:1055–1078
9. Owe M, Richard DEJ, Walker J (2001) A methodology for surface soil moisture and vegetation optical depth retrieval using the microwave polarization difference index. IEEE Trans Geosci Remote Sens 39:1643–1654
10. Choudhury BJ, Tucker CJ, Golus RE, Newcomb WW (1987) Monitoring vegetation using Nimbus-7 scanning multichannel microwave radiometer's data. Int J Remote Sens 8:533–538
11. Njoku EG, Chan SK (2006) Vegetation and surface roughness effects on AMSR-E land observations. Remote Sens Environ 100:190–199

12. Boori MS, Vozenilek V, Burian J (2014) Land-cover disturbances due to tourism in Czech Republic. Advances in Intelligent Systems and Computing, vol. 303. Springer, Switzerland, pp 63–72. doi:10.1007/978-3-319-08156-4-7
13. Paloscia S, Pampaloni P (1988) Microwave polarization index for monitoring vegetation growth. IEEE Trans Geosci Remote Sens 26:617–621
14. Boori MS, Amaro VE (2011) A remote sensing approach for vulnerability and environmental change in Apodi valley region, Northeast Brazil. Int J Environ Earth Sci Eng 5(2):01–11
15. Boori MS, Amaro VE, Vital H (2010) Coastal ecological sensitivity and risk assessment: a case study of sea level change in Apodi River (Atlantic Ocean), Northeast Brazil. Int J Environ Earth Sci Eng 4(11):44–53
16. Clara SD, Jeffrey PW, Peter JS, Richard AM, Thomas RH (2009) An evaluation of AMSR-E derived soil moisture over Australia. Remote Sens Environ 113:703–710
17. Chris D (2008) The contribution of AMSR-E 18.7 and 10.7 GHz measurements to improved boreal forest snow water equivalent retrievals. Remote Sens Environ 112:2701–2710
18. Lubin D, Garrity C, Ramseier RO, Whritner RH (1997) Total sea ice concentration retrieval from the SSM/I 85.5 GHz channels during the Arctic summer. Remote Sens Environ 62:63–76
19. Boori MS, Amaro VE (2010) Land use change detection for environmental management: using multi-temporal, satellite data in Apodi Valley of northeastern Brazil. Appl GIS Int J 6 (2):1–15

Optimal Path Problem with Possibilistic Weights

Jan Caha and Jiří Dvorský

Abstract The selection of optimal path is one of the classic problems in graph theory. Its utilization have various practical uses ranging from the transportation, civil engineering and other applications. Rarely those applications take into account the uncertainty of the weights of the graph. However this uncertainty can have high impact on the results. Several studies offer solution by implementing the fuzzy arithmetic for calculation of the optimal path but even in those cases neither of those studies proposed complete solution to the problem of ranking of the fuzzy numbers. In the study the ranking system based on the Theory of Possibility is used. The biggest advantage of this approach is that it very well addresses the indistinguishability of fuzzy numbers. Lengths of the paths are compared based on the possibility and the necessity of being smaller than the alternative. The algorithm offers the user more information than only the optimal path, instead the list of possible solutions is calculated and the alternatives can be ranked using the possibility and the necessity to identify the possibly best variant.

Keywords Fuzzy numbers · Dijkstra algorithm · Optimal path · Uncertainty

1 Introduction

The selection of optimal or least-cost path through space is one of the common issues in the GIS. The optimal path may be chosen either in a network or on a surface. In both cases the algorithms used for selecting optimal path are based on graph theory, so there is actually little difference between the raster and the vector

J. Caha (✉) · J. Dvorský
Faculty of Science, Department of Geoinformatics, Palacký University,
17. Listopadu 50, 771 46 Olomouc, Czech Republic
e-mail: jan.caha@upol.cz

J. Dvorský
e-mail: jiri.dvorsky@upol.cz

I. Ivan et al. (eds.), *Geoinformatics for Intelligent Transportation*,
Lecture Notes in Geoinformation and Cartography,
DOI 10.1007/978-3-319-11463-7_3

datasets. The range of possible utilization is very wide, from route planning to many civil engineering applications especially in construction of various networks [1].

Like any other type of data even data for selecting optimal path are affected by uncertainty. The main uncertainty affecting selection of optimal path is the uncertainty of weights or in other words cost for travelling from one node to another. These weights of edges can represent many real world phenomena, for example geographical distance of nodes, time necessary to cover the distance or amount of fuel needed for this particular distance. While distance can be measured quite exactly it is not particularly suitable as a measure for finding optimal path [2], mainly because distance alone does not tell anything about fitness of the solution. On the other hand, the time and/or amount of fuel necessary for travel are good indicators for optimal path selection. Yet none of those two can be expressed exactly for real world problems. Both of them are highly dependant on many other variables and thus unfit to be expressed as a crisp number [3]. It is much better to express them as a vague and ill-know values, using fuzzy set theory as fuzzy numbers [4].

Modifications of the Dijkstra and other algorithms for selection of the optimal path were studied in several studies [1–9]. All of those papers aims at calculating the optimal or the shortest path in a network when the uncertainty of the arc weights is presented in the graph, however each of these studies utilize different ways to obtain the results. The process has two main challenges that have to be addressed in order to produce the algorithm. These challenges are addition of the fuzzy numbers and their ranking. The addition of fuzzy numbers is usually described for the triangular and the trapezoidal fuzzy numbers [3, 4, 6], however these are not all the possible shapes of the fuzzy numbers and other variants can be also used. The addition is presented for mentioned shapes mainly because it can be easily implemented and calculated. But there are more general solutions that work for variety of other fuzzy number shapes [10]. Some authors [4] even use methods that provides a crisp value as the result of addition of fuzzy numbers. While this may be easier for further ranking of the results it leads to the loss of information about vagueness and/or imprecision of the fuzzy number.

The second challenge that need to be solved is ranking of fuzzy numbers. As noted by Dubois and Prade [11] there is no natural total-ordering structure for a set of fuzzy numbers and many of the approaches to the problem are either counter-intuitive and/or consider only one point of view on the matter. Some studies propose algorithms where any of indices for comparison of fuzzy numbers can be used [6]. While some use specific indice or even distance of fuzzy numbers for their ranking [2, 9]. While all mentioned approaches have their possible use, none of them really address the problem of indistinguishability and overlap of fuzzy numbers, which certainly should be solved. The solution can be found in use of Possibility theory and indices proposed by Dubois and Prade [11].

The main advantage of the proposed algorithm is in generalization of fuzzy numbers addition. There is no assumption about shape of fuzzy numbers, instead the methods that use piecewise linear fuzzy number are used. Such fuzzy numbers can have any shape. The framework of Possibility theory is used for ranking of

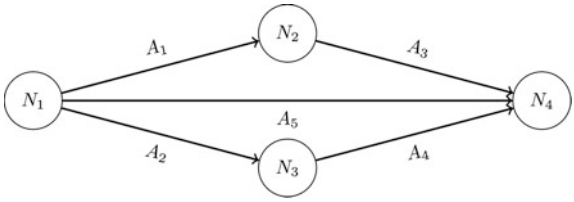

Fig. 1 Simple graph with N_i nodes and directed arcs A_j

fuzzy numbers for calculation of possibility and necessity of equality and/or exceedance of fuzzy numbers.

The structure of paper is following: Sect. 2 offers basic preliminaries and notions of graph theory, for further elaborations about this topic please see [12]. Section 2.1 briefly summarizes informations about Fuzzy numbers, addition of Fuzzy numbers and ranking of Fuzzy numbers in framework of possibility theory. The proposed Algorithm is shown in Sect. 3 and a case study is presented in Sect. 4. The discussion and conclusions are presented in Sect. 5.

Prior to explanation of the algorithm some basic definitions need to be set up, the full reference can be found in Bondy and Murty [12]. Through the work we consider directed weighted network $G(N, A)$ that consist of set of nodes $N = \{1, ..., n\}$ and a set of directed arcs $A = \{1, ..., m\}$. Each of these arcs is defined by an ordered pair of nodes (i, j) that $i, j \in N$ and never $i \neq j$. Since the arcs are directed then $A(i, j) \neq A(j, i)$. Each of these arcs has a weight, that specifies cost for passing from start to final node. Usually this weight w_k is specified as a crisp positive number and it is used to identify the optimal path from starting node to the destination (Fig. 1).

The selection of optimal path is a process of selecting path from node N_i to node N_j, where the sum of the weights is minimal. There are many algorithms that solve the problem proposed by Bellman–Ford et al. [7]. Between these algorithms the Dijkstra algorithm [13] is undoubtedly one of the most commonly used, not only in practical applications, but also in scientific studies [4].

2 Fuzzy Numbers and Possibility Theory

In case when there is need to model uncertainty that originates in indistinguishability, vagues etc. it is not suitable to use statistical approaches and alternative approaches is necessary [10]. Alternative framework for all essential operations can be found in Fuzzy set theory and Possibility theory.

2.1 Fuzzy Numbers

Fuzzy numbers are special cases of convex, normal fuzzy sets defined on $\mathbb{R}$ with at least piecewise continuous membership function, that represent vague, imprecise or

ill-known value [10]. There are several types of fuzzy numbers, commonly used are triangular and trapezoidal ones, however other shapes are possible as well [10]. Triangular and trapezoidal fuzzy numbers are often used because calculations with them and their comparison can be done relatively easily, but it is much better if calculations and comparisons can be done for any shape of fuzzy numbers.

The most general type of fuzzy numbers that can be utilized for calculations are so called piecewise linear fuzzy numbers, these fuzzy numbers are defined as a set of α-cuts [10]. They can approximate any given shape and in their most simple representation are equal to triangular or trapezoidal fuzzy numbers.

If there is need to combine fuzzy numbers with classic crisp values then crisp numbers are treated as special case of fuzzy number, where all α-cuts are the same degenerative interval [10].

2.2 Fuzzy Arithmetic

In order to perform basic arithmetic operations with fuzzy numbers there is need for apparatus that allows and specifies such operations. The most general form of such rule is specified by so called extension principle [14], however this particular definition is complicated in terms of implementation, so alternative approaches that utilize decomposition theorem and interval arithmetic are used [10]. The decomposition theorem states that every fuzzy number (or generally any fuzzy set) $\tilde{\mathrm{A}}$ can be described by associated sequence of α-cuts. An α-cut is an interval where all the objects have membership at least equal to α. Formally it can is written as: $cut_\alpha\left(\tilde{\mathrm{A}}\right) = \tilde{\mathrm{A}}_\alpha = x \in X | \mu_{\tilde{\mathrm{A}}}(x) \geq \alpha\}$ [10]. Such α-cut of a fuzzy number is always closed interval $A_\alpha = [\underline{a_\alpha}, \overline{a_\alpha}]$. The only necessary arithmetic operation for determination of shortest path is addition, using decomposition theorem and interval arithmetic the addition of fuzzy number $\tilde{A}$, $\tilde{B}$ is [15]:

$$A_\alpha + B_\alpha = [\underline{a_\alpha} + \underline{b_\alpha}, \overline{a_\alpha} + \overline{b_\alpha}] \tag{1}$$

for each $\alpha \in [0, 1]$. Using this approach the addition of any two fuzzy numbers is possible.

2.3 Possibility Theory

To allow decision making based on fuzzy numbers there is a need for a system that will allow ranking of fuzzy numbers. There are several such systems however most of them consider only one point of view on the problem [11]. The complete set of ranking indices in the framework of possibility theory was proposed in [11]. This ranking system uses possibility and necessity measures to determine relation of two fuzzy numbers.

Utilization of possibility theory allows also semantically describe fuzzy numbers as possibility distributions [16]. This semantic than help us explaining what such fuzzy numbers mean. The values with membership value 1 are believed to be absolutely possible or unsurprising, thus they should cove the most likely result. With decreasing degree of membership the possibility of obtaining given result decreases and the surprise rises. When membership value reaches 0 then such result is impossible (or almost impossible at some cases) and the surprise that such result would present is maximal. Such semantics helps with practical explanation what the results truly mean.

To asses position of fuzzy number $\tilde{X}$ to the fuzzy number $\tilde{Y}$ four indices are needed [11]. Two of them define possibility and necessity that $\tilde{X}$ is at least equal or greater than $\tilde{Y}$:

$$\prod_{\tilde{X}}([\tilde{Y},\infty)) = \sup_x \min(\mu_{\tilde{X}}(x), \sup_{y\le x} \min(\mu_{\tilde{Y}}(y)) \tag{2}$$

$$\mathcal{N}_{\tilde{X}}([\tilde{Y},\infty)) = \inf_x \max(1-\mu_{\tilde{X}}(x), \sup_{y\le x} (\mu_{\tilde{Y}}(y)) \tag{3}$$

The other two determine if $\tilde{X}$ is strictly greater than $\tilde{Y}$:

$$\prod_{\tilde{X}}(]\tilde{Y},\infty)) = \sup_x \min(\mu_{\tilde{X}}(x), \inf_{y\le x} 1-\mu_{\tilde{Y}}(y)) \tag{4}$$

$$\mathcal{N}_{\tilde{X}}(]\tilde{Y},\infty)) = \inf_x \max(1-\mu_{\tilde{X}}(x), \inf_{y\ge x} 1-\mu_{\tilde{Y}}(y)) \tag{5}$$

Together these indices allow comparison of any two fuzzy numbers, based on pairwise comparison any set of fuzzy numbers can be sorted.

For both set of indices there are four situations of the combinations of possibility and necessity that can be outcome of the calculation. In this paragraph both relations—at least equal or greater, and strictly greater—are referred as relation, because the descriptions are valid for both pairs of indices. The first situation is when $\prod_{\tilde{X}}\left([\tilde{Y},\infty)\right) = \mathcal{N}_{\tilde{Y}}\left([\tilde{Y},\infty)\right) = 0$ which means that $\tilde{X}$ is definitely does not fulfil the given relation to $\tilde{Y}$. Then there is opposite situation $\prod_{\tilde{X}}\left([\tilde{Y},\infty)\right) = \mathcal{N}_{\tilde{Y}}\left([\tilde{Y},\infty)\right) = 1$, in which $\tilde{X}$ completely satisfy the relation. The other two relations contains some uncertainty, because they indicate certain results but they can not provide them absolutely. The first of those is situation when $\prod_{\tilde{X}}\left([\tilde{Y},\infty)\right) > 0$ and $\mathcal{N}_{\tilde{Y}}\left([\tilde{Y},\infty)\right) = 0$. This means that there is possibility that $\tilde{X}$ might satisfy the relation, but it is not necessary. Obviously that means that the indicators are not strong. The last possible combination of values is $\prod_{\tilde{X}}\left([\tilde{Y},\infty)\right) = 1$ and $\mathcal{N}_{\tilde{Y}}\left([\tilde{Y},\infty)\right) > 0$. In such case again it the relation is not satisfied absolutely but the indicators are much stronger than in previous case.

3 The Algorithm

The Dijkstra algorithm was proposed in 1959 [13] and it purpose is to identify shortest path between given source node of the graph and all the other nodes. With small modification it can be also used to identify shortest path from starting node to the destination node [4]. It is this variant of the algorithm which will be shown. The algorithm is relatively simple and makes use of only two operations—addition and comparison of crisp numbers. The algorithm works in several steps [4]:

1. assign all nodes distance value: zero for the starting node and infinity for all others
2. set all nodes as unvisited, set starting node as current
3. calculate cumulative distances from current node to all its neighbours, if the distance is smaller then previously recorded distance then overwrite the distance and write the previous node
4. set all neighbours of the current node as visited
5. move to next unvisited node
6. if all the nodes were visited stop the algorithm.

The distance from one node to another is equal to the weight of the arc between those nodes in the necessary direction. The distance of node N_i from starting node is equal to the sum of distances between those two nodes. For each node we store the distance from the starting node and also the previous node on the path from starting node. That way the shortest path from any node to the starting node can be identified easily.

From the definition of the algorithm it is obvious that there is only one solution to the problem of finding optimal path between two nodes if such path exists. However identification of such ideal path is only possible in the environment without uncertainty. As soon as uncertainty is introduced there maybe be several solutions that can be hard or impossible to order. For the modified version of Dijkstra algorithm there is no assumption of one ideal path, in fact there is assumption that several such paths exist and that there are differences that allow their basic ordering.

There are several modifications to the algorithm. First is that all the weights in graph are expected to be fuzzy numbers. The calculation on distances from starting node to neighboring nodes is done according to decomposition theorem and Eq. (1). The second change of the algorithm is that for each node the list of distances is stored (Code Sample 1).

Code Sample 1. Dijkstra algorithm (modified from: [4])

```
function Dijkstra(Graph, source):
  for each vertex v in Graph:           // Initializations
    v.distanceList.add(infinity);       // Each vertex stores list of
distances
  end for

  source.distanceList.add(0);           // Distance from source to source
  Q = the set of all nodes in Graph;

  while Q is not empty:                 // The main loop

    u = vertex in Q with smallest distance to last visited node or source;
    remove u from Q;

    if u.distanceList.contains(infinity):
      break;                                        // all remaining vertices
are
    end if                                          // inaccessible from source

    for each neighbor v of u:   // where v has not yet been removed from Q
                                // the distance is calculated for fuzzy
numbers
      newDistanceList = calculateDistance(u.distanceList, dist_between(u,
v));
      v.distanceList = compareFuzzyValues(v.distanceList, newDistanceList);

      select new v in Q;      // Reorder v in the Queue

    end for
  end while

  return distancesLists of all nodes;
end function
```

When calculating distance of new node there is necessity to take into account all the possible paths to this node and add the new distance to all of them (Code Sample 2).

Code Sample 2. Calculation of distances for node

```
//each node may contain more than one solution, the function calculates those
function calculateDistance(distanceList, distance)
  for each distance i in distanceList:
    distanceList[i] = distanceList[i] + distance; // according to Eq.(1)
  end for
  return distanceList;
end function
```

The next step in the algorithm is comparison of the calculated distance with the distances already known for the node. Possibility and necessity is calculated according to Eqs. (2) and (3). There are 3 possible outcomes of the comparison the new values to the already known distances. First the necessity result may be equal to 1. Which means that it is definitely bigger, in such case the value is of no interest because the alternative is for sure shorter. If the values of necessity and possibility are both equal to zero than the value is definitely smaller and it should replace the originally recorded values. If $\prod_{\tilde{X}}\left(\left[\tilde{Y},\infty\right)\right) > 0$ and $\mathcal{N}_{\tilde{Y}}\left(\left[\tilde{Y},\infty\right)\right) < 1$, that is and indicator, that there is overlap between two values and there is no clear preference

which is one is actually smaller. In such case the new value is added to the list (Code Sample 3).

The described algorithm provides list of distances for each node. This list can be ordered according to pairwise comparisons of fuzzy numbers in the list to produce best possible outcome. Also all several outcomes can be presented with ranking according to Eqs. (2) and (3).

Code Sample 3. Comparison of fuzzy distances stored in two lists

```
//comparison of existing list of distances store for node with list of new
nodes
function compareFuzzyValues(distanceList, newDistanceList):

  addToList = false;

  if distanceList is empty:
    distanceList = newDistanceList;

  else:
    for each newDistance in newDistanceList:
      for each distance in distanceList:
        possibility = possibility(newDistance >= distance); // using Eq.(2)
        necessity = necessity(newDistance >= distance);     // using Eq.(3)

        if necessity = 1:
          break;
        end if

        if possibility = 0:
          remove distance from distanceList;
          addToList = true;
        end if

        if possibility > 0 and necessity < 1:
          addToList = true;
        end if
      end for

        if addToList = true:
          add newDistance to distanceList;
        end if
    end for
  end if

  return distanceList;
end function
```

The algorithm can be implemented according to the Code Samples 1, 2, and 3. The addition of fuzzy numbers as well as their ranking is computationally much more complicated operation than same operations with crisp numbers. Also the algorithm does not search only for one solution but rather for a set solutions which is also more computationally expensive than the classic Dijkstra Algorithm. Based on these facts it can be reasoned that the algorithm will be both computationally and time demanding when compared to classic Dijkstra algorithm. But these are properties of the algorithm that on the other hand allows calculation with the uncertainty.

4 Case Study

The case study shows rather simple example of a graph with weights represented as fuzzy numbers or possibility distributions. This case study may describe real word example of travelling in the city where weights show time necessary to reach the node. Obviously time cannot be expressed exactly because it may depend on external conditions that are unknown at the time, when the model was created. Such conditions could be weather, time when the the travel should be made, amount of traffic etc. Because none of those conditions can be know in advance, it is reasonable to model them as possibility distributions.

The example used in case study is obvious. A simple graph containing 4 nodes and 5 directed arcs (Fig. 2). **Node *a* is a starting point of path and destination node is *d***. From the visualization of the graph it is visible that 3 paths can be identified: a → b → d, a → c → d and finally direct path from a → d. Since all the weights of the graph are defined as triplets in form $[A_{0,}A_1 = A_1, A_0]$ they represents triangular fuzzy numbers. Known property of fuzzy numbers is that if they are aggregated the result is again triangular number [10]. So the Eq. (1) is applied only for α values of 0 and 1. Obtained results are summarized in Table 1.

Results can be best asses when they are visualized (Fig. 3). Now the ranking needs to established. Since the interest is in finding values that are smaller or equal to the given value the Eqs. (2) and (3) will be used to calculate possibility and necessity.

The comparison of the obtained results is summarized in Table 2. From that can be reasoned that solution a → d is the worst as it has possibility and necessity of at least equality to both other solution equal to 1. Also a → c → d ≥ a → d has both possibility and necessity equal to 0 which excludes this solution from set of possible shortest paths. From comparison of solutions a → b → d and a → c → d it is clear that there is no strict ordering of these solutions, because there is quite a big

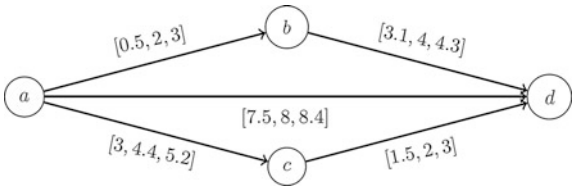

Fig. 2 Simple graph with fuzzy weights

Table 1 Resulting path and their lengths of the case study

Path	Triangular number
a → b → d	[3.6, 6, 7.3]
a → c → d	[4.5, 6.4, 8.2]
a → d	[7.5, 8, 8.4]

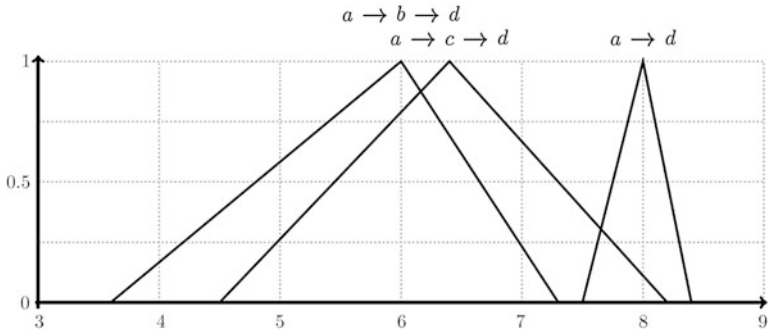

Fig. 3 Results of case study compared in a graph

Table 2 Comparison of the resulting paths

Comparison	Possibility	Necessity
a → b → d ≥ a → c → d	0.875	0.349
a → c → d ≥ a → d	0	0
a → c → d ≥ a → b → d	1	0.651
a → c → d ≥ a → d	0.304	0
a → d ≥ a → b → d	1	1
a → d ≥ a → c → d	1	1

overlap. But even such solutions can be ordered, there is higher both possibility and necessity of a → c → d ≥ a → b → d than a → b → d ≥ a → c → d. Than can be interpreted as a → b → d being more suitable solution. However the fact that neither of indices is equal to 1 means that the solutions can not be distinguished very well, in fact they are rather similar (Fig. 3). According to those facts the results of the algorithm can be shortly summarized by defining solutions a → b → d and a → c → d as acceptable solutions, while a → d is unacceptable solution (Table 3).

Such cases are classic situations when presenting both solution and their ranking would be useful for decision maker. Mainly because the solutions are quite similar and there is possibility that choosing any of those might lead to optimal decision. Unfortunately because of the presented uncertainty the solutions can not be ranked directly.

Table 3 Results of the algorithm

Path	Status
a → b → d	Accepted
a → c → d	Accepted
a → d	Not accepted

5 Discussion and Conclusion

The presented modification of the Dijkstra algorithm aims to provide better support of decision making in situations where uncertainty of the data exists. It should be helpful mainly by providing all solutions that can not be distinguished, or in other words that have rather high similarity. This is archived by utilization of Fuzzy set theory and Possibility theory to manage the uncertainty and the vagueness through the calculation. The results obtained from the algorithm provide the user not only with one optimal path but also with other options that are quite similar under the given amount of uncertainty.

The use of fuzzy numbers as weights in the graph allows better modelling of the real world situations where the time to travel from one point to another can not be specified exactly, or other similar cases. Specifying the time as a crisp number can be too much idealization and simplification of the problem, because the algorithms for finding optimal path then produce way to idealized solutions that do not take into account either uncertainty or the amount of dissimilarity of the solutions.

The proposed algorithm proposes solution to both challenges, that were mentioned previously. It allows identification of optimal path in uncertain environment. This uncertain or vague environment is however better model of reality than exact environment, where all the values are expected to be known precisely. The second issue is addressed by providing not only one solution but a list of solutions. This provides more alternatives that can be ranked using possibility and necessity measures.

The variant of Dijkstra algorithm is in GIS also used for selecting least cost paths on surfaces [1]. The proposed algorithm can be used for calculating optimal path on surfaces that contain uncertainty, especially on so called fuzzy surfaces. Further studies of the topic could be focus on this issue—selection of optimal paths on fuzzy surfaces.

Acknowledgments The authors gratefully acknowledge the support by the Operational Program Education for Competitiveness—European Social Fund (projects CZ.1.07/2.3.00/20.0170 and CZ.1.07/2.2.00/28.0078 of the Ministry of Education, Youth and Sports of the Czech Republic).

References

1. Yu C, Lee J, Munro-Stasiuk MJ (2003) Extensions to least-cost path algorithms for roadway planning. Int J Geogr Inf Sci 17(4):361–376
2. Mahdavi I, Nourifar R, Heidarzade A, Amiri NM (2009) A dynamic programming approach for finding shortest chains in a fuzzy network. Appl Soft Comput 9(2):503–511
3. Okada S, Oper T (2000) A shortest path problem on a network with fuzzy arc lengths. Fuzzy Sets Syst 109(1):129–140
4. Deng Y, Chen Y, Zhang Y, Mahadevan S (2012) Fuzzy Dijkstra algorithm for shortest path problem under uncertain environment. Appl Soft Comput 12(3):1231–1237

5. Ghatee M, Hashemi SM (2009) Application of fuzzy minimum cost flow problems to network design under uncertainty. Fuzzy Sets Syst 160(22):3263–3289
6. Hernandes F, Lamata MT, Verdegay JL, Yamakami A (2007) The shortest path problem on networks with fuzzy parameters. Fuzzy Sets Syst 158(14):1561–1570
7. Ji X, Iwamura K, Shao Z (2007) New models for shortest path problem with fuzzy arc lengths. Appl Math Model 31(2):259–269
8. Okada S (2004) Fuzzy shortest path problems incorporating interactivity among paths. Fuzzy Sets Syst 142(3):335–357
9. Tajdin A, Mahdavi I, Mahdavi-Amiri N, Sadeghpour-Gildeh B (2010) Computing a fuzzy shortest path in a network with mixed fuzzy arc lengths using α-cuts. Comput Math Appl 60 (4):989–1002
10. Hanss M (2005) Applied fuzzy arithmetic: an introduction with engineering applications. Springer, Berlin
11. Dubois D, Prade H (1983) Ranking fuzzy numbers in the setting of possibility theory. Inf Sci 30(3):183–224
12. Bondy JA, Murty USR (2008) Graph theory. Springer, New York
13. Dijkstra EW (1959) A note on two problems in connexion with graphs. Numer Math 1 (1):269–271
14. Zadeh LA (1965) Fuzzy sets. Inf Control 8(3):338–353
15. Moore RE, Kearfott RB, Cloud MJ (2009) Introduction to interval analysis. Society for Industrial and Applied Mathematics, Philadelphia
16. Zadeh LA (1978) Fuzzy sets as a basis for a theory of possibility. Fuzzy Sets Syst 1:3–28

Optimal Placement of the Bike Rental Stations and Their Capacities in Olomouc

Zdena Dobešová and Radek Hýbner

Abstract Several towns over the whole world run the network of the station for rent a bike for municipal transport. The town Olomouc has good condition for bike transport. The town is flat, and private transport by bike is very often. There is the opportunity to prepare the network of bike rental station. The rent out the bike is assumed for daily transport of inhabitants or tourists and visitors. The presented study shows the analysis of optimal placement of the rental station in Olomouc. The spatial analysis is based on data about street lines, cycling lines and numbers of inhabitants and others. Extension Network Analyst for ArcGIS was used for location and allocation analyses. Moreover, the suggestion of capacities (number of position for bikes) for each station was calculated. The result is two variants for 3 and 4 min walking time to the rental station.

Keywords Rental station · Cycling · Location analysis · Allocation analysis

1 Introduction

Valencia, Santander, Seville, Barcelona, London, Dublin, Lyon, Paris, Marseille, Luxembourg, Wien and many other cities have the bicycle renting public service. Bike-sharing is becoming more and more frequent mean of transport in the European and World cities. Cycling supplements the public transport in a good way in towns. Cycling fill the gap between walking that is very slow and public transport. In case of traffic jam, the cycling is the quickest way of transport.

Z. Dobešová (✉) · R. Hýbner
Department of Geoinformatics, Palacký University, 17 listopadu 50, 771 46 Olomouc, Czech Republic
e-mail: zdena.dobesova@upol.cz

R. Hýbner
e-mail: rad.hyb@volny.cz

I. Ivan et al. (eds.), *Geoinformatics for Intelligent Transportation*,
Lecture Notes in Geoinformation and Cartography,
DOI 10.1007/978-3-319-11463-7_4

Many case studies and realization (San Francisco, Lisbon, Seattle) exist for several towns [1–3]. The inspiration was the real experience with the system Valenbisi in Valencia [4]. Only one solution exists in the Czech Republic. Bicycle renting public service HOMEPORT PRAHA exists in Prague, municipal part Karlín. Presented solution suggests the placement of stations for the whole city Olomouc. This study did not concern to the economical, technical or operating aspects of bike sharing. The main aim was to analyze spatial situation and conditions for optimal location of bike rental stations in town Olomouc using GIS. The analysis was solved as geoinformatics task. Spatial analyses are very often used for exploration of the urban environment [5].

Several case studies were explored. Midgley [6] mentions four generations of bike sharing. The first solution appeared in Amsterdam (1960), La Rochelle (1976) a Cambridge (1993). Bicycles were for free for inhabitants. The second generation locked the bicycles in the rental stations. The loan of a bicycle was by inserting a coin (Danish towns Farso and Grena in 1991). The third generation started in Copenhagen at 1995. The users paid the annual fee to rent a bicycle. The using of bicycle is free for the first 30 min. It is necessary to pay a small fee when the time is longer than 30 min. Now it is the most realized solution in many towns.

The spatial distribution of rental stations considers some facts in studied case studies. The distance between two of stations is recommended from 300 to 500 m [7]. The study for Paris recommended about 10 rental stations per km^2. Localization of stations must primarily consider the highest moving of inhabitant. The influences are a number of inhabitant on permanent address, commuters to schools and jobs, the closeness to the shops, the cultural and sport facilities (stadiums, theatres, cinemas, museums, concert halls, markets, department stores etc.).

The presented solution is individual solution for Olomouc city. The suggested method is own developed method that is partially inspirited by presented case studies. The method has considered source data and their structure and also their availability for city Olomouc and census in the Czech Republic. The synthesizing solution arose from detail research of case studies over the whole world and detail study of condition in city Olomouc.

2 Step of Analysis

Case study for Olomouc city consists of several steps. The first step was the data collection and the update of street lines and especial bicycle path and bicycle lane. It was assumed to locate the rental station near the bicycle path and line. The second step was the collection data about the number of inhabitants, commuting people to localize source and target area with high citizen motion. These data and data about land use were the base for the creation of “raster of suitable areas”. The raster of suitable areas was the first output of spatial analysis.

Analyses Minimize Facilities and Maximise Coverage from the set of Location-Allocation Analyses were the next step. Task Minimize Facilities determines the

minimal number of facilities that cover maximum demand points. This analysis determines the suitable number of the rental station. The address data was input to the location analysis as demand points. The last step was the suggestion of capacity of stations.

3 Raster of Suitable Areas

The first spatial analysis was the creation of suitable areas for location of rental stations. Suitable areas were created as a weighted raster that expressed the high population movement. The pixel size was discussed. The sizes 10 and 20 m were tested. The size 10 m better expresses the situation near the streets in the centre of the town.

Input data for the raster were vector data: street lines, bicycle lane/path, station of public transport and railway stations. All these data were actualized and verified in summer 2012 [8]. Stations of public transport and railway stations are important. The continuation of bus transport with cycling is supposed [7]. Buffer zones (50 m) of these points and the line vector data were converted to the rasters. In addition, another data were considered. Data about commuters were taken from the Czech Statistical Office. Commuters are supposed to be a client of rental stations. Number of commuters was originally assigned to the street lines. Accommodation facilities and their capacities were multiplied by 0.29. The occupation of hotels is 29 % in average. All these data and address points with the number of inhabitants were converted to the separate rasters. The last input data was vector polygon theme—land use that was also converted to the raster [9]. The building block areas and water had value 0. All rasters were reclassified.

Using tool Raster Calculator from Map Algebra toolset was created the final raster of suitable areas. The scale of weight was from 0 to 9. The weight 0 means "unsuitable area", the weight 1–3 means "not much suitable area", the weight 4–6 means "suitable area" and the weight 7–9 means "the most suitable area". The detail part of raster of suitable areas is in Fig. 1. The first step of analysis—calculation of raster of suitable areas was tested for two municipal parts of town. One part was from the centre of town, and the second one was neighbourhood municipal part.

Finally, the weights of suitability from raster were assigned to the address points. These address points were the input for next network analyses as potential places of self-service stations.

The steps of input data preparing and next spatial processing were assumed to record as a model (data flow diagram) in ModelBuilder. The advantage would be an automatic batch processing and repetitive using of model [10, 11]. The idea was not realized due to the necessity of manual setting of class in reclassifying process.

Fig. 1 Part of the raster of suitable areas

4 Network Analyses

Extension Network Analyst for ArcGIS was used for the next steps of analysis. The data structure—Network dataset was based on feature class street line (contains also pavements). Network dataset is necessary for next network analyses.

4.1 Minimize Facilities Analysis

Analysis Minimize Facilities solves the minimal number of stations. The principle is to localize facilities to allocate to them the maximum of demand points in specified distance. Address points with the weight in interval 5–9 were taken as candidate points. Weight was taken from raster of suitable areas. The interval was a crucial decision. There were only 15 address points in interval 7–9 (the most suitable area) and 263 points in interval 6–9. Small number of candidate points produces all points as result facilities [12]. The better choice was interval 5–9. Total number of candidate points was 1,663 address points. Search tolerance was set to 200 m [8]. The input parameter is also impedance in minutes. Two values were set: 3 and 4 min for two runs of analysis. The result was only the number of station, not their localisation. Quantities were 87 stations for 3 min and 43 for 4 min. The quantities are very different in case of small change of time.

4.2 Maximize Coverage

Subsequently, the localization of stations was solved by function Maximize Coverage. This function needs as input parameter the number of facilities. The results of previous analysis Minimize Facilities were used. This analysis tries to place the limited number of points to maximize the covered area. The amount of candidate points was taken bigger than in the previous analysis. Points with weight 4 were also considered. Total number of candidate points was 4,645. Output of that analysis was lines that connected demand points with their localized facilities (rental stations). Finally, the polygons belonging to localized facilities were obtained by analysis Service Area. The polygons were solved as not overlapping polygons. For both versions (3 and 4 min) service areas were determinated.

5 Proposal of Capacities for Stations

Final step was a suggestion of capacity for each station. Capacity means the number of position (stands) for bicycles in station. Base information was the service area of each station. The area, that was covered by station, was determined by tool Service Area from extension Network Analyst for ArcGIS. For each 78 stations were determined 78 polygons of service areas (Fig. 2). The polygon features class was joined with the point layer of address points with the number of inhabitants. Total number of inhabitants that belong to each service area was calculated (Fig. 3).

Although the technical realisation did not propose, the sizes of stations were suggested in that case study. The modules from 10 up to 40 positions were considered (modules with 10, 15, 20, 25, 30, 35 and 40 stands). The inspiration was taken from other cities. Table 1 shows the situation in some European cities. The rental services have more stand than bicycles to guarantee space for parking. The ration is about 10. The number of bicycles and stands per 1,000 inhabitants very vary in cities. The redistribution of bicycles between stations is sometimes necessary. It happens especially in the morning when commuters arrive at the main railway station, and bike rental station is empty very quickly. Inverse situation is in the afternoon.

The limits for the number of inhabitants for modular rental station were experimentally suggested achieving average number of 6.85 stands per 1,000 inhabitants (Table 2).

According to calculated number of inhabitants in each service area the size of capacity was manually assigned to the rental stations. Final localization of rental stations and their capacities are on the map in Fig. 4. Each station is labelled by the suggested capacity.

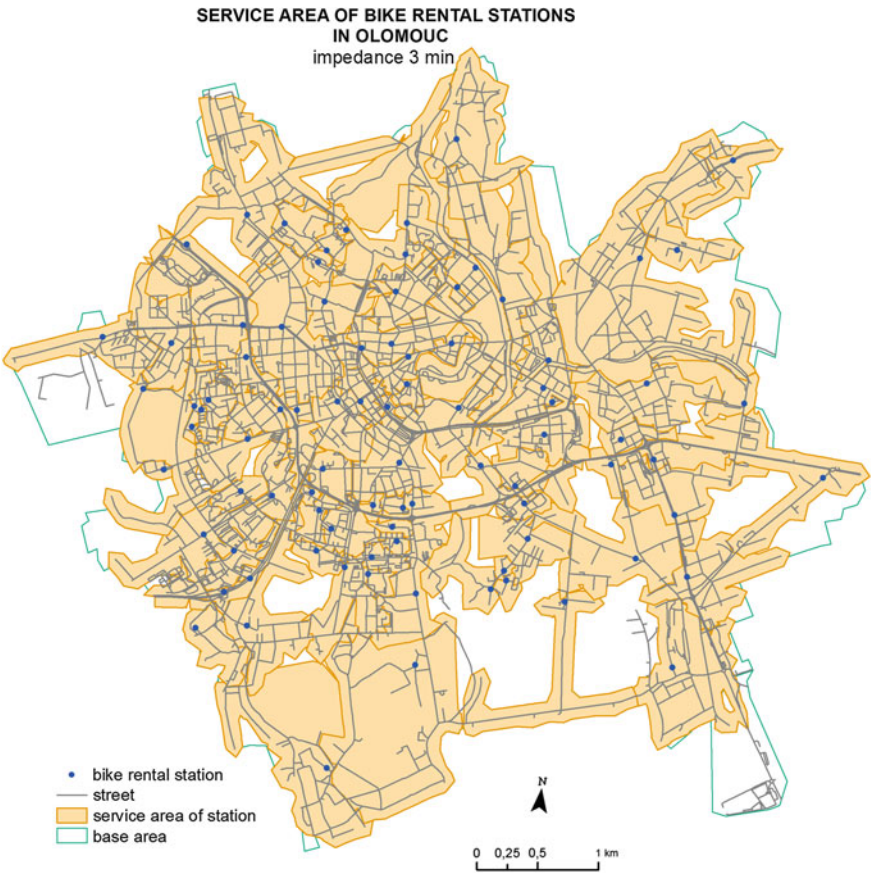

Fig. 2 Service area of bike rental stations in Olomouc [8]

6 Results

The case study has two possible solutions. The first one is for maximum 3 min walking to the station. In that case, the number of the bike rental station is 87. When the maximum walking time is 4 min the number of stations is 43. The first solution is preferred (Fig. 4). When the station is empty and no bicycle is here, the person has to go to the next station. Total time is 6 min in the first solution or 8 min in the second solution. The 6 min are limitation that be practically accepted by cyclists. Comparison of results is Table 3.

The real location of station must consider the traffic situation, owner condition in realisation. Local condition must be verified. A small shift up to 50–100 m can be accepted. The optimal distance between stations is from 300 to 500 m [7]. Very often the station occupies one or two parking places that is owned by municipality.

Fig. 3 Bike rental station in Valencia [4]

Table 1 Comparison of the number of bicycles and stands per 1,000 inhabitants in European cities [6]

City	Number of bicycles/ 1,000 inhabitants	Number of stands/ 1,000 inhabitants
Paris	9.6	13.9
Lyon	6.1	8.8
Rennes	4.8	7.0
Copenhagen	4.0	5.8
Stockholm	4.0	5.8
Barcelona	3.7	5.4
Brussels	1.1	1.6
Frankfurt	1.1	1.6
Oslo	0.5	0.7
Wien	0.4	0.6

Table 2 Suggested category of capacities for impedance 3 min [8]

Capacity	Limit number of inhabitants	Number of stands/1,000 inhabitants
10	1,000	10
15	2,000	7.5
20	3,000	6.67
25	4,000	6.25
30	5,000	6
35	6,000	5.86
40	7,000	5.71

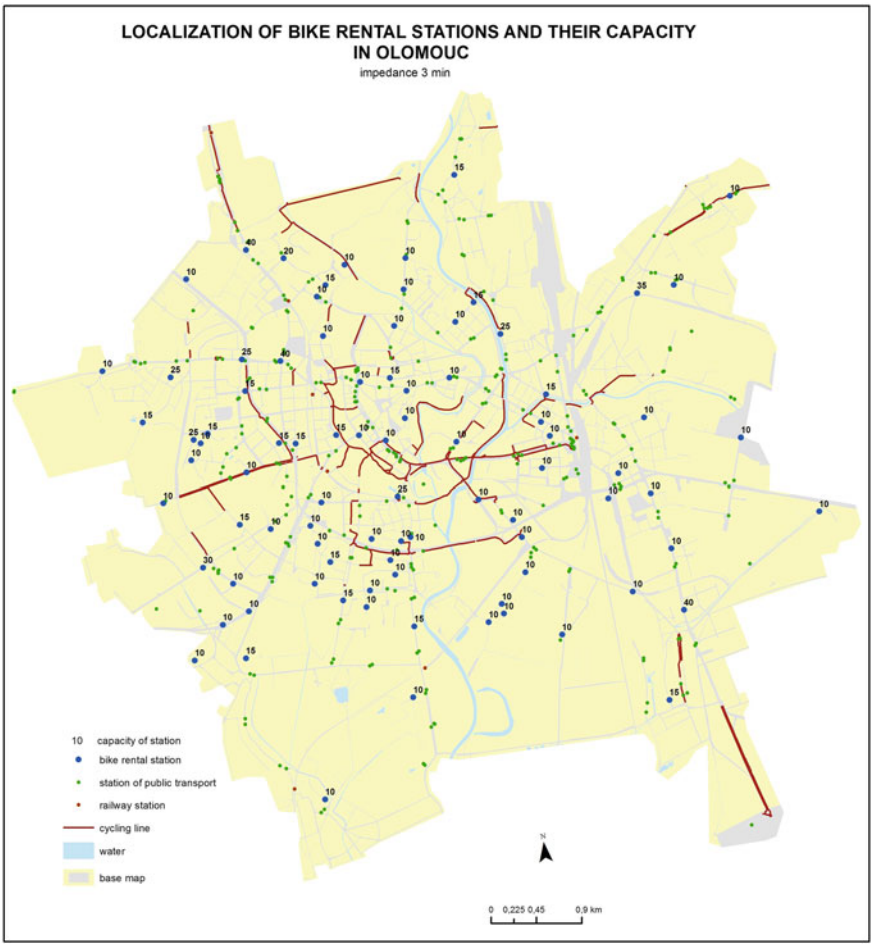

Fig. 4 Localization of bike rental stations and their capacity [8]

Table 3 Comparison of two solutions [8]

Impedance	3 min	4 min
Total number of stations	87	43
Number of covered inhabitants	90,408	90,322
Total capacity of stations	1,175	755
Average number of inhabitants per one stand	76.9	199.6
Average number of stands per 1,000 inhabitants	13	8.4
Number of bicycles in flotilla	646	415

The terrain investigation, discussion and refining must be used before final realisation of the network of bike rental station. This theoretical output produced by network analyses was handed to municipal government of Olomouc city to consider it in new cycling strategy for the city.

Acknowledgments Work was supported by the project CZ.1.07/2.3.00/20.0166.

References

1. Chen F (2011) A GIS suitability model on optimal locations for bike-sharing stations: a case study in the city of San Francisco. http://www.ocf.berkeley.edu/~fncchen/portfolio/%5BPAPER%5D%20A%20GIS%20Suitability%20Model%20on%20Optimal%20Locations%20for%20Bikesharing%20Stations.pdf. Accessed 7 Apr 2013
2. Martinez LM, Caetano L, Eiro T, Cruz F (2012) An optimization algorithm to establish the location of stations of a mixed fleet biking system: an application to the city of Lisbon. Conference EWGT, Paris, 10–13 Sept. http://www.lvmt.fr/ewgt2012/compendium_109.pdf. Accessed 8 Apr 2013
3. Wuerzer T, Mason S, Youngerman R (2012) Boise bike share location analysis. http://sspa.boisestate.edu/planning/files/2012/12/Boise-Bike-Share-Location-Analysis.pdf. Accessed 8 Apr 2013
4. Ajuntament de Valencia (2013) Valenbisi, En Valencia, di sí a la bici. http://www.valenbisi.com/. Accessed 7 Oct 2013
5. Sedlák P, Komárková J, Jedlička M, Hlásný R, Černovská I (2010) Modelling of spatial analyses processes for purpose of detection of weak points in barrier-free environment. In: Narsingh D et al (ed) Applied computer science, Proceedings of international conference on ACS, WSEAS Press, Malta, pp 419–412
6. Midgley P (2011) Bicycle-sharing schemes: enhancing sustainable mobility in urban areas. http://www.un.org/esa/dsd/resources/res_pdfs/csd-19/Background-Paper8-P.Midgley-Bicycle.pdf. Accessed 10 Apr 2013
7. Bike Share Program Investigation (2009) Phase 1 report: best practices investigation final report. http://www.smartcommute.ca/media/uploads/pdf/bike_share_best_practices_2009.pdf. Accessed 10 Apr 2013
8. Hýbner R (2013) Návrh optimálního rozmístění stanic půjčoven kol a jejich kapacit v Olomouci (Design of the optimal placement of the bike rental stations and their capacities in Olomouc) diploma thesis, Department of geoinformatics. Palacký University, Olomouc
9. Burian J, Brus J, Vozenilek V (2013) Development of Olomouc city in 1930–2009: based on analysis of functional areas. J Map 9(1):64–67

10. Dobesova Z, Dobes P (2012) Comparison of visual languages in geographic information systems. Erwing M, Stapleton G, Costagliola G (eds) Proceedings of IEEE symposium on visual languages and human centric computing, VL/HCC 2012 IEEE, Innsbruck, p 245
11. Dobesova Z (2013) Using the "Physics" of notation to analyse ModelBuilder diagrams. In: Proceedings of SGEM 2013 13th international multidisciplinary scientific geoconference, vol 1, STEF92 Technology Ltd., Sofia, pp 595–602
12. Valchařová D (2012) Alokační a lokační analýzy města Olomouce. (Location and allocation analyses in town Olomouc) diploma thesis, Department of geoinformatics, Palacký University, Olomouc

Detecting Spatial and Temporal Route Information of GPS Traces

Tao Feng and Harry J.P. Timmermans

Abstract This paper aims at detecting route information of GPS traces to represent spatial and temporal information of trips. A Bayesian belief network model is used to calculate the probability of a road matching a GPS log point. The algorithm incorporates road network topology, distance from trace nodes to road segments, the angle between two lines, direction difference, accuracy of measured GPS log point, and position of roads. GPS data collected in the Eindhoven region, The Netherlands, is used to examine the performance of this algorithm. Results based on a small sample show that the algorithm has a good performance in both processing efficiency and prediction accuracy of correctly identified instances. Prediction accuracy using a small sample is 87.02 %.

Keywords Bayesian belief network · GPS · Map matching · Road network

1 Introduction

Detecting route information of GPS traces has been an important research topic in recent years in transportation. Various map matching algorithms have been proposed with the aim to match some geographical locations or points with the existing network data. For vehicle-based traffic research, it can provide microscopic spatial-temporal information for a specific vehicle. This would be beneficial to the requirements of many research topics such as route choice simulation, emission and energy consumption analysis, travel demand forecasting, travel behaviour analysis, etc. Especially, with the increasing applications of new technologies such as GPS,

T. Feng (✉) · H.J.P. Timmermans
Urban Planning Group, Department of the Built Environment,
Eindhoven University of Technology, Vertigo 8.21,
5600 MB Eindhoven, The Netherlands
e-mail: t.feng@tue.nl

H.J.P. Timmermans
e-mail: h.j.p.timmermans@tue.nl

I. Ivan et al. (eds.), *Geoinformatics for Intelligent Transportation*,
Lecture Notes in Geoinformation and Cartography,
DOI 10.1007/978-3-319-11463-7_5

WIFI, Bluetooth as well as applications of smart phones in data collection, the requirement of an efficient and valid map matching algorithm to identify the exact locations of the trace points on network data becomes extremely important.

Basically, to identify whether a node belongs to a specific road segment (link) is not straightforward because of the difference between the spatial locations of the node and the link, road network topology and the accuracy of geographical measurement. This can be more complicated if a node is located in an area surrounded by high density buildings where the strength of the satellite signals heavily influences the accuracy of the location measurement. In addition, the variety in some special cases, like U-turn, passing through a round-about, lane changing, also increases the complexity to design map matching algorithms. A well-performed model should not only handle these main research issues, but provide sufficient robustness and uncertainty measurement in the model to be applicable in different contexts.

Due to the fact that GPS data fluctuate according to the contextual information, like the weather, urban density, sensitivity of the GPS sensor, etc., the traces measured on a temporal scale using the same device can have different accuracy. Therefore, the algorithm is necessary to be flexible enough to capture such uncertainty. From a long-term view of perspective, it seems to be important that the designed algorithm incorporates a learning function into the model in the sense that the estimated parameters could be adjusted through an intelligent learning procedure, which will then increase the overall accuracy of the map matching results with more data coming in.

A common approach for map matching, which has been adopted empirically, is by means of spatial analysis functions provided by geographical information systems (GIS) tools. The buffering area along with the geographical objects, i.e. lines or nodes, are created first, and used to match other geographical data where various criteria of overlapping filters are set in advance. Such a method is popularly applied because it is convenient to implement, but it needs to set the threshold of the searching radius which can be different according to different accuracy of the measurement. For example, Du and Aultmann-Hall [1] have empirically used a 10 m threshold to create the buffer and match the road network with GPS points. Although this threshold value has been shown to have acceptable accuracy, the method cannot meet the requirement when matching personal traces. In particular, the variation of the coordinates leads to the dilemma that some nodes either cannot be recognized as belonging to any roads in case of a small search threshold or are overly matched in case of a big radius.

A prototype map matching algorithm was developed by using the distance from node to node, the distance from nodes to lines and/or lines to lines [2]. These algorithms are consistent in the sense the distance was considered as the only decision variable. This can be problematic in real applications because of the ignorance of other important variables, like the connectivity of road segments. Although such algorithms have shown a good performance regarding the processing speed, the matching accuracy is difficult to ensure.

Recently, research appeared to incorporate more influential variables into the map matching process, like the angle between the directions of two lines, the connectivity of network topology and accuracy of the GPS measurements [3–5]. From a methodological point of view, existing map matching algorithms vary from ad hoc rules to advanced learning-based algorithms, i.e. fuzzy set, Hidden-Markov algorithm, probability hypothesis, etc. For instance, Pyo et al. [6] proposed the multiple hypothesis probability (MHP) algorithms for map matching. The method was further adopted and extended to the application of matching with GPS data [7]. Quddus et al. [8] introduced fuzzy logic theory to map matching with road networks. Some of the important variables, like the search space based on the error ellipse derived from the error variances, the perpendicular distance from a position fix to the link, the bearing of the link, and the direction of the vehicle, are incorporated. Six rules were created for fuzzy inference. The model was shown to be more accurate than previous models. However, it needs some expert knowledge to determine the fuzzy set.

Ren [4] proposed advanced algorithms for pedestrian and/or wheelchair navigation services. A Hidden-Markov model and a so-called multi-sensor approach, which incorporates the accelerometer into map matching, were used. Bierlaire et al. [5] proposed a probabilistic algorithm, which can be very useful for smart phone data. The model showed good efficiency and provided an opportunity to measure the uncertainty of the candidate road sets. However, the model needs some simplified assumptions in real applications. White et al. [9] and Quddus et al. [10] provide more detailed literature reviews on the main existing map matching algorithms.

Unlike the empirical methods, these advanced algorithms can potentially better handle the complexity in map matching procedures. Nevertheless, a well-performed algorithm should be flexible enough to measure the uncertainty of matched roads, and be capable to incorporate the major influential factors to ensure prediction accuracy. Therefore, it is still needs to further improve the performance of map matching algorithms. Considering the increasing number of applications of Bayesian Belief Networks (BBN) in different fields of research and their superiority relative to other algorithms [11, 12], it seems adequate to examine the feasibility of this algorithm in map matching. Therefore, in this paper, we will develop a map matching algorithm which incorporates the BBN model. The model incorporates some major influential factors, including distance to road, connectivity between two road segments, direction difference of two line objects, the accuracy of GPS measurement and the direction difference between two adjacent links. The method is evaluated using the GPS data collected in the Eindhoven region, The Netherlands.

2 Algorithm

To identify whether a road segment matched a GPS point, it is necessary to incorporate the influential factors. In the following discussion, we will first illustrate the main influential factors we adopted, followed by a presentation of the proposed algorithm.

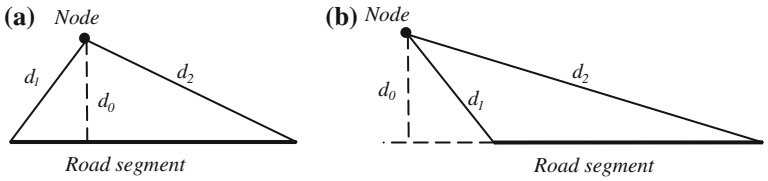

Fig. 1 Distance between the a node to a road segment. **a** Direct perpendicular distance. **b** Indirect perpendicular distance

2.1 Control Variables

2.1.1 Distance to Road

The distance between two geographical objects represents the correlation between spatial locations. The road segment, which is mostly closed to the referenced node, has a high probability to be the correct road. However, the distances from a GPS point to a specific road segment vary in terms of the spatial correlation between the two geographical objects. As shown in Fig. 1, there could be three types of distances between a node to a line, which are the perpendicular distance (d_0) and the distances from the node to the end nodes (d_1 and d_2) of the link.

In most of cases, the perpendicular distance was considered as an efficient measurement. Other distances might be used to calculate angle information of the virtual triangular to provide further location information. In our case, we take the closest distance between the node and the road. In another words, it is the perpendicular distance (d_0) as in the case of Fig. 1a and d_1 as in the case of Fig. 1b. In this way, every road segment in the candidate set can be differentiated through the shortest distance from a node to a road.

2.1.2 Direction Difference

Despite that the distance measures the reference information for a single node it does not say anything about the sequence information. The integral consideration of two or more adjacent nodes can provide information in both time and direction dimensions. Basically, the direction between the line connecting two adjacent nodes should be consistent in some extent with the direction of the matched link. Moreover, it can also benefit to the identification of whether there happens a turning action which mostly indicates a cross section closed to the node (Fig. 2a).

To further identify the correlation between the line of two nodes and the road segment, we use the angle information by incorporating the direction of the lines, as shown in Fig. 2b. In order to determine the degree of the angle consistently between a location and multiple road candidates, the direction of the road and two nodes are pre-set in advance. As shown in Fig. 2b, to ensure that Road 1 and the link

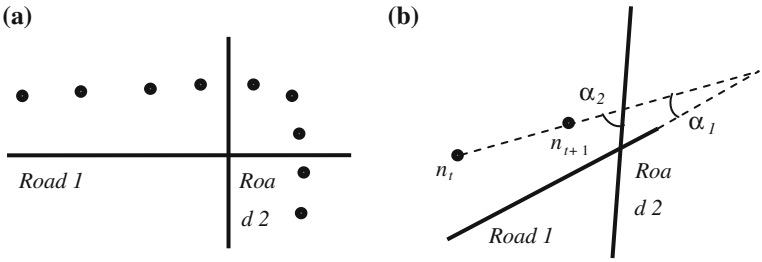

Fig. 2 Spatial pattern of log points in cross-sections. **a** Changing direction. **b** No turns

connecting the two nodes has to be in the same direction to confirm the angle of α rather than 180 − α. For the sake of simplicity, in practice, we restrict the angle as to be less than 90°.

2.1.3 Connectivity

Apart from the distance and direction information, one of the most important factors is the connectivity, which means the topology information of the road and cross sections in the geographical representation. This variable is quite important to filter out the un-reasonable roads and increase search efficiency. In practice, only these roads, which are connected at least at one node with the previously confirmed road segment, are treated as connected.

2.1.4 Other Factors

The accuracy of GPS data depends on signal strength, sensitivity of the sensor and the spatial context of the travel environment. In principle, the more satellites, the less noise in the measurements. In addition, the difference in complexity of traveling environment results into different travel patterns in the sense that travel speed in the high density city centres and suburban areas differ significantly. Therefore, it is also necessary to incorporate velocity information and accuracy of the GPS measurements.

2.2 The BBN Model

The method we adopted here is the Bayesian Belief Network (BBN), which replaces ad hoc rules with a dynamic structure, leading to improved classification if consistent evidence is obtained over time from more samples (more traces).

A Bayesian belief network (also called Bayes net) is a graphical representation of the conditional probability and causality relationships between variables. The model is described qualitatively by directed acyclic graphs where nodes and edges represent variables and the dependencies between variables. The nodes where the edge originates and ends are called the parent and the child, respectively. Bayesian belief networks allow for probabilistic inference to be performed, indicating that the probability of each value of a node can be computed when the values of the other variables are known.

The nodes that can be reached from other nodes are called descendent. In Bayesian network, each variable is independent of its non-descendent given the state of its parents. Since the independence among the variables are clearly defined, not all joint probabilities in the Bayesian system need to be calculated, which provides an efficient way to compute the posterior probabilities. Suppose the set of variables in a BBN is $\{A_1, A_2, \ldots, A_n\}$ and that *parents* (A_i) denotes the set of parents of the node A_i in the BBN. Then the joint probability distribution for $\{A_1, A_2, \ldots, A_n\}$ can be calculated from the product of individual probabilities of the nodes:

$$P(A_i, \ldots, A_n) = \prod_{i=1}^{n} P(A_i | parents(A_i)) \quad (1)$$

In our case, the Bayesian belief network represents the multiple relationships between different spatial, temporal and other factors, including errors in the technology itself (input), and the facet of the candidate road segment that we wish to identify (output). We use a Bayesian belief network to impute automatically the probability for each road segment in a filtered road set.

Figure 3 shows the network structure that we use to infer the matched road segment with respect to GPS traces. A candidate road segment is treated as a function of the states of the variables included in the BBN.

To what extent a road segment is matched with a location may be partly determined by the information of the previously matched data. For example,

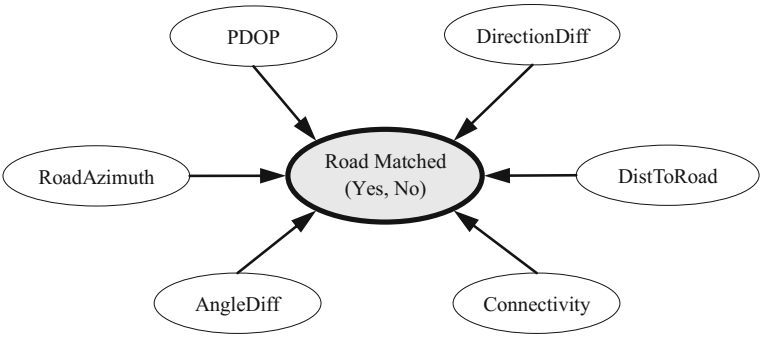

Fig. 3 Model structure for the inference of map matching

traveling along a straight route will in general have a pattern that the directions of the adjacent links connecting two GPS log points are similar. While turning across a road section may result into significant difference between the directions. Therefore, we consider three variables as the sequence information, the connectivity (Connectivity), the angle difference between the directions of two adjacent links (AngleDiff), and the direction difference between the link connecting two nodes and the matched road segment (DirectionDiff).

Here, the connectivity indicates whether two adjacent road segments are connected each other. For example, to impute the probability of road segment i, we take the previously matched road segment $i - 1$ as a reference, and check whether the current road i connects with the road $i - 1$. This means we keep the information of the previous matched road segment temporally to identify the potential road segment for the current location. In case that two adjacent locations identified a same road segment i, the connectivity is set as true.

The DirectionDiff can be calculated as mentioned previously. The angle difference (AngleDiff) is the absolute value of the difference between two adjacent directions of the virtual links, as mentioned above. In case of the starting node, the direction is set to 0. Therefore, the angle difference between the second link and the previous link equals to the value of the direction with respect to the second GPS log point.

In the model, we include two variables for the accuracy of the measurements, the Position Dilution of Precision (PDOP) and the number of satellites (NSATS). The variable PDOP is a measure of overall uncertainty of a GPS position, represents the quality of GPS signals. A PDOP value of 1 indicates a good satellite configuration and high-quality data; conversely, PDOP values above 8 are considered poor. The quality of the data decreases as the PDOP value increases.

The variable (DistToRoad) is the perpendicular distance from a node to a road segment as presented above (Fig. 1). The variable of RoadAzimuth measures the angle of the matched line object in a spherical coordinate system. Assume that a vector from an origin to a point of interest is projected perpendicularly onto a reference plane. Then the angle between the projected vector and a reference vector on the reference plane is called the azimuth. Therefore, the azimuth information indicates position of a road, which may provide useful input in combination with other location variables.

The output variable is whether a road segment is the matched road. In this case, it has two levels, yes or no. For each candidate road segment, we infer the probability through the conditional probabilities among input variables and the output variable. For a set of found options, the road segment, which has the highest probability, is taken as the rightly matched road.

3 GPS Data and Implementations

The GPS data used in this paper were collected in the urban area of Eindhoven, The Netherlands. One of the main purposes of this GPS data collection is to find valuable merits of peoples activity-travel trajectories in a long term. Every participant was required to join the survey for a period of three months. People carried the GPS logger, downloaded and uploaded their GPS data to the website. The data was then processed using the program of TraceAnnotator to generate the possible activity and travel data. Details about the TraceAnnotator can refer to the paper by Moiseeva et al. [13]. A web-based prompted recall procedure, which allows people to validate their historical data by modification, filling, removing or inserting in case of missing or incorrect data, was adopted. Additionally, respondents were also asked to provide some demography information and the locations where they visit frequently.

Individuals carried the GPS logger, named Bluetooth A++ Pro. The device has a good sensor embedded, which can receive well signals within trains. This capability decreases in some extent the noise induced by signals in urban area, however, the overall accuracy of the GPS data is in general rather acceptable especially for traveling data, like car for example. The GPS devices were configured to record data in every 3 s. The recorded information includes: date, time, longitude, latitude, speed, distance, accuracy of the measurement (like PDOP, HDOP, VDOP etc.), and number of satellites.

Although the data collected in the Eindhoven region was targeted as a large scale of research projects where all available transportation modes and various activity types were included, in this paper, we are especially interested in the trips by car to test the efficiency of the proposed map matching algorithm. In addition, since the training of the BBN model needs some facts that can determine the conditional probabilities among the input variables and the road segment, we extract the trips by car, which have detailed recorded diary.

The road network data includes all the road segments of the whole Netherlands. There are three categories of roads: the national road, the provincial road and the local road. Figure 4 shows the distribution of the GPS log points and road categories. As a consequence, a total of 10 trips, including 1,227 GPS points are selected as a test sample.

In order to evaluate the efficiency of the proposed method, we labelled in the dataset the true road segments for every GPS log point using GIS. A filter was designed specifically to search the set of candidate road segments for a GPS coordinates. More specifically, a buffer with the given radius (di) for a GPS point i was created based on the coordinates, and the road segments which touch with the buffer were taken into the choice set.

To determine a feasible value of search radius will help improving the searching efficiency of the whole algorithms. Since the GPS traces are influenced by various indicators like number of satellites, weather, etc., the spatial pattern of the log points vary even for a same road segments. The empirical values of 2.5 and 11.4 (unit: meter)

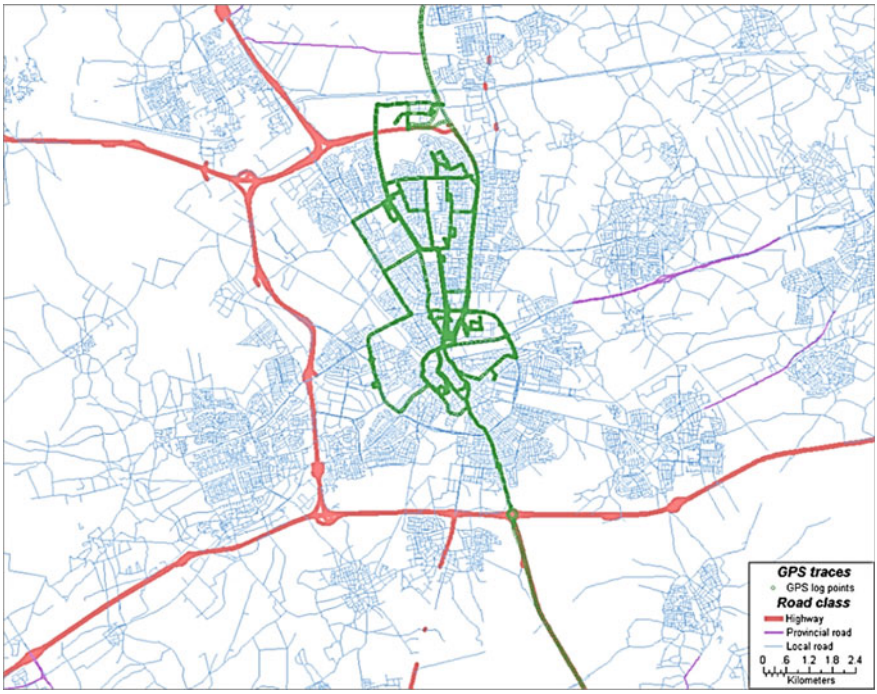

Fig. 4 Distribution of the GPS log points on the road network of The Netherlands

have been used to classify the data quality of good and poor [4]. As shown in Fig. 5, the distances to the same road from GPS log points of the same individual among different days are different.

Because the search process is memory intensive in that the searching time increases with the increase of the search radius. Here, in order to increase the efficiency of the searching procedure, the search radius was set dynamically according to the value of PDOP. We use 20 m as the searching radius if the PDOP has a value less than 3 and 50 m otherwise (Eq. 2).

$$d_i = \begin{cases} 20, & if\ PDOP \leq 3 \\ 50, & if\ PDOP > 3 \end{cases} \tag{2}$$

In the process of BBN training, the filter was first implemented for every log point in the sample to generate a set of candidate road segments. Then the input variables in the BBN model were calculated for each road segment and the GPS coordinates. A new dataset where each row represents the pattern of matched or unmatched road segment and their relevant attribute variables was created. As presented above, we incorporated variables relevant to speed, connectivity, spatial distance to the specified road segment, direction and the accuracy of GPS log measurements.

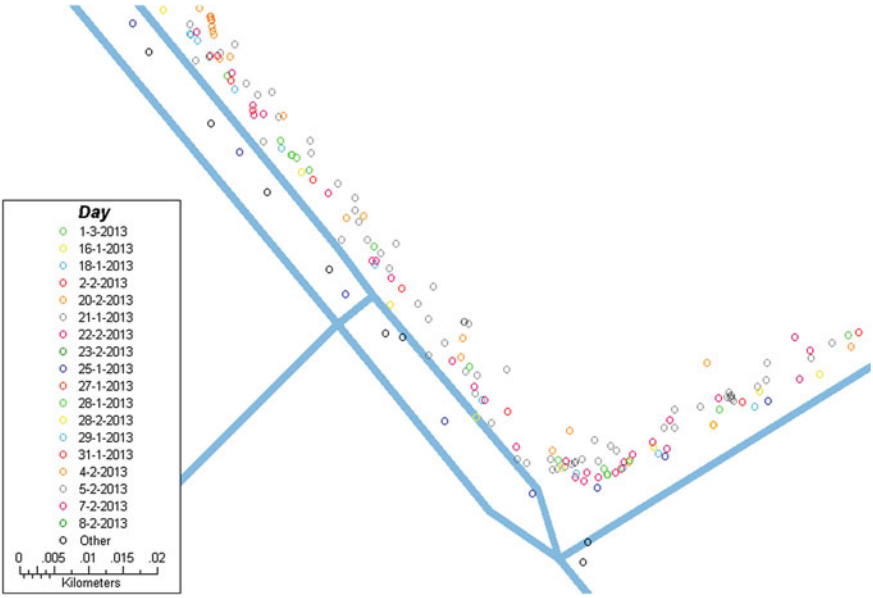

Fig. 5 Distances from the GPS log points of different days to road segments

The true sample data was prepared using the carefully recorded diary and the road network data within GIS. The locations, which cannot match with any road segments, were excluded. We divided the sample data into two datasets, one is for training purpose and the other is for test purpose. The datasets were selected randomly in terms of trips and road categories, by setting 75 and 25 % as the training and test dataset, respectively.

Since the connectivity is considered as one of the determinant variables, it is important to find the first road segment of the starting log point (origin). Because of the effect of signal issue in the activity locations, the log points which are closed.to the true activity location might be fluctuated. Moreover, a prompted recall cannot ensure the mentioned location as a truth. Therefore, we add some additional filters in assisting the identification of the origin. More specifically, we include the information of personal profiles and the validated location names in combination with the activity type. In concrete, if the personal profile is available in terms of the activity type, we picked the coordinates of their personal locations directly from the database of personal locations. Otherwise, the location names will be used for online geo-coding to find a valid coordinates through Google service. Finally, if both the personal profiles and location names are missing or incomplete for some reasons, we fetch the original GPS traces according to the start time and/or end time of the activity. Finally, the coordinates of the origin are generated as to provide references of map matching for the consequent GPS log points. A detailed implementation procedure is depicted in Fig. 6.

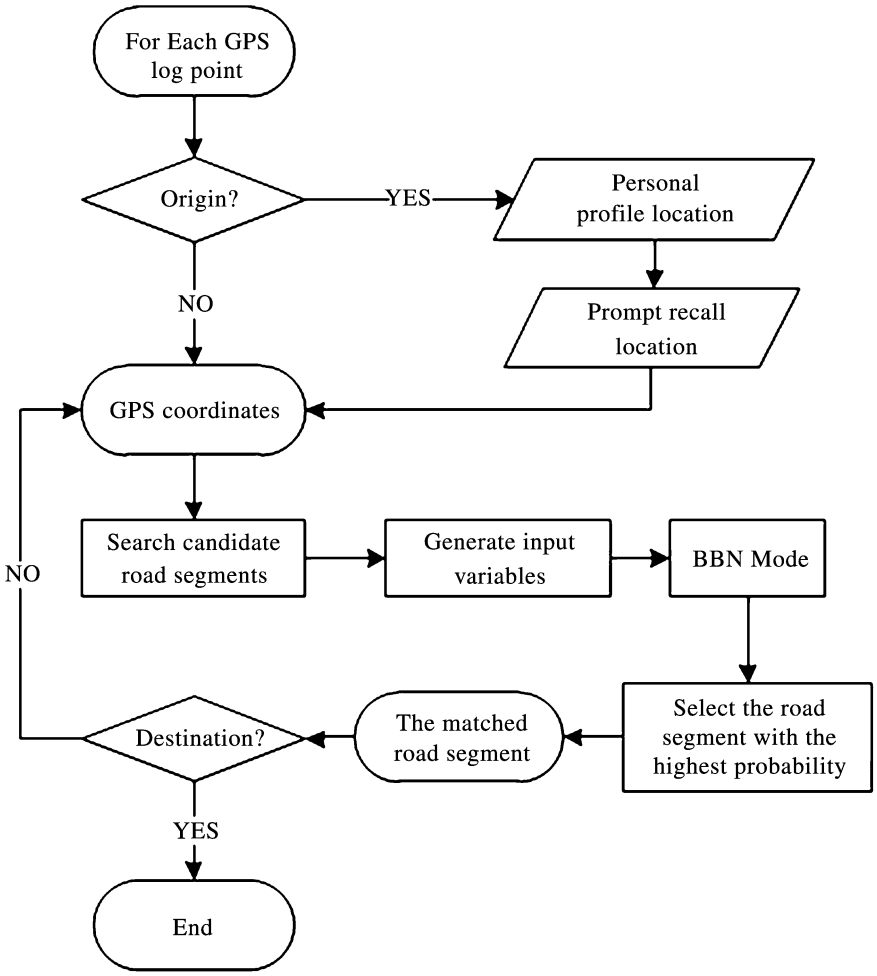

Fig. 6 Flowchart of the implementation steps

As shown in the flowchart, the map matching process starts from the origin and ends at the destination of a trip. The detection of real origin is necessary since the traces during activity episode fluctuate in general. Taking the first data record as the starting node can be sometimes problematic because the device needs some time to configure at the beginning of start. Since the recognition of real activity location is out of the scope of this research, we simply check on the personal profile data that the respondents supported. In addition, we also use the prompted recall data to double-confirm the exact location and obtain the coordinates through a geo-coding process.

After the recognition of the origin point, the candidate road segments are fetched and relevant input variables are generated. The selection of the road segment follows the prediction of the BBN model. The selected road will be the one with a

highest probability among all the candidate road segments. In this sense, the un-selected road segments also have a value of probability, which on the other hand measures the uncertainty of the map matching algorithm.

In addition, it should be noted that, for each GPS log point, the connectivity is considered here as one of the input variables to identify the road segment. This is different from the hard constraint, which only considers connected road segments and excludes the potential roads which are not connected with the previous road segment. In some cases, it is possible that a road segment is incorrectly matched or a road segment is too short to be matched with any locations. Therefore, relaxing the connectivity as a hard constraint will avoid the possible error propagation in case that one road segment was recognized incorrectly. In order to ensure that the matched road segments are sections of a same route, we post process the matched data by checking from the origin to the destination. For example, if there is one road segment which does not connect with both the previous and the forward road segments, the end node of the previous road will be connected with the start node of the forward road by using the shortest path algorithm.

4 Results

Because for each log point in the training dataset, a set of candidate road segments were gathered in advance, in which each road segment has a label on whether it is a matched road (true) or not (false). The inter-dependency correlations among input and output variables are then set up in terms of the ground truth. Then the data can be used for training the model to obtain the potential interdependency correlations, which can be used for prediction.

Table 1 shows an example of the conditional probabilities for the connectivity variable specifically. The conditional probability here indicates the extent of the matching dependency on whether two road segments are connected. The percentage of rightly matched is the relative value by comparing the number of data records, which are matched correctly divided by the total sample. It represents the relative accuracy based on the current dataset. As one can see that the probability of rightly matched road reaches 0.832, if the current road connects with the previous road. For un-matched roads, the percentage of the non-connected (0.535) is slightly higher than that of the connected (0.465). This is reasonable in that the probability of

Table 1 Conditional probability of connectivity

The rightly matched road	Connect with the previous road (connectivity)	
	Yes	No
True	0.832	0.168
False	0.465	0.535

un-matched roads is dependent on the size of candidate road sets and the cross-effects of other input variables.

For these roads that are in the candidate road set (here, the label is False) but not the matched roads, the connectivity results into a percentage of 0.465 and 0.535 for connected and unconnected road segments, respectively. This means the unconnected roads are more possible (0.535 vs. 0.465) to be un-matched road than matched roads, indicating the connectivity correlation will benefit to matching the road correctly.

In order to evaluate the performance of the proposed BBN model, we use the results according to the indicators of the correctly classified instances (CCI), incorrectly classified instances (ICI) and Kappa value (Kappa). The ICI, being the other round of CCI, labels the percentage of incorrectly matched data. The kappa statistic measures the agreement of prediction with the true class [14]. Here, the value of 0 and 1 signifies incomplete and complete agreement, respectively. A higher value of Kappa indicates a better performance of the model.

Table 2 presents the details of the prediction accuracy. It is found that the accuracy of correctly classified instances 87.02 %. This means the BBN model has a good performance in matching the GPS data. The level of Kappa for BBN model is 0.577, which is also satisfied in this context.

Table 3 shows the results of hit ratio for the two classes of the output variable in the BBN model. Hit ratio is a measure of business performance traditionally associated with sales. It is normally a matrix which includes all the combinations of different classes in the prediction result. Here, the hit ratio shows how accurate a road was matched. The higher is the value, the more accurate are the matched results. Since we set the variable into 2 levels, one is the right road segment, and the other is the found road segments but not the right road. We found for both classes, the accuracy percentages are 56.19 and 95.64 %, respectively. These ratios are calculated based on the whole candidate road segments, which means that the more number of candidate road, the lower of the level of confirmed ratio, because only one road among the candidate roads can be labeled as the right road. This is why the ratio of confirmed yes is lower than that of the confirmed no, because the number of unmatched roads in the candidate road set is large.

Table 2 Prediction accuracy and model performance

	CCI	ICI	Kappa
All samples	87.018 %	12.983 %	0.577

Table 3 Results of the hit ratio

	Confirmed yes	Confirmed no
Hit ratio	56.19 %	95.64 %

5 Summary, Conclusions and Discussion

Identifying the location of a GPS point on a road segment has been an important research issue in transportation planning, transport modeling and environmental analysis. In route choice simulations, the GPS data provides the merit with more accurate and detailed real-time information, which is impossible to approximate in traditional stated choice experiments. Moreover, the matched roads in combination with the time information will also contribute to providing more possibilities in microscopic simulation of traffic flow and environmental analyses.

Development of an efficient map matching algorithm is of high importance in different research fields. Due to the fact previous methods are not efficient enough in the aspect of flexibility and learning capability, in this paper, we proposed an algorithm using Bayesian belief network model for map matching of GPS data. Variables employed in the model are distance to road, difference of directions, difference of angles of two adjacent links, connectivity, number of satellites and PDOP. The algorithm is investigated by using the data collected in the Eindhoven region, The Netherlands. Simulation results showed that the BBN model shows a good performance in recognizing the road segments with an accuracy of 87 % (correctly classified instances).

As one may argue that the accuracy of GPS data is questionable, which are a common issue in this study as well as others related to map matching algorithms, such data should not give main influences on the matching results. Although the extreme unrealistic data appear not much frequent in our GPS data, it is always true that the effect of the noise data should be handled well. Therefore, when applying this algorithm in real applications, a process to filter such data out is necessary. Moreover, the algorithm needs to be improved by designing it more flexible with respect to these inaccurate data.

As presented in the paper, the performance of the algorithm was evaluated through a carefully recorded dataset. This was considered as a feasible way to confirm the validity of this algorithm, because the validation of an algorithm in the context of map matching is not much straightforward. There needs additional effort to provide example data where sufficient ground truth and various special cases should be included. In spite of the acceptable efficiency of Bayesian network in map matching (87 %), one cannot say it is a better algorithm than others at this moment because of the difference in the GPS data used. Future research will go further to examine some other algorithms by using the same data set to see the possible superiority of the proposed algorithm.

As to test the efficiency of this algorithm, in this paper, a prototype of an enhanced map matching algorithm was proposed and examined through a small sample data. However, it is necessary in future work to include more sample data to further check the generality in large scale applications. Since the current algorithm spent much time in referencing the geo-objects in GIS, future research should consider the processing speed to make it realisable real-time applications. In a more general context, various special cases, which are common in GPS data, like passing through

a cross-section, U-turn, driving through round-about and traveling off-roads, are necessary to take into account. Facts representing the special cases should be extracted in advance from large GPS samples. To that end a more flexible map matching algorithm will incorporate the capability to comprehensively deal with different cases.

References

1. Du J, Aultman-Hall L (2007) Increasing the accuracy of trip rate information from passive multi-day GPS travel datasets: automatic trip end identification issues. Transp Res Part A Policy Pract 41(3):220–232
2. Bernstein D, Kornhauser A (1998) An introduction to map matching for personal navigation assistants. Available via DIALOG. http://www.njtude.org/reports/mapmatchintro.pdf
3. Quddus MA, Noland RB, Ochieng WY (2009) The effects of navigation sensors and spatial road network data quality on the performance of map matching algorithms. Geoinformatica 13 (1):85–108
4. Ren M (2012) Advanced map matching technologies and techniques for pedestrian/wheelchair navigation. Ph.D dissertation, School of Information Sciences, University of Pittsburgh
5. Bierlaire M, Chen J, Newman J (2013) A probabilistic map matching method for smartphone GPS data. Transp Res Part C Emerg Technol 26:78–98
6. Pyo JS, Shin DH, Sung TK (2001) Development of a map matching method using the multiple hypothesis technique, Intelligent transportation systems. In: Proceedings IEEE, pp 23–27
7. Schuessler N, Axhausen KW (2009) Processing raw data from global positioning systems without additional information. Transp Res Record J Transp Res Board 2105:28–36
8. Quddus MA, Noland RB, Ochieng WY (2006) A high accuracy fuzzy logic based map matching algorithm for road transport. J Intell Transp Syst 10(3):103–115
9. White C (2000) Some map matching algorithms for personal navigation assistants. Transp Res Part C Emerg Technol 8(1–6):91–108
10. Quddus MA, Ochieng WY, Noland RB (2007) Current map-matching algorithms for transport applications: state-of-the art and future research directions. Transp Res Part C Emerg Technol 15(5):312–328
11. Rudloff C, Ray M (2010) Detecting travel modes and profiling commuter habits solely based on GPS data. In: Transportation research board 89th annual meeting, Washington DC, USA, 10–14 Jan
12. Feng T, Timmermans HJP (2013) Transportation mode recognition using GPS and accelerometer data. Transp Res Part C Emerg Technol 37:118–130
13. Moiseeva A, Jessuren J, Timmermans HJP (2010) Semiautomatic imputation of activity travel diaries: use of global positioning system traces, prompted recall, and context-sensitive learning algorithms. Transp Res Record J Transp Res Board 2183:60–68
14. Hall M, Frank E, Holmes G, Pfahringer B, Reutemann P, Witten IH (2009) The WEKA data mining software: an update. SIGKDD Explor 11(1):10–18

Impact of Particular Indicators of Urban Development of Cities in the Czech Republic on Average Road Traffic Intensity

Vladimír Holubec and Lena Halounová

Abstract This paper deals with the dependency between the development of road traffic intensity and several statistic and spatial indicators, which are monitored in cities of the Czech Republic. Road traffic intensity was used as the basic phenomenon. The other city indicators are residential, productive, recreational and other areas, population and many other indicators. This analysis is a part of a large research focused on last 40 years in cities of various sizes, traits, and location in the country during last 40 years in 10 years' time steps. Stagnating or even a decreasing number of inhabitants of cities on one side and increasing road traffic intensity is a typical characteristic in most cities. The fact concerns both cars, and lorries; motorcycle form of transport has receded for more than 80 % during these 40 years. The paper shows that the urban development is strongly dependent on historical developments of individual cities. It means that influence of individual indicators varies in individual cities. There was an important difference between the period before and after the political change in 1989. The aim of the paper was to analyse a long period of urban development of a high number of Czech cities and to determine if their development can be generalized for all of them or it is more individual. Future situation of cities can be more reliably derived from the historical development of individual cities than from deep statistical analyses of a higher number of cities. The result will help urban engineers for urban areas modelling.

Keywords Land use · Development · Road traffic intensity · Urban area · ArcGIS

V. Holubec (✉) · L. Halounová
Department of Mapping and Cartography, Faculty of Civil Engineering, Czech Technical University in Prague, Thákurova 7, 166 29 Praha 6, Czech Republic
e-mail: vladimir.holubec@fsv.cvut.cz

L. Halounová
e-mail: lena.halounova@fsv.cvut.cz

I. Ivan et al. (eds.), *Geoinformatics for Intelligent Transportation*,
Lecture Notes in Geoinformation and Cartography,
DOI 10.1007/978-3-319-11463-7_6

1 Introduction

Since 1950s of the 20th century, cities of the Czech Republic have changed at a varying extent due to their technical and social development with regard to two different political and economic systems. Development and consequences of these changes have reflected a quality of our living space in our present cities. All consequences cannot be classified as positive. In order to avoid these negative consequences, analysis of the history is needed. It was the main goal of the COST Project —Modelling of urban areas to lower the negative influences of human activities.

The project dealt with a detailed evaluation of relations among urban development indicators to prepare a set of recommendations for a sustainable development of urban areas. It was processed between 2010 and 2012 at the Department of Mapping and Cartography of the Faculty of Civil Engineering at CTU in Prague. Project included analysis of the cities of the Czech Republic from the point of view of the road traffic and urban development determined by land use classes and some statistical data. Land use classes called functional classes which consist of—residential areas, production areas, recreational areas, other areas and transportation areas. The project was originally processed for fifty cities. However, all data were not available for all cities. Therefore only 36 cities were fully-processed.

This article is a part of a broader comparative study of the above-mentioned COST project. The main topic of this paper is to analyse various attributes which can influence road traffic. These attributes as indicators of the cities' development are described in Chap. 3. The relationship was processed within fifty selected cities in the Czech Republic by a methodology which was developed by Vepřek [1].

Road traffic is an import source of air pollution, noise, and many other problems of present life on one side and therefore it plays a substantial role in the urban area environment. On the other side, the world has changed and relies very intensively on road traffic. Land use in urban areas has an important influence on road traffic intensity, which is one of its characteristics in these areas. Road traffic intensity—as measured in the Czech Republic—is the number of various types of vehicles passing through determined locations on selected roads in 24-h periods. The analysis is based on seeking the dependency between road traffic intensity and particular land use and statistic indicators (Table 1). This relation is expressed by a correlation coefficient CCAI (see Chap. 3).

2 Current State

Urbanisation as a phenomenon of the last 50 years is a phenomenon which occurs in most countries of the world. It is the reason why urban development is analysed by many authors in many countries. The goal of these analyses is to determine the indicators which can be managed to lower the negative impacts of urbanisation from the increasing noise and emissions of road vehicles, e.g.

Table 1 List of processed indicators

Name of indicators	Number of analysed cities (at least in one time span)
A. Agricultural area in the administrative city area	36
B. Forest area in the administrative city area	36
C. The area of water bodies in the administrative city area	36
D. Built-up areas and courtyards in the administrative city area	36
E. Other areas and barren land in the administrative city area	36
F. Traffic areas in the core area	36
H. Productive area in the core city area	36
I. Residential area in the core city area	36
J. Recreational areas in the core city area	36
K. Other areas in the core city area	36
L. Population of the city	36
M. Number of inhabitants using public transport system daily	23
N. The population growth	36
O. Economically active population	36
P. Number of inhabitants commuting to work	22
Q. CO_2 emissions from large sources	23
R. Dust emissions from large sources	23

Litman [2] describes the methods for evaluating how transport planning decisions influence land use—and how land use planning decisions affect transport. He uses 12 factors as a location of development relative to the regional urban centre, which reduces vehicle mileage per capita. The higher number of people or jobs per unit areas reduces the vehicle ownership, etc. He mentions that actual impacts will vary depending on specific conditions and combinations of applied factors.

Similar argumentation about the relation between transportation and land use can be found in Jacobson [3] who states that land use type distribution and transportation system are interdependent. It means that transportation elements have an influence on land structure and land use has an effect on the transportation network shape. This relation is extremely important because—from the point of view of road traffic—it can define our living space especially in cities, where the type of transportation is defined by its location, and the density of population and spatial structure of land use types in the area. For example, the street layout with the funnel type of major traffic arterials causes congestion in major streets and buildings are set far apart by vast parking areas, and wide access roads and that discourages walking among them.

The affects of various land use characteristics on travel activity were analysed in many other publications, e.g. Ristimäki and Kalenoja [4].

The relation between transport and land use has an impact on business analysis, especially access management. Banister [5] emphasizes that transportation infrastructure is one of the crucial phenomena of economic development. Transportation is a source of carbon emissions, which are assumed to have an influence on global

climate change. If we want to keep the economy on its trend with the support of transportation, we have to deal with the reduction of energy and emissions in transportation, although this problem is very tough, some small successes have happened.

The trend of the growth of road traffic, which has been increasing, is unsustainable [6]. As a solution, they suggest reducing energy consumption based on a change of travel habits (shorter distances and slower speeds, with a more flexible interpretation of time constraints) with regard to the land use planning. The solution of the low carbon transport system is outlined in Banister et al. [7] so as behavioural options and possible demand reductions.

The link between land use planning and energy consumption can be presented with convincible data in scientific outputs. However, they show how difficult is to determine the relation between land use and the consumption of energy in transportation with regard to social economic powers. Regression analysis shows that variable values of urban forms can contribute to change transportation energy consumption by 10 %. Therefore the knowledge of the consequential benefits (e.g. of energy saving or quality improvement of the environment) is needed.

Some other authors focus on this topic from the point of view of commuting. Ma, Banister [8] deal with commuting and its efficiency linked to the urban form. They take into account excess-commuting (additional journey-to-work travel represented by the difference between the actual average commute and the smallest possible average commute, given the spatial configuration of workplaces and residential sites). Another type of analysis is an analysis of urban expansion by the gradient analysis of multi-temporal data and influence of road traffic [9].

Smart Growth is a current analysis looking for decisions in smart planning, where the fact how land use plans will affect road traffic intensity is known. The analysis includes an integration of different land uses in closer proximity by promoting higher densities with a mixture of land uses, revitalization of cities, protection of sensitive or classic environments (e.g. farm, open space), etc. It can be shown as an example of locating houses, shops and offices in their common neighbourhood. This approach improves access for residents and employees and allows lowering of road traffic intensity. This is a typical scale of New Urbanism [3].

To successful solve this problem, cooperation between many branches must be analysed (economics, planning, technological innovations, etc.) [3, 5]. Jacobson [3] highlighted the cooperation between local and county governments.

3 Data

3.1 Spatial Data

The data which were used in the project were spatial and non-spatial. The spatial data had two different sources. One of them were the statistical data of the Czech Office of Survey, Mapping and Cadastre (COSMOC). The data are regularly

(yearly) updated from land use of all parcels in the Czech Republic. The data determine forest areas, water areas, agriculture areas, built-up areas and courtyards, and other areas and barren soil in administrative city areas—indicators A, B, C, D, E, I in Table 1. Administrative city areas are entire city areas of individual cities in individual years. They were used in all cities in 1995, 2000 and 2005, in some of them also in 1970, 1980 and 1990. List of indicators used only in 2 time periods column in Table 3 shows cities with 1995 and 2000 data only.

A core city area is an administrative area of a given city at the end of 1970s. The first half of the 1980s was the first period when some villages neighbouring of cities became parts of these cities, the second half of the 1980s was the second period. Their land enlarged original administrative areas of these cities. Original city areas (before joining) were separated from these villages by agricultural or forested areas. They did not have a common historical development. It was the reason why the authors analysed the dependence of the road intensity also on land use of core areas of cities. All land use areas (residential, productive, traffic, recreational and other areas) in core city areas were processed by an image analysis and interpretation. These land use areas were derived from city plans (vector data) and aerial orthophotos and satellite images (raster data). City plans represent the actual state of land use of cities and plans for their future. However, their list of land use classes is more detailed—specifying detailed classes of all land use classes. These detailed classes were merged into the above-mentioned five land use = functional classes. The real state was verified and/or corrected using both types of remote sensing data for all cities in GIS. Orthophoto data were provided by COSMOC. Landsat data of the appropriate years were the satellite remote sensing data downloaded from http://glovis.usgs.gov. GIS vector data of land use/functional classes were a source of spatial data—indicators F, G, H, I, J, K in Table 1. The functional class areas can be dated by the remote sensing data measurement. Time difference between analysed years (1970, 1980, 1990, 2000, and 2005) and the remote sensing data were less than 3 years.

3.2 Non-spatial Data

Non-spatial statistical data (population data) are from the Czech Statistical Office web site (www.czso.cz). They are updated at least once per year. These are L, M, N, O, and P indicators in Table 1.

Road traffic intensity data are collected and archived since 1968 by the Road and Motorway Directorate and are from 1973, 1980, 1990, 1995, 2000, and 2005. The Directorate measures a number of passing vehicles in selected points in 24 h. These points ((determined by their Identification numbers and geographical coordinates) are located on important roads of various classes in the entire country—both in, and out of urban areas. We defined average road traffic intensity for the analysis. The average road traffic intensity is a sum of the measured intensities in all points of one city divided by the number of measured points. This value allowed us to compare

cities with unequal number of points where road traffic intensities were measured. The number of points varied from 3 to more than 60. Indicators Q and R were provided by the Faculty of Economy.

3.3 List of Used Indicators for Correlation

18 types of indicators were used for the correlation. Table 1 shows a complete list of all indicators (in the first column) and number of cities where the indicator was used (second column). They were not complete for all analysed years in all cities. Correlation coefficients were calculated from all available values of each indicator of individual cities.

4 Method

4.1 Correlation Analysis

The analysis of urban development and road traffic in many cities was performed by the statistical processing. Correlation analysis was used as a basic tool and correlation coefficients were evaluated for all cities.

The correlation analysis was evaluated for a correlation coefficient CCAI between an average road traffic intensity and particular statistic indicators. The average road traffic intensity is a sum of all measured road traffic intensities (number of vehicles passing through the location in 24 h) in individual cities divided by number of locations where the measurement was performed.

The correlation coefficient equation

$$CCAI(x,y) = \frac{\sum(x - x_{av}).\sum(y - y_{av})}{\sqrt{\sum(x - x_{av})^2.\sum(y - y_{av})^2}} \quad (1)$$

was used to find dependence between indicators in Table 1 road traffic intensity as the most important source of pollution in urban areas in most cities of the Czech Republic.

The correlation coefficient CCAI as a single value for each city shows how strong the linear dependency between traffic intensity and the particular indicator is. This correlation coefficient was determined for three periods: 1970–2005, 1970–1990, and 1995–2005 in Microsoft Excel ("corel" function). Values of the correlation coefficient were divided into five classes (Table 2):

For a better assessment of each type of a motor vehicles, the "unit vehicle" (UV) variable was developed. This variable is defined by: $UV = 2 * T + O + 0.5 * M$, where T is the number of trucks, O is the number of cars and M is the number of motorcycles [10].

Table 2 Dependency type distribution

Dependency	Absolute value of correlation coefficient
Very strong	0.800–1.000
Strong	0.600–0.799
Inconclusive	0.400–0.599
Weak	0.200–0.399
Very weak	0.000–0.199

All correlation coefficients cannot be determined for each city since the data were insufficient for some cities [11]. For correlation analysis, it is case the result of the correlation coefficient has two values only: −1 or +1 [11], but this cannot reflect the true intensity of dependency, but only its orientation (direct/indirect correlation). In Table 4, there is a list of cities where the CCAI was not computed from all indicators. The correlation coefficient was computed from all indicators for Olomouc, Liberec, Hradec Králové, Ústí nad Labem, Pardubice, Zlín, Kladno, and Chomutov. The correlation coefficients were not computed for Prague (Fig. 1).

The correlation coefficient shows if the development of one variable depends strongly (high correlation) on the development of the other. We have received values for 17 indicators in 36 cities in 3 time spans with the above-mentioned missing values of indicators (Table 3). To make an overall evaluation for all cities, we decided to compare individual time spans individually for all indicators and individual indicators among themselves in these individual periods.

Due to the lack of certain data in several periods and cities, two approaches to evaluate correlations of all cities were used.

The first approach uses a procedure of weighted sum. Six extreme values of correlation (3 positive and 3 negative) are chosen for each city. Each of the three values of each indicator is weighted by values 1–3 (min. to max.—positive and negative). The most important indicators are selected by the sum of these values.

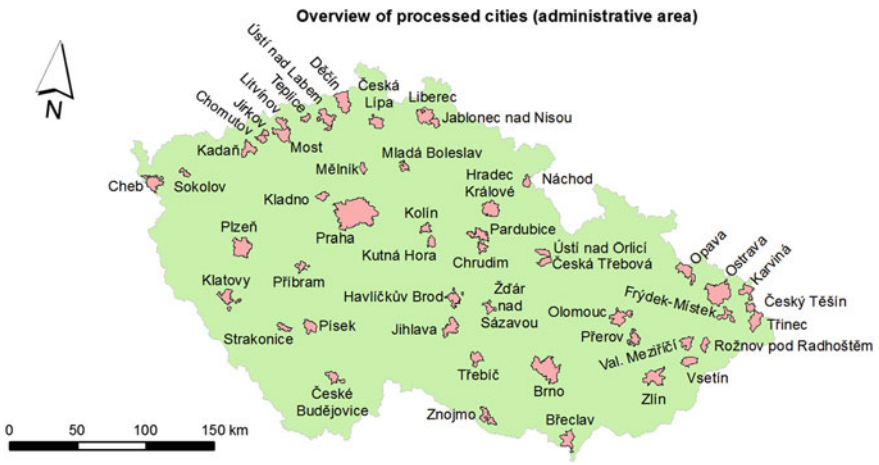

Fig. 1 Administrative areas of processed cities in the Czech Republic

Table 3 List of used indicators for each city

City	List of indicators which were used	List of indicators used only in 2 periods	List of indicators which cannot be used
Brno	A, B, C, D, E, G, L, M, N, O, P, Q, R		F, H, I, J, K
Ostrava	F, H, I, J, K, L, M, N, O, P, Q, R	A, B, C, D, E, G	
Plzeň	A, B, C, D, E, F, G, H, I, J, K, L, M, N, O, Q, R	P	
Most	A, B, C, D, E, F, G, H, I, J, K, L, N	M	O, P, Q, R
Karviná	A, B, C, D, E, F, G, H, I, K, L, N		J, M, O, P, Q, R
Frýdek-Místek	A, B, C, D, E, F, G, H, I, K, L, N, O		J, M, P, Q, R
Opava	A, B, C, D, E, G, I, L, N	M	F, H, J, K, O, P, Q, R
Děčín	F, H, I, J, K, L, N	A, B, C, D, E, G, M	O, P, Q, R
Teplice	A, B, C, D, E, F, G, H, I, J, K, L, N	M	O, P, Q, R
Jihlava	A, B, C, D, E, F, G, H, I, J, K, L, N	M	O, P, Q, R
Přerov	F, H, I, J, K, L, N	A, C, D, E, G	B, M, O, P, Q, R
Jablonec nad Nisou	F, H, I, J, K, L, N, O, Q, R	A, B, D, E, G	C, M, P
Mladá Boleslav	A, B, C, D, E, F, G, H, I, J, K, L, N		M, O, P, Q, R
Třebíč	A, B, C, D, E, F, G, I, J, K, L, N	H	M, O, P, Q, R
Česká Lípa		A, B, C, D, E, G, L, N	F, H, I, J, K, M, O, P, Q, R
Znojmo	A, B, C, D, E, F, G, H, I, J, K, L, N, O, P, R	Q	M
Příbram	F, H, I, J, K, L, N, O, P, Q, R	A, B, D, E, G	C, M
Cheb	F, H, I, J, K, L, M, N, O, Q, R	A, C, D, E, G, P	B
Kolín	A, B, C, D, E, F, G, H, I, J, K, L, N, O, P, Q, R		M
Písek	F, H, I, J, K, L, N	A, B, C, D, E, G	M, O, P, Q, R
Vsetín	F, H, I, J, L, N	A, B, C, D, E, G	K, M, O, P, Q, R
Valašské Meziříčí	A, B, E, F, G, H, I, J, K, L, N		C, D, M, O, P, Q, R
Litvínov	A, B, C, D, E, F, G, H, I, J, L, N	M	K, O, P, Q, R
Český Těšín	F, H, I, J, K, L, N	A, B, C, D, E, G	M, O, P, Q, R

(continued)

Table 3 (continued)

City	List of indicators which were used	List of indicators used only in 2 periods	List of indicators which cannot be used
Břeclav		A, B, C, E, L, N	D, F, G, H, I, J, K, M, O, P, Q, R
Sokolov	A, B, C, D, E, F, G, H, I, J, K, L, N		M, O, P, Q, R
Havlíčkův Brod	A, B, C, D, E, F, G, H, I, J, K, L, N		M, O, P, Q, R
Žďár nad Sázavou	A, B, C, D, E, F, G, H, I, J, K, L, N, O, P, Q, R		M
Chrudim	A, D, E, F, G, H, I, J, K, L, N, O, P, Q, R		B, C, M
Strakonice	A, B, D, E, F, G, H, I, J, K, L, N		C, M, O, P, Q, R
Klatovy	A, B, C, D, E, F, G, H, I, J, K, L, M, N, O, Q, R	P	
Kutná Hora	A, B, C, D, E, G, H, I, J, L, N, O, P, Q, R		F, K, M
Jirkov	L, N		A, B, C, D, E, F, G, H, I, J, K, M, O, P, Q, R
Náchod	A, B, C, D, E, F, G, H, I, J, K, L, N, O, P, R		Q, M
Mělník	A, B, C, D, E, F, G, H, I, J, K, L, N, O, P, Q, R		M
Kadaň	F, H, I, J, K, L, N		A, B, C, D, E, G, M, O, P, Q, R
Rožnov pod Radhoštěm	A, D, E, F, G, H, I, J, L, N		B, C, K, M, O, P, Q, R
Česká Třebová	F, H, I, J, K, L, N	A, B, D, E, G	C, M, O, P, Q, R
Ústí nad Orlicí	F, H, I, J, K, L, N	A, B, C, E, G	D, M, O, P, Q, R

The second approach uses a sum of all correlation coefficient values in cities where all indicators were known. This was done by 3 ways:

- sum of absolute values of the correlation coefficient
- sum of positive values of the correlation coefficient
- sum of negative values of the correlation coefficient.

Sum of absolute values shows which indicators have the highest influence on the road traffic intensity regardless their sign. Low values prove a low correlation both positive, and negative. Sums of positive/negative correlation coefficients of all cities of individual indicators in one time span present which indicator has the highest

positive/negative influence to the road traffic intensity in that span. The final calculation of the average values of correlation coefficients (one value for one indicator of all cities unlike the sums mentioned above) was used to show what the dependence of road traffic intensity in all cities to indicators as one value for each indicator. This value does not show variability of individual cities as it smoothens them out by averaging.

4.2 Multiple Linear Regression

Multiple linear regression (MLR) is a multivariate statistical technique. It was performed on software called SPSS (Statistical Package for the Social Sciences). SPSS is a computer program used for statistical analysis and further for survey authoring and deployment, data mining, text analytics, and collaboration and deployment. MLR can model the linear relationship between a dependent variable and more than one explanatory (independent) variable. The mathematical formula applied to the explanatory variables to best explain or predict the dependent variable is the following:

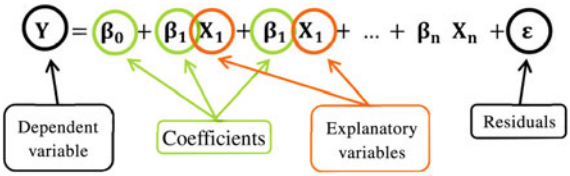

A dependent variable (ARTI) is the variable representing the process which should be predicted or understood. Explanatory variables (attributes of population, land use, etc.) are the variables used to model or to predict the dependent variable values. The dependent variable is a function of the explanatory variables. Regression coefficients are values, one for each explanatory variable, that represent the strength and the type of the relationship the explanatory variable has to the dependent variable [12]. There are a few main assumptions of a regression analysis.

1. Independent variables should not be highly intercorrelated (the assumption of the absence of multicollinearity). Multicollinearity leads to an unstable correlation matrix and can produce unreliable regression estimates, significance levels and confidence intervals.
2. There will not be outliers that could distort results.
3. The variables are related in a linear fashion. Since multiple regression is based on Pearson's correlation coefficient, which is only sensitive to linear relationships, gross departures from linearity will mean that important relationships will remain undetected.
4. The variables are normally distributed [13].

In order to prevent the multicollinearity, values of explanatory variables were modified by creating an interaction variable (e.g. Population density).

This method was used to analyse not only the data by a different tool, but to also analyse different development due to the political and therefore economical regime. The political change was in 1989. The analyses were done separately for the 1970–1990, 1995–2005, and 2000–2005. Comparison of individual time spans shows if the political change in 1989 has had an influence on the dependence between road traffic and all indicators. The new political regime changed ownership from the state one to a private one of many industrial non-industrial objects, changed a system of planning, etc.

5 Results

5.1 Correlation Analysis

The data with the strongest influence to the road traffic development in the cities were determined from CCAI. From the point of view of frequency of extreme values (positive and negative) of indicators, indicator N (Population growth) was a parameter with the highest negative correlation for 50 % of the analysed cities. Indicator K (Other areas of land use in the core area) was a parameter with the highest positive correlation in 16 % of the analysed cities.

The first approach of the analysis uses a procedure of weighted sum. Six extreme values of correlation (3 positive and 3 negative) are chosen for each city where each of the three values of each indicator is weighted by values 1–3. The most important indicators are selected by the sum of these values. By this approach, the highest sum of the weighs has N indicator (population growth), which is followed by I indicator (Residential area in the core area) and R indicator (Dust emissions from large sources). The highest sum of the positive weigh has I indicator (Residential area in the core area). The highest sum of the negative weighs has N indicator (Population growth).

The second approach uses a sum of correlation coefficient, and sum of negative values of the correlation coefficient.

This approach takes into account all values, so the indicators with lower contributions to the final value are also included. This approach is figured in the charts below.

It is shown (Fig. 2) that R indicator (Dust emissions from large sources) has the highest absolute value of the CCAI correlation coefficient from all processed cities for which all indicators was known in more than two time spans. These values show that Dust emissions (R indicator) and Residential area in the core city area (I indicator) have the highest influence on road traffic intensity, however, their influence can be both negative and positive (see Figs. 3 and 4).

Figure 3 presents the Residential area in the core area (indicator I) to have the highest direct influence to the average road traffic intensity. The positive influence does not occur in all cities.

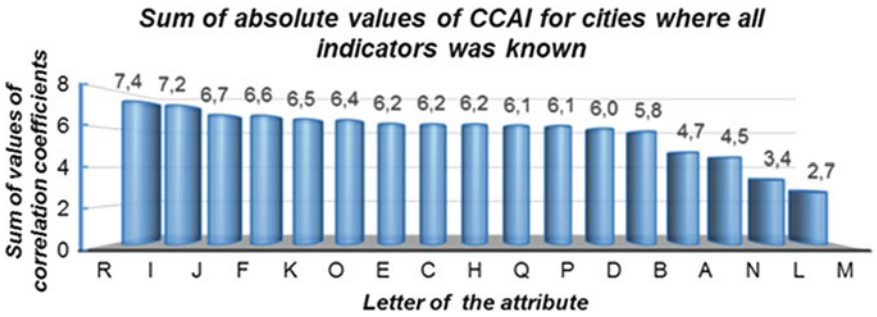

Fig. 2 Chart of sum of absolute values of CCAI

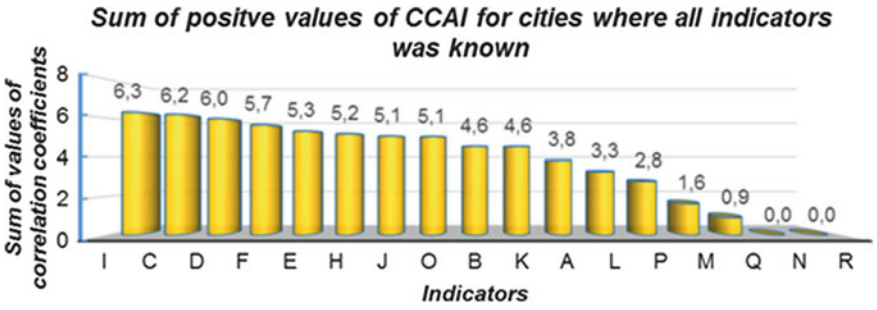

Fig. 3 Chart of sum of positive values of CCAI

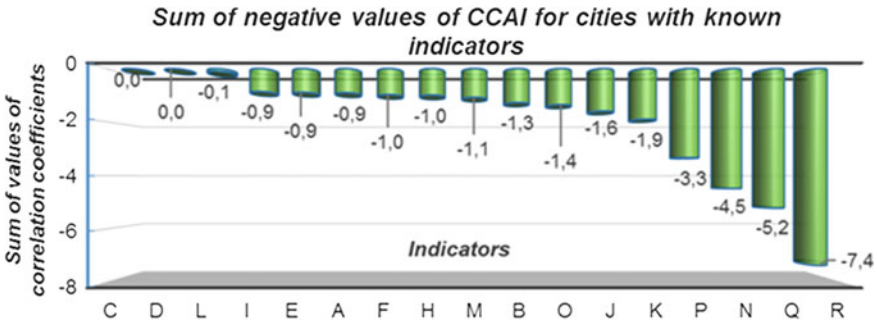

Fig. 4 Chart of sum of negative values of CCAI

The indicator R (Dust emissions from large sources) has the highest negative sum (Fig. 4) and the lowest positive sum (Fig. 3) since this indicator has negative correlation coefficient for each city in this analysis. Therefore this indicator can be proclaimed as an indirect correlation indicator. What is interesting, is that indicator L (Population of the city) with one of the lowest negative sum is only in the middle of positive sum has also a low positive sum.

Average values of the absolute correlation coefficient values were also processed but unlike the above charts from all processed cities. It ensues from Fig. 4 that the highest average CCAI has F indicator (Traffic areas in the core area). This result was expected since it is obvious that traffic areas have a strong impact on traffic development.

5.2 Multiple Linear Regression Analysis

Results of the multiple linear regression are in Table 4 where ARTI is average road traffic intensity. It was the tool, which showed us differences among individual time spans.

Table 4 Multiple regression models explaining average road traffic intensity

Year	R_a^2[%]	Items (sum) type of attributes	Explaining variable
Models explaining the ARTI			
1970	15.3	25(25) *P* + *E* + *L*	Population
1980	47.4	23(25) *P* + *E* + *L*	Population Recreational areas
1990	53.6	23(25) *P* + *E* + *L*	Population Recreational areas
1995	80.4	18(25) *P*	Population aged 0–14 Immigrants
2000	47.3	25(25) *P*	Population Population aged 0–14
2005	60.4	25(25) *P*	Population Population aged 0–14
Opposite contribution			
2005	99.1	10(25) *P* + *L*	Population Population aged 0–14 Female residents Total population growth Traffic areas
1970–1980–1990	49.0	67(75) *P* + *E* + *L*	Population Births Economically act. population Recreational areas
1995–2000–2005	60.3	68(75) *P*	Population Population aged 0–14
2000–2005	94.2	15(75) *P* + *L*	Population Population aged 0–14 Total population growth Traffic areas

P Population, *E* Economic situation, *L* Land use

6 Conclusion

This analysis showed the impact of particular indicators on the average road traffic intensity. It is a step to the next analysis, where some of the indicators (for example E, A, Q) can be analysed deeper. It means the analysis of cities regarding the comparison of particular indicators from the point of view of their influence. It should answer the question, what is the difference among cities which makes the indicators influence differently.

Indicator R (Dust emissions from large sources) has the highest absolute influence (Fig. 2) and it is in the middle of average values of CCAI (Fig. 5). It is interesting that indicator Q (CO_2 emissions from large sources), N (Population growth) and R (Dust emissions from large sources) are the most important indirect indicators having only negative correlation values. Indicator F (Traffic areas in the core area) was the most important indicator in the table of average CCAI. The credibility of this indicator is emphasized, because this indicator was monitored in 36 cities (Table 1) (even in all 49 cities analysed in the project). A negative result of this indicator was only in Chomutov (a transit city).The second most important indicator is Q (CO_2 emissions from large sources). This indicator belongs to a group with a lower positive sum of CCAI and a higher negative sum of CCAI. It seems to be an un-expected result. However, traffic is a significant source of CO_2 emissions. This can be shown in all big cities not only in the Czech Republic; road traffic intensity is a great source of CO_2 emissions in centres of these cities. Therefore it is obvious that the road traffic in core city areas has a strong influence to the overall volume of CO_2 emissions.

On the other side, one of the lowest value indicator among all categories is the Population of the city (L). There are four cities (Děčín, Chomutov, Mělník a Litvínov) with the lowest correlation coefficient in this indicator which is—in the absolute value—lower than 0.1. The prevailing part of their traffic is created by transit, which affects resulting average value of CCAI There are two indicators, which have no negative correlation coefficient value in 8 cities processed in this

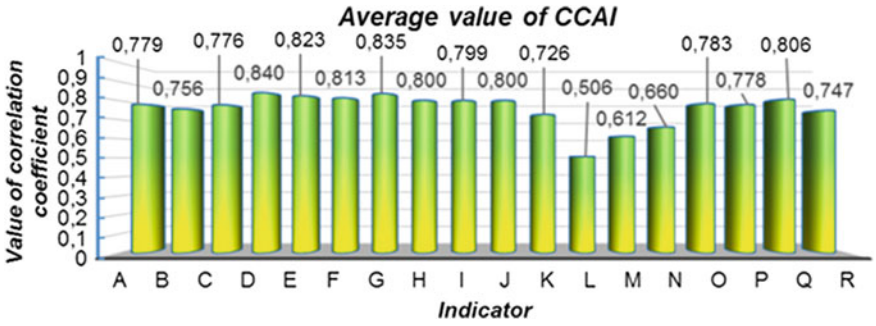

Fig. 5 Chart of average values of CCAI (from absolute value of CCAI)

analysis—C (The area of water bodies in the administrative city area) and D (Built-up areas and courtyards in the administrative city area).

Results of MLR taking into account the more detailed data about population proved a high complexity of the dependence and ambiguity of results from two different evaluations. They highlighted influence of population data and suppressed spatial data showing significant influence of recreational and traffic areas differently in three analysed periods.

This part of the project confirmed the results published already in Halounová [14] that urban development and its impact on the road traffic (analysed here as average road traffic intensity in cities) of individual cities substantially differs among cities. The difference was found in unequal value of correlation coefficients of individual indicators of individual cities. It was found that each indicator has both direct and indirect impact in the whole group of cities. These correlation coefficients proved that the functional classes and their areas describing residential areas in core city areas, traffic and productive areas have the strongest direct impact to the road traffic intensity from the whole group view. It was also determined by other authors (see Chap. 2).

All indicators used can be derived or found for all cities at least in the several previous years. Results of this part of the project showed that prediction of the impact of the future development of a city on road traffic intensity should be analysed rather from the historical development of the last 25 years than from the a model made from many cities. The analysis should take into account not only spatial indicators, but also the number of inhabitants, economically active population, and number of inhabitants commuting to work.

The future work will be focused on spatial distribution, fractionalisation, road network density, GDP, etc., in the cities. These phenomena were not taken into account in this phase of the research.

References

1. Vepřek K (2009) Metodika hodnocení efektivnosti rozvoje silniční sítě z hlediska urbanizace/ Methodology of evaluation of affectivity of the road traffic development from the urbanisation point of view (in Czech only). Prague
2. Litman TA, Steele R (2013) How land use factors affect travel behaviour. Land use impacts on transport, Transport Policy Institute. Available via DIALOG. http://www.vtpi.org/landtravel.pdf. Accessed 18 Oct 2013
3. Jacobson E (2003) The transportation-land use connection. Transportation and Growth Management, School of Urban Studies and Planning, College of Urban and Public Affairs, Portland State University, Portland
4. Ristimäki M, Kalenoja H (2011) Travel-related zones of urban form in urban and peri-urban areas. In: Track 11, 3rd world planning school congress, Perth
5. Banister D (2011) Cities, mobility and climate change. J Transp Geogr 19:1538–1546
6. Banister D (2011) The trilogy of distance, speed and time. J Transp Geogr 19:950–959
7. Banister D, Anderton K, Bonilla D, Givoni M, Schwanen T (2011) Transportation and the environment. Annu Rev Environ Resour 36:247–270

8. Ma KR, Banister D (2007) Urban spatial change and excess commuting. Environ Plann 39:630–646
9. Fan F, Wang Y, Qiu M, Wang Z (2009) Evaluating the temporal and spatial urban expansion patterns of Guangzhou from 1979 to 2003 by remote sensing and GIS methods. Int J Geogr Inf Sci 23(11):1371–1388
10. Stolbenková P (2012) Analysis of various indicator influences in road traffic in GIS (master thesis in English). FCE CTU in Prague, Prague
11. Hornik D (2013) Spatial changes in selected urban areas of the Czech Republic (master thesis in Czech). FCE CTU in Prague, Prague
12. ESRI (2011) ArcGIS help library: regression analysis basics. Available via DIALOG. http://help.arcgis.com/en/arcgisdesktop/10.0/help/index.html#/Regression_analysis_basics/005p00000023000000/
13. de Vauss D (2002) Analysing social science data. Sage, London
14. Halounová L (2013). Relation between road traffic intensity and urban development in cities of the Czech Republic, GIS Ostrava 2013

Time of Day Dependency of Public Transport Accessibility in the Czech Republic

Jiří Horák, Igor Ivan and David Fojtík

Abstract The accessibility evaluation of public transport is based on commuting to work conditions in Czech municipalities. Searching in time schedules are supported by client-server parallel processing. Three indicators are calculated for each municipality, district and region. Their evaluation proves the significant differences between commuting times. It indicates that traditional commuting pattern still persists in time schedules. The analysis of how regional differences in accessibility are changed according to commuting time intervals shows that accessibility for late morning is significantly decreased (compare to early morning) in all districts except of Prague and surrounding districts. The most dramatic drop of accessibility (more than 4 times) is recognised in the central part of the country. The combined evaluation of both-way accessibility for public transport discovers areas with serious restrictions on commuting to afternoon and night work shift using.

Keywords Commuting · Public transport · Time of day · Accessibility

1 Introduction

Accessibility is usually perceived as a relative "nearness" of one place to other places. One of the most complex definitions of accessibility reflects "the extent to which the land-use transport system enables (groups of) individuals or goods to

J. Horák (✉) · I. Ivan
Institute of Geoinformatics, VSB-Technical University of Ostrava, 17. Listopadu 15, 70800 Ostrava, Czech Republic
e-mail: jiri.horak@vsb.cz

I. Ivan
e-mail: igor.ivan@vsb.cz

D. Fojtík
Department of Control Systems and Instrumentation, Faculty of Mechanical Engineering, VSB-Technical University of Ostrava, 17. Listopadu 15, 70800 Ostrava, Czech Republic
e-mail: david.fojtik@vsb.cz

I. Ivan et al. (eds.), *Geoinformatics for Intelligent Transportation*,
Lecture Notes in Geoinformation and Cartography,
DOI 10.1007/978-3-319-11463-7_7

reach activities or destinations by means of a (combination of) transport mode(s)" [1]. Overall, no accessibility measure including all criteria exists [2]. Geurs and Wee [3] identified four basic types of accessibility measures:

1. Infrastructure-based measures are used for evaluation of the performance or service level of transport infrastructure. Measures like "level of congestion" or "average travelling speed on the road network" or "public transport stop accessibility" [4] are frequently utilized in transport planning.
2. Location-based measures are applied for analysing accessibility at locations. Typically the neighbourhood of the locality is searched for relevant objects (i.e. locations of services), connectivity between the evaluated location and each found object is measured and partial results are aggregated. Examples are "total shopping area within 1 km diameter from a residence" or "number of jobs available within 1 h limit of journey from a residence". These measures are preferred in geographical studies or urban planning.
3. Person-based measures evaluate accessibility at the individual level and focus on limitations of individual's freedom of action in the environment in the context of space–time geography [5]. These may include series of locations (visited by the person), duration of mandatory activities in these locations, the time budgets for flexible activities and other conditions like capacity or speed of transport system.
4. Utility-based measures may analyse and evaluate economic benefits that people collect by utilisation of the spatially distributed activities.

The second group summarizes rates of the level of connectivity among given locations.

One of the possibilities to measure the connectivity (location-based measure) is to calculate frequencies of transit connections or vehicles i.e. Cebollada [6]. Such analyses are quite popular—i.e. Hůrský [7], Marada et al. [8] evaluate public transport time schedules for 2000 and 2006 years using weighted frequency of connections. For the urban environment, Križan [9] uses the number of city transport links in Bratislava. Recently, usually the frequency of bus/train arrives for each stop is used [10, 11]. Nevertheless, the frequency measures cannot cover all aspects. Such indicators do not provide any evaluation of requirements or travel costs expressed in time, distance or monetary cost. To measure accessibility level of a locality or to offer well accessible services, it is necessary to track each possible connection, recognise and record its parameters and evaluate the accessibility or connectivity between places by the process of selection and aggregation of possible individual journeys.

Evaluation of location-based measures of accessibility depends on adjustment of parameters of the established transport model. Usually following parameters are required: origin, destination, travel limits (i.e. maximal duration of the journey, maximal distance, maximal number of changes) and also time settings need to be specified (time intervals to start and to finish the journey).

The accessibility evaluation significantly depends on the purpose of commuting [12]. This study is focused on commuting to work, thus according to country-wide

and regional working time conditions the parameters for limiting public transport conditions are set.

Except of the sensitivity to basic parameters setting, typical location-based measures usually suffer from following limitations: they do not take into account individuals' behaviour (perceptions and preferences), no capacity restrictions are applied, no possibility to combine destinations is included and only one-way transport is used for calculation. The last limitation has been discussed by Šeděnková et al. [13] arguing that especially for the 2nd work shift, the number of accessible municipalities is decreased in average by 80 % if a return connection is requested, what reveals the real weaknesses of the public transport system. Also Ivan et al. [14] emphasized the importance of return connection existence after the work shift in evaluations of public transport accessibility. The average decrease of accessible municipalities due to missing return connection is about 50 % for the morning shift and almost 90 % for the afternoon shift.

The accessibility is usually studied according to a transport mode used for a journey. In the Czech Republic (CR) the public transportation still represents a very important mode for commuting. In 2011, 56.9 % of passengers used public transport (11.5 % excluding urban public transport). According to the total passenger transport performance (expressed in passenger-kms) the share of public transport is 39.6 % (25.5 % excluding urban public transport) [15].

Improvement of commuting conditions represents one of the important ways, how to provide better conditions for employees and attract missing labour force [16]. Better understanding of the public transport potential remains essential for improved land use and urban planning, decreasing of social, rural-urban and peripheral-agglomeration disparities, and more efficient utilisation of public budgets.

Even though the understanding of public transit accessibility is important for encouraging mode shifts to reduce car reliance and is essential for the wellbeing of non-car households, still the relatively little research on accessibility using public transit exists [17, 18]. The public transport accessibility in CR is evaluated by i.e. Seidenglanz [19] or Marada and Květoň [20] who are usually focused on rural and peripheral areas documenting their bad transport serviceability. Kraft and Vančura [21] compare conditions of accessibility of Prague by public transport and by car. They discover the more significant variability of time accessibility and average speed is in the case of public transport.

One of the most important issues in choosing a travel mode is the dependency on time of day because the time is more important than distance or monetary costs [22, 23].

The demand for transportation changes during the day. Usually used evaluation is focused on selection of "the best appropriate" time slot (typically morning) and did not take into account other requests arisen during the day. From the practical point of view the bad accessibility in secondary time slots may be serious barriers for commuting to services, for taking a job with more work shifts or for applying flexible working hours.

The aim of the study is to evaluate accessibility across the Czech Republic and assess the dependency on time slots used for commuting by public transport.

2 Methodology

The accessibility evaluation of particular municipality is based on commuting conditions to all other municipalities within 100 km (Euclidean distance) and within CR. The influence of this distance limitation can be specified based on real inter-municipal commuting from 2011 census data. From 935,186 of daily commuters who specified origin and destination of their trips, 98.5 % are commuting within 100 km (Euclidean distance). Remaining 1.5 % commuters indicate usage of regional public transport in 23 % which represents a segment of missing 0.3 % commuters. Nevertheless this segment also includes suspicious answers and potential errors in the census data, thus the remaining part of commuting (above 100 km) can be neglected. It is worth to note that the accessibility evaluation is based mainly on relative territorial and temporal comparisons where the influence of distance limit is eliminated.

The transport connections were searched in valid time schedules of buses and trains using information system of CHAPS Ltd. Each existing transport connection was evaluated and characteristics of all connections matching given conditions were stored to the database (departure time, arrival time, time duration, cost and number of changes).

The time for requesting a public transport connection was limited to several time intervals. Considering more than 28 % (1.11 million) of all employees work in multi-shift operation (forth in the EU28 rank) (more in CSU [24]), commuting for 3 work shifts were tested (1st work shift with 3 possible starting times). In all cases, the latest time of arrival was set to 15 min before the beginning of the shift and similar time interval was applied after the shift is over. Commuting time periods were coupled to assure both appropriate arrival to workplace and not postponed return home after work [16]. The access and egress of public transport has not been evaluated, for more information about influence of door-to-door commuting (see Ivan [4]).

The extent and demandingness of processing requires building a database of public transport connections. A SW application TRAM was developed using client-server technology [25] and parallel processing on a group of computers. The client part consists of approx. 30 computers with special software for connection searching fully utilizing multi-core processors. The process of building the database contains two main phases [25]:

1. searching phase, including massive searching of various possible public transport connections by 700 connections batches,
2. data analyses and recording of transport connection parameters for the optimal commuting variant.

The programme returns several possible connections for commuting matching requested conditions. Each of them is evaluated (multicriteria evaluation including duration, price, distance and departure/arrival fitting) and finally, the most optimal (i.e. not the shortest) variant is chosen.

Table 1 Time intervals for selection and evaluation of public transport possibilities

Start of the work-shift	Earliest departure (BF)	Latest arrival (BF)	Earliest departure (AF)	Latest arrival (AF)
6:00	4:30	5:45	14:15	15:30
8:00	6:30	7:45	16:15	17:30
9:00	7:30	8:45	17:15	18:30
14:00	12:30	13:45	22:15	23:30
22:00	20:30	21:45	6:15	7:30

BF before the work-shift, *AF* after the work-shift

In this study the processing (6,279,563 combinations of municipalities) was performed on 35 computers and the time of processing was about 40 h. Data was processed by Trčka [26].

The conditions of public transportation for commuting were evaluated for each year in the period of 2007–2011 using valid transport timetables for these dates: 23.9.2007, 8.9.2008, 26.9.2009, 14.6.2010, and 5.10.2011. The parameters were set according to the Table 1. The maximum number of connection changes was 5 and the maximal duration was set to 60 min.

The time settings obviously do not cover all commuting possibilities (arrival and departure schedules) but those called "suitable" commuting conditions or connections.

The parameters of the optimal variant for commuting are stored to the database. Finally, data is aggregated and used for the accessibility evaluation. Usually levels of municipalities, districts (LAU1), and regions (NUTS3) are used for analysis.

The transport accessibility was assessed mainly using following indicators:

- The **rate of accessible municipalities** (*RA*), which is defined as the number of accessible municipalities per number of all municipalities tested for existing transport connection (in %) on certain time (*h*) in case of one-way travelling. The best accessible municipality has the highest value of *RA*.

$$RA_{h,i} = \frac{NMA_{h,i}}{NMT_{h,i}} * 100 \quad [\%]$$

  where *NMA* is the number of accessible municipalities, *NMT* is the total number of municipalities within a given Euclidean distance (i.e. 100 km), *h* is hour and *i* is the index of municipality.
- The **rate of missing return connection** (*RMRC*) expresses the existence of a return suitable connection after the work shift to the residential municipality. The best accessible municipality poses the lowest value of *RMRC*. Zero value means that each municipality accessible by one-way connection (under the given conditions) also provides a suitable return connection to residential municipality after the end of the shift.

$$RMRC_{h,i} = \frac{NMAOW_{h,i} - NMATW_{h,i}}{NMAOW_{h,i}} * 100 \quad [\%]$$

where *NMAOW* is the number of accessible municipalities for one-way journey and *NMATW* is the number of accessible municipalities for both-way journey. The best conditions have municipalities with both the high RA and the low RMRC (for the same time interval).

- The **rate of both-way accessible municipalities** (*RBWA*) provides information about the relative number of accessible municipalities for both-way commuting on a certain time (*h*). The zero value highlights municipalities with only one-way commuting possibilities and simultaneously without destinations with a suitable return connection. When no one-way commuting exists, *RBWA* is set to −1 (see formula bellow) and labelled as "no commuting". The best accessible municipality for both-way commuting has the highest value of *RBWA*.

$$RBWA_{h,i} = \begin{cases} -1 & \text{if } \mathrm{RA_{h,i}} = 0 \\ \frac{\mathrm{RA_{h,i}} * (100 - \mathrm{RMRC_{h,i}})}{100} & \text{if } \mathrm{RA_{h,i}} > 0 \end{cases}$$

Indicators calculated for each municipality have been aggregated to higher geographical units, successively districts (LAU1), regions (NUTS3) and country (NUTS0).

3 Public Transport Accessibility in 2011

The average rate of accessible municipalities is 0.44 % in CR, thus only approx. a half percent of all municipalities within 100 km (Euclidean distance) is available by public transport under the given conditions (see methodology). The value of *RA* oscillates between 0.64 % (interval 4:30–5:45 or 6:30–7:45) and 0.14 % (interval 20:30–21:45) (Table 2). While the rate of accessible municipalities is almost the same for early morning intervals, it is dramatically decreased to 46 % of the previous value only 1 h later. Then the indicator reaches 74 % of the maximal RA

Table 2 Number (*NA*) and rate (*RA*) of accessible municipalities in the Czech Republic according to commuting time intervals

Time interval	RA	$RA_{relative}$ (%)	RA > 1 % (%)	$RA_{relative}$ > 1 % (%)	NA	NA > 10 (%)	$NA_{relative}$ > 10 (%)
4:30–5:45	0.64	100	1,561	100	2,697	43	100
6:30–7:45	0.64	100	1,513	100	2,521	40	100
7:30–8:45	0.30	46	545	35	1,161	19	44
12:30–13:45	0.47	74	944	61	1,968	32	75
20:30–21:45	0.14	26	148	10	444	7	17

in the lunch time (commuting to second shift). For commuting to 3rd work shift commuting, the value goes down again and represents only 26 % of the maximal value. These changes generally demonstrate the significant differences between accessibilities measured for different time intervals during a day.

If a certain limit is adopted to define well accessible residential municipalities, i. e., those with 1 % as minimal level of accessible municipalities (within 100 km) in the given time interval, even stronger differences in results are revealed (Fig. 1). The average accessibility for time interval 7:30–8:45 is only 35 % of the accessibility for the early morning time interval. RA for time interval 12:30–13:45 is about 61 % and only 10 % for time interval 20:30–21:45.

The level of accessibility can be specified also in absolute values as the number of accessible municipalities within 100 km (*NA*). Obviously, this indicator provides more concrete insight into the number of potential destinations and choices for commuting. Nevertheless there are also serious drawbacks, mainly variable size of municipalities and the edge effect near national border [16].

The distribution of municipalities according to the number of accessible destinations on specified time intervals is depicted in Table 2 and Fig. 2. Early morning (C6, C8) and afternoon (C14) time intervals are characterized by similar results, while results for late morning (C9) and late evening (C22) intervals reveal much worse values. From all 6,252 municipalities, there are about 1,000 without commuting possibility for commuting at 4:30–5:45 and 6:30–7:45, about 1,400 at 12:30–13:45, but about 2,900 at 7:30–8:45 (almost three times more than 1 h before) and almost 4,000 at 20:30–21:45. Based on these results, 6, 8, or 14 o'clock

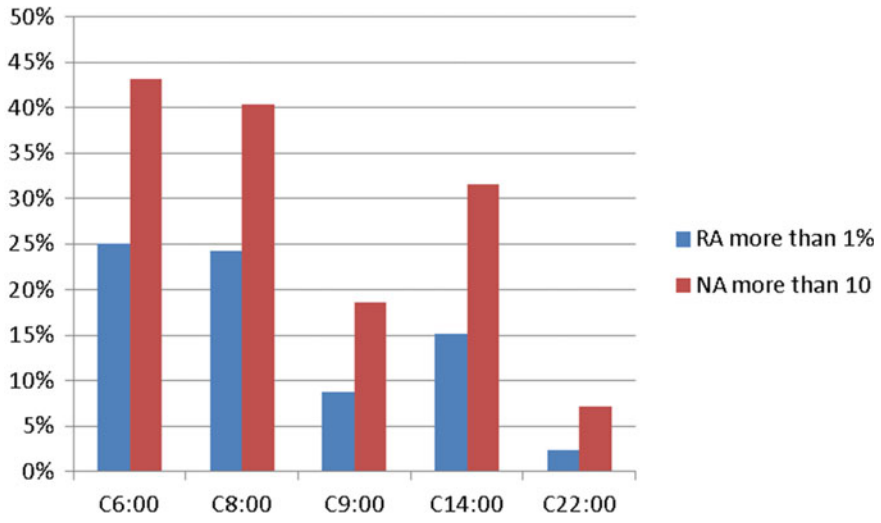

Fig. 1 The share of well accessible municipalities (above limits in *RA* and *NA*) according to the time of day

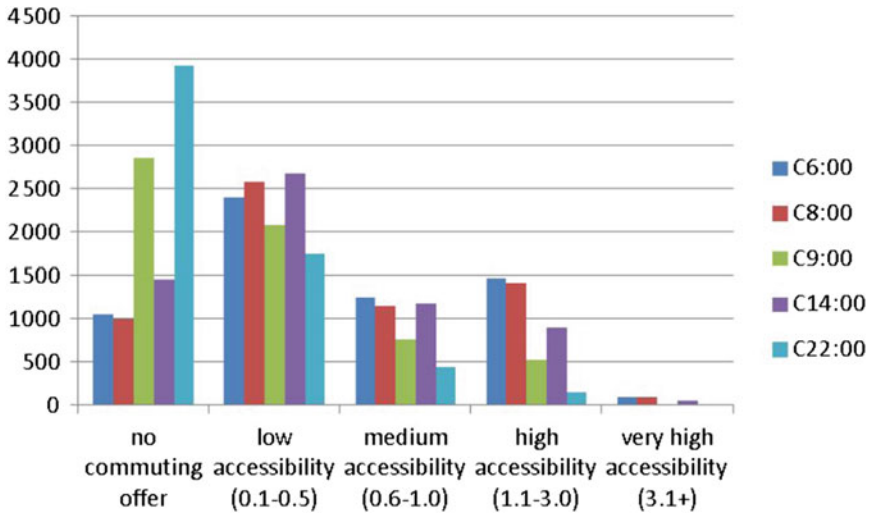

Fig. 2 Number of Czech municipalities in 5 categories of accessibility according to time of day

can be considered as suitable hours for commuting by public transport, while 9 and 22 o'clock are handicapped hours.

Commuters can travel to more than 10 municipalities from 43 % of municipalities if they commute at 6 o'clock, accordingly from 40 % of municipalities at 8 o'clock, from 19 % at 9 o'clock, from 32 % at 14 o'clock, and only from 7 % for night shift commuting. This data can be recalculated to relative comparison where the base is the average of 6 and 8 o'clock commuting. These relative results are quite close to the results of average accessibility to all municipalities (except of decreased value for 22 o'clock, see Table 2).

Results indicate the persistence of traditional commuting pattern in time schedules (mainly travel to the work early in the morning), additionally also the dependency of public transport accessibility evaluation on time dimension and finally a case of public transport obstacles in supporting flexible working hours or part-time jobs.

Further, **regional differences** have been analysed.

The average rate of accessible municipalities for districts (LAU1) for time intervals 4:30–5:45 and 20:30–21:45 are portrayed in Fig. 3. The results for early morning interval show specific trends, mainly relatively high level of accessibility in eastern districts and in the three largest cities (Prague, Brno, Ostrava—AB, BM, OV). Districts with lower accessibility are clustered in the central Bohemia close to Prague what may be caused by dominant position of Prague with lower accessibility level of smaller municipalities in surroundings (many of them can be classified as Prague's suburbia). The pattern of evening accessibility proves lower accessibility in almost all districts except of the three largest cities and several districts close to borders (eastern Moravia and two isolated districts in the NW part). The geographical distribution of

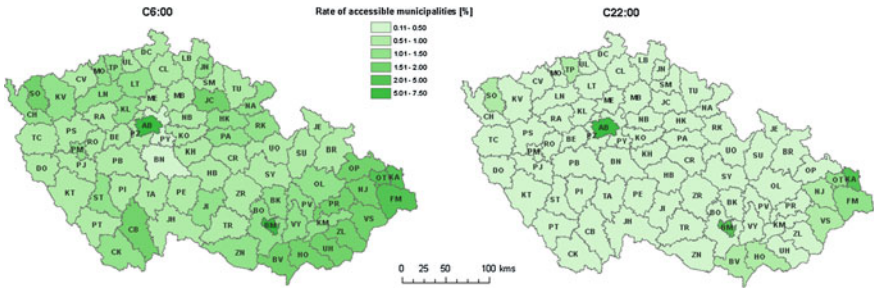

Fig. 3 Average rate of accessible municipalities (*RA*) aggregated to level of Czech districts (LAU1) at 4:30–5:45 (*left*) and 20:30–21:45 (*right*)

regions with better accessibility for night-shift commuting corresponds to regions with higher levels of employers with multi-shift operation (mostly NW, NE and central areas).

Figure 4 depicts the changes of the rate of accessible municipalities (*RA*) from early morning to late morning and to evening. For commuting at 9 o'clock, only three regions indicate an increase of accessibility—Prague and surrounding districts (AB, PZ, PY) what may correspond to later starts of working hours. Very low changes in accessibility are evident in Brno and its surrounding (BM, BO) and surprisingly also in Karlovy Vary district (KV). Small decrease of accessibility (about 10–30 %) is found in the NE part of the CR (Moravian-Silesian region), partially in the SE part of the CR, western border regions and central Bohemia. Vice versa, a central part of the CR (near regional borders of Vysočina, South Moravia, South Bohemia and Pardubice region) shows a substantial drop of the accessibility level (RA_9 is more than 4 times smaller than RA_6). Results for commuting at 22 o'clock provide generally similar spatial pattern—shrinkage of well serviced areas around Prague (AB) and Brno (BM), persisting better situation around Ostrava (OV) and overall substantial decreasing of accessibility in almost all other districts.

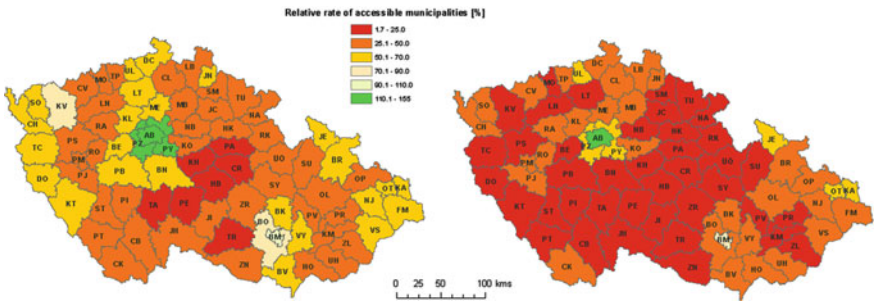

Fig. 4 Relative rate of accessible municipalities aggregated to level of Czech districts (LAU1) for time interval 7:30–8:45 (*left*) and for the time interval 20:30–21:45 (*right*) related to the results for time interval 4:30–5:45 (in %)

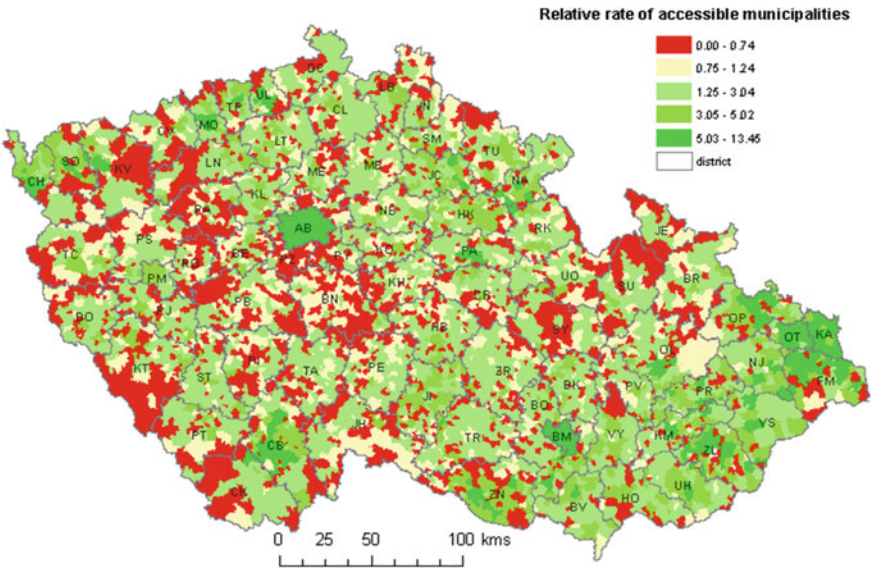

Fig. 5 Relative rate of accessible municipalities (compare to the average of the CR) for time interval 4:30–5:45

To avoid the ecological fallacy, the situation for particular municipalities is depicted in Fig. 5. These results show a high variability. The number of accessible municipalities is normalized to the average of the CR. Municipalities in the last interval (red colour) are below 75 % of the national average and members of top three intervals (green) are about more than 25 % above the average. The general trend that has been discovered for the district level is confirmed on municipal level and areas of higher accessibility in eastern parts of the country contain a few isolated municipalities with below-average accessibility. Municipalities with the lowest accessibility are concentrated in mountain areas (peripheral parts in Bohemia), in central Bohemia (BN, PB, RO, RA) and in some other isolated smaller areas.

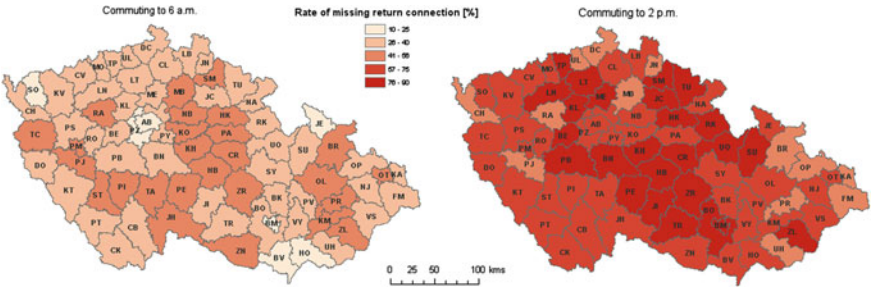

Fig. 6 Average rate of missing return connection in municipalities aggregated to level of Czech districts (LAU1) for time interval 4:30–5:45 (*left*) and 12:30–13:45 (*right*)

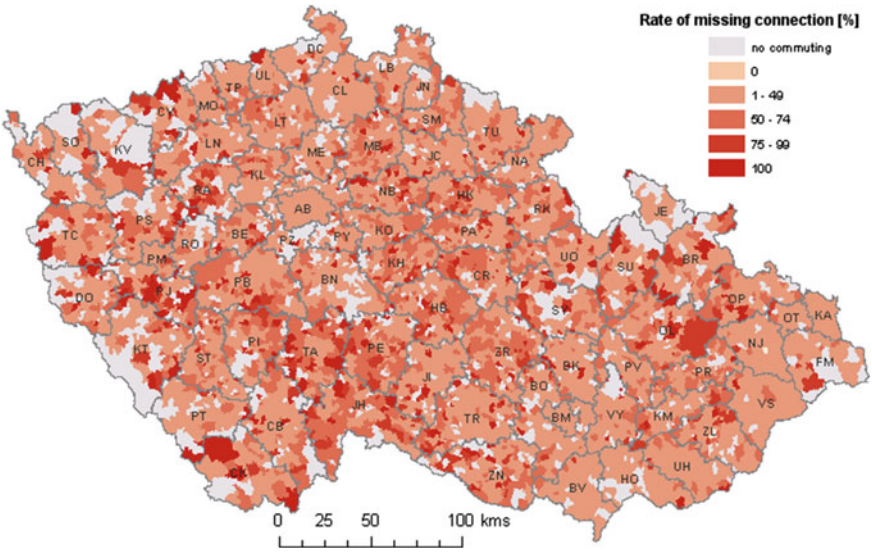

Fig. 7 Rate of missing return connection in municipalities for time interval 4:30–5:45

Concerning **the rate of missing return connection**, the situation is much better for the morning hours than during the afternoon (what is caused by bad public transport conditions for return journey after 22:15). For the 1st work shift starting at 6 o'clock, the best situation is in Prague and Brno, followed by several other isolated districts. To the opposite the worst situation for return journeys after the 1st work shift is in the ring of districts around central Bohemia, mainly close to the border between Bohemia and Moravia (JH, PE, HB, ZR, CR), the belt in central Moravia (ZL, KM, PR, OL, BR), surprisingly also 3rd and 4th largest cities Ostrava (OT) and Plzen (PM), and several others (Fig. 6).

The situation within particular districts is usually not homogeneous (see Fig. 7). Often even neighbouring municipalities are largely different in the availability of return connection.

The rate of missing return connection for the 2nd work shift is much more problematic. The average rate is almost 2 times worse than early in the morning, but the regional differences are not so strong. Most of districts have more than half municipalities without suitable returning connections. The worst situation is again in the centre part of the CR (mainly the Vysočina region, districts as HB, ZR, TR, JI, PE etc.), Brno and some parts of NE and NW Bohemia (Fig. 6).

It is worth to note that any interpretation must take into account that good conditions of return connection existence are also assigned to areas with a very low one-way connectivity (a very low number of accessible municipalities results in higher probability of return connection existence and thus also significantly lower rate of missing return connection). That is why a combined evaluation of both-way accessibility has been adopted.

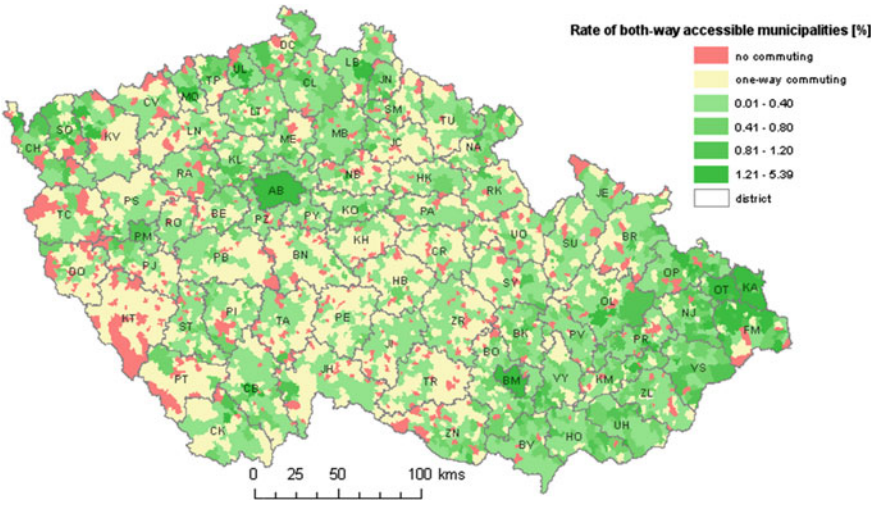

Fig. 8 Rate of both-way accessible municipalities for commuting to 2nd work shift

The **combined evaluation of both-way accessibility** is based on the rate of both-way accessible municipalities (see Methodology) (Fig. 8).

The combined evaluation of public transport accessibility for the 3rd work shift (Fig. 9) shows only several municipalities without any return connection, what is a logical result of low rate of missing return connection for this time. Many municipalities have no possibility to commute (even in one-way) but the remaining

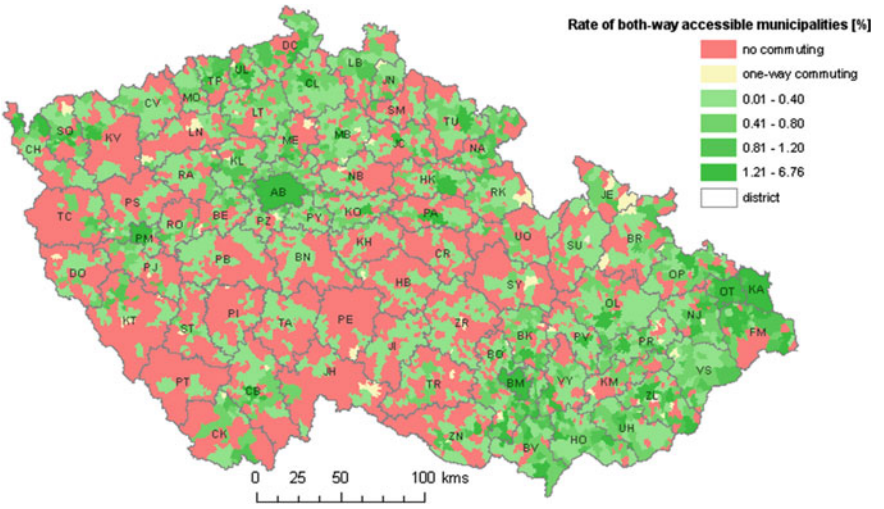

Fig. 9 Rate of both-way accessible municipalities for commuting to 3rd work shift

municipalities show relatively good both-way accessibility. The best conditions are around largest cities, nevertheless important differences in the size of such agglomerations exist—the largest accessible agglomeration is around Ostrava (OT, KA, NJ, FM, OP, VS), in S-E Moravia (BV, HO, UH), partially also in central Moravia (PR). To the opposite, the Plzeň agglomeration (PM, 4th largest city) is quite small with a diameter similar to the significantly less populated Trutnov agglomeration (TU).

4 Development of Accessibility

The development of accessibility has been evaluated using both main indicators—*RA* and *RMRC*—aggregated for the regional (NUTS3) level.

Concerning *RA* (Fig. 10) Prague (red line) shows unique development comparing to other regions. This difference is getting stronger suggesting that improvements of Prague's accessibility are more rapid than in other regions. Since 2009 besides Prague two eastern regions (Moravian-Silesian and Zlin regions) are getting separated in accessibility from the others (approx. 50–100 % more than other regions except of Prague).

According to the rate of both-way accessible municipalities, the best situation is again in Prague and also here the situation has been getting better since 2009. The other regions demonstrate only small changes (significant decrease of accessibility was indicated in Ústí region between 2007 and 2008 what is explained by the exchange of regional public transport operator). Higher changes in the both-way

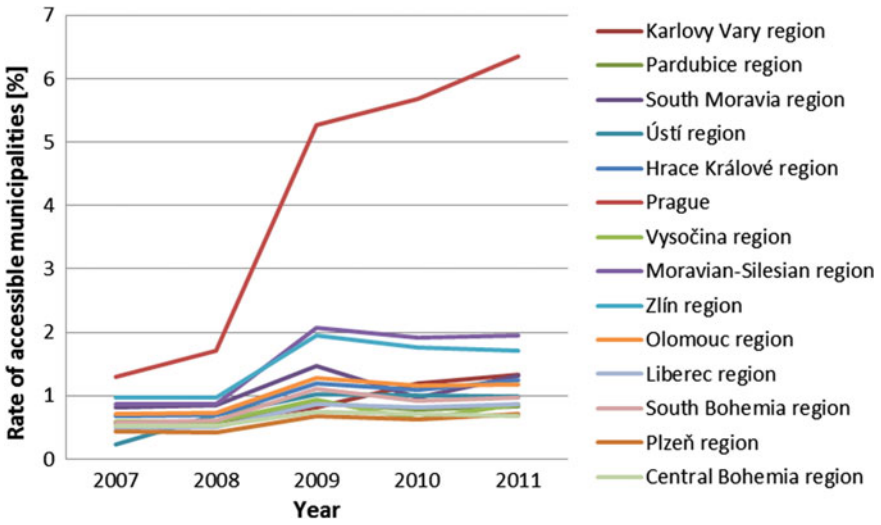

Fig. 10 The development of the rate of accessible municipalities for commuting at the interval 4:30–5:45 between 2007 and 2011 in Czech NUTS3 regions (modified from [26])

accessibility level were recorded in 2010, when a temporary increase of return connections was discovered in some regions. Similar development was recognised also in other time intervals except of commuting to 3rd work shift where the accessibility was significantly decreased in the Moravia-Silesian region and in the central Moravia part, nevertheless their accessibility is still on a good level comparing to other parts of the country.

5 Conclusion

The accessibility evaluation for public transport is based on commuting to work conditions in Czech municipalities.

The transport connections are searched in valid time schedules of buses and trains. The client-server architecture is adopted and client part consists of dozens of computers equipped with SW application TRAM. Parallel processing using multi-core processors effectively process more than 6 million of combinations for commuting between municipalities. The commuting time for connection search is limited to several selected time intervals. Commuting for three work shifts is tested (1st work shift with 3 possible starting times). Also possibility of suitable return journey (from work place to residence) is taken into account.

Three indicators are used for the analysis. The rate of accessible municipalities is defined as the ratio between the number of accessible municipalities and the number of all municipalities tested for commuting at certain time in case of one-way travelling. The rate of missing return connection expresses the chance of suitable return after the work shift back to the residential municipality. The rate of both-way accessible municipalities provides information about the relative number of accessible municipalities for both-way commuting at a certain time. Indicators are calculated for each municipality and then aggregated to districts (LAU1) or regions (NUTS3).

The evaluation results prove the significant differences between analysed time slots used for commuting. Rates of accessible municipalities for the Czech Republic is almost the same for two early morning intervals, while 1 h later the rate is dramatically decreased to 46 % of the previous value. In the lunch time the indicator rises again. Its value for evening hours falls down to 26 % of the morning value.

It indicates, the traditional commuting pattern (go to the work early in the morning) still persists in time schedules and flexible working hours or part-time jobs are still not adequately supported by public transport operators.

The analysis of regional differences in accessibility changes according commuting times shows that in all districts the accessibility for late morning is decreased (compare to early morning) except of Prague and surrounding districts. The most dramatic drop of accessibility (more than 4 times) is recognised in the central part of the country (border parts for Vysočina, South Moravia, South Bohemia and Pardubice regions).

The combined evaluation of both-way accessibility discovers areas (i.e. Klatovy district) where almost no municipality has a possibility for suitable both-way commuting for the 2nd work shift. It may be a serious problem for some occupations (mainly in service sector such as shop assistants). As expected, better conditions for 3rd work shift are around big cities, nevertheless important differences in the size of such agglomerations exist. The largest accessible agglomeration is around Ostrava and in the SE Moravia, while the Plzeň agglomeration (4th largest city) remains quite small.

The development of accessibility in 5 years (2007–2011) in the Czech NUTS3 regions indicates the divergent situation of Prague, the Moravian-Silesian and Zlin regions compared to quite stable worse situation in other regions.

Acknowledgments The data and the transport searching engine are provided by courtesy of CHAPS Ltd. Application has been developed as a part of Higher Education Development Fund—FRVŠ 956/2013/B1.

References

1. Geurs KT, Ritsema van Eck JR (2001) Accessibility measures: review and applications. RIVM Report 408505 006. National Institute of Public Health and the Environment
2. Vanderbulcke G, Steenberghen T, Thomas I (2009) Mapping accessibility in Belgium: a tool for land-use and transport planning? J Transp Geogr 17(1):39–53
3. Geurs K, Wee B (2004) Accessibility evaluation of land-use and transport strategies: review and research directions. J Transp Geogr 12(2):127–140
4. Ivan I (2010) Docházka na zastávku a její vliv na dojížďku do zaměstnání. Geografie 115 (4):393–412. ISSN:1212-0014
5. Hagerstrand T (1970) What about people in regional science? People Reg Sci Assoc 24 (1):7–21
6. Cebollada A (2009) Mobility and labour market exclusion in the Barcelona metropolitan region. J Transp Geogr 17(3):226–233
7. Hůrský J (1978) Regionalizace České socialistické republiky na základě spádu osobní dopravy. Studia Geographica, Geografický ústav ČSAV, Brno, p 182
8. Marada M, Květoň V, Vondráčková P (2010) Doprava a geografická organizace společnosti v Česku. Česká geografická společnost, Geographica. Praha, p 165
9. Križan F (2007) Regionálna typológia územia Bratislavy na základe dostupnosti supermarketov a hypermarketov. Geografický časopis 59(4):373–385
10. Currie G (2010) Quantifying spatial gaps in public transport supply based on social needs. J Transp Geogr 18:31–41
11. Yigitcanlar T, Sipe N, Evans R, Pitot M (2007) A GIS-based land use and public transport accessibility indexing model. Aust Plan 44(3):30–37
12. Goodchild MF, Jannele DG (2004) Spatially integrated social science. Oxford University Press, Oxford, p 456. ISBN:0-19-515270-0
13. Šeděnková M, Horák J, Ivan I, Fojtík D (2009) Hodnocení rozdílů při sledování dojížďky do zaměstnání jedním či oběma směry. In: Proc. Sympozium GIS Ostrava 2009, Ostrava, p 13
14. Ivan I, Horák J, Šeděnková M (2009) Public transport accessibility in the Czech Republic. In: Proceedings of ERSA congress, Lodz, Poland, p 18, 25–29 Aug 2009
15. Transport Yearbook (2011) Ministry of transportation, Prague. https://www.sydos.cz/cs/rocenka_pdf/Rocenka_dopravy_2011.pdf

16. Horák J, Šeděnková M, Horáková B (2008) Public transport accessibility based on time schedule analyses. In: Svatoňová H et al Geography in Czechia and Slovakia. Theory and practice at the onset of 21st Century. Brno, p 500. ISBN:978-80-210-4600-9
17. Mavoa S, Witten K, McCreanor T, O'Sullivan D (2012) GIS based destination accessibility via public transit and walking in Auckland, New Zealand. J Transport Geogr 20(1):15–22
18. Jánošíková Ľ, Kubáni A (2000) Dopravná dostupnosť obcí. Komunikácie 2(4):9–15. ISSN:1335-4205
19. Seidenglanz D (2007) Dopravní charakteristiky venkovského prostoru. Katedra Regionální geografie a regionálního rozvoje PřF Masarykovy univerzity v Brně, Disertační práce. Brno, p 196
20. Marada M, Květoň V (2006) Význam dopravní obslužnosti v rozvoji venkovských oblastí. In Proceedings of the conference "Venkov je náš svět". Czech Agriculture University Prague, pp 422–431
21. Kraft S, Vančura M (2008) Regionální vyhodnocení efektivity dopravního systému České republiky a jeho prostorových dopadů. XI. Mezinárodní kolokvium o regionálních vědách. KRES, ESF, Brno, pp 252–260. ISBN:978-80-210-4625-2
22. Salon D (2009) Neighborhoods, cars, and commuting in New York City: a discrete choice approach. Transport Res A Pol 43(2):180–196
23. Lei TL, Church RL (2010) Mapping transit-based access: integrating GIS, routes and schedules. Int J Geogr Inf Sci 24:283–304
24. CSU (2013) Analýza: Ženy pracují na směny stejně často jako muži, p 6. http://www.czso.cz/csu/csu.nsf/informace/czam110413analyza13.doc
25. Fojtík D, Horák J, Šeděnková M, Ivan I (2009) Software support for automatic creating database of public transport connections. In: Proceedings of international Carpathian control conference ICCC 2009, Zakopane, Poland, pp. 517–520, 24–27 May 2009. ISBN:8389772-51-5
26. Trčka J (2013) Vývoj dopravní obslužnosti v ČR ve vybraném období. Diploma thesis, VSB-TU Ostrava

Automatic Generation of 3D Building Models from Point Clouds

Vojtěch Hron and Lena Halounová

Abstract Point cloud is a product of laser scanning (terrestrial/airborne) or it can be derived from automatic image matching. Both techniques are very modern and progressive methods of non-selective collection of spatial data. The representation of buildings through point cloud is not appropriate for many applications. Handling with a set of data points, covering large areas is also very hardware consuming. For these reasons, it is suitable to represent individual buildings as spatial objects, called 3D models. This paper is a review of fully automatic generation of 3D building models from point clouds. It compares the solutions of various academic institutes and analyzes current commercial software products that process this task. In this work, data point clouds collected by airborne laser scanning will be used as an input. A major influence on the generation of 3D building models have the density and quality of the point cloud, which are determined by scanning parameters. For this reason, various input datasets will be tested.

Keywords 3D building models · Point clouds · Airborne laser scanning · LiDAR

1 Introduction

Spatial data are very popular and in demand nowadays. Due to its great popularity, this data type and high requirements for the accuracy and topicality lead to their more frequent acquisition. The acquired data have a great information potential. Manual interpretation of spatial information is in fact extremely time consuming and it is impossible to repeat it with the same result due to the human factor. Fully

V. Hron (✉) · L. Halounová
Faculty of Civil Engineering, Department of Geomatics, Czech Technical University in Prague, Thákurova 7, 166 29 Prague 6, Czech Republic
e-mail: vojtech.hron@fsv.cvut.cz

L. Halounová
e-mail: lena.halounova@fsv.cvut.cz

I. Ivan et al. (eds.), *Geoinformatics for Intelligent Transportation*,
Lecture Notes in Geoinformation and Cartography,
DOI 10.1007/978-3-319-11463-7_8

automatic methods of processing are used with increasing amounts of data that must be processed in shorter time periods. Current automatic techniques are still under development and can only partially exploit the potential of the data. The real potential of the data is usually unused. This issue is therefore a challenge for experts from a wide range of disciplines like remote sensing, photogrammetry or computer vision.

The most common form of spatial elevation data is a point cloud which can be obtained by active sensors like airborne laser scanning (ALS) systems which use the Light Detection and Ranging (LiDAR) principle. The spatial data can be also derived by image matching techniques using satellite or aerial images. Point cloud data represent the surface geometry by an object independent distribution of points with uniform quality, however, this form of representation is not appropriate for many applications. For more sophisticated tasks, a generalization and simplification of the digital surface model (DSM) is necessary. The generation of 3D building models is just such the case. The fields of application of 3D building models are quite various such as visualizations, urban planning, environmental monitoring (for example air pollution, propagation of road traffic noise etc.), propagation of electromagnetic waves for telecommunication applications and the generation of flood maps.

Image matching techniques are very popular and progressive methods nowadays, however, they are extremely dependent on the quality of input aerial images. Ground sampling distances (GSD) and overlaps between images have a major impact on the acquisition of high quality outputs. Most of the presented results were typically achieved by high quality input datasets with large forward and side overlaps between images and GSD under 10 cm. Data with these specifications can be collected relatively easily from small areas, but it seems that it will not be economic to collect such data for large areas for entire countries. This paper gives a review of the possibility of fully automatic generation of 3D building models from point clouds covering large areas. For this reason, point clouds collected only by airborne laser scanning will be used as input data in this paper.

2 Related Work

The first important task in 3D building reconstruction is the identification of points describing the buildings. These points represent mainly building roofs and their parts in case they were collected from the air. The second important task is the segmentation and conversion of these roof parts into geometrically and topologically correct building models. These tasks are really challenging and most scientific papers solve this problem using other external sources of information like maps or even better ground plans. Building ground plans can be obtained from digital cadastral maps or GIS layers containing building footprints. This information can rapidly help for building reconstructions as no sophisticated algorithms must be used for the classification of raw point cloud [1]. The buildings are reconstructed on

the position of their footprints and the shape of these footprints can be used for the exact determination of the buildings outer walls. The roof planes can be detected by using ground plan lines. The assumption is that the normal direction of roof planes is usually perpendicular to one of the ground plane lines [2–4]. The shape of the building outline can be used for a decomposition of a building as a combination of simple roof elements [5–7].

The combination of different data sources is a great idea for solving complex tasks. Many countries have digital cadastral maps and it is therefore possible to use ground plans for 3D city modelling. Unfortunately, additional data sources like digital ground plans are not available for every country. Supporting data can be also outdated in relation to the time of acquisition of elevation data or can come from untrusted sources. The use of maps is also problematic. The positions of buildings are known with some uncertainties due to map inaccuracy and generalization. These uncertainties are not higher than 0.5 m [8], however, they strongly depend on the quality and scale of the maps. The original form of the maps (digital or paper) is also important.

Using ground plans can be often quite complicated. Ground plans are based on cadastral maps that register only the outer walls. A large number of buildings have different shapes of their ground plans and roof footprints. Modern houses have typically large roof overhangs over the outer walls. It is illustratively presented in Fig. 1.

This problem is solved by the Czech Land Survey Office. The Czech Republic has an old cadastral map, which contains many errors as a result of many decades of a continuous operation. Most users want consistent and especially actual data sets. Now there is an effort to fix these errors using point clouds acquired by ALS for the new altimetry mapping. Automatic detection of buildings can be also used for updating and revision of the cadastral map and other derived products. Manual validation of millions of buildings is not feasible from the perspective of the whole country. It is also necessary to use a very sophisticated full-automatic solution which is independent on other sources.

Fig. 1 *Left* Orthoimage of two buildings with roof overhangs (*green line*) over the outer walls (*cyan line*). *Right* Oblique image of the same buildings taken from the east

In one approach, which is explained in detail [9], a robust algorithm for the autonomous reconstruction of buildings from sparse LiDAR data was used. No prior knowledge and supplementary sources were needed in this paper. The classification of the point cloud into terrain and off-terrain points was done by a filtering process that uses global functions in the form of orthogonal polynomials. The iteration process was based on a fitted function that passes between laser points. In the subsequent iterations, the degree of the polynomial was decreased. The reduction of the polygon degree was done in accordance with an evaluation of the residuals. The assumption was that terrain points have negative residuals and off-terrain points have positive residuals. The final result was reached when the iteration did not change the shape of the terrain, so only the terrain points influenced the polynomial [10]. Separated areas of off-terrain points were then filtered by size and height above the ground. Filtered points that created planes as roof parts were further grouped into segments and classified in unique roof faces. Between roof faces, topological relations were identified and from this information, an adjacency graph was created which was very useful for the determination of roof types. The crease edges between the roof faces were computed by the plane intersection. Boundaries of buildings were derived from their roof edges that were detected using the Hough Transformation. It was an approximate solution with lines that were geometrically incorrect, they were not parallel and rectangular. Extracted lines were also fixed using an adjustment with specific weights for roof edges according to their classification into three classes: horizontal crease edges, non-horizontal crease edges and border lines. The adjustment was not a destructive operation so it had no influence on topology. The generation of buildings was completed after the adjustment of their bounding lines.

This solution [9] is much more sophisticated than the one that is described in Haala and Brenner [1], where the shapes of buildings were determined by a segmentation of DSM in the raster form and a subsequent extraction of planar regions. The planar range image segmentation algorithm [11] was used because it was fast, essentially simple and scored very well if compared to other algorithms [12]. The algorithm is based on the segmentation of a regular DSM grid into straight 3D line segments which are used as a starting position for the region growing process. The main advantage of this algorithm is that it requires no *a priori* knowledge. However, the algorithm has a problem with the precise extraction of region boundaries. The author solved this problem by using ground plans. The problem was bypassed instead of being solved.

The following part of the text is dedicated to an analysis of commercial software, which is designed for the automatic generation of 3D building models.

3 Methodology and Data

The automatic generation of 3D building models will be tested in ENVI LiDAR (more detailed in [13]). Other commercial products are INPHO Building Generator, tridicon CityModeller and tridicon BuildingFinder. INPHO Building Generator and

tridicon CityModeller allow the generation of 3D building models from point clouds and building footprints. Tridicon BuildingFinder generates building footprints and 3D buildings only from oriented aerial images. These software products have not yet been tested.

4 ENVI LiDAR

ENVI LiDAR (E3De in the past, further only the software) comes from Exelis VIS (Visual Information Solutions) that focuses on the development of software products for analysis and visualization of geo-information. A trial version of the software (version 3.2, January 2013) was obtained from the company ARCDATA PRAHA s.r.o., which is a distributor of Exelis VIS products for the Czech Republic.

The software is designed for automatic processing and interactive control of ALS data (Fig. 2). The result of processing is a classification of raw point cloud into several classes (terrain, buildings, trees, power lines and poles). Classified data can be used for the creation of elevation models (DTM and DSM) and 3D models of buildings and vegetation that can be exported and used in other software products.

Input data can be in binary format LAS (LiDAR/Laser data exchange format) or ASCII. The software enables you to work with the georeferenced data in any projection and geodetic datum. The recommended density of the point cloud is greater than 1–2 points per square meter. The data processing runs completely automatically without the need of human intervention. The setup processing is done in the only dialog window with three tabs.

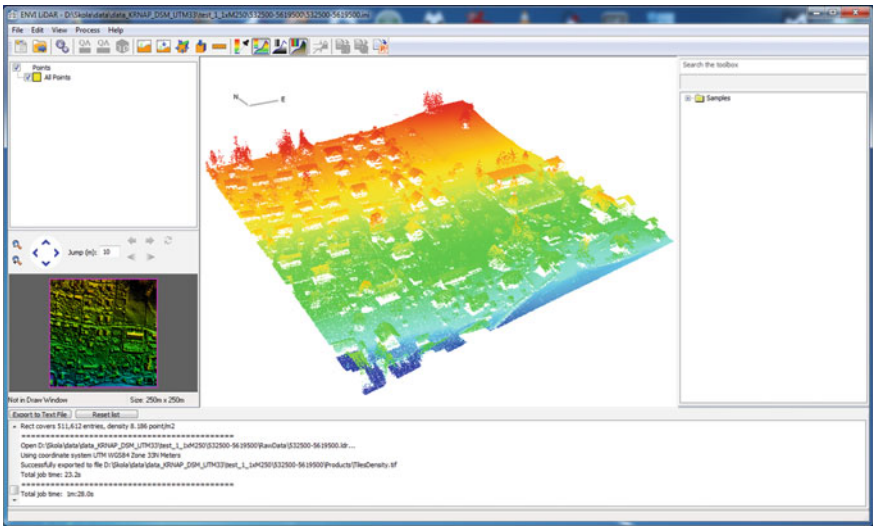

Fig. 2 Interface of the software and visualization of raw point cloud (colour hypsometry, perspective view)

4.1 Input Data Quality

Software testing was performed on three datasets with different densities of point clouds. The first and second dataset covered the identical area (part of the city Rokytnice nad Jizerou) and so their outputs can be compared to each other. Sample dataset attached to the software was a very dense point cloud and thus represents an interesting source suitable for precise modelling.

4.2 Classification of Point Cloud

Figure 3 (top) shows point clouds in the colour hypsometry in relation to the height of the terrain. The colour range is not created from absolute height values, but from relative heights of points above the ground. This type of visualization eliminates the height disparity of the terrain, which gives a better idea about objects on the ground (buildings and vegetation). Classification results are in Fig. 3 (bottom), where each class is displayed in a different colour.

Input datasets were classified into four classes (terrain, buildings, other and unprocessed). Figure 3 shows that the terrain was identified correctly in both datasets, however, it does not apply to the buildings. In the first dataset, almost no buildings were found. This is due to the too sparse point cloud from this dataset. Points representing most of the buildings were classified incorrectly into the class other. The result of the classification of buildings in the second dataset is significantly better. All buildings have been identified. The class other contains only those points that represent vegetation (trees and shrubs) and small objects with low height (outhouses, greenhouses, fences, cars etc.).

The result of the classification of the sparse point cloud from the first dataset is not satisfying. Changes of the recommended setting did not lead to improved results. For this reason, the first dataset is not suitable for building modelling. The next part of the analysis considers only the remaining two datasets in Table 1 (#2 and #3).

The following Fig. 4 shows only a part of the test area. It is approximately the central part of the second dataset. The classification result can be evaluated easily by a visual comparison of the orthoimage [Fig. 4 (left)] and the classified point cloud [Fig. 4 (right)]. A good classification is a prerequisite for the subsequent automatic generation of 3D building models.

4.3 Creation of 3D Building Models

The automatic generation of 3D building models is based on the RANSAC (RANdom SAmple Consensus) method [14]. The principle of this method is to find

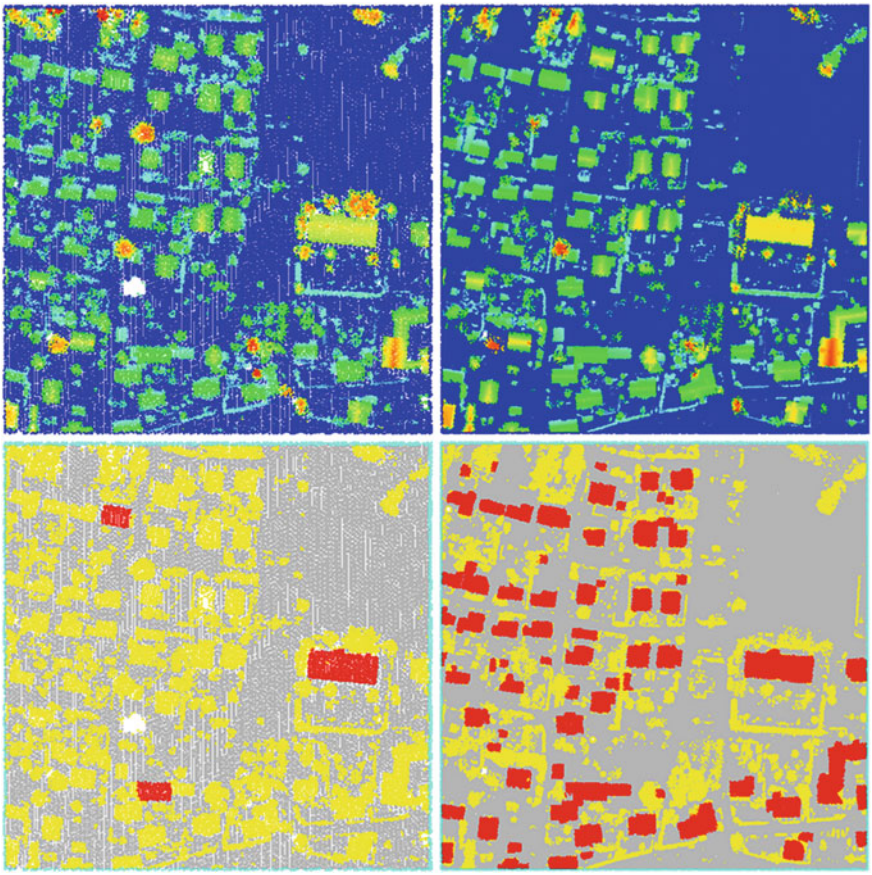

Fig. 3 Datasets: #1—Czech Land Survey Office [*left*] and #2—Krkonoše Mountains National Park [*right*]. *Top* Raw point clouds (colour hypsometry in relation to the height of the terrain). *Bottom* Classified point clouds: terrain (*gray*), buildings (*red*), other (*yellow*), unprocessed (*cyan*)

Table 1 Comparison of input data; #—dataset N^{o}

#	Owner of data	Area	Average density (p/m^2)
1	Czech Land Survey Office	Rokytnice nad Jizerou (Czech Republic)	1.2
2	Krkonoše Mountains National Park	Rokytnice nad Jizerou (Czech Republic)	8.2
3	ENVI LiDAR sample data	Kleinwolkersdorf (Austria)	21.8

geometric primitives by interleaving planes through the point cloud. The software interleaves planes exclusively from the points that were classified into the class buildings. This approach reduces the amount of data that must be analyzed (Fig. 5).

Fig. 4 Detail of the second dataset: orthoimage [*left*] and classified point cloud [*right*]: terrain (*gray*), buildings (*red*) and other (*yellow*)

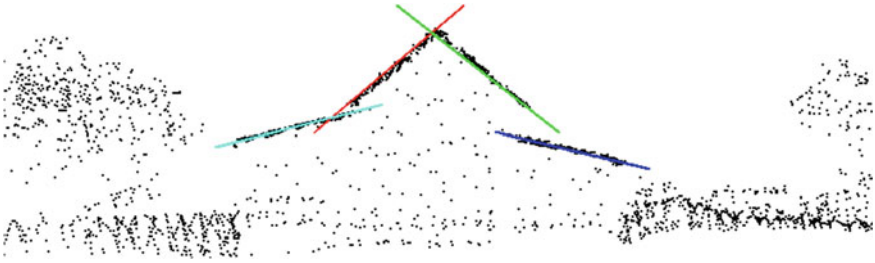

Fig. 5 Profile of the point cloud with interleaved planes through the roof faces

The created 3D models of buildings can be visualized as wire-frame objects or more realistic 3D objects covered by textures. The following figure shows a plan view of the wire-frame models of buildings [Fig. 6 (left)] and 3D view of textured models of the buildings [Fig. 6 (right)].

In the software settings, it is possible to define a desired form of the generated models. The models of buildings can be in the form of models with the real shape of the roofs (LoD 2—Level of Detail 2) or box models (LoD 1—Level of Detail 1) with a choice of the height (the lowest point on the roof, the average height of the roof, and the highest point on the roof).

The quality of the created 3D building models with real shapes of roof (LoD 2) is not ideal. During the detailed inspection of individual buildings, it was discovered that the algorithm does not produce real building models. All buildings are composed of several smaller parts (irregular polyhedrons) that are adjacent or overlap each other. It gives an impression of real building models. Unfortunately, the software does not contain any knowledge base of buildings or roof shapes. For this

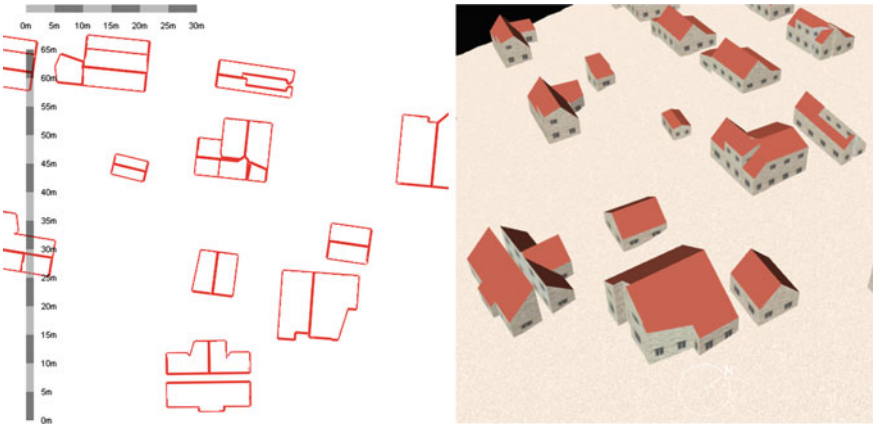

Fig. 6 3D building models in LoD2 created from the second dataset, plan view of the wire-frame models [*left*] and 3D view of the textured models [*right*]

reason, the building models are highly incorrect. Some buildings were split into smaller parts, although the building identification in the point cloud was good (see Fig. 6—building down in the middle).

Figure 7 demonstrates the result that can be achieved by using an extremely dense point cloud. In this case, the third dataset with point cloud density approximately 20 points per square meter was used. Figure 7 [left] shows that the produced building model is composed of seven parts. It is not a single object. The building model is very accurate and does not contain any glaring errors, therefore the result can be regarded as satisfactory.

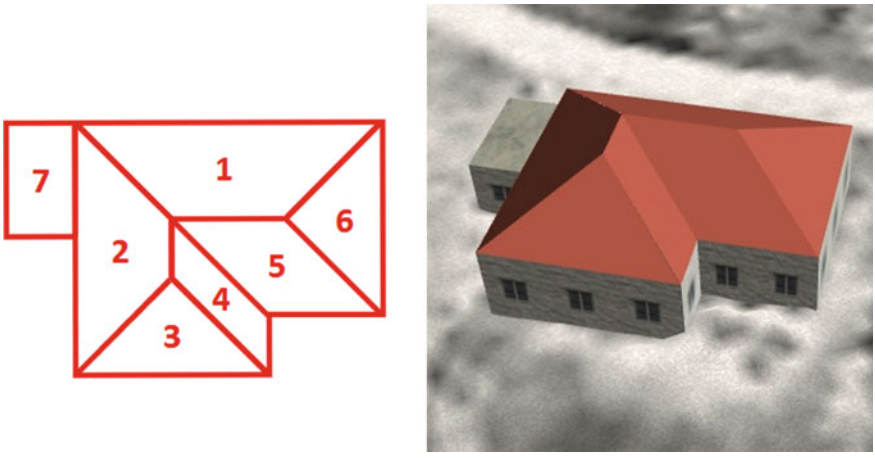

Fig. 7 3D building model in LoD2 created from the third dataset, plan view of the wire-frame model [*left*] and 3D view of the textured model [*right*]

5 Conclusions

The software has a user-friendly graphical interface that is quite intuitive and allows users to view analyzed data in several options. Data processing is very well described in the Help section. The main advantage of this software is the possibility of automatic data processing, which is controlled by user-defined parameters. However, the description of the parameters is not very detailed in the Help of the software. Options are described in general and very tersely in the text. A user does not have sufficient insight into the internal functionality of the software.

The processes of the point cloud classification and modelling of buildings are very robust but they are not too sensitive to changes of optional parameters. This can be considered as an advantage and disadvantage at the same time. The modification of some parameters did not lead to the desired changes in the final result. For this reason, recommended settings were used in most cases. An implemented method analyzes the data locally and without the use of any knowledge base of buildings or roof shapes. The building model is created by a group of smaller parts (irregular polyhedrons). The software does not create real building models, but only groups of spatial primitives.

The main weakness of the software is its necessity to use high-quality input data. Processing of different data sets showed that for achieving high-quality building models, it is necessary to use a very dense point cloud as an input (20 points per square meter and more). Unfortunately, point clouds with this density are not typical. The missing knowledge base of building and roof shapes, and a poor control of the implemented algorithm make the processing of sparse point clouds difficult. Applying a sparse point cloud (up to 10 points per square meter) results in the creation of building models with a lower quality.

At the end of this paper, it should be mentioned that a detailed 3D city model consists of an accurate digital terrain model and high-quality 3D models of buildings and grown vegetation and all objects alongside roads. The data will become a normal part of the visualization of such space to allow designers to enlarge their data sources and geographic data for further processing and modelling. They will enable specialists to control and even improve conditions of the road traffic to be safer and passable. All these spatial data have a great importance for intelligent transportation, therefore they are quite important.

References

1. Haala N, Brenner C (1997) Generation of 3D city models from airborne laser scanning data. In: Proceedings 3rd EARSEL workshop on LIDAR remote sensing on land and sea, Tallinn, Estonia, 17–19 July, pp 105–112
2. Haala N, Anders KH (1997) Acquisition of 3D urban models by analysis of aerial images, digital surface models and existing 2D building information. Integrating photogrammetric techniques with scene analysis and machine vision III, Orlando, FL, United States, 21–23

April. Proceedings of SPIE—the international society for optical engineering, vol 3072, pp 212–222
3. Jibrini H, Paparoditis N, Deseilligny MP, Maitre H (2000) Automatic building reconstruction from very high resolution aerial stereopairs using cadastral ground plans. In: 19th ISPRS congress, Amsterdam, The Netherlands, 16–23 July
4. Vosselman G, Dijkman ST (2001) 3D building model reconstruction from point clouds and ground plans. Int Arch Photogramm Remote Sens Spat Inf Sci 34(Part 3/W4):37–43
5. Haala N, Brenner C, Anders KH (1998) 3D urban GIS from laser altimeter and 2D map data. Int Arch Photogramm Remote Sens 32(Part 3/1):339–346
6. Brenner C (2000) Towards fully automatic generation of city models. 19th ISPRS congress, Amsterdam, The Netherlands, 16–23 July. Int Arch Photogramm Remote Sens 33(Part B3/1):85–92
7. Vosselman G (2002) Fusion of laser scanning data, maps, and aerial photographs for building reconstruction. International geoscience and remote sensing symposium (IGARSS), Toronto, Ont., Canada, 24–28 June, pp 85–88
8. Suveg I, Vosselman G (2000) 3D reconstruction of building models. 19th ISPRS congress, Amsterdam, The Netherlands, 16–23 July. Int Arch Photogramm Remote Sens 33(Part B2):538–545
9. Nizar AA, Filin S, Doytsher Y (2006) Reconstruction of buildings from airborne laser scanning data. Prospecting for geospatial information integration, Reno, NV, United States, 1–5 May. Am Soci Photogramm Remote Sens 2:988–997
10. Akel NA, Zilberstein O, Doytsher Y (2004) A robust method used with orthogonal polynomials and road network for automatic terrain surface extraction from LiDAR data in urban areas. 20th ISPRS congress, Istanbul, Turkey, 12–23 July. Int Arch Photogramm Remote Sens Spat Inf Sci 35(part B3):243–248
11. Jiang X, Bunke H (1994) Fast segmentation of range images into planar regions by scan line grouping. Mach Vis Appl 7(2):115–122
12. Hoover A et al (1996) An experimental comparison of range image segmentation algorithms. IEEE Trans Pattern Anal Mach Intell 18(7):673–689
13. ENVI LiDAR Help (part of the software installation), Exelis visual information solutions. Document version 3.2., c 2012, 2013-06-11
14. Fischler MA, Bolles RC (1981) Random sample consensus: a paradigm for model fitting with applications to image analysis and automated cartography. Commun ACM 24(6):381–395

Towards a Solution for the Public Web-Based GIS Monitoring and Alerting System

Jitka Hübnerová

Abstract This paper deals with the issue of interoperability of heterogeneous sensor systems and the availability of their data from a global perspective. We show the application of previously developed WEDA architecture style into a GIS based experimental system and we present the performance analysis results of the system. The paper also presents its strengths as being a firewall-friendly, web-standards based solution that can be plugged into existing applications without needing to completely rewrite them (which is good when using OGC Sensor Web Enablement services). The paper compares the new style with styles which are used today in OGC Webservices. We then present an alpha version of the experimental system with eventing enhancements that are available with the new style. These principles will be applied from the experimental system to the final draft specification and API after more tests. If such a web-service standard meets the new binding possibilities, alerting will become widely accessible and GIS viewers and sensors can improve user-experience, loading/publishing sensor data or loading pipelined WMS tiles as well.

Keywords Sensor web · Web services · Web sockets · Performance · Complex event processing

1 Introduction

As the amount of sensor data is growing, more people want to see the data from the sensors online via the web. OGC SWE standards [1] enable the web-based discovery, exchange and processing of sensor observations, as well as the tasking of

J. Hübnerová (✉)
Faculty of Mechatronics, Informatics and Interdisciplinary Studies,
Institute of Novel Technologies and Applied Informatics, Technical University of Liberec, Studentská 2, 461 17 Liberec, Czech Republic
e-mail: jitka.hubnerova@tul.cz

I. Ivan et al. (eds.), *Geoinformatics for Intelligent Transportation*,
Lecture Notes in Geoinformation and Cartography,
DOI 10.1007/978-3-319-11463-7_9

sensors systems. SWE is technology to enable the implementation of Sensor Webs. Wildfires, river basins, tsunami alerts, and environmental risk management are just some of the uses of OGC's interoperability framework for web-based access and control of sensors and sensor data. One of the SWE standard's services, the relatively new Sensor Observation Service (SOS, 2008), provides an API (application programming interface) that allows web servers to collect data from subscribed sensors and public to explore their nearly real-time data. The goal of OGC Sensor Web Enablement SOS is to provide access to observations from plug and play sensors and sensor systems in a standard way that is consistent for all sensor systems including remote, in situ, fixed and mobile sensors. SOS standard is based on the REST (SOS 1.0) or SOAP (SOS 2.0) protocols. SOAP/REST protocols are the implementation of web services (and web services are a well-known application of SOA—service oriented architecture). Messages are exchanged using a request–reply pattern and interaction is synchronously initiated by client. The question is *if the standards are prepared today to be as interactive and interconnected to be usable from a global perspective*. Many sensor systems are built at a local level and their read-only data is published on the web. There is a large space for *linking these autonomous systems to the big sensor web and evaluating different event types with some higher automated logic or with preferences defined by each user*. As with other SOAP web services, performance may also become an issue and can negatively impact the user experience. Each request uses a shared HTTP persistent connection over a single TCP connection (in the best case) and waits for its response before another request can proceed. Web browsers open a memory-reasonable number of connections (for example 6 for Chrome) to partly overcome such limitations and developers use AJAX that prevents UI blockage (browser communicates synchronously). But the performance problem and other web service limitations still remains. At the time of writing, SOS standard are becoming known in web mapping software and first implementations exist (for example OpenLayers javascript library provides a very limited functionality for requesting the SOS service). So as we can see, for Sensor Observation Service, the mechanism is publicly available and open, which can overcome its other disadvantages. As for other OpenGIS standards, we think that this specification will become broadly popular in future. However, because of technology limitations, this web service stack cannot be used for real-time monitoring and alerting in particular. In the next few chapters we want to *describe our approach to overcome these limitations and also to present a version of an experimental system that we use to measure its performance parameters and to tune the specification draft*.

In 2003, Gartner introduced [2] a new terminology to describe a design paradigm based on events: Event-Driven Architecture (EDA). EDA [3, 4] defines a methodology for designing and implementing applications and systems in which events are transmitted between decoupled software components and services. Event objects are sent from an event source to the event consumer in asynchronous messages at times determined by the event source. Pushing event objects proactively reduces latency (the time required to respond to an event), compared to waiting for consumers to pull event objects (for example, by repeatedly asking if

any new data is available = polling). EDA had many forms during the years when it was used in local networks and now it is often discussed in relation to SOA and how these two can interact. This can be a very interesting feature when used in a World-Wide-Web environment for many uses and especially for sensor data publication and monitoring problems. Theoretical discipline (without practical application) which tries to combine these architectures is called SOA 2.0 (SOA 2.0 = SOA + EDA). Only local area network (LAN) monitoring and alerting systems are widely used today. One type of their output is sending SMS/e-mail messages to the specified group of users (e.g. crisis team) if some threshold is exceeded. This system is good for crisis team disaster early warning and is built with reliability in mind. *Such systems are not available to the public today*. For the public, another OGC Sensor Web Enablement standard was proposed and named Sensor Alert Service (and a very new Sensor Event Service). These SOA web service specifications have some disadvantages in transport binding which is firewall unfriendly (XMPP protocol for SAS) or requires the consumer to have a public endpoint address (SES). As we know, IPv4 is still the leading specification and not many users own such an address. From a global public monitoring and alerting perspective, these solutions are still weak for the task (and as a result they are not well-known).

The motivation for our work was dealing with performance issues of web services at first. After we built an API and experimental GIS-based system, new opportunities and topology enhancements were discovered. In the first part of the text we introduce some fundamentals of the proposed style to understand the concept and contribute with a comparison of the new concept with the style used today. Next we will describe the experimental system and publish the results of performance analysis. We would like to create another experimental system in future which should show a reduction in the time needed to load WMS tiles from the GIS server by pipelining enhancements of developed API (but that is not topic of this paper). This will show us how pipelining the capabilities of our architecture style can improve the performance of such a very common use. Finally we will describe topology and event processing enhancements which are interesting especially for “GIS on the web” use-cases and can be used for building a publicly available alerting solution (deployable to the cloud SaaS environment). The resulting description will be transformed to the draft specification and API after more tests on the experimental system.

2 Changing Architecture Style

The Weda architectural style is a hybrid architectural style that we have derived from other network-based standards, such as web services [5] and HTML5 websockets [6] to get a practical real-time SOA 2.0 [7] solution for WWW. It provides a uniform connector interface to the client and server implementers allowing them to extend their existing web services (SOAP 1.2, REST, POX) with a new type of

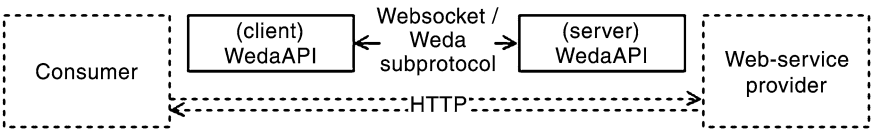

Fig. 1 Blackbox overview of Weda

endpoints and binding while keeping their HTTP server endpoints to legacy clients alongside Weda endpoints (Fig. 1).

New possibilities grew with the arrival of Websockets. Websockets is a technology that provides bi-directional, full duplex communication over a single TCP socket. It is designed to be implemented in web browsers and web servers and traverses firewalls, proxies, and routers seamlessly and leverages Cross-Origin Resource Sharing (CORS). The communication channel can be protected against eaves-dropping with TLS, much like HTTPS. The default ports are 80 or 443, so enterprises are not required to open additional ports in their firewalls.

2.1 Comparison of Web Services Architectural Styles

We can identify three classes of Web services (Table 1):

- REST-compliant Web services, in which the primary purpose of the service is to manipulate XML representations of Web resources using a uniform set of "stateless" operations.
- RPC-compliant Web services, in which the service may expose an arbitrary set of operations.
- WEDA-compliant Web services, in which the service can use asynchronous message passing which can provide us eventing behaviour as well as call and return.

We developed an informal (IANA or RPC based) [8] as well as a formal (timed automata) specification [9], whose purpose is to ensure the interoperability between Weda implementers. The list of topics covered is: Weda gateway, Weda endpoints (also for non-public client endpoints), Addressing, Weda transport binding, Contracts, Weda subprotocol, Weda service description, model checking and verification. All of the components were implemented into the beta version of Weda API. The aim of future development is to provide an easily pluggable library in more programming languages, which has a simple interface but robust and self-contained implementation.

Table 1 Comparison of web services architectural styles

Attribute	WEDA-style	REST-style	RPC-style
Architecture	SOA 2.0	SOA	SOA
Distributed system type	Hybrid (message passing and call/return)	Call/return	Call/return
Addressability	Multiple endpoints per service (clients, server)	Unique URI address per resource	One endpoint per service
Common transport	HTML5 WebSockets	HTTP	HTTP
State	Statefull	Stateless	Stateless
Flow control	Asynchronous	Synchronous	Synchronous (over FW-friendly transport)
Process com. models	One-to-one, one-to-many, many-to-many	One-to-one	One-to-one
Latency	Best (after improving admission and flow control)	Good	Good
Throughput	Extremely high	Bad	Bad
Instance context	Per session	Per call	Per call
Scalability	Best in terms of concurrent clients	Good	Good
Coupling	Loose (only event type definitions in duplex contracts)	Functionally tightly coupled (MIME types in self-descriptive resource representations)	Functionally tightly coupled (operations and data types in contract)
Data interface	Inherited (no restriction)	Generic (e.g. HTTP verbs, MIME)	Service description (e.g. WSDL)
Common data format	Inherited (no restriction)	HTTP resource representation, XML, JSON	SOAP
Deployment topologies	Enterprise service bus	Hub and spoke (centralized)	Hub and spoke (centralized)
Coordination	Esb's native functions for orchestration and choreography, no scheduler	Resource-oriented workflows (theoretical-atom, rss, dynamic hyperlinks in practice)	Service-oriented workflows, scheduler required
Coordination	Esb's native functions for orchestration and choreography, no scheduler	Resource-oriented workflows (theoretical-atom, rss, dynamic hyperlinks in practice)	Service-oriented workflows, scheduler required

3 Experimental System

We have built two experimental "GIS on the web" systems with WEDA API. Experience and data obtained from these experiments were used for calibrating the model. Both experimental systems use the same server-side implementation and only client implementations differ as one was developed as a thick client and the other as a thin client (Fig. 2).

3.1 Server Side

The server side consists of a database layer, data access layer, web-service and server-side Weda API.

- *Database layer*—Sensor data is stored in the spatial database Observations Data Model (ODM). Version 1.1 [10] is a generic template for the observations DB. For example the SpatialReferences table provides specifications of the location of an observation site to record the name and EPSG code of each spatial reference system used. The database was running inside a MSSQL 2008 environment. We used more types of data, for example hydrologic data from CUAHSI-HIS.
- *Data access layer*—Our data access layer provides us mapping of conceptual schema to data schema, isolation from the relational database and database schema and other features.

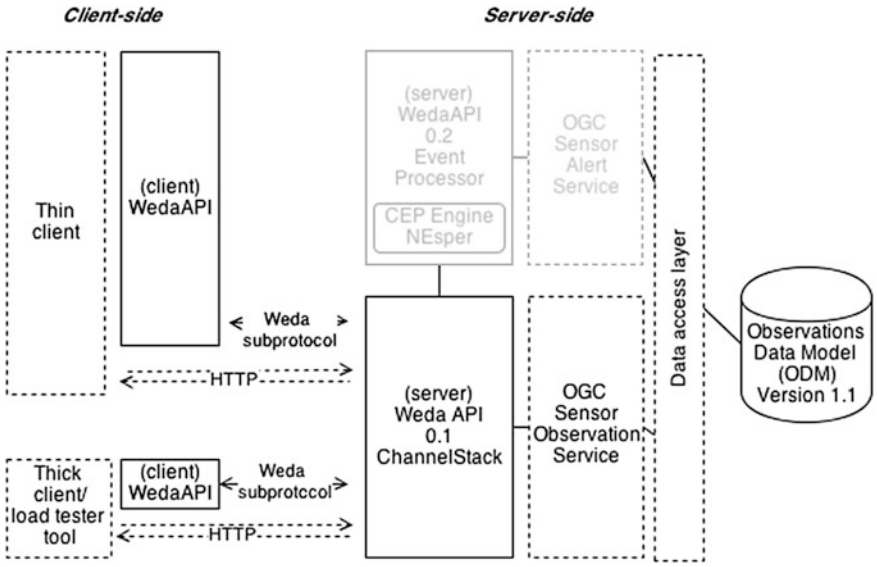

Fig. 2 Overview of experimental systems

- *Web service*—As we wanted to be sure that the existing service could be extended, we chose OGC Sensor Observation Service [11] as part of our experimental system. The server solution consists of the implementation of standard SOS webservice without changes in contracts and business logic (the goal). For spatial data, Renci (Renaissance Computing Institute) OpenGIS implementation was used to bring us API for using Gml, Ows, SensorML or Tml specifications. In the first version of samples we use its Core and Enhanced extensions with GetCapabilities, DescribeSensor, GetObservation and GetFeatureOfInterest operations. In the future version transactional extension of SWE SOS can be implemented especially with a proposal of one-way InsertObservation operation and broadcast event that new observation arrived for all clients.
- *Weda API*—Other projects undergoing development are WedaAPI and layers of the Weda eventing processor (will be integrated to WedaAPI after more tests). The WebSocket server used is RFC6455 Super-WebSocket implementation. The Weda eventing processor integrates a Complex event processing engine NEsper—the widely used CEP engine offering runtime for .Net. CEP server runs independently and has its own long running lifetime over the requests. REST-compliant Web services, in which the primary purpose of the service is to manipulate XML representations of Web resources using a uniform set of "stateless" operations.
- RPC-compliant Web services, in which the service may expose an arbitrary set of operations.
- WEDA-compliant Web services, in which the service can use asynchronous message passing which can provide us eventing behaviour as well as call and return.

3.2 Thin Client

Figure 3 shows the web client interface of our thin-client connected to the server. Both clients read the geo-spatial data from the OGC SOS service by Weda ChannelStack—transport and message binding and subprotocol. This client acts as GIS Web map reader with WMS and SOS layers. It is implemented with ASP.NET MVC3 and JavaScript using OpenLayers. We extended its Protocol.SOS javascript library to be capable of connecting to the Weda endpoint. The use for the client is as a public GIS Viewer system which presents SOS service data graphically upon the public WMS layer while that data is loaded over Weda. End developers can build a nice viewer with many features according to Weda capabilities. This client was not considered as a benchmarking environment. Nevertheless some response time logging is contained in source so the user can optimize the application after displaying the response time information in the browser's console.

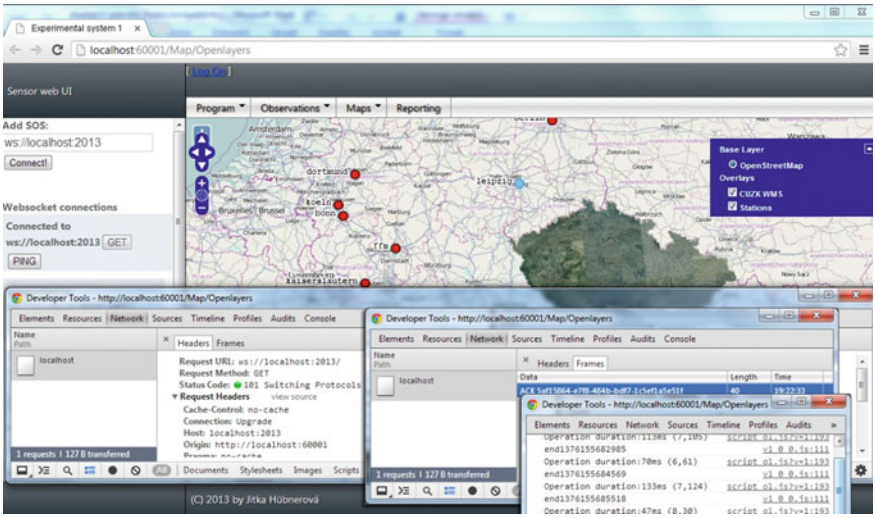

Fig. 3 Experimental system with thin client interface

3.3 Thick Client

Figure 4 shows the desktop client interface of our thick-client. It is implemented in C#.Net Winforms. The desktop client application was extended to be a load testing tool. As Websocket is a new protocol, there are no load testing tools that can act over WebSocket and none extensible with some subprotocols. This client allows us to do real benchmarks of Weda against REST and SOAP over HTTP SOS service. Legacy SOAP/REST endpoints are also invoked and used in benchmarks as baseline.

4 Performance Analysis

We measured response time instability of Weda by invoking number of requests (according to SOS GetCapabilities, DescribeSensor, GetObservation and GetFeatureOfInterest operations) from the thick client application and collecting the responses with metadata about server processing times and other parameters (such as 20 kB amount of transferred data per request etc.).

The load generator was hosted on 4xIntel Xeon running at 2.5 Ghz, Windows 8, 2 GB of RAM, 1Mbps downlink network connection and 100 Kbps uplink network connection. The location of the load generator was 4 network hops away from the server hosting the service. Reverse proxy (no caching) was placed between the client and server. The average packet round trip time was 33 ms and constituted less

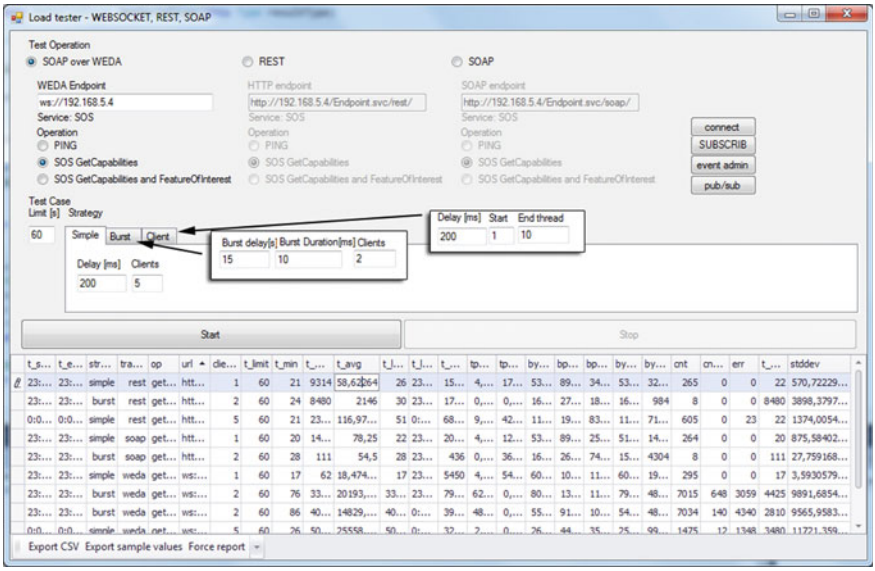

Fig. 4 Experimental system with thick client interface

than 1 % of the service time. The server was hosted on an Intel Core i7 2670qm running at 2.2 Ghz, 4GB DDR3 665 MHz, Windows 7 professional sp1 64bit. The database server (MSSQL 2008 R2) was running on the same host as the Weda server so its latency is included in total amount of RPT. It was found that RPT times mainly consist of latency of data access layer (99 %). The test case for measuring response time instability has been defined with constant payload of GetCapabilities operation invoked at OGC SOS webservice. Every 10 s for 3 h a request was sent and results were measured to give us more than 1,000 samples. The server processed each request by proper serialization at each layer up to the bottom data access layer. Backward propagation of results was packed into response frames by Weda API and metadata about server processing times was glued into the response. An illustration of setup and measuring points can be seen in Fig. 5.

RTT includes a time for request forwarding achieved by our reverse proxy. This was used to simulate such a device's delay. The Weda architectural style is a hybrid architectural style that we have derived from other network-based standards, such as web services [5] and HTML5 web-sockets [6] to get a practical real-time SOA 2.0 [7].

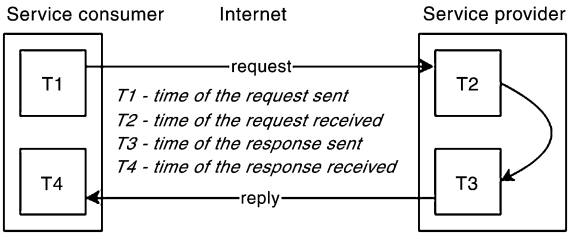

Fig. 5 Benchmark setup

$$RT = T4 - T1 \tag{1}$$

$$RPT = T3 - T2 \tag{2}$$

$$RTT = (T2 - T1) + (T4 - T3) = (T4 - T1) - (T3 - T2) = RT - RPT \tag{3}$$

Performance trends and variance results are shown in Fig. 6. It can be seen that response times are constant for 50 % (1,600–1,700 ms) samples. 73 % of the sample's RT were around the 95th percentile. 26 % of samples have uncertain response time varying from 2 to 11 s (four times more than average value). RTT is the main part of RT value. Its distribution is very similar to RT as 48 % of RTTs are between 1,600 and 1,700 ms. One small peak can be found at 4.5 s where 7 % of samples are situated.

Table 2 shows the statistics of the test. A ratio between standard deviation and average value is used as an uncertainty measure. From the table we can see that RT and RTT have a relatively small variance but RPT has significant instability which does not affect the final RT by much.

A very small amount of samples are significantly affected by RPT giving more than 1 s to total RT. From this point there is no chance to significantly improve performance by improving serialization technique (except adding the compression) or dealing much with the implementation. In our other work we use these results to predict response time instability formula.

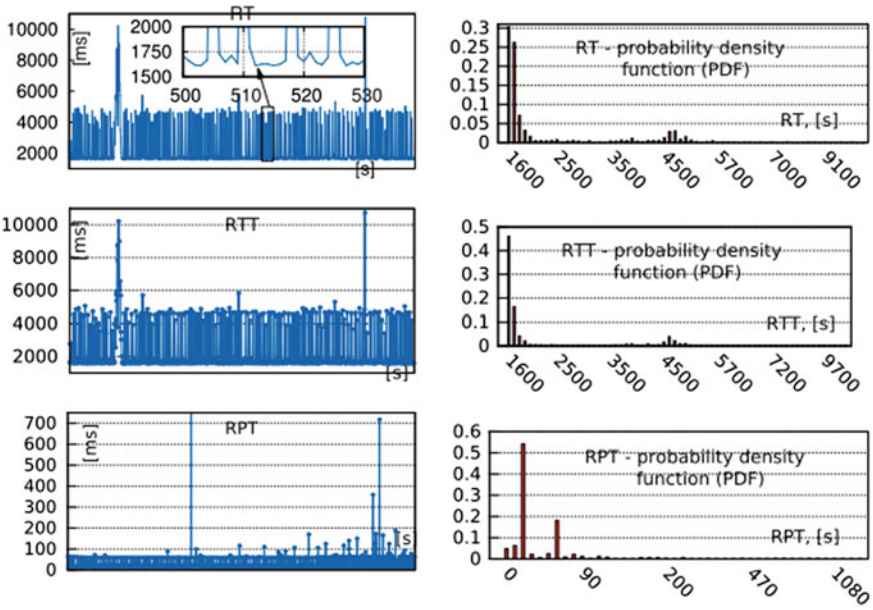

Fig. 6 Performance trends and probability density of RT, RTT, RPT

Table 2 Performance statistics: RT, RPT, RTT

	Min (ms)	Max (ms)	Avg (ms)	95th (ms)	Std.dev.	Std.dev/ Avg (%)
RPT	10	1,280	31	18	54	940
RTT	1,580	10,754	2,197	1,630	1,244	56.6
RT	1,608	10,773	2,258	1,669	1,243	55.8
Ping RTT	32	367	40	35	3	1.7

4.1 Baseline Benchmarks

We performed many benchmark measurements to compare Weda against REST and SOAP/RPC web services. These results and comparative graphs are out of the scope of this paper, so here I only wish to add some findings on interesting quality attributes.

- *Findings on the throughput attribute*—from "burst-based test cases" we can learn that synchronous styles (SOAP over HTTP and REST) can only achieve a small amount of turns compared to Weda-style. Weda-style has a 40-times higher throughput, but as such it is more susceptible to DDoS attacks without a robust admission control mechanism (tests ran without any admission control mechanism implemented). A great way of dealing with overwhelming issues is to add an admission control mechanism at each input queue. It is a matter for discussion if such a mechanism should be required directly in WebSocket specification (not in Weda-style).
- *Findings on the scalability attribute*—very interesting results were obtained from the "constant count of samples per burst test case," which suppressed the differences caused by asynchronous or synchronous transport. We saw that throughput increases exponentially with the number of clients for Weda-style. RPC and REST-styles have their peak-throughput relatively low at a count of 6 clients (each client invoked exactly 10 samples per burst every 1 s). Weda-style proves that it is more scalable in terms of concurrent clients.
- *Findings on the response time attribute*—peak-throughputs can negatively impact Weda-style (the next version should deal with it with an admission/flow control mechanism). To suppress this behaviour we prepared a test case where conditions were set in a way leading to very similar throughput behaviour (we prevented Weda-style to send/process more samples than other styles). From the results we obtained that Weda's 90th percentile response time is lowest and unaffected by incrementing client count unlike the RPC and REST-style. This test case shows that Weda-style responsiveness is a little bit better than for RPC and REST-style.

5 Event Processing Enhancements

The main building block of web based GIS monitoring and alerting solutions is contained inside the Weda specification—the use of duplex services. This enables message exchange patterns in which both endpoints can send messages to the other independently. A duplex service, therefore, can send messages back to the client endpoint, providing event-like behaviour. Duplex communication occurs when a client connects to a service and provides the service with a channel at which the service can send messages back to the client. We can benefit from the client's Weda endpoint which is accessible from the server. To implement the push mechanism, the client must implement a client-specific contract called a callback contract. As we created our experimental system before the SES standard was proposed, our experiments contain an easier WS-Eventing [12] contract (other WS-Notification [13] OASIS-Standard is bind able to the model). There are three types of services needed in enhancements:

1. Subscription and notification management
2. Default public integration point for sensors, monitoring systems and other event sources
3. Integration point for admin tools for statement/topic management.

As shown in Fig. 7, the Weda event processor consists of a dispatcher component, four event processing services which can be running on separate instances and one CEP engine. Complex event processing is technology to transform single, low-level events into aggregated, high-level events by looking across event streams. Many message types are transmitted here as SOAP management operations, events, subscription messages, registered EPL rules and rule actions. Implementation of eventing enhancements is now integrated in an experimental system only. After

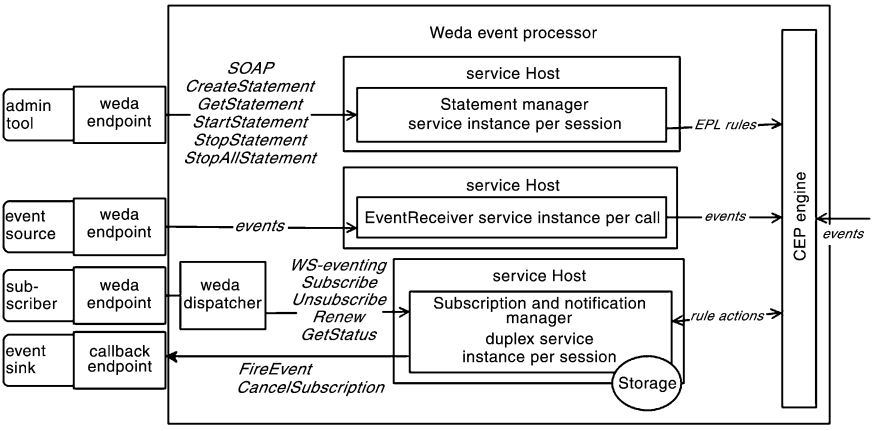

Fig. 7 High-level process view of Weda event processor and its relationship to EDA components

stabilization of API and testing with SES specification, it will be integrated directly into WEDA API. In the scope of this paper we will only highlight some of the components that build together the practical implementation of SOA 2.0 architecture.

- For example the Notification manager component reacts on rule actions from the CEP server and parses the list of subscriber's topics to make the correct push of an event to appropriate event sink. Events are defined by the end application. An example of event-type (SASAlert) follows:

```
<?xml version="1.0" encoding="UTF-8"?>
  <SASAlert xmlns="http://www.opengis.net/sas"
   xmlns:xsi="http://www.w3.org/2001/XMLSchema-instance"><Header>
        <AlertMessageStructure>
          <sas:QuantityProperty>
             <sas:Content definition="urn:ogc:def:property:OGC:Temperature"
   uom="Cel">-0.9</sas:Content>
          </sas:QuantityProperty>
        </AlertMessageStructure>
      </Header>
      <Body>51.96 7.607 70.0 2009-10-17T02:27:04Z 0 30</Body>
  </SASAlert>
```

- Event generator integration point—EventReceiver metadata service is the main integration point for monitoring systems, network sensors and other event generators (event sources) which send an event into the CEP server for further processing.
- Statement manager metadata service is an integration point for any administration tool that allows definition of topics. Thanks to the StatementManager service, experts can provide a set of rules that may change over time, due to the dynamic nature of the domain. Client application behaviour can be changed only by changing the set of rules, nothing has to be programmed. An example rule provided as EPL statement follows. This example statement fires as soon as a LocationSensor of a certain device does not fire events for 10 s. Every user can then subscribe for this topic.

```
SELECT count(*), Identifier FROM LocationSensor.win:
time(10 s)
GROUP BY LocationSensor.Identifier HAVING count(*) = 0
```

6 Conclusions

In this work, the author presents the application (experimental system) of the WEDA architectural style for developing "GIS on the web" solutions. The paper also shows performance results measured on the system. It shows that RT is stable

and good enough to be used in real-time and also summarizes other benchmark findings from a number of different test cases. The system can improve the performance of sensor web services and thanks to the presented "event processing enhancements" it extends messaging capabilities for publicly available monitoring and alerting sensor webs. There are many applications for this system from small ones (e.g. warning the public or farmers within a range of 10 km before an approaching storm or hail) to bigger ones (monitoring of emissions in real time by informing the public to close windows and alerting the relevant authorities after exceeding permitted limits) or building automata that can warn before some critical event occurs (if water exceeds the threshold at Liblín and Zvíkovec and it is raining in Beroun, then clients are alerted from Beroun to Praha 11–13). With this technology, results from very different sensor types can be processed together and cross calculated. Users can define their own preferences for what to monitor and alert for. The resulting trend analysis can be made available on a global level and deployed in the cloud environment.

Acknowledgments This work was supported by the Ministry of Education of the Czech Republic within the SGS project no. 78001/115 on the Technical University of Liberec.

References

1. Botts M, Percivall G, Reed C, Davidson J (2008) OGC sensor web enablement: overview and high level architecture. In: Nittel S, Labrinidis A, Stefanidis A (eds) GeoSensor networks, volume 4540 of lecture notes in computer science, Berlin, 17–20 Sept 2007, Springer, pp 175–190
2. COM-20-2737 (2003) Event-driven applications: definition and taxonomy. Gartner, Stamford
3. Etzion O, Chandy M, Ammon RV, Schulte R (2006) Event-driven architectures and complex event processing. IEEE international conference on services computing, IEEE, Sept 2006
4. Chandy KM, Charpentier M, Capponi A (2007) Towards a theory of events. In: Proceedings of the 2007 inaugural international conference on distributed event-based systems, DEBS '07, ACM, New York, USA, pp 180–187
5. Group WW (2013) Web services glossary (2004) Available via DIALOG. http://www.w3.org/TR/ws-gloss/. Accessed Oct 2013
6. RFC6455 (2011) The WebSocket protocol. IETF, California
7. Levina O, Stantchev V (2009) Realizing event-driven SOA. In: Perry M, Sasaki H, Ehmann M, Bellot G, Dini O (eds) Fourth international conference on Internet and Web applications and services, Venice/Mestre, Italy, 24–28 May 2009, IEEE Computer Society, Washington, pp 37–42
8. Hübnerová J (2013) Weda—new architectural style for world-wide-web architecture. In: Proceedings of ISAT 2013, 34th international conference information systems architecture and technology, Sept 2013, Poland, Institute of Informatics Wrocław University of Technology, Poland, ISBN 978-83-7493-804-4
9. Hübnerová J (2013) Model based analysis and formal verification of WEDA architectural style. In: Proceedings of IEEE international conference on informatics and applications (ICIA), Poland, Sept 2013, Poland, IEEE, Poland, ISBN 978-1-4673-5255-0
10. Tarboton D, Jeffery S, Horsburgh TD, Maidmen JS (2013) Cuahsi community observations data model (ODM), version 1.1, design specifications

11. OGC 06-009r6 (2008) Sensor observation service v.1.0.0. OpenGIS implementation standard, Open geospatial consortium
12. Box D, Cabrera LF et al (2004) Web services eventing (WS-eventing) specification. Available via DIALOG. http://download.boulder.ibm.com/ibmdl/pub/software/dw/specs/ws-eventing/WS-Eventing.pdf. Accessed Oct 2013
13. Graham S et al (2006) Web services notification (WS-notification) version 1.0. Available via DIALOG. https://www.oasis-open.org/committees/tc_home.php?wg_abbrev=wsn#technical. Accessed Oct 2013
14. Clements P, Kazman R, Klein M (2001) Evaluating software architectures: methods and case studies. Addison-Wesley, Boston

Demand and Supply of Transport Connections for Commuting in the Czech Republic

Igor Ivan and Jiří Horák

Abstract The question of modal split or modal share for commuting is still very relevant topic in the studies of transport issues. This paper deals with evaluating of real demands for individual and public transport using for daily commuting between municipalities in the Czech Republic based on data from census 2011. Results discover a strong relationship between individual transport use and geographical location. The highest share of individual transport is in western areas and less populated municipalities. Concurrently the public transport supply is analysed based on data from the Database of public transport connections which has been developing by authors since 2007. Comparing evaluated transport demand and supply, all municipalities are divided into 12 categories. Various demographical (age, education, population) and geographical (altitude, area, distance to regional and national borders, x and y coordinates) factors including commuting time are studied and discussed in four most extreme groups. Typically small demand and small supply for public transport is correlated with high car ownership index, small number of residents, and closeness of regional borders (internal peripheries).

Keywords Commuting · Public transport · Individual transport · Modal split

1 Introduction

The decision of mode choice remains a crucial issue in studying transport geography. However some countries have been successful in shifting car users onto public transport, others are struggling despite their effort to make public transport

I. Ivan (✉) · J. Horák
Institute of Geoinformatics, VSB-Technical University of Ostrava, 17. Listopadu 15, 708 00 Ostrava, Czech Republic
e-mail: igor.ivan@vsb.cz

J. Horák
e-mail: jiri.horak@vsb.cz

I. Ivan et al. (eds.), *Geoinformatics for Intelligent Transportation*,
Lecture Notes in Geoinformation and Cartography,
DOI 10.1007/978-3-319-11463-7_10

more attractive. The modal split is related to numerous relevant more or less success factors, ranging from *individual mode choice*, which in turn depends on individual and mode characteristics, to *land use* and population density. But two of them are considered as the most important—the travel time and the level of variability of travel time [1]. Unlike price and other factors, time spent on travelling is an absolute constraint which cannot be increased infinitely [2, 3]. Particularly in case of regular short-distance trips, i.e. commuting to work, the commuter's behaviour minimises the economical and time costs needed for the trip. The preference of one of these two aspects—price and time—is crucial for the final transport mode selection.

It is not just about the time of transport (in-vehicle time), but also about the time for journey preparation (varying according to its length, purpose and frequency), walking to public transport stop, waiting for the vehicle (positive influence of regular time schedule), time for eventual vehicle changes and waiting for follow-up connection, walking to the final destination from stop. All of these parts create the out-vehicle time [3]. The same situation is valid also for the journey back to home after the end of the work-shift. Additionally the passengers are more sensitive to out-of-vehicle times than in-vehicle time (in range 1.5–2.3 times more). Particular phases of out-of-vehicle times are quite variable. The walking and waiting time is perceived mostly negatively (except very long journeys) and in case of commuting using public transport the walking times can make up 24–30 % the time of the whole journey (averagely 800 m) in the Czech Republic compared to individual car transport with distance about 50/160 m in rural/urban environment. All of out-vehicle time parts are generally more time consuming in case of mass public transport. Not only that out-vehicle and in-vehicle time is perceived differently, but also generally the time is perceived differently, and each individual has its own travel time budget. Its size is derived from how time is valued, which is in turn related to wages [4]. From the time point of view, it can be assumed that public transport is preferred if the in-vehicle and out-vehicle time of commuting meets the needs of the commuter, otherwise commuter must rely on individual transport.

This general modal split based only on travel time is further influenced by price of travel. The individual car transport is more monetary expensive than the commuting by public transport. Each individual has also own money budget, similarly as in case of time. If the prize exceeds the individual's budget, commuter has the only possibility to use public transport even the commuting time is partly over the time budget. In the worst case, the people cannot commute at all and either they have to move closer or to prefer a job in better accessible areas. For regular travelling between two places, public transport providers offer cheaper seasonal ticket in order to increase the share of public transport in commuting trips to work [4]. The owning such seasonal ticket increases the probability that an individual will use public transport and create larger resistivity to new cheaper opportunities (such as ridesharing with colleague, purchase of a new car). On the other hand, White [5]

has noted that owning a car makes the probability of using it for daily activities (including commuting) much higher, even if it does not provide any economic benefits and an appropriate public transport connection exists. Then, the public transport will be used only under rare circumstances (journey to the city centre, to a party etc.). Additionally the car is shared also by other members of the family, either as passengers for journeys to work, school (ridesharing) or as drivers for their own needs (carsharing). So, the decrease of public transport use is higher than the average for one person. Each new car in a family substitutes about 200–250 local journeys by public transport per family and year. This effect is more significant in case of the first car and smaller for additional cars. Therefore, policies aimed at discouraging car ownership with activities such as high registration fees or annual excise duties, hoping to reduce the share of car use for trips to work. Unsurprisingly, GDP per capita is also positively correlated with car share. Also other more or less significant individual factors have influence on final mode choice such as ecological lifestyle, subjective perception of public transport, personal image, comfort of travelling etc.

Socio-economic and other subjective factors have been found to be very important in explaining commuting behaviour. Nevertheless, land use is considered as equally important factor for final mode choice and has a clear relationship with travel behaviour [4]. Following seven main dimensions of land use factors have been identified: (1) density; (2) diversity/mixed use; (3) design and infrastructure (including parking, and conditions for walking and cycling), (4) destination accessibility; (5) accessibility to public transport; (6) demand management; and (7) demographics [6, 7].

In this paper, we compare the demand and supply of two transport modes—public and individual—in relation to commuting in the Czech Republic. The goal is to answer three questions: (1) Where are the main areas/flows using individual transport? (2) What kind of commuters is travelling here? (3) Do they have any alternative in public transport use? The demand is based on the data from census 2011 and characterized as real modal-split used for commuting between a pair of municipalities. By contrast, the majority of the existing Czech geographical studies on commuting mode choice have been conducted based on data from census 2001 without consideration whether any alternative exists, i.e. [8–14]. We add another perspective and utilise our data from the database of public transport connections (described below). Combining these two data sources we classify municipalities into several categories based on the level of real public transport use for commuting (demand) and the number of municipalities accessible by public transport (supply). Additionally we select the typical members of the most extreme groups considering various aspects. The remainder of this paper is organised as follows: Sect. 2 describes the data used; Sect. 3 presents the commuting modal-split; Sect. 3.1 describes the supply of public transport connections; Sect. 4 presents the results of combining both data sources and finally; Sect. 4 summarises the main findings.

2 Data

Commuting flow data comes from census 2011 with the decisive moment at midnight from 25 to 26 March 2011. It provides information about all commuting flows with the origin municipality within the Czech Republic (destination can be in foreign country). The commuter is defined as an employee or a student (commuting to school and to work is distinguished in data) who has the job or school out of the residential municipality (this can differ from official address in the ID card). The commuting within the same municipality is not considered by statistics as commuting. Altogether, the table contains 178,171 records and 1,551,918 commuters are travelling between these pairs of municipalities (general volume of data are summarised in Table 1). Standard list of parameters has been further extended about the modal share between seven analysed transport modes for all of 178,171 records—car (driver); car (passenger); train; bus; urban public transport (some transport links operate also outside the municipality area); motorcycle; and bicycle. The frequency of transport mode use within one municipality combination is often higher than number of commuters. This is caused by the possibility of respondents to choose more options if they are using a combination of them. Due to all possible combinations, this inconsistency causes only small problem in case of individual and public transport combination. Only 0.5 % of all respondents selected this combination as the used transport way for commuting what makes it irrelevant. Combination of public and individual transport such as park and ride, bike and ride play only negligible role in the Czech Republic.

Finally the data set has been reduced based on two criterias (1) both, origin and destination of commuting must be within the Czech Republic (commuting to foreign country has been excluded); (2) in case we compare the real modal share with existing public transport connection, we work only with commuting flows within 100 km (Euclidean distance). This distance selection is important to make this data consistent with the second data source (see text below).

The final number of records and commuters is in Table 1.

The second data used in this paper are from the Database of transport connections which has been developed and three times a year updated since 2007. This database contains all combination of municipalities within 100 km (Euclidean distance) with

Table 1 Number of records and commuters in data set from census 2011

	Number of records	Number of commuters	Commuting to work		Commuting to school	
			Total	On daily basis	Total	On daily basis
Domestic and foreign commuting	178,171	1,551,918	1,125,337	953,190	426,581	302,955
Domestic commuting	165,347	1,508,711	1,089,876	935,186	418,835	299,324
Domestic commuting within 100 km	143,591	1,427,475	1,050,933	921,010	376,542	291,719

information about public transport connections between each pair. A municipality is defined by the main public transport stop suggested by the valid time tables. The database contains travel time, number of changes, price and existence of return connection for each combination of municipalities and five time intervals (to 6, 7, 8, 14 and 22 o'clock) which define the beginnings of three work shifts. Each public transport connection must fulfil these criterias: (1) the Euclidean distance between municipalities is less than 100 km; (2) the duration is less than 90 min; (3) number of changes is 5 and smaller; (4) arrival time cannot be earlier than 60 min before; and (5) departure time from commuter's residence cannot be earlier than 120 min before arrival (more in [15, 16]).

Valid timetables have been used to search all public transport connections using buses and trains (no urban transport) for the 8 March 2011 (similar date as the decisive moment of census). For the municipality level, the database contains 12,579,133 combinations with further information of transport connections to 6, 7, 8, 14 and 22 o'clock. From this volume, 721,826 combinations have at least one connection for at least one commuting time.

3 Modal Split of Commuting

Following Rodrigue et al. [17] we define modal split or mode share as the proportion of trips that is made by each transport mode. Compared to the modal options in our data set, census results in general distinguish 14 different modal options including their combinations. From the public transport modes bus is used for commuting with 18.8 %, following by urban transport with 6.6 % and train with 6.2 %. The most often, commuters are using car as drivers with 36.3 % and as passengers as 7.6 %. The other individual transport modes have only negligible usage—motorbikes with 0.1 %, bicycle with 1.4 %. Combination of different transport modes are not as common as was expected with the highest share of bus and urban transport combination (3.3 %) and train and urban transport with 2.6 %. Other combinations have the share below 2 % and about 10 % of commuters did not respond this answer.

For the needs of this paper, we work with modified data set from census as specified above and only domestic daily commuting is analysed. For all of 935,186 daily commuters, 1,283,421 cases of transport option uses are stored in the data set. This inconsistency is explained above. Transport options have been aggregated to two groups. First group consists of 803,601 users (63 %) of cars as driver; cars as passenger; motorcycles and bicycles and is named as individual transport and the second group is named as public transport and consists of 479,820 users (37 %) of trains; buses and vehicles of urban public transport. Daily commuters prefer individual transport compared to general commuting with the share about 51 %.

The spatial variability of individual transport share is high with east-west gradient as it is portrayed in the map (Fig. 1). The spatial variability in case of public transport share is inverted. No employee is commuting or no given transport option is in case of 561 municipalities from 6,251 of municipalities in the Czech Republic.

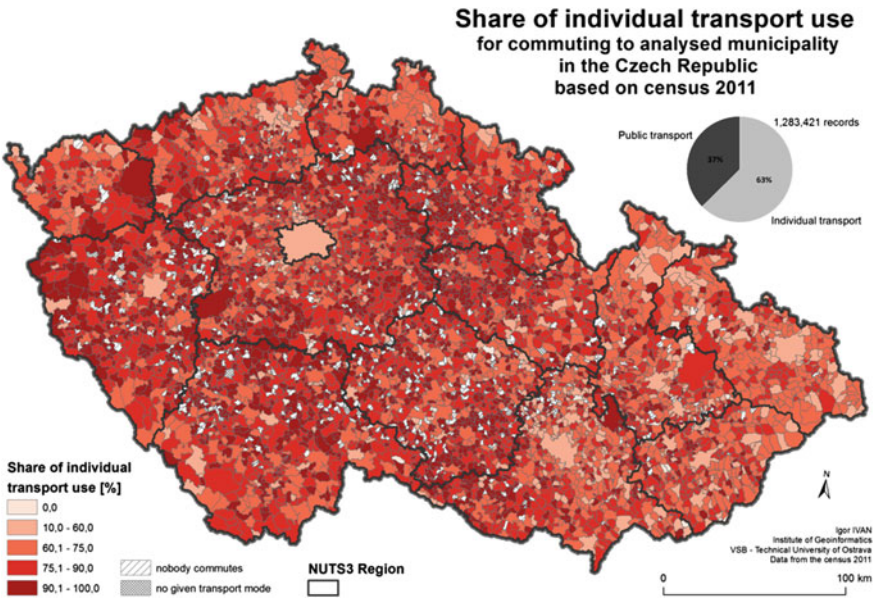

Fig. 1 Share of individual transport use for daily commuting in the Czech Republic (2011)

Nevertheless these are only low-populated municipalities. The most populated cities have the share of individual transport between 40 and 60 % what is significantly below the average. This confirms the Pearson correlation coefficient between the population (aged 15–64) and frequency of individual or public transport use which is slightly higher in case of public transport mode (0.987 and 0.975). If we analyse the correlation between the population (15–64) and share of individual or public transport use, the correlation coefficient is negative in case of individual transport ($R = -0.084$). This is even more evident if only municipalities above 10,000 residents are included ($R = -0.452$ for individual transport). The more populated is the city the smaller is the share of individual transport use and this relationship is getting stronger.

The level of individual transport use is getting higher in the direction from the eastern to the western parts of the Czech Republic (see Fig. 1). This general spatial trend is also confirmed by negative Person correlation coefficient between the share of individual transport use and the x coordinates ($R = -0.195$). Also the correlation between the population (15–64) and the x coordinates has been analysed to exclude the influence of relationship between the population size and individual transport share. Nevertheless, this correlation is very small, not statistically significant and even positive ($R = 0.009$). So there may play an important role some different influences and the supply of public transport connections (Fig. 2) can be the one with the biggest importance.

It has been discussed that the mode decision is influenced by many more or less important factors which significantly depend on individual's subjective opinion.

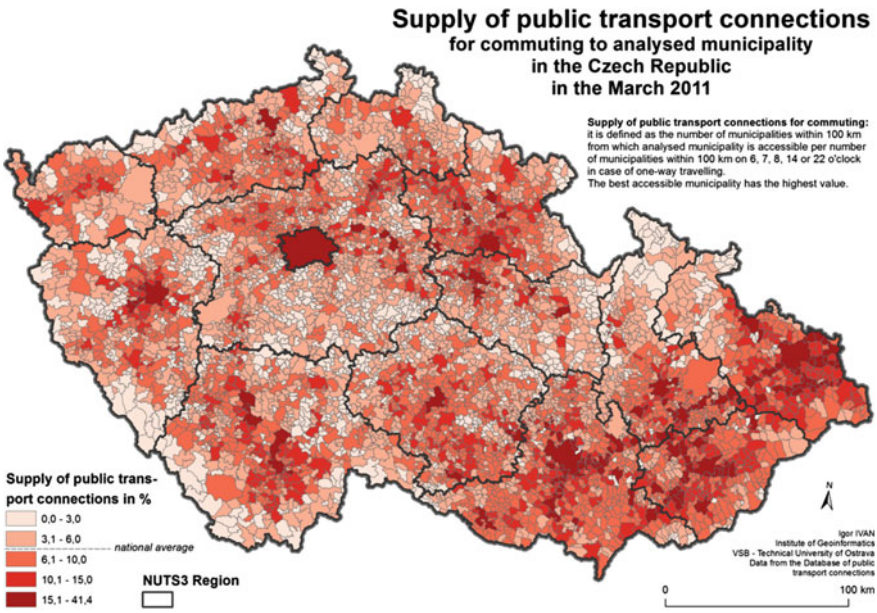

Fig. 2 Supply of public transport connections to analysed municipality in the Czech Republic (2011)

The crucial aspect in this choice is existence of an alternative. If no public transport connection exists the commuter must rely on individual transport. It is not an easy task to evaluate the supply of public transport connection at the municipality level. Commonly used indicator for such evaluating is the number of links servicing the municipality. But this indicator suffers several problems, i.e. there can be only one or a few frequent links connecting only several and still the same municipalities, these links can arriving and departing at wrong time for commuting needs. We have developed a new indicator for evaluating the supply of public transport connections and defined it as the number of municipalities within 100 km from which analysed municipality is accessible per number of municipalities within 100 km on 6, 7, 8, 14 or 22 o'clock in case of one-way travelling. The map (Fig. 2) shows spatial distribution of supply and on the first look it is clear that the general distribution is opposite to that in the previous map (Fig. 1). So the best accessibility by public transport is in case of the biggest cities what is again confirmed by positive and statistically significant ($p = 0.01$) correlation ($R = 0.257$). If only cities above 10,000 residents are analysed, the correlation is even 0.621.

Similarly also the spatial trend from west to east is evident and confirmed by positive and statistically significant ($p = 0.01$) correlation ($R = 0.277$) which is even bigger than in case of the population size. Also in this case correlation is higher without municipalities below 10,000 residents but the increase is not as high as in the previous case ($R = 0.336$).

3.1 Demand and Supply of Transport Connections for Commuting

The share of individual transport use and level of public transport services are mutually interlinked. If the share of individual transport use goes higher the provider of public transport should react on such decrease of passengers and reduce provided transport services. On the other hand, the share of individual transport can decrease when the number of accessible municipalities is higher in correct commuting times. The map (Fig. 3) describes the relationship between previously defined supply of public transport services and demand for public transport services defined as the share of public transport use for commuting. All municipalities have been divided into 12 categories depending on the size of both indicators. The first three categories (shadow colours) contain only 38 municipalities with no use of public transport for commuting. The median of commuting employees to these municipalities is equal to 1 so they have only negligible impact (47 commuters). All remained municipalities have been divided into 3 × 3 categories corresponding to three quantiles of these two distributions.

Several geographical (x, y coordinate; distance to national and regional border; area; altitude) and demographical (age end education of commuters; number of residents aged 15–64) aspects and commuting time have been analysed to find typical members of the most extreme four categories. All analysed factors are

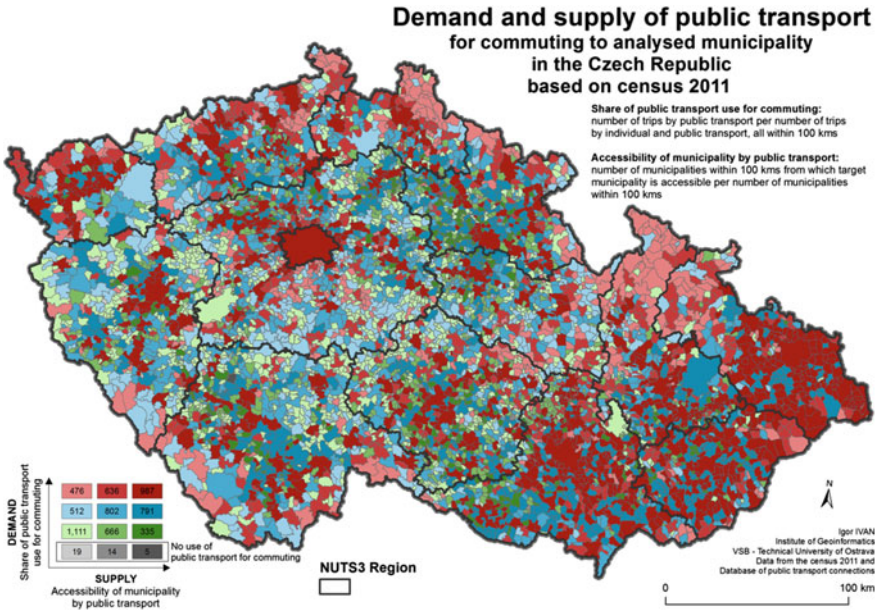

Fig. 3 Demand and supply of public transport for commuting to analysed municipality in the Czech Republic (2011)

statistically significant between groups except commuters with basic education and aged 30–49. The light green category consisting of 1,111 municipalities (18 %) is typical due to small demand for public transport and also small supply of such services. Its members are destinations most often for older commuters (above 50 years) with secondary education without final exam and lower who commute typically up to 15 min. Typical aspects of these municipalities are very high car ownership index, so these people rely on cars and more than 60 % people (aged over 18) own private car. These municipalities have the smallest average number of residents (138) and are located typically in higher altitudes in western areas, significantly more distant from national and closer to regional borders—internal peripheries. These facts are proved also in the map (Fig. 3) where the group members are located along regional borders of Bohemian regions (western parts).

The dark red group consists of 987 municipalities which are typical by high supply and demand for public transport for commuting to analysed municipality. According to current trends in transport policy this is an ideal case. These commuters use to be younger with the highest levels of education (complete secondary and tertiary) and commuting for longer time (above 15 min but also above 60 min). Residents show very small car ownership index. The municipalities of this group belong to the biggest and largest, located more often in the eastern and northern parts of the country, closer to national borders and far from regional borders. Based on the map, they are concentrated in the Moravian part of the country (east) and in the northern parts of Bohemia (similarly as members of dark blue group).

The smallest number of municipalities (335) belongs to dark green transitional group and they have high supply of public transport, but the commuters are rarely using it for daily commuting. Employees commuting to these municipalities are usually younger 30 years, with full secondary education. Compared to the next group, commuters to these destinations commute for shorter time, rarely above 15 min. So, residents do not use public transport despite a good level of public transport accessibility because their travel time is very short. These municipalities are small (both by population and area), in lower altitudes, in southern areas, closer to national border and more distant from regional borders. Indicated spatial influences seem to be confirmed in the map with the increased occurrence of such municipalities in the Vysocina Region and South Bohemian Region.

Municipalities with high demands for public transport but with low supply of these services belong to the light red group (476 municipalities). Residents are usually older with various levels of education. A typical attribute of commuters is longer time spent by journey to work. They have the highest share of trips between 30 and more minutes. The accessibility of public transport is low but the commuters probably do not have any other option and they rely on this mode of transport. These municipalities are located more in eastern and northern areas and in areas with higher altitude. They are close to national and regional borders, large but sparsely populated. The map proves these geographical findings—two main clusters of such municipalities are Jeseniky mountains (N-E part) and Krkonoše and Jizerské mountains (N part).

4 Conclusion

The study is based on data from census 2011 (daily commuting between municipalities, demographical attributes), the register of cars (car ownership), and the Database of public transport connections (description of public transport conditions in municipalities).

The strong relationship between individual transport use and geographical location has been proved. The highest share of individual transport is in western areas and less populated municipalities. According to the local transport demand and supply, municipalities are divided into 12 categories. A correlation analysis with many demographical (age, education, population) and geographical (altitude, area, distance to regional and national borders, x and y coordinates) factors including commuting time enable to characterize following groups of municipalities by selected attributes:

- 1st group with small demand and small supply for public transport indicates high car ownership index, small number of residents, high altitude, and closeness of regional borders (internal peripheries).
- 2nd group with high supply and demand for public transport shows very small car ownership index, closeness to country border (external peripheries), younger population with higher education (complete secondary and tertiary) and longer commuting time. These municipalities are located very often in eastern parts of the country.
- 3rd group with high supply of public transport but low utilisation in commuting is probably interlinked with short commuting time, young and middle educated population in smaller municipalities.
- 4th group with high demands for public transport but with low supply of such services is typical by longer commuting time (above 30 min), in peripheral mountain areas, with older population. These municipalities are mostly clustered in two larger areas.

The result shows typical features of transport choice conditions in the country. Further research should focus more on regional differences to deliver adjusted recommendations to regional transport decision makers.

Acknowledgments Application has been developed as a part of higher education development fund—frvš 956/2013/b1. Authors thank the agency for financial support.

References

1. van Vugt M, van Lange PAM, Meertens RM (1996) Commuting by car or public transportation? A social dilemma analysis of travel mode judgements. Eur J Soc Psychol 26 (3):373–395
2. Bhat C, Koppelman FS (1999) A retrospective and prospective survey of time-use research. Transportation 26(2):119–139

3. Vande Walle S, Steenberghen T (2006) Space and time related determinants of public transport use in trip chains. Transp Res Part A Policy Pract 40(2):151–162
4. Vale DS (2013) Does commuting time tolerance impede sustainable urban mobility? Analysing the impacts on commuting behaviour as a result of workplace relocation to a mixed-use centre in Lisbon. J Transp Geogr 30:38–48
5. White P (2002) Public Transport. Spon Press, London. ISBN 0-415-25772-7
6. Banister D (2011) Cities, mobility and climate change. J Transp Geogr 19:1538–1546
7. Litman T (2011) Land use impacts on transport—how land use factors affect travel behavior. Victoria Transport Policy Institute, Vitoria, p 80
8. Čermák Z (1993) Geografické aspekty prostorové mobility obyvatelstva. [kandidátská disertační práce], přírodovědecká fakulta univerzity Karlovy, katedra sociální geografie a regionálního rozvoje, Praha
9. Čtrnáct P (1983) Dojížďka do zaměstnání podle výsledků sčítání 1980. Demografie 25(3): 221–233 (FSÚ, Praha)
10. Hampl M (2004) Současný vývoj geografické organizace a změny v dojížďce za prací a do škol v Česku. Geografie - Sborník ČGS 109(3):205–222
11. Hůrský J (1969) Metody grafického znázornění dojížďky do práce. Rozpravy ČSAV, řada matematických a přírodních věd, 79 (3). Academia, Praha
12. Macka M, Králová M (1977) Kvalitativní změny ve vývoji dojíždění do zaměstnání v ČSR. Studia geographica 61:67–74 (GÚ ČSAV, Brno)
13. Řehák S (1988) Dojížďka do zaměstnání v ČSSR. Sborník prací 19, Současný stav a dynamika prostorových struktur měst a regionů v PLR a ČSSR. GGÚ ČSAV, Brno, pp 83–95
14. Szczyrba Z, Toušek V (2004) Vyjížďka a dojížďka do zaměstnání v České republice; Změny v období transformace. In: Przeksztalcenia regionalnych struktur funkcjonalno-przestrzennych, VIII/2, Wroclaw, 21–31
15. Fojtík D, Ivan I, Horák J (2011) Database of public transport connections—its creation and use. In: Proceedings of the 2011 12th international carpathian control conference, ICCC'2011, pp 115–119
16. Ivan I, Horák J, Fojtík D, Inspektor T (2013) Evaluation of public transport accessibility at municipality level in the Czech Republic. In: GeoConference on informatics, geoinformatics and remote sensing, conference proceedings 1, ISBN:978-954-91818-9-0, p 1088
17. Rodrigue JP, Comtois C, Slack B (2009) The geography of transport systems. Routledge, New York, p 368

Train Platforming Problem

Ľudmila Jánošíková and Michal Krempl

Abstract The train platforming problem consists in the allocation of passenger trains to platforms in a railway station. One of the important problems a dispatcher has to solve, especially in a large railway station, is to decide, at which platform track an approaching train should arrive. There is a tool helping him in his job called the track occupancy plan. The plan specifies for each arriving or departing train the platform track along with the time slot during which the track will be occupied by the train. This paper deals with a method for computer-aided design of the track occupancy plan. The problem is formulated as a bi-criterion mixed integer programming problem. The first objective is to minimise the deviations of the arrival and departure times proposed by the model from the times specified by the timetable. The second criterion maximises the desirability of the platform tracks to be assigned to the trains. The model is solved using a lexicographic approach and the local branching algorithm. The model was verified by using the real data of Prague main station. Results of the experiments are included.

Keywords Train platforming · Scheduling · Mixed integer mathematical programming · Multiple-objective programming

Ľ. Jánošíková (✉)
Faculty of Management Science and Informatics, Department of Mathematical Methods and Operations Research, University of Žilina, Univerzitná 1, 010 26 Žilina
Slovak Republic
e-mail: Ludmila.Janosikova@fri.uniza.sk

M. Krempl
Faculty of Mechanical Engineering, Institute of Transport, VŠB Technical University of Ostrava, 17. Listopadu 15, 708 33 Ostrava - Poruba, Czech Republic
e-mail: michal.krempl.st@vsb.cz

I. Ivan et al. (eds.), *Geoinformatics for Intelligent Transportation*,
Lecture Notes in Geoinformation and Cartography,
DOI 10.1007/978-3-319-11463-7_11

1 Introduction

The train platforming problem is a subproblem of the generation of a timetable for a railway company. The generation of a timetable is a hierarchical process. At the first stage, a preliminary timetable for the whole network is proposed. In this phase, a macroscopic viewpoint at the railway network is applied. Stations are considered as black boxes. Capacity limits of particular stations and the movement of trains inside the stations are not taken into account. Then, at the second stage, a microscopic viewpoint related to stations is applied. At every station, the network timetable is checked whether it is feasible with respect to capacity, safety and train operators' preferences. This process results in a track occupancy plan which specifies for each arriving or departing train the platform track along with the time slot during which the track will be occupied by the train. Cargo trains do not affect the plan since they travel mostly in night, when there are fewer passenger trains, they use different tracks in the station, and in case of conflicting movements they can wait at the entry signal.

In the Czech and Slovak Republic, planning train movements through the station is done by hand, using planner's experience and a set of rules determined by a railway company. The main goal of this research is to design a more sophisticated approach which would serve as a planner's decision supporting tool and result in a better track occupancy plan. Improvement in the plan quality results in:

1. better management of train operation in the station, namely:
   (a) shorter times of routes occupation by arriving and departing trains,
   (b) uniform workload of the infrastructure elements, such as tracks, switches, and platforms, which leads to a more robust plan resistant to random disturbances;
2. higher service quality perceived by passengers, namely:
   (a) shorter distances needed for changing trains,
   (b) more appropriate platforms (platforms near to ticket sales points and to the station entrance, platforms equipped by station shops or catering etc.),
   (c) less probability of changing the planned platform when the train delays;
3. meeting train operators' requirements on arrival and departure times and platforms assigned to trains.

Routing and scheduling trains at a station has been studied by researchers in countries, where large, busy stations with capacity constraints can be found. Billionet [1] addresses only the routing problem. The problem is modelled using a graph theory and the integer programming formulation of the resulting graph colouring problem is solved. However, the k colouring problem is not indeed an optimisation problem, it means any feasible solution is acceptable and the problem formulation does not reflect the solution quality, such as route lengths or platform preferences for individual trains. Zwaneveld [2] and Zwaneveld et al. [3] formulate

the problem of train routing as a weighted node packing problem, using bivalent programming, while the solution algorithm applies the branch-and-cut method. A disadvantage of the above presented models is that the calculations connected with them are computationally too complex and time consuming. Another, practically oriented approach has given up on applying the integer programming methods, and replaced them by the heuristics, solving the scheduling and routing problems at a time [4]. The algorithm incorporates, or considers, the operational rules, costs, preferences and trade-offs, which are applied by experts creating plans manually. The shortcoming of this approach is obvious: since it is a heuristics, the optimality of the resulting plan is not guaranteed.

Other way of research, e.g. Bažant and Kavička [5], Chakroborty and Vikram [6], has been directed at operational train management. In real time it is necessary to reflect the requirements of the operation burdened with irregularities, i.e. to re-schedule the arrival and departure times, and/or re-route trains.

In this paper we propose a mixed integer programming (MIP), bi-criteria model of the train platforming problem. The problem can be solved by a lexicographic approach, where particular criteria are ranked according to their importance.

2 Problem Formulation

The train platforming problem consists of the following partial issues. For each train,

- a platform track must be specified at which the train should arrive; the platform track assignment determines the route, on which the train approaches,
- arrival time at the platform and departure time from the platform need to be determined.

The solution should minimise deviations from the planned arrival and departure times and maximise the total preferences for platforms and routes.

The inputs to the mathematical programming model are as follow:

1. track layout of the station, which is necessary for determining feasible platform tracks for a train and conflicting routes,
2. list of trains, where the data required for each train include:
   (a) planned time of its arrival at the platform,
   (b) planned time of its departure from the platform,
   (c) line on which the train arrives (in-line) and departs (out-line),
   (d) list of feasible platform tracks with their desirability for the train,
   (e) category of the train.

All time data are given in minutes.

Further on we present the formulation of the MIP model. First we need to explain the symbols used:

Subscripts which in the mathematical model represent objects

i, i', j	train
k, k'	platform track

Input parameters (constants)

t_i^{Pa}	planned arrival time of train i at the platform
t_i^{Pd}	planned departure time of train i
t^{Cn}	standard amount of time passengers take to change trains (depends on particular railway station)
I_i	arrival line track (in-line) for train i
O_i	departure line track (out-line) for train i
c_i	category of train i; $c_i = 1$ for regional stopping trains and increases with the speed and distance travelled by the train. We have to divide train into categories, because international fast express trains have obviously higher importance than the regional ones. Delays of international trains can commit more traffic problems and extra costs than delays of regional trains
$t^{\min}$	minimum dwell time of a train at the platform
$t^{\max}$	maximum time interval, in which two train movements are tested for a conflict
p_{ik}	preference coefficient; it reflects the desirability of the assignment of platform track k to train i
s_{ik}	number of switches on the route of train i from the arrival line track to platform track k and from platform track k to the departure line track
$s_i^{\min}$	number of switches on the shortest train route in the station
$s_i^{\max}$	number of switches on the longest train route in the station
$a(l, k, l', k')$	coefficient, which has value *true*, if the route connecting line l to platform track k conflicts with the route connecting line l' to platform track k'; if there exists any route connecting line l to track k and any route connecting line l' to track k' such that these two routes do not conflict, then $a(l, k, l', k')$ = false. If both trains use the same station or line tracks (i.e. $k = k'$ or $l = l'$), then $a(l, k, l', k')$ = true. The existence of route conflicts can be identified in advance from a detailed map of the track layout.

We adopted the concept of conflicting routes and conflict solving from Carey and Carville [4]. If two trains are on conflicting routes we must ensure that there is at least a required minimum headway (time interval) between them, for safety and signalling reasons. For example, let $h(i, k, i', k')^{da}$ be the minimum headway required between train i departing from track k and the next train i' arriving at track k'. The superscripts d and a denote departure and arrival, and the order of the superscripts indicates the order of the trains, i.e., train i is followed by i'. Similarly we have $h(i, k, i', k')^{aa}$, $h(i, k, i', k')^{ad}$ and $h(i, k, i', k')^{dd}$ for combinations arrival—arrival, arrival—departure,

departure—departure. We need not introduce subscripts to denote the in-lines or out-lines used by trains since for an arriving train i the in-line is already specified by I_i, and for a departing train i the out-line is specified by O_i.

The preference coefficient p_{ik} may reflect:

- operator's preferences of platforms,
- the distance of the track k to the connecting trains,
- the length of the route used by train i arriving to or departing from platform track k. The smoother and shorter the route is, the less the possibility of a conflict with other trains is, hence the probability of delay propagation decreases.

In our model, coefficient p_{ik} is set according to the following formula:

$$p_{ik} = \begin{cases} 1 & \text{if track } k \text{ is the planned (or desired) track for train } i \\ 0.9 & \text{if track } k \text{ is located at the same platform as the planned track} \\ 0.8\left(\frac{s_i^{\max} - s_{ik}}{s_i^{\max} - s_i^{\min}}\right) & \text{otherwise} \end{cases}$$

Sets of objects

K	set of all platform tracks
$K(i)$	set of feasible platform tracks for train i
U	set of all arriving, departing, and transit trains
$W(j)$	set of all connecting trains, which has to wait for train j
$V^{aa} = \{(i,j) : i,j \in U,\ i<j, \lvert t_i^{Pa} - t_j^{Pa}\rvert \le t^{\max}\}$	set of ordered pairs of those trains that may arrive concurrently
$V^{ad} = \{(i,j) : i,j \in U,\ i<j, \lvert t_i^{Pa} - t_j^{Pd}\rvert \le t^{\max}\}$	set of ordered pairs of those trains that arriving train i and departing train j may travel concurrently
$V^{da} = \{(i,j) : i,j \in U,\ i<j, \lvert t_i^{Pd} - t_j^{Pa}\rvert \le t^{\max}\}$	set of ordered pairs of those trains that departing train i and arriving train j may travel concurrently
$V^{dd} = \{(i,j) : i,j \in U,\ i<j, \lvert t_i^{Pd} - t_j^{Pd}\rvert \le t^{\max}\}$	set of ordered pairs of those trains that may depart concurrently

Decision and Auxiliary Variables of the Model

$$\text{for } i,j \in U,\ k \in K(i) : x_{ik} = \begin{cases} 1 & \text{if track } k \text{ is assinged to train } i \\ 0 & \text{otherwise} \end{cases}$$

u_i difference between the planned and real arrival time of train i at a platform, $i \in U$

v_i difference between the planned and real departure time of train i from a platform, $i \in U$.

The following auxiliary variables $\boldsymbol{y}$ are introduced for the couple of those trains i and j that may travel concurrently. They enable to express safety headways between conflicting trains.

$$\text{for } i,j \in U,\ i<j : y_{ij}^{aa} = \begin{cases} 1 & \text{if train } i \text{ arrives before train } j \text{ arrives} \\ 0 & \text{otherwise} \end{cases}$$

$$\text{for } (i,j) \in V^{ad} : y_{ij}^{ad} = \begin{cases} 1 & \text{if train } i \text{ arrives before train } j \text{ departs} \\ 0 & \text{otherwise} \end{cases}$$

$$\text{for } (i,j) \in V^{da} : y_{ij}^{da} = \begin{cases} 1 & \text{if train } i \text{ departs before train } j \text{ arrives} \\ 0 & \text{otherwise} \end{cases}$$

$$\text{for } (i,j) \in V^{dd} : y_{ij}^{dd} = \begin{cases} 1 & \text{if train } i \text{ departs before train } j \text{ arrives} \\ 0 & \text{otherwise} \end{cases}$$

After these preliminaries, the mathematical model can be written as follows:

$$\textit{minimise} \quad \sum_{i \in U} c_i(u_i + v_i) \tag{1}$$

$$\textit{maximise} \quad \sum_{i \in U} \sum_{k \in K(i)} p_{ik} x_{ik} \tag{2}$$

subject to

$$v_i + t_i^{Pd} \geq u_i + t_i^{Pa} + t^{\min} \quad \forall i \in U \tag{3}$$

$$v_i + t_i^{Pd} \geq u_j + t_j^{Pa} + t^{Cn} \quad \forall j \in U;\ i \in W(j) \tag{4}$$

$$\begin{aligned} &u_{i'} + t_{i'}^{Pa} \geq u_i + t_i^{Pa} + h(i,k,i',k')^{aa} - M(1 - y_{ii'}^{aa}) - M(1 - x_{ik}) - M(1 - x_{i'k'}) \\ &\forall (i,i') \in V^{aa}, k \in K(i), k' \in K(i') : a(I_i,k,I_{i'},k') \end{aligned} \tag{5}$$

$$\begin{aligned} &u_i + t_i^{Pa} \geq u_{i'} + t_{i'}^{Pa} + h(i',k',i,k)^{aa} - M y_{ii'}^{aa} - M(1 - x_{ik}) - M(1 - x_{i'k'}) \\ &\forall (i,i') \in V^{aa}, k \in K(i), k' \in K(i') : a(I_i,k,I_{i'},k') \end{aligned} \tag{6}$$

Constraints (7)–(12) are specified for the other combinations of arrival—departure and have similar meaning as (5) and (6).

$$\begin{aligned} &u_i + t_i^{Pa} \geq v_{i'} + t_{i'}^{Pd} + h(i',k,i,k)^{da} - M y_{ii'}^{aa} - M(1 - x_{ik}) - M(1 - x_{i'k}) \\ &\forall (i,j) \in U, i<j, k \in K(i) \cap K(i') \end{aligned} \tag{7}$$

$$\begin{aligned} &u_{i'} + t_{i'}^{Pa} \geq v_i + t_i^{Pd} + h(i,k,i',k)^{da} - M(1 - y_{ii'}^{aa}) - M(1 - x_{ik}) - M(1 - x_{i'k}) \\ &\forall (i,j) \in U, i<j, k \in K(i) \cap K(i') \end{aligned} \tag{8}$$

$$y_{ij}^{aa} = 1 \quad \forall i,j \in U, i \neq j, I_i = I_j, t_i^{Pa} \leq t_j^{Pa} \tag{9}$$

$$\sum_{k \in K(i)} x_{ik} = 1 \quad \forall i \in U \tag{10}$$

$$u_i, v_i \geq 0 \quad \forall i \in U \tag{11}$$

$$x_{ik} \in \{0,1\} \quad \forall i \in U \; \forall k \in K(i) \tag{12}$$

$$y_{ij}^{aa} \in \{0,1\} \quad \forall i,j \in U, i<j \tag{13}$$

$$y_{ij}^{ad} \in \{0,1\} \quad \forall (i,j) \in V^{ad} \tag{14}$$

$$y_{ij}^{da} \in \{0,1\} \quad \forall (i,j) \in V^{da} \tag{15}$$

$$y_{ij}^{dd} \in \{0,1\} \quad \forall (i,j) \in V^{dd} \tag{16}$$

Model Description

Objective function (1) minimises the weighted deviations of the arrival and departure times proposed by the model from the times specified by the timetable. The weights cause that long-distance/high-speed trains will respect planned times and regional trains will be postponed if necessary. The second criterion maximises the desirability of the platform tracks to be assigned to the trains.

Constraint (3) ensures that a minimum dwell time needed for boarding and alighting must be kept.

Constraint (4) states that connecting train i with real departure $v_i + t_i^{Pd}$ has to wait in station to time at least $u_j + t_j^{Pa} + t^{Cn}$.

Constraints (5)–(12) ensure that a minimum headway will be kept between conflicting trains. More precisely, constraint (5) states that if trains i and i' have planned arrival times within $t^{\max}$ and train i arrives at platform track k before train i' arrives at track k', i.e.

$$x_{ik} = 1, \; x_{i'k'} = 1, \; y_{ii'}^{aa} = 1 \tag{17}$$

and trains are on conflicting routes (i.e. $a(I_i, k, I_{i'}, k')$ is *true*), then train i' is allowed to arrive at least $h(i, k, i', k')^{aa}$ minutes later than train i. If at least one of the conditions (23) is not met (e.g. train i is not assigned to track k), then constraint (5) becomes irrelevant as the right-hand side is negative (M is a suitably picked high positive number). If train i' is followed by train i ($y_{ii'}^{aa} = 0$), then i is allowed to arrive at least $h(i', k', i, k)^{aa}$ minutes later than i', which is ensured by constraint (6). Constraints (7)–(12) have a similar meaning for the other combinations of arrival—departure.

Constraints (13)–(14) ensure that a train will not be dispatched to an occupied track. If train i' is followed by train i ($y_{ii'}^{aa} = 0$) and both trains arrive at the same track k, then i is allowed to arrive at least $h(i', k, i, k)^{da}$ minutes after train i' leaves

track k, which is expressed by constraint (13). Constraint (14) holds for the reverse order of trains i, i'.

Constraint (15) states that y_{ij}^{aa} is 1 if train i is followed by train j at the arrival and both trains travel on the same in-line.

Constraint (16) ensures that each train is always dispatched to exactly one platform track.

The remaining obligatory constraints (17)–(22) specify the definition domains of the variables.

This multiple-criteria optimisation problem was solved using the lexicographic approach, where the objective functions are ranked according to their importance. In the problem at hand, the first objective function (i.e. to meet the timetable) is more important that the second one (i.e. to respect track preferences). This ordering reflects how decisions are currently made in practice. The solution technique consists of two steps. In the first step the problem (1), (3)–(22) is solved giving the best value of the weighted sum of deviations f_1^{best}. Then the constraint

$$\sum_{i \in U} c_i(u_i + v_i) \leq f_1^{best} \tag{18}$$

is added and the model (2)–(22), (24) is solved. Because both MIP problems are hard and the optimal solutions cannot be found within a reasonable time limit, we decided to implement the local branching heuristic [7] using the general optimisation software *Xpress*.

3 Case Study

The model was verified by using the real data of Prague main station and the timetable valid for the years 2004/2005. Prague main station is a large station that at the given time had 7 platforms, 17 platform tracks and 8 arrival or departure line tracks. According to the timetable 2004/2005, the station dealt with 288 regular passenger trains per a weekday. We could use any timetable for validation, however we used the timetable valid for 2004/2005 because we knew that it was done with some mistakes. We wanted to demonstrate that our model is valid, can detect every possible conflict in the timetable and suggest its solution.

Since the model with 288 trains contains 41,279 variables and 595,323 constraints, it is not possible to solve it to optimality in a reasonable time. That is why the decomposition of the problem must be done. The planning period (a day) was divided into shorter time periods. They were chosen in such a way so that the morning and evening peak hours were taken as a whole and the rest of the day was divided into shorter periods with approximately the same number of trains. The resulting time intervals can be seen in Table 1.

Table 1 Results of experiments for the decomposed planning period and shortened change time

Time interval	No. of trains	No. of variables	No. of constraints	Value of 1st objective function	Value of 2nd objective function	Delay on arrival (min)	Delay on departure (min)	No. of trains allocated to different platform
0:00–5:00	20	393	6,960	0	20.0	0	0	0
5:00–8:00	56	2,280	41,965	12	54.6	2	2	5
8:00–10:00	45	1,576	32,870	13	41.8	0	5	8
10:00–12:00	37	1,091	21,692	6	35.2	0	2	5
12:00–15:00	52	1,943	35,804	11	47.9	1	2	9
15:00–18:00	54	1,993	35,028	6	54.0	0	2	0
18:00–24:00	77	3,682	57,842	14	75.7	2	4	4

Table 2 Results of experiments for the decomposed planning period and normal change time

Time interval	No. of trains	No. of variables	No. of constraints	Value of 1st objective function	Value of 2nd objective function	Delay on arrival (min)	Delay on departure (min)	No. of trains allocated to different platform
0:00–5:00	20	393	6,960	10	20.0	0	8	0
5:00–8:00	56	2,280	41,965	12	54.6	2	2	5
8:00–10:00	45	1,576	32,870	13	41.8	0	5	8
10:00–12:00	37	1,091	21,692	12	35.2	0	4	5
12:00–15:00	52	1,943	35,804	11	47.9	1	2	10
15:00–18:00	54	1,993	35,028	6	54.0	0	2	0
18:00–24:00	77	3,682	57,842	14	75.7	2	4	4

For every time interval, the mathematical programming model was solved using the lexicographic approach described in the previous section. In case that the exact algorithm (branch and bound method) did not finish in a predetermined computational time (30 min) then the local branching heuristic was applied.

The computational experiments were performed for a shortened change time which is 4 min in Prague main stations, as well as for the normal change time (8 min). The results for the shortened time are reported in Table 1 and for the normal change time in Table 2.

The results of computational experiments show that the timetable was not correct with regard to safety requirements. There were some trains travelling on conflicting routes concurrently. That is why their desired arrival or departure times could not be kept. Moreover, in some cases the original timetable did not respect desired time passengers need to change trains. However the model respects such connections. The best solution proposed by the model with the shortened change time delays 3 trains at arrival by 5 min and 12 trains at departure by 17 min in total, and dispatches 31 (11 %) trains to platform tracks different from the planned ones. Departures of 7 trains are postponed by 1 min and 5 trains by 2 min. For the normal change time, 3 trains are delayed at arrival by 5 min and 16 trains are delayed at departure by 27 min in total (8 trains by 1 min, 6 trains by 2 min, 1 train by 3 min and 1 train by 4 min). 32 trains are dispatched to platform tracks different from the planned ones.

Other experiments were performed to investigate:

- how decomposition of planning period influences the computational time and the quality of obtained solution within 30 min limit for computing,
- how train delays influence the track occupancy plan,
- efficiency of the branch and bound and local branching methods.

4 Conclusion

In the paper, a mixed integer programming model for the train platforming problem at a passenger railway station is described. The model proposes a track occupancy plan that respects safety constraints for train movements and relations between connecting trains, minimises deviations of the arrival and departure times from the timetable and maximises the desirability of the platform tracks to be assigned to the trains. The model could serve as a planner's decision supporting tool.

Acknowledgments This research was supported by the Scientific Grant Agency of the Ministry of Education of the Slovak Republic and the Slovak Academy of Sciences under project VEGA 1/0296/12 "Public service systems with fair access to service" and by the Slovak Research and Development Agency under project APVV-0760-11 "Designing of Fair Service Systems on Transportation Networks".

References

1. Billionet A (2003) Using integer programming to solve the train-platforming problem. Transp Sci 37(2):213–222
2. Zwaneveld PJ (1997) Railway planning—routing of trains and allocation of passenger lines. Ph. D. thesis, Erasmus University Rotterdam, Rotterdam, The Netherlands
3. Zwaneveld PJ, Kroon LG, van Hoesel SPM (2001) Routing trains through a railway station based on a node packing model. Eur J Oper Res 128:14–33
4. Carey M, Carville S (2003) Scheduling and platforming trains at busy complex stations. Transp Res Part A 37:195–224
5. Bažant M, Kavička A (2009) Artificial neural network as a support of platform track assignment within simulation models reflecting passenger railway stations. Proc Inst Mech Eng Part F J Rail Rapid Transit 223(5):505–515
6. Chakroborty P, Vikram D (2008) Optimum assignment of trains to platforms under partial schedule compliance. Transp Res Part B Methodol 42(2):169–184
7. Fischetti M, Lodi A, Salvagnin D (2009) Just MIP it! In: Maniezzo V, Stützle T, Voß S (eds) Matheuristics. Springer, New York, pp 39–70

Examples of the Implementation of Fuzzy Models in Tourism in the South Moravian Region

Pavel Kolisko

Abstract In geospatial information systems we often come across concepts expressing imprecision, incompleteness, uncertainty or vagueness, just like in everyday life. The degree of uncertainty or vagueness can be expressed through fuzzy set theory by membership functions. The fuzzy sets are more suitable for modelling of the vague phenomena than the classical crisp sets. We ordinarily find out spatial features which are not exactly bounded but are verbally determined. There are two examples of fuzzy exploitation in the South Moravian Region in this paper. Multicriteria decision making of tourism areas uses elementary fuzzy logic knowledge and assessment of bike trail difficulty which is considered according to the compositional rule of inference especially by Mamdani's method and defuzzification processes. The analyses apply the raster modelling using software ArcGIS 10.1, geoprocessing tools and programming language Python.

Keywords GIS · Fuzzy set · Fuzzy logic · Multicriteria decision making · Fuzzy inference · Modus ponens · Compositional rule of inference · Defuzzification · Centroid · Center of gravity · Center of sums

1 Introduction

The term "fuzzy logic" was described by Lofti A. Zadeh in 1965. This many-valued logic characterizes wispy, unclear, vague, uncertain meaning [1]. In usual life we utilize unconfined terms such as steep slope, near the forest. We can speak about "linguistic variables" with linguistic values [2]. Real situations are modelled better by using fuzzy sets with uncertain boundary. Each element is in the set more or less. It is indicated by a degree of membership to a fuzzy set, by value between zero and

P. Kolisko (✉)
Faculty of Science, Department of Geography, Masaryk University, Kotlářská 2, Brno, Czech Republic
e-mail: 248680@mail.muni.cz

I. Ivan et al. (eds.), *Geoinformatics for Intelligent Transportation*,
Lecture Notes in Geoinformation and Cartography,
DOI 10.1007/978-3-319-11463-7_12

one. Fuzzy sets are perceived as generalization of classical crisp sets which are their specific case. Quality "to be fuzzy" is often expressed as ambiguity, not as inaccuracy or uncertainty.

Definition of fuzzy set using the characteristic function.

Let $\boldsymbol{X}$ be a universe set (crisp set). A fuzzy set A of the universe $\boldsymbol{X}$ is defined by a characteristic function called membership function μ_A such that $\mu_A : \boldsymbol{X} \rightarrow \langle 0, 1 \rangle$ where $\mu_A(x)$ is the membership value of x in A.

The membership value assigns a degree of membership to a fuzzy set to any element.

$\mu_A(x) = 1$	element x belongs to a fuzzy set for sure
$\mu_A(x) = 0$	element x doesn't belong to a fuzzy set for sure
$0 < \mu_A(x) < 1$	we aren't sure if element x belongs to a fuzzy set.

Each function $\boldsymbol{X} \rightarrow \langle 0, 1 \rangle$ determines any fuzzy set definitely.

The membership degree to the fuzzy set is specified by mathematical functions [3].

We usually compose the membership functions of elementary linear functions. These are trapezoidal, triangular, S-shaped and L-shaped membership functions. We often use more complicated rounded functions, too as Gaussian function, bell-shaped function, sinusoidal function etc.

2 Operations on Fuzzy Sets and Fuzzy Logic

Operations complement, union and intersection on fuzzy sets are defined in similar way as on crisp sets [4].

The standard intersection of two fuzzy sets A and B is a fuzzy set with the membership function defined by

$$\mu_{A \cap B}(x) = \min(\mu_A(x), \mu_B(x)). \quad \text{Zadeh's intersection}$$

The standard union of two fuzzy sets A and B is a fuzzy set with the membership function defined by

$$\mu_{A \cup B}(x) = \max(\mu_A(x), \mu_B(x)) \quad \text{Zadeh's union}$$

The standard complement of fuzzy set A is a fuzzy set with the membership function defined by

$$\mu_{\bar{A}}(x) = 1 - \mu_A(x) \quad \text{Zadeh's complement}$$

Functions for modelling fuzzy conjunction are called triangular norms (t-norms), for fuzzy disjunction triangular conorms (t-conorms). They are assumed as functions of two variables defined on a unit square.

Basic t-norms

$T_M(x,y) = \min(x,y)$ Minimum t-norm

$T_P(x,y) = xy$ product t-norm

$T_L(x,y) = \max(0, x+y-1)$ Łukasiewicz t-norm

$T_D(x,y) = \begin{cases} \min(x,y) & \text{if max(x,y) = 1} \\ 0 & \text{else} \end{cases}$ drastic t-norm

The drastic t-norm is the smallest t-norm and the minimum t-norm is the largest t-norm, because we have $T_D(x,y) \leq T_L(x,y) \leq T_P(x,y) \leq T_M(x,y)$.

Basic t-conorms

$S_M(x,y) = \min(x,y)$ Maximum t-conorm

$S_P(x,y) = x+y-xy$ probabilistic t-conorm

$S_L(x,y) = \min(1, x+y)$ Łukasiewicz t-conorm

$S_D(x,y) = \begin{cases} \max(x,y) & \text{if min(x,y) = 0} \\ 1 & \text{else} \end{cases}$ drastic t-conorm

The maximum t-conorm S_M is the smallest t- conorm, drastic t-conorm is the largest t-conorm, because we have $S_D(x,y) \geq S_L(x,y) \geq S_P(x,y) \geq S_M(x,y)$.

Now we can generalize expression of fuzzy sets union and intersection.

The intersection of fuzzy sets based on t-norm T is the fuzzy set with the membership function defined by

$$\mu_{A \cap_T B}(x) = T(\mu_A(x), \mu_B(x)).$$

The union of fuzzy sets based on t-conorm T is the fuzzy set with the membership function defined by

$$\mu_{A \cup_S B}(x) = S(\mu_A(x), \mu_B(x)).$$

Therefore, the standard intersection and union are special cases $A \cap B = A \cap_{T_M} B$ and $A \cup B = A \cup_{S_M} B$.

The fuzzy negation, the complement of the fuzzy set and various implications are defined similarly [5].

2.1 Fuzzy Relations

Let $\boldsymbol{X}$, $\boldsymbol{Y}$ be crisp sets. A binary fuzzy relation R from $\boldsymbol{X}$ to $\boldsymbol{Y}$ is any fuzzy subset R of the set $\boldsymbol{X} \times \boldsymbol{Y}$. Fuzzy relation R is described by the membership function $\mu_R : \boldsymbol{X} \times \boldsymbol{Y} \rightarrow \langle 0, 1 \rangle$.

We can define intersection on t-norm T and union on t-conorm S.

$$\mu_{A\cap_T B}(x,y) = T(\mu_A(x,y), \mu_B(x,y))$$
$$\mu_{A\cup_S B}(x,y) = S(\mu_A(x,y), \mu_B(x,y))$$

Definition composition of fuzzy relations

Let $\boldsymbol{X}$, $\boldsymbol{Y}$, $\boldsymbol{Z}$ be crisp sets, A, B binary fuzzy relations and T t-norm. Then sup-T composition of fuzzy relations A and B is fuzzy relation $C = A \circ_T B$ with the membership function $\mu_C(x,z) = \sup_{y\in Y} T(\mu_A(x,y), \mu_B(x,y))$.

3 Fuzzy Inference and Generalized Modus Ponens

The fuzzy inference is a process which is applied to reasoning based on vague concept. The inductive method *modus tollens* and the deductive method *modus ponens* are the basic rules of inference in binary logic. In modus ponens we infer validity of a propositional formula q from validity of implication $p \Rightarrow q$ and validity of premise of a propositional formula p.

3.1 Generalized Modus Ponens

In fuzzy reasoning we use a generalized modus ponens according to following statement, where A, B, A', B' are fuzzy sets, X, Y linguistic variables. The scheme consists of a rule or a premise (prerequisite), an observing and a conclusion (consequence).

Rule	if X is A, then Y is B
Observing	X is A'
Conclusion	Y is B'

The observing does not have to correspond to the premise in the rule. According to finding degree of comparison between premise X is A in the rule and current observing X is A' it happens modification conclusion Y is B in the rule and getting value B' of variable Y. If it is $A' = A$ in observing, it have to be valid $B' = B$. In fact, we operate more rules, input and output variables.

Example:

Rule	if the slope is moderate, the bike trail difficulty is easy
Observing	slope is steeper
Conclusion	bike trail difficulty is harder

3.2 Compositional Rule of Inference

Practically we need to interpret verbal values of sets *A, B* mathematically and define the rule of fuzzy relation *R* between variables *X, Y*. We use the compositional rule of inference for assignment value B' of variable *Y*, which corresponds with value A' of variable *X*.

We can get term, where the set B' is the sup-min composition of the fuzzy set A' and the fuzzy relation *R*, written as $B' = A' \circ R$ with the membership [6]

$$\mu_{B'}(y) = \sup_{x \in X} \min(\mu_{A'}(x), \mu_R(x, y)) \quad \text{standard intersection}$$

or generally

$$\mu_{B'}(y) = \sup_{x \in X} \quad T(\mu_{A'}(x), \mu_R(x, y)) \quad \text{union based on t-norm } T$$

Rule	(X, Y) is $R(A, B)$
Observing	X is A' compositional rule of inference on t-norm T
Conclusion	Y is B', $B' = A' \circ_T R(A, B)$

We have to keep generalized modus ponens during relational reasoning, too, i.e. $A \circ_T R(A, B) = B$.

The fuzzy relations can be modelled by a logical implication or by a cartesian product T^* based on t-norm. We confine to the second possibility and we get:

$$\mu_{R(A,B)}(x, y) = T^*(\mu_A(x), \mu_B(y))$$
$$\mu_{B'}(y) = \sup_{x \in X} \quad \min(\mu_{A'}(x), T^* \mu_A(x), \mu_B(y)))$$

We can generalize the properties to t-norm *T*:

$$\mu_{B'}(y) = \sup_{x \in X} \; T(\mu_{A'}(x), \; T^*(\mu_A(x), \; \mu_B(y)))$$

If we choose $T = T^* = T_M$ we get:

$$\mu_{B'}(y) = \sup_{x \in X} \; \min(\mu_{A'}(x), \; \min(\mu_A(x), \; \mu_B(y))) \quad \textit{Mamdani's method}$$

For $T = T_M$ and $T^* = T_P$, it is: [5].

$$\mu_{B'}(y) = \sup_{x \in X} \; \min(\mu_{A'}(x), \; \mu_A(x) \cdot \mu_B(y)) \quad \textit{Larsen's method}$$

4 Mamdani's Method

Let's have a look at Mamdani's method in detail [7].

Let $B = \{P_1, P_2, \ldots, P_k\}$ be a knowledge base with k rules for n input variables $X_1, X_2, \ldots, X_n$ and one output variable Y. Each of the variables X_i have the verbal value $A_{i,j}$ in j-th rule, variable Y has the verbal value B_j, where $i = 1, 2, \ldots, n$, $j = 1, 2, \ldots, k$. For Mamdani's regulator are defined:

Rules	P_1 :	if X_1 is A_{11} and X_2 is A_{21} and $\cdots$ and X_n is A_{n1}, then Y is B_1
	P_2 :	if X_1 is A_{12} and X_2 is A_{22} and $\cdots$ and X_n is A_{n2}, then Y is B_2
	$\ldots$	
	P_k :	if X_1 is A_{1k} and X_2 is A_{2k} and $\ldots$ and X_n is A_{nk} then Y is B_k
Observing	X_1 is A'_1 and X_2 is A'_2 and$\ldots$and X_n is A'_n	
Conclusion	Y is B'	

Because the effort with the whole of the relation is numerically arduous, it is preferable to use the approach FITA (first inference then aggregation), which means reasoning of conclusion rule-by-rule, where the final aggregate conclusion is $B' = \bigcup_{j=1}^{k} B'_j$.

Therefore $\mu_{B'}(y)$ can be presented as $\mu_{B'}(y) = \max_{j=1}^{k} \mu_{B'_j}(y) = \max_{j=1}^{k} \min\left(w_j, \mu_{B_j}(y)\right)$, where $w_j = \min\left(w_{1j}, w_{2j}, \ldots, w_{nj}\right)$ is the total weight of j-th rule, numbers $w_{1j}, w_{2j}, \ldots, w_{nj}$ are particular degrees of fulfilment of the premises in j-th rule X_1 is A_{1j}, X_2 is $A_{2j}, \ldots,$ X_n is A_{nj}.

We can generalize the properties to t-norm T.

Consider the generalisation of t-norm T for an intersection and t-norm T^* for an assignment of the relation (Fig. 1). The membership function for degrees $w_j = T\left(w_{1j}, w_{2j}, \ldots, w_{nj}\right)$ is defined as $\mu_{B'}(y) = \max_{j=1}^{k} \mu_{B'_j}(y) = \max_{j=1}^{k} T^*\left(w_j, \mu_{B_j}(y)\right)$.

For Larsen's method is written $T = T_M$ and $T^* = T_P$.

5 Defuzzification

If we apply crisp inputs, the results of inference are fuzzy outputs. We often need to find the particular real value of output by defuzzification. There are several methods to defuzzify. We can distribute them to methods searching the most acceptable solution and methods of the best compromise [8].

The methods of the most acceptable solution are presented by the methods of the most important maximum with selection of the biggest value of the membership functions placed leftmost, middlemost or rightmost—Left of Maximum (LoM), Mean of Maximum (MoM), Right of Maximum (RoM).

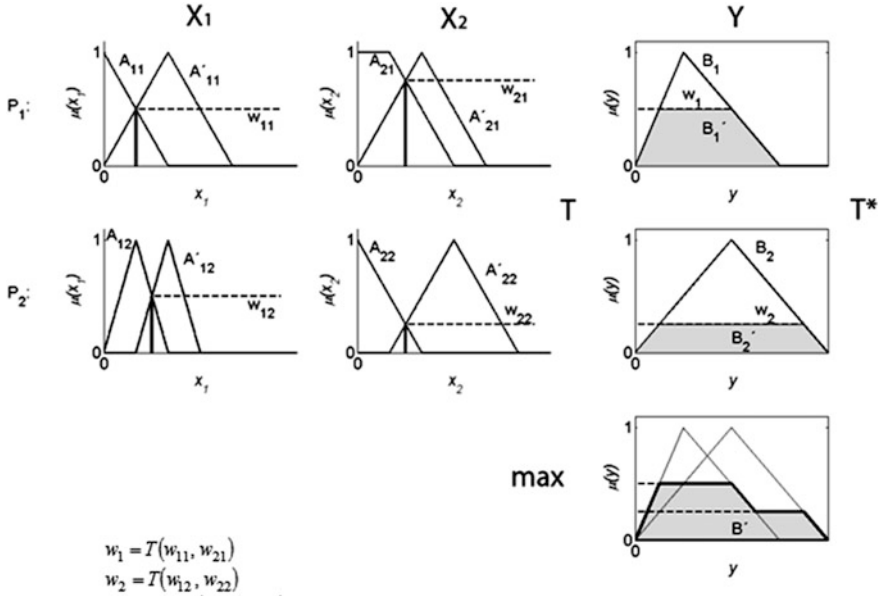

$$w_1 = T(w_{11}, w_{21})$$
$$w_2 = T(w_{12}, w_{22})$$
$$\mu_{B_1'}(y) = T^*(w_1, \mu_{B_1}(y))$$
$$\mu_{B_2'}(y) = T^*(w_2, \mu_{B_2}(y))$$
$$\mu_{B'}(y) = \max(\mu_{B_1'}(y), \mu_{B_2'}(y))$$
$$\mu_{B'}(y) = \max_{j=1}^{2} T^*(T(w_{1j}, w_{2j}), \mu_{B_j}(y))$$

Fig. 1 Illustrative scheme of the universal regulator with two rules, two input variables and one output variable

Methods of the best compromise include:

Center of Gravity (CoG)—the centroid of area (the centroid of the plane figure given by union of the part areas bounded by particular membership functions).
Center of Sums (CoS)—the centroid of sums (the centroid of the plane figure given by function, which is equal to the sum of the particular membership functions in the rules)
Center of Maximum (CoM)—the centroid of singletons (the centroid of the typical values, e.g. MoM, for the particular membership functions of the rules).

5.1 CoG

It makes for finding the first coordinate of the centroid of area bounded by the membership function $\mu_{B'}$. The method is mathematically difficult because we need to know the membership function and calculate the Riemann integrals. In the

reasoning of conclusion rule-by-rule $B' = \bigcup_{j=1}^{k} B'_j$ is $\mu_{B'}(y) = \max_{1 \le j \le k} \mu_{B'_j}(y)$. The situation is simpler, if the universe of the output variable is discrete subset of real numbers $Y = \{y_1, y_2, \ldots, y_r\}$.

$$y_{B'}^{CoG} = \frac{\int_Y \mu_{B'}(y)\, y\, dy}{\int_Y \mu_{B'}(y)\, dy} = \frac{\int_Y \left(\max_{1 \le j \le k} \mu_{B'_j}(y) \right) y\, dy}{\int_Y \left(\max_{1 \le j \le k} \mu_{B'_j}(y) \right) dy} \quad \text{continuous membership function}$$

$$y_{B'}^{CoG} = \frac{\sum_{i=1}^{r} \mu_{B'}(y_i) y_i}{\sum_{i=1}^{r} \mu_{B'}(y_i)} \quad \text{discrete membership function}$$

5.2 CoS [6]

It serves to find the first coordinate of the centroid of area which is bounded by the function defined as sum of the membership functions $\mu_{B'_j}$. The method is easy-to-use because it does not need to determine the conclusion B'. If the particular conclusions of rules do not overlap, the result of the method CoS is the same as for the method CoG.

$$y_{B'_j}^{CoS} = \frac{\int_Y \left(\sum_{1 \le j \le k} \mu_{B'_j}(y) \right) y\, dy}{\int_Y \left(\sum_{1 \le j \le k} \mu_{B'_j}(y) \right) dy} = \frac{\sum_{1 \le j \le k} \left(\int_Y \mu_{B'_j}(y)\, y\, dy \right)}{\sum_{1 \le j \le k} \left(\int_Y \mu_{B'_j}(y)\, dy \right)} \quad \text{continuous membership function}$$

$$y_{B'_j}^{CoS} = \frac{\sum_{i=1}^{r} y_i \sum_{j=1}^{k} \mu_{B'_j}(y_i)}{\sum_{i=1}^{r} \sum_{j=1}^{k} \mu_{B'_j}(y_i)} \quad \text{discrete membership function}$$

5.3 CoM

The first coordinate of the membership function is written for each conclusion of rule by the method of the most important maximum (Mean of Maximum) and the result is the centroid of singletons.

$$y_{B'_j}^{CoM} = \frac{\sum_{j=1}^{k} y_j \cdot \mu_{B'_j}(y_j)}{\sum_{j=1}^{k} \mu_{B'_j}(y_j)}$$

6 Multicriteria Decision Making of Tourist Areas

The multicriteria decision analysis was required by officials of The Department of Regional Development to make out the most important tourist areas especially for family with children in the South Moravian Region. This assignment was determined by several required parameters. In our aspect we wanted to consider healthy environment, forest accessibility, proximity of bodies of water, optimum distance of the important roads, near historical and cultural monuments and density of the bike and hiking trails.

The evaluation was made both by fuzzy sets and crisp sets in order to compare them. The fuzzy raster maps were the results. The choice of the expression of the membership functions was performed by software to plotting mathematical curves. Below there are mentioned particular criteria, data sources (RA—regional authority data), qualities and units. Then the selected tools from Spatial Analyst Tools with their configuration follow.

Environmentally significant areas (Ea)—**protected areas, natural parks (data RA, distance, meter)**

Overlay—Fuzzy Membership—Small (midpoint 500, spread 2) (Fig. 2).

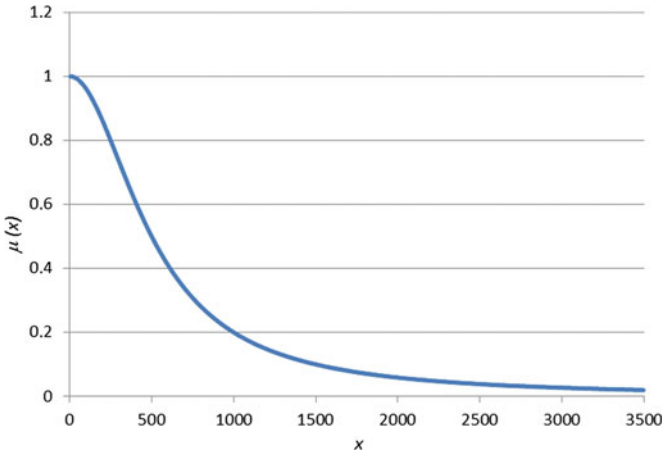

Fig. 2 Membership function—environment

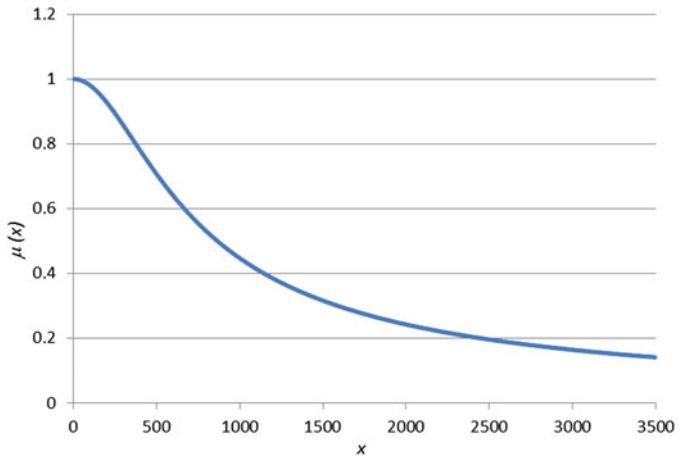

Fig. 3 Membership function—forests

$$\mu(x) = \frac{1}{1 + \left(\frac{x}{500}\right)^2}$$

Forests accessibility (Fa) (data CEDA StreetNet, distance, meter)

Overlay—Fuzzy Membership—Small (midpoint 500, spread 2)—Somewhat (dilatation) (Fig. 3).

$$\mu(x) = \sqrt{\frac{1}{1 + \left(\frac{x}{500}\right)^2}}$$

Bodies of water (Bv) (data CEDA StreetNet, distance, meter)

Map Algebra—Raster calculator (Fig. 4).

$$\mu(x) = \begin{cases} 1 & \text{if } x < 100 \\ \frac{4000 - x}{3900} & \text{if } 100 \le x \le 4000 \\ 0 & \text{if } x > 1000 \end{cases}$$

Roads (Ro)—motorways and national roads (data CEDA StreetNet, distance, meter)

Map Algebra—Raster calculator (Fig. 5)

$$\mu(x) = \begin{cases} x \le 4000 & \text{if } \frac{1}{2}\left(1 - \cos\left(\pi \frac{x}{4000}\right)\right) \\ 4000 < x < 10000 & \text{if } 1 \\ 10000 \le x \le 30000 & \text{if } \frac{30000 - x}{20000} \\ x > 30000 & \text{if } 0 \end{cases}$$

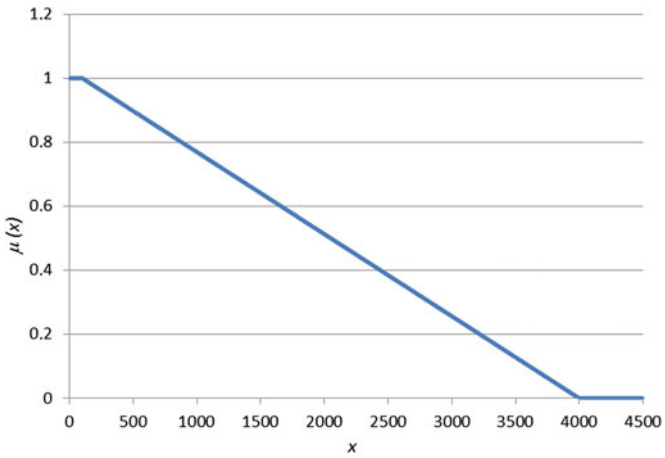

$$\text{for crisp sets} \quad \mu(x) = \begin{cases} 1 & \text{if} \quad x \le 2000 \\ 0 & \text{if} \quad x > 2000 \end{cases}$$

Fig. 4 Membership function—water

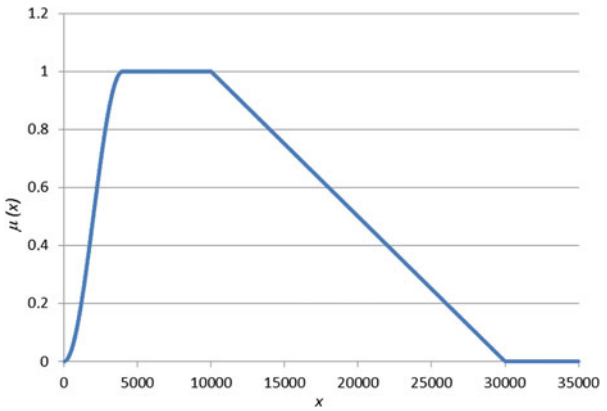

$$\text{for crisp sets} \quad \mu(x) = \begin{cases} 0 & \text{if} \quad x < 4000 \\ 1 & \text{if} \quad 4000 \le x < 20000 \\ 0 & \text{if} \quad x \ge 20000 \end{cases}$$

Fig. 5 Membership function—roads

Historical and cultural monuments (Hm) **(data RA, distance, meter)**
Map Algebra—Raster calculator (Fig. 6)

$$\mu(x) = \begin{cases} 1 & \text{if} \quad x < 500 \\ \frac{15000 - x}{14500} & \text{if} \quad 500 \le x \le 15000 \\ 0 & \text{if} \quad x > 15000 \end{cases}$$

Bike trails (Bt)—net density (data RA)
Density—Kernel Density (radius 3 km), normalization
Hiking trails (Ht)—net density (data RA)
Density—Kernel Density (radius 3 km), normalization

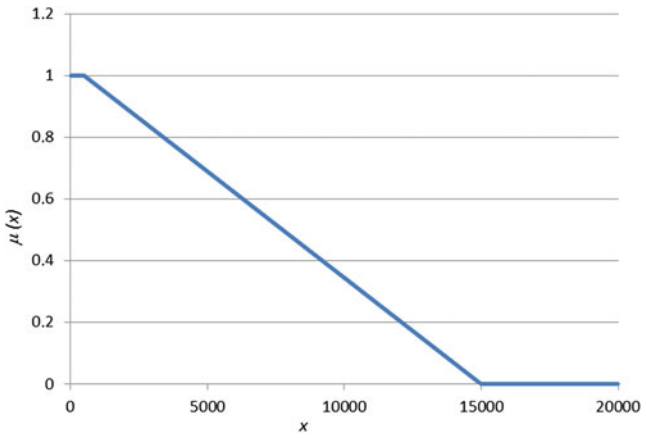

for crisp sets

$$\mu(x) = \begin{cases} 1 & \text{if} \quad x \leq 7000 \\ 0 & \text{if} \quad x > 2000 \end{cases}$$

Fig. 6 Membership function—monuments

6.1 Using ModelBuilder

The logical model of raster analysis is created in ModelBuilder. In the preliminary stage the necessary data are collected and then union, selection, buffering and density are executed. The vector data are converted to raster data. If it is possible,

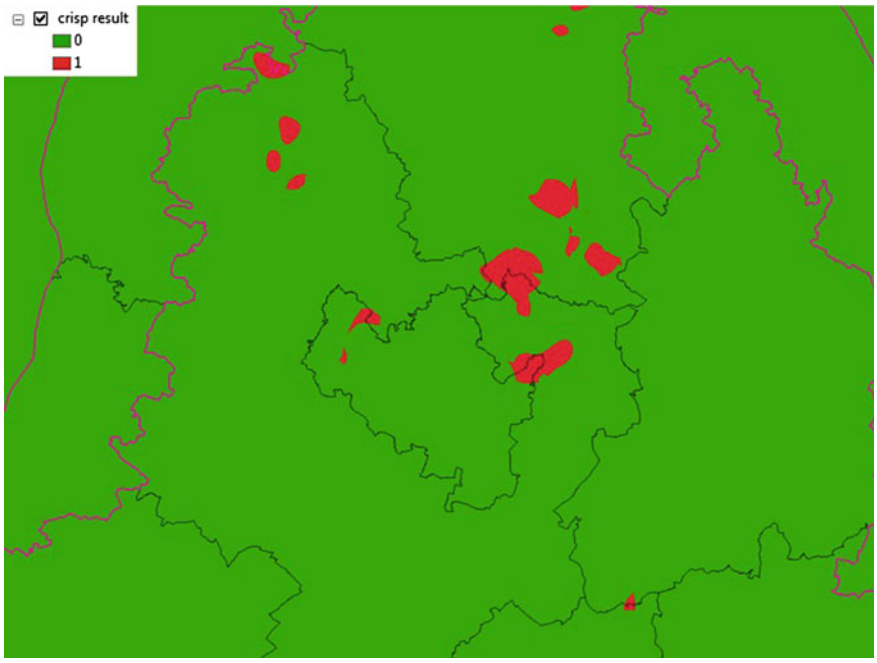

Fig. 7 The result of analysis near Brno and surrounding—crisp sets

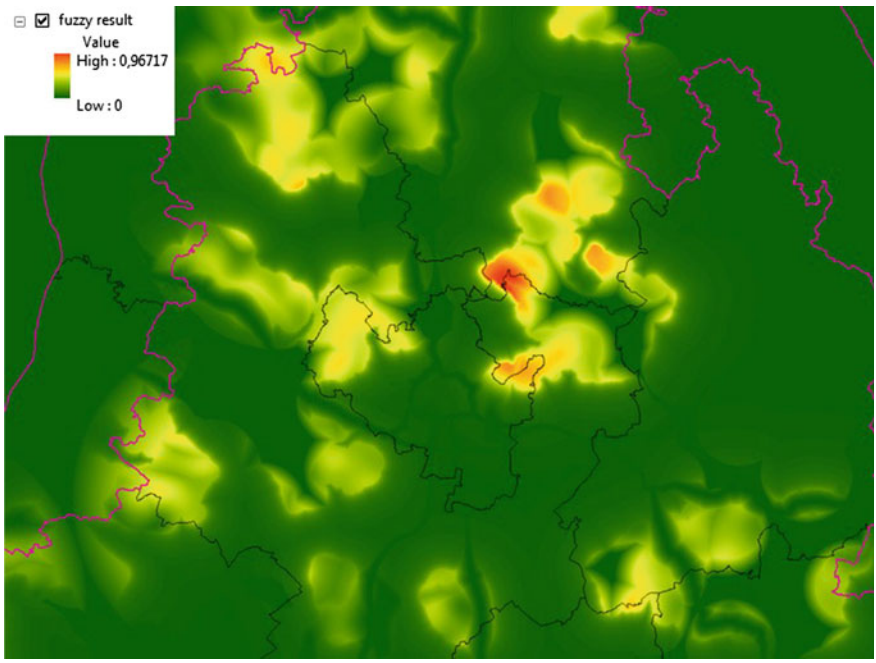

Fig. 8 The result of analysis near Brno and surrounding—fuzzy sets

the data reclassification and eventually euclidean distance are computed. Finally we can implement the raster operations to progressive evaluation of result according to desired expression written as (Fig. 7)

$$Ea \cap Fa \cap Bv \cap Ro \cap Hm \cap (Bt \cup Ht)$$

Our intent of this spatial model was to represent a base map for analysis of tourism regions in South Moravia. Final fuzzy map (Fig. 8) depends on the expression and description of the problem, determination of particular criteria and assignment of the degree of membership to fuzzy sets. It is important to specify operations on fuzzy sets (in this case standard intersection and union). The data quality is essential.

6.2 Conclusion

This multicriteria decision analysis carries the obtaining of the basic spatial placement of significant tourist areas. It provides the results determined to compare with statistical data such as the attendance and the attractiveness of region, the substantiation of the low attendance in some places, finding their developing, linkup to public services and the direct consequences for hiking and bike trails.

7 Solution of Bike Trail Difficulty Rating

When we think about cycle route, we consider time, weather, trail length, points of interest and we solve the route difficultness or demandingness, too. We find out the route quality and suitability for different categories of target bikers. Bike trail difficulty recognizes whether the route is suitable for families with children, for recreational sportsmen, maybe for athletes. In 2003 and 2005 the projects were made with intent to collect information about cycle routes and their facilities. In 2007 the data were updated by terrain research, especially the status of surface and difficulty of bike trails.

During actual checking well-known routes it was verified that the characteristic of bike trail difficulty has already disagreed with the reality. Each rating depends on time, it is affected by the subjective view and data collection is a hard task in terrain. Therefore, we need to utilize another approach for instance by fuzzy reasoning. The slope and the quality or the type of the road surface which were chosen as analytical inputs impact on the difficulty.

The data are published on the web cycling portal of the South Moravian Region http://www.cyklo-jizni-morava.cz, including the interactive bike trail map with choosing routes and points of interest.

The modelling is accomplished over rasters in ArcGIS 10.1 using ModelBuilder and geoprocessing tools, especially Spatial Analyst Tools—Fuzzy Membership, Fuzzy Overlay, Raster Calculator, Cell Statistics and Python.

7.1 Methods

We use two input variables, X_1 for the type of the road surface and X_2 for the angle of the slope (both defined by crisp values) and output variable Y for the bike trail difficulty.

Assume the following input and output fuzzy subsets which are given by verbal values and rules representing their relationship.

Type of road surface (data CEDA StreetNet 2012)

K_1 paved roads (asphalt, pavement, concrete)
K_2 maintained roads (unpaved, gravel)
K_3 other unpaved roads (forest and cart roads)

Angle of slope (DMT 2012, in degrees, cells size 10 m)

S_1 moderate slope
S_2 steep slope

Bike trail difficulty

D_1 small difficulty—easy difficult roads (suitable for families with children)

D_2 intermediate difficulty—more difficult roads (suitable for recreational sportsmen)

D_3 hard difficulty—very difficult roads (suitable for athletes)

Rules	P_1 : if X_1 is K_1 and X_2 is S_1, then Y is D_1
	P_2 : if X_1 is K_2 and X_2 is S_1, then Y is D_1
	P_3 : if X_1 is K_3 and X_2 is S_1, then Y is D_2
	P_4 : if X_1 is K_1 and X_2 is S_2, then Y is D_2
	P_5 : if X_1 is K_2 and X_2 is S_2, then Y is D_3
	P_6 : if X_1 is K_3 and X_2 is S_2, then Y is D_3
Observing	X_1 is K' and X_2 is S'
Conclusion	Y is D'

The fuzzy sets K_1, K_2, K_3 were given by the bell-shaped membership function Near (Midpoint 0, Spread 0.0001) available in the geoprocessing tools of ArcMap in the category Fuzzy Membership (Fig. 9). The function expresses the close localization of the road as a fuzzy line [9] in network of roads (x_1—distance from the road in meters).

Next figures show settings that define S_1, S_2 and D_1, D_2, D_3 (Figs. 10 and 11)

I applied and compared several regulators and defuzzification methods and did the interpretation rule-by-rule. We declare w_j as the total weight of the j-th rule

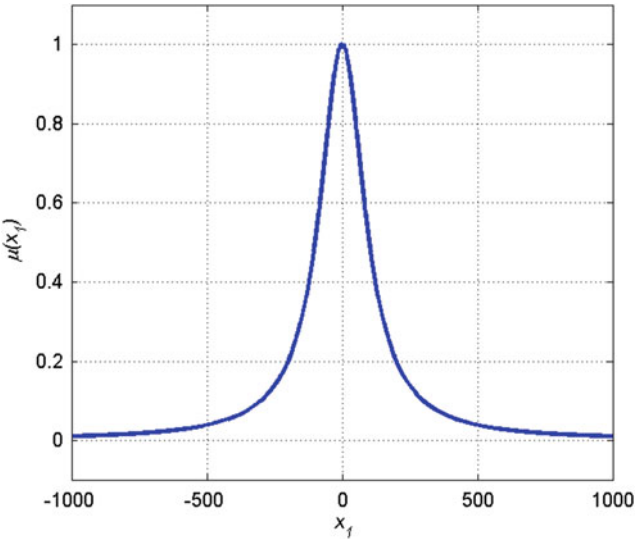

$$\mu(x_1) = \frac{1}{1 + 0{,}0001\, x_1^{\,2}}$$

Fig. 9 Membership function for roads

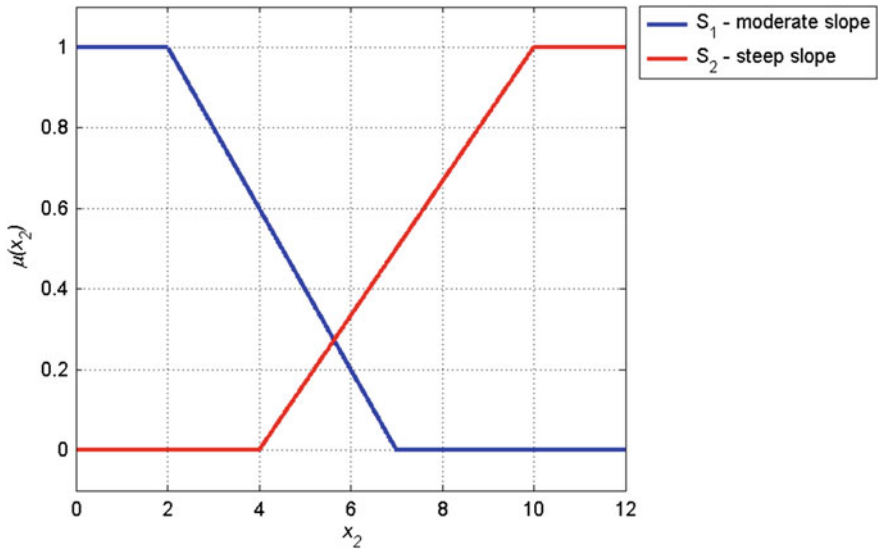

Fig. 10 Membership function for slope

worked from particular weights of premises (roads, slope) w_{1j}, w_{2j}. The membership function of conclusion of the j-th rule is written $\mu_{D'_j}(y)$. This is the most important applied methods.

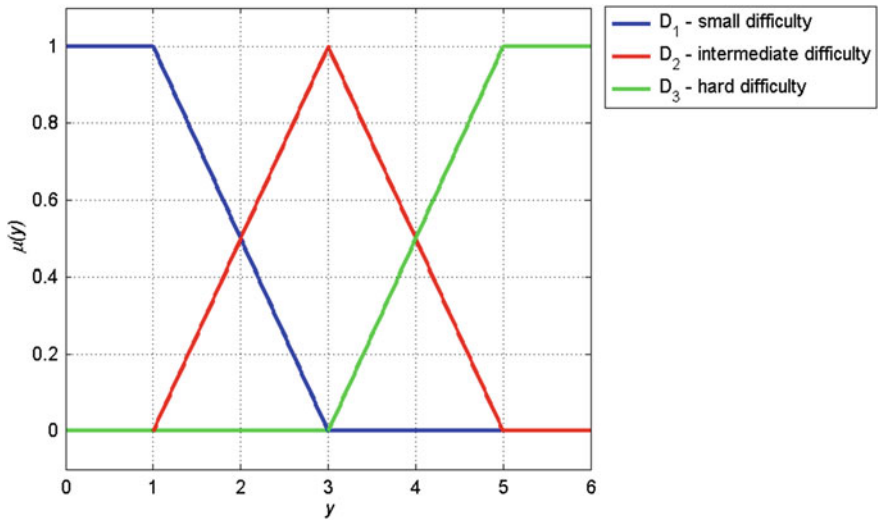

Fig. 11 Membership function for difficulty of road

Mamdani's method (COS-TM-TM, COM-TM-TM)

$$\mu_{D'}(y) = \max_{j=1}^{k} T_M\Big(T_M\big(w_{1j}, w_{2j}\big), \mu_{D_j}(y)\Big) = \max_{j=1}^{k} \min\Big(\min\big(w_{1j}, w_{2j}\big), \mu_{D_j}(y)\Big)$$

Larsen's method (COS-TP-TM)

$$\mu_{D'}(y) = \max_{j=1}^{k} T_P\Big(T_M\big(w_{1j}, w_{2j}\big), \mu_{D_j}(y)\Big) = \max_{j=1}^{k} \Big(\min\big(w_{1j}, w_{2j}\big) \cdot \mu_{D_j}(y)\Big)$$

7.2 Mamdani's Method (COS-TM-TM)

Considering evaluation of the road surface and reasoning of conclusion rule-by-rule, we will choose (COS-TM-TM) the centroid of sums which means calculation.

$$y_{D'_j}^{CoS} = \frac{\sum\limits_{1\le j\le 6}\left(\int\limits_{\boldsymbol{Y}} \mu_{D'_j}(y)\; y\; dy\right)}{\sum\limits_{1\le j\le 6}\left(\int\limits_{\boldsymbol{Y}} \mu_{D'_j}(y)\; dy\right)}$$

$$= \frac{\int\limits_{\boldsymbol{Y}} \mu_{D'_1}(y)\; y\; dy + \int\limits_{\boldsymbol{Y}} \mu_{D'_2}(y)\; y\; dy + \int\limits_{\boldsymbol{Y}} \mu_{D'_3}(y)\; y\; dy + \int\limits_{\boldsymbol{Y}} \mu_{D'_4}(y)\; y\; dy + \int\limits_{\boldsymbol{Y}} \mu_{D'_5}(y)\; y\; dy + \int\limits_{\boldsymbol{Y}} \mu_{D'_6}(y)\; y\; dy}{\int\limits_{\boldsymbol{Y}} \mu_{D'_1}(y) dy + \int\limits_{\boldsymbol{Y}} \mu_{D'_2}(y)\; dy + \int\limits_{\boldsymbol{Y}} \mu_{D'_3}(y)\; dy + \int\limits_{\boldsymbol{Y}} \mu_{D'_4}(y)\; dy + \int\limits_{\boldsymbol{Y}} \mu_{D'_5}(y)\; dy + \int\limits_{\boldsymbol{Y}} \mu_{D'_6}(y)\; dy}$$

The total weight of the j-th rule w_j is the minimum of the particular weights of the premises (roads, slope) w_{1j}, w_{2j} in this rule (simply signed w). The membership function of the conclusion of the j-th rule is presented as $\mu_{D'_j}(y) = \min\Big(w_j, \mu_{D_j}(y)\Big)$. The membership $\mu_{D_j}(y)$ is simply denoted $\mu(y)$.

In the first and the second rule we evaluate small difficulty D_1 (Fig. 12).

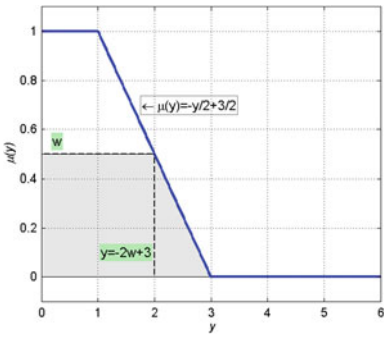

$$\int_0^{-2w+3} w\; y\; dy + \int_{-2w+3}^{3} \left(-\frac{y}{2}+\frac{3}{2}\right) y\; dy = \underline{\frac{2}{3}w^3 - 3w^2 + \frac{9}{2}w}$$

and

$$\int_0^{-2w+3} w\; dy + \int_{-2w+3}^{3} \left(-\frac{y}{2}+\frac{3}{2}\right) dy = \underline{-w^2 + 3w}$$

Fig. 12 Membership function for small difficulty

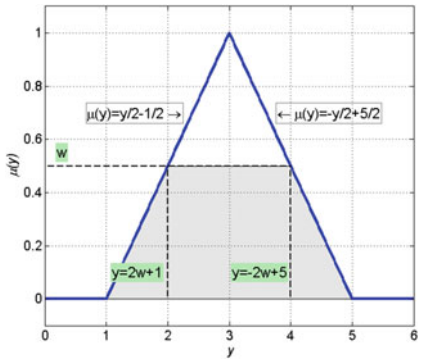

$$\int_{1}^{2w+1}\left(\frac{y}{2}-\frac{1}{2}\right)y\,dy+\int_{2w+1}^{-2w+5}w\;y\;dy+$$

$$+\int_{-2w+5}^{5}\left(-\frac{y}{2}+\frac{5}{2}\right)y\,dy=\underline{-6w^2+12w}$$

and

$$\int_{1}^{2w+1}\left(\frac{y}{2}-\frac{1}{2}\right)dy+\int_{2w+1}^{-2w+5}w\,dy+$$

$$+\int_{-2w+5}^{5}\left(-\frac{y}{2}+\frac{5}{2}\right)dy=\underline{-2w^2+4w}$$

Fig. 13 Membership function for intermediate difficulty

In the third and the fourth rule we evaluate intermediate difficulty D_2 (Fig. 13). In the fifth and the sixth rule we evaluate hard difficulty D_3 (Fig. 14).

$$\int_{3}^{2w+3}\left(\frac{y}{2}-\frac{3}{2}\right)y\,dy+\int_{2w+3}^{6}w\;y\;dy=\underline{-\frac{2}{3}w^3-3w^2+\frac{27}{2}}$$

and

$$\int_{3}^{2w+3}\left(\frac{y}{2}-\frac{3}{2}\right)dy+\int_{2w+3}^{6}w\,dy=\underline{-w^2+3w}$$

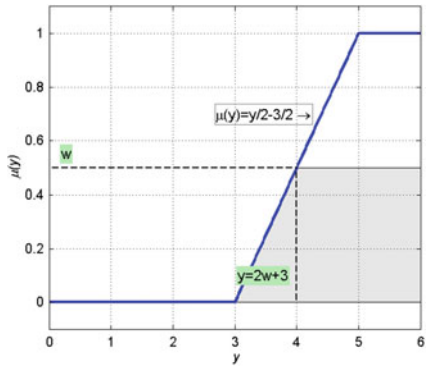

$$\int_{3}^{2w+3}\left(\frac{y}{2}-\frac{3}{2}\right)y\,dy+\int_{2w+3}^{6}w\;y\;dy=\underline{-\frac{2}{3}w^3-3w^2+\frac{27}{2}}$$

and

$$\int_{3}^{2w+3}\left(\frac{y}{2}-\frac{3}{2}\right)dy+\int_{2w+3}^{6}w\,dy=\underline{-w^2+3w}$$

Fig. 14 Membership function for hard difficulty

7.3 Mamdani's Method (COM-TM-TM)

We evaluate by the centroid of singletons Center of Maximum (COM-TM-TM) using the mean of the maximum.

$$y_{D'_j}^{CoM} = \frac{\sum_{j=1}^{k} y_j \cdot \mu_{D'_j}(y_j)}{\sum_{j=1}^{k} \mu_{D'_j}(y_j)}$$

$$= \frac{y_1 \cdot \mu_{D'_1}(y_1) + y_2 \cdot \mu_{D'_2}(y_2) + y_3 \cdot \mu_{D'_3}(y_3) + y_4 \cdot \mu_{D'_4}(y_4) + y_5 \cdot \mu_{D'_5}(y_5) + y_6 \cdot \mu_{D'_6}(y_6)}{\mu_{D'_1}(y_1) + \mu_{D'_2}(y_2) + \mu_{D'_3}(y_3) + \mu_{D'_4}(y_4) + \mu_{D'_5}(y_5) + \mu_{D'_6}(y_6)}$$

By substituting values:

$$= \frac{\frac{0-2w_1+3}{2} \cdot w_1 + \frac{0-2w_2+3}{2} \cdot w_2 + \frac{2w_3+1-2w_3+5}{2} \cdot w_3 + \frac{2w_4+1-2w_4+5}{2} \cdot w_4}{w_1 + w_2 + w_3 + w_4 + w_5 + w_6}$$

$$\frac{+\frac{2w_5+3+6}{2} \cdot w_5 + \frac{2w_6+3+6}{2} \cdot w_6}{w_1 + w_2 + w_3 + w_4 + w_5 + w_6}$$

$$= \frac{-w_1^2 + \frac{3}{2}w_1 - w_2^2 + \frac{3}{2}w_2 + 3 \cdot w_3 + 3 \cdot w_4 + w_5^2 + \frac{9}{2}w_5 + w_6^2 + \frac{9}{2}w_6}{w_1 + w_2 + w_3 + w_4 + w_5 + w_6}$$

The models of Mamdani's methods in ModelBuilder are shown in Fig. 15.

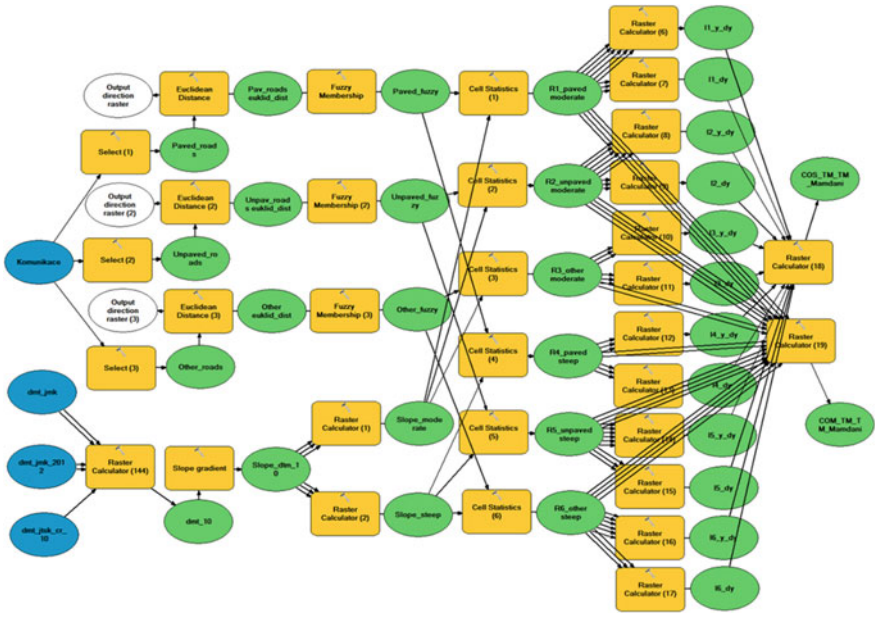

Fig. 15 The models of Mamdani's methods (COS-TM-TM, COM-TM-TM)

7.4 Comparison of the Methods and Defuzzification

The data of well-known parts of the bike trails which were possible to classify were selected to compare the best methods. We can use the comparison of the maximum, minimum, arithmetic mean and standard deviation according to the difficulty of the bike trails, then we monitored frequency histograms.

Mamdani's method is well representative with defuzzification CoS but also with defuzzification CoM, where there is the bigger value range and the higher frequency on the intervals of the maximum occurrence.

Larsen's method has similar characteristics. However, it is not suitable for the bike trails with the intermediate difficulty and highlights the bike trails with the small and hard difficulty.

The table compares the percentage of the bike trails suitable for the membership in interval $\langle 0,25;\ 1\rangle$ according to small, intermediate and hard difficulty having regard to their whole choice for the individual difficulties and the choosing methods. (Table 1)

The sum value of the percentages expresses the precision of the individual method. We can see that Mamdani's method bluntly dominates, especially with defuzzification CoS.

The results of Larsen's method are quite good. This method is not much reliable in the evaluation of the intermediate difficult bike trails. It significantly competes with Mamdani's method within the small and hard difficult bike trails. These methods are compared at the selected region (Fig. 16), where Mamdani's method with defuzzification CoM is characterized by big differences and Larsen's method by small differences of values of the bike difficulty. Mamdani's method with defuzzification CoS is the most reliable.

We choose the bike trail difficulty obtained by Mamdani's method with the defuzzification CoS for another analytical processing. It will permit to reclassify the attribute of the current bike difficulty and to add the difficulty of the other roads for the routing as the finding of the optimal road according to the difficulty.

7.5 Making Use of Mamdani's Raster to Finding the Bike Trail Rating

We assume that Mamdani's raster with defuzzification CoS is the main input to our analysis. The aim of this way is rating of all roads, not only cycle trails, registered in street net feature class.

Table 1 Part of suitable bike trails for membership $\langle 0,25;\ 1\rangle$

Difficulty	Small (%)	Intermediate (%)	Hard (%)	All (%)
COS-TM-TM	96.6	83.7	73.7	**84.1**
COM-TM-TM	97.1	75.0	74.5	76.0
COS-TP-TM	97.1	67.9	74.8	69.4

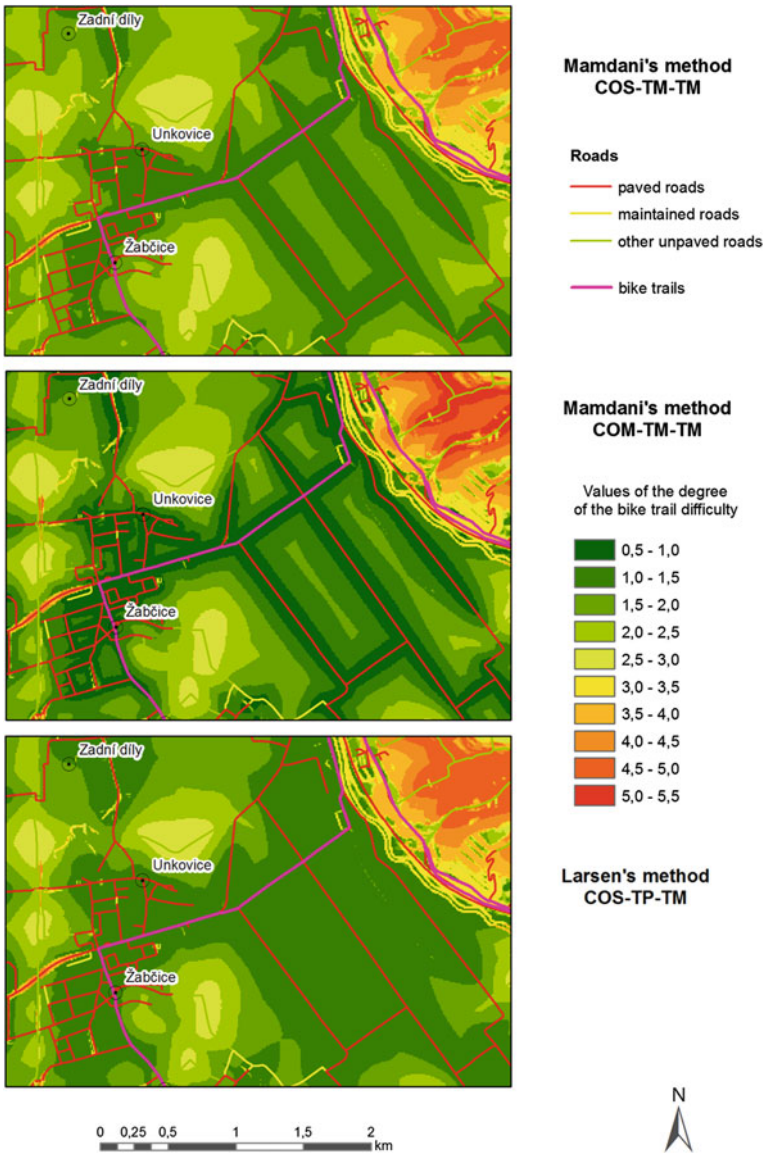

Fig. 16 Comparison of the methods in the region detail

First, we perform the extract of the cells of this raster that corresponds to roads defined by a buffer mask. Then the raster is converted to point feature class with the attribute from raster. The aspect as the slope direction is added to every point which obtains the near information about distance to the nearest road line, too. Finally, we extract and join the value of the difference Mamdani's raster and Mamdani's "null"

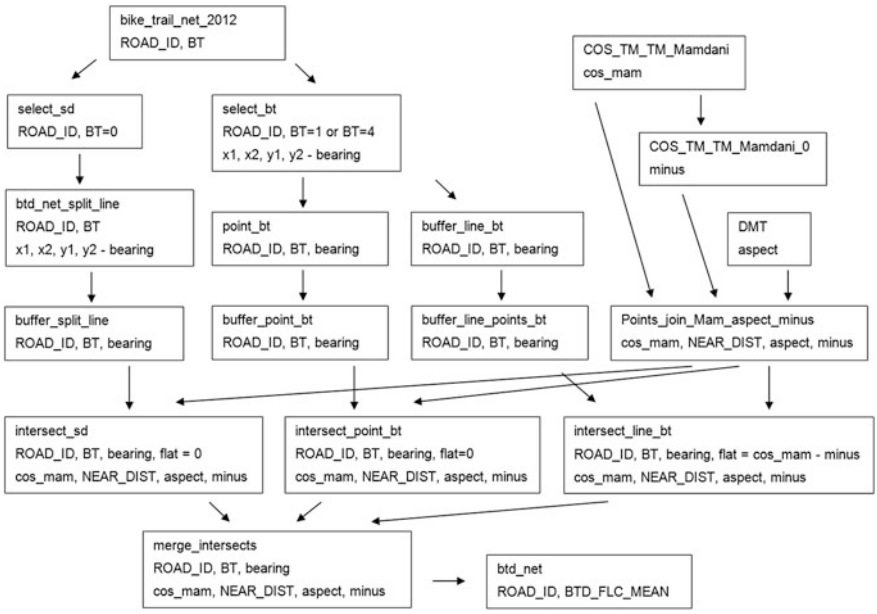

Fig. 17 Scheme for analysis by Python—layers and their important attributes

raster which doesn't consider the altitude. This difference influences the increase of the road difficulty compared to the flat surface. These steps are implemented by ModelBuilder and point feature class is the result—feature class called Points_join_Mam_aspect_minus in Fig. 17.

The next part takes open-source programming language Python that is both powerful and easy to learn. Particular steps are reflected in the following scheme (Fig. 17) where these components are used.

Explanatory text:

bike_trail_net_2012	input feature class involving street net and bike trail sections with actual fields
select_sd	selection of bike trails except bridges and tunnels
btd_net_split_line	seperation of bike trail sections to line segments, new geometry and completion bearing attribute (azimuth)
buffer_split_line	10 m buffer of the line segments, bearing (line azimuth)
select_bt	selection of bridges and tunnels
point_bt	beginnings and endings of bridges and tunnels
buffer_point_bt	10 m buffer of endpoints of bridges and tunnels
buffer_line_bt	10 buffer of line of bridges and tunnels
buffer_line_points_bt	symmetrical difference buffer_line_bt and buffer_point_bt
intersect_sd	intersect buffer_split_line and Points_join_Mam_aspect_minus
intersect_point_bt	intersect buffer_point_bt and Points_join_Mam_aspect_minus

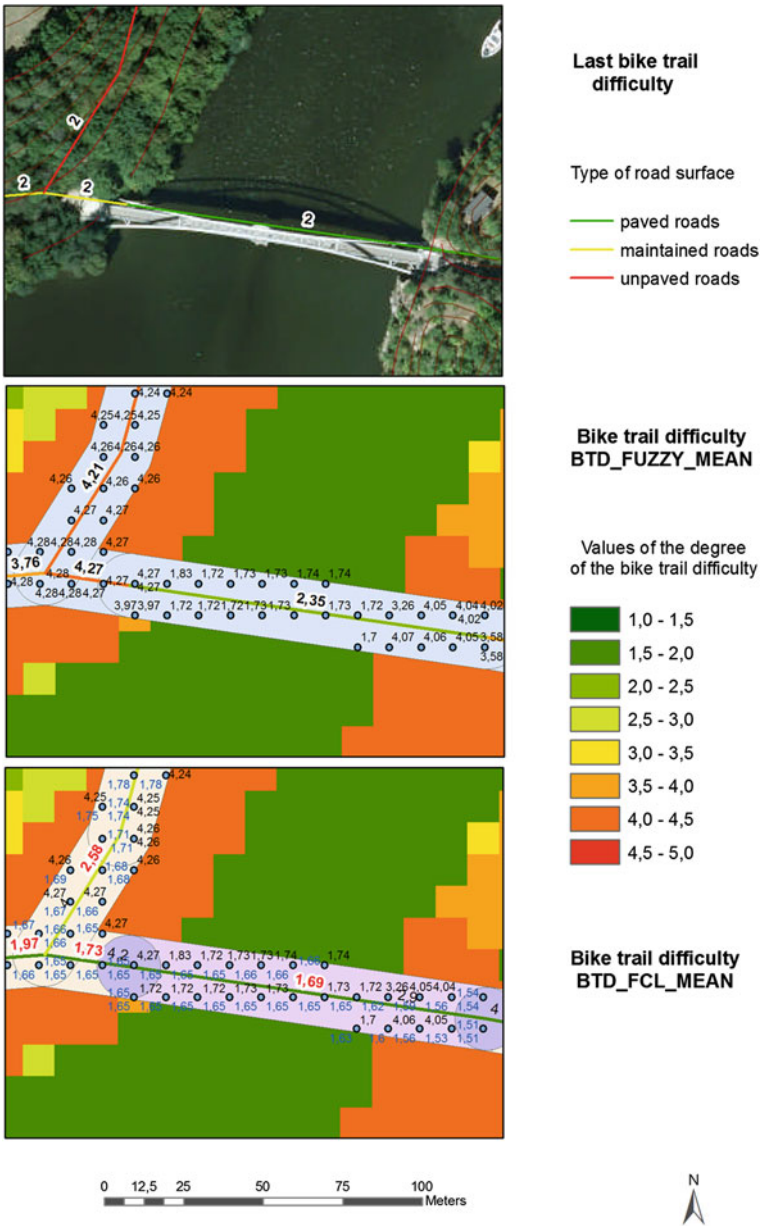

Fig. 18 Comparison of the last bike trail rating, bike trail rating BTD_FUZZY_MEAN and BTD_FCL_MEAN

intersect_line_bt	intersect buffer_line_points_bt and Points_join_Mam_aspect_minus
merge_intersects	merge of all intersects
btd_net	output bike trail sections with assignment of new bike trail difficulty

The most important step by Python creates btd table for joining to btd_net feature class with new bike trail difficulty field. Initial testing script worked with all points from feature class merge_intersects and calculated only arithmetic mean of particular roads according to road id. Because the points are in the different distance from road line it is more accurate to think about weighted average in the context of fuzzy membership of points. In the distance 10 m is membership 0 and on the line is membership 1 (BTD_FUZZY_MEAN).

In this approach we can see the biggest problem in the line direction compared with the slope direction. Bike trail sections in the direction of the contour line have a hard difficulty. And that also brought me to the fact that it will be useful to take the current difficulty from Mamdani's raster for the line segments in direction slope line and use difficulty from Mamdani's "null" raster (flat surface) for the segments in direction contour line. Consequently, the difficulty depends on the difference these rasters and the angle between the slope direction and the road line azimuth. The product of this deviation of straight lines and the ninetieth of this difference means the reduction of difficulty (BTD_FCL_MEAN).

Finally, I tried to reduce mistakes for short road sections and roads in bridges and at tunnels. The difficulty of the bridges and tunnels road is specified mainly by points at their beginning and ending. The points along the line are reduced to the flat value (Fig. 18).

8 Conclusion

The bike trail difficulty is important readout for planning routes of bike tours. Mainly, it depends on the quality of the road surface and the slope. We can express the requests for the bike trail difficulty fairly verbally by rules that are processed using the fuzzy sets and the compositional rule of inference and Mamdani's method. This method has reached the best effect with the defuzzification the centroid of sums and using the integral calculus.

The main aim of this paper is the exploitation and map presentation of the results on the web cycling portal of the South Moravian Region http://www.cyklo-jizni-morava.cz/. The analysis extends the difficulty of the bike trails to all roads. Considering fuzzy approach we can imagine the region compactly as a whole of the seamless bike trail difficulty raster fuzzy map and as the map of bike trail difficulty rating. The reclassification of the current difficulty and the update of the road difficulty network are very important to the improvement of the bike routing

depending on the required target group (family with children, recreational sportsman and athlete).

There are some inaccuracies and problems especially on the connections of the miscellaneous types of roads. I have some ideas to improve the actual bike rating and remove the found mistakes. It is the opportunity to use more rules in Mamdani's method or eventually add other linguistic variables such as elevation and road length.

References

1. Zadeh LA (1965) Fuzzy sets. Inf Control 8(3):338–353
2. Zadeh LA (1975) The concept of a linguistic variable and its application to approximate reasoning. Inf Sci 8(3):199–249
3. Kainz W (2010) mathematical principles of GIS. Available via DIALOG. http://homepage.univie.ac.at/Wolfgang.Kainz/Lehrveranstaltungen/15th_Nordic_Summer_School/The_Mathematics_of_GIS_Draft.pdf. Accessed 10 Oct 2013
4. Jura P (2003) Základy fuzzy logiky pro řízení a modelování. VUTIUM, Brno
5. Navara M, Olšák P (2002) Základy fuzzy množin. Skriptum ČVUT, Praha
6. Kolesárová A, Kováčová M (2004) Fuzzy množiny a ich aplikácie. Slovenská technická univerzita, Bratislava
7. Mamdani EH, Assilian S (1975) An experiment in linguistic synthesis with a fuzzy logic controller. Int J Man Mach Stud 7(1):1–13
8. Modrlák O (2004) Teorie automatického řízení II. - Fuzzy řízení a regulace. Technická universita v Liberci, Praha
9. Machalova J (2011) Modelling of chosen selectable factors of the develop of tourism with geographic it and fuzzy sets using. Acta Univ. Agric. et Silvic. Mendel. Brun. LIX(2): 189–198

Photovoltaics as an Element of Intelligent Transport System Development

Krystyna Kurowska, Hubert Kryszk and Ewa Kietlińska

Abstract Intelligent Transport System (ITS) means advanced applications aiming at providing innovative services related to different means of transport and traffic management as well as providing important information to traffic participants. Currently, ITS is applied within the areas of large cities. It is inevitable that the system should be applied in all locations where it may contribute to road safety improvement or streamlining the traffic. Application of photovoltaics as the renewable energy source for necessary devices (information signs, warning signs, variable contents signs, monitoring and lighting) is an opportunity for common application of ITS. Photovoltaics can be used practically in every location and, first of all, locations difficult to access to power grid. Based on the example of the Region of Warmia and Mazury in north-eastern Poland the current use of photovoltaics for providing power for road infrastructure was identified. Information concerning use of photovoltaic panels in marking of the national roads in the region was obtained from the General Directorate of National Roads and Motorways (GDDKiA), branch in Olsztyn. GIS tools were used for identification of the existing road signs supplied by photovoltaics. The MapInfo Professional application was applied for development of the appropriate subject map. According to the opinion of the authors the need exists for development of the pan-European GIS system containing information on the existing ITS and indicating key locations in which such a system should be implemented. Photovoltaics is the element facilitating ITS implementation in new difficult to access locations outside urban areas.

K. Kurowska (✉) · H. Kryszk
Department of Planning and Spatial Engineering, Faculty of Geodesy and Land Management, University of Warmia and Mazury in Olsztyn, Prawocheńskiego Street 15, 10-724 Olsztyn, Poland
e-mail: krystyna.kurowska@uwm.edu.pl

H. Kryszk
e-mail: hubert.kryszk@uwm.edu.pl

E. Kietlińska
IMAGIS S.A, Górczewska 2212/226, 01-460 Warsaw, Poland
e-mail: eva.kietlinska@imagis.pl

I. Ivan et al. (eds.), *Geoinformatics for Intelligent Transportation*,
Lecture Notes in Geoinformation and Cartography,
DOI 10.1007/978-3-319-11463-7_13

Keywords National roads · Renewable energy sources · Photovoltaics · GIS tools · Road safety · Intelligent transport system

1 Introduction

During the times of progressing socioeconomic development and general globalisation, mobility and possibility of development of modern, safe, productive and natural environment friendly transport system is the key issue. According to Koźlak [1], transport systems development must consider the need for increasing effectiveness of their operation coupled with limiting the negative consequences of transport development. According to the Strategy of Transport Development by 2020 [2], increasing territorial access and improving safety of traffic participants as well as transport sector effectiveness improvement by establishing a consistent and user friendly transport system in the national (local), European and global dimension is the main objective of the national transport policy. Implementation of the intelligent transport system is such a solution very strongly supported by the European Union.

Intelligent Transport Systems (ITS) are advanced applications which without embodying intelligence as such aim to provide innovative services relating to different modes of transport and traffic management and enable various users to be better informed and make safer, more coordinated and 'smarter' use of transport networks [3]. ITS represent a combination of IT and communication solutions with transport infrastructure and vehicles aiming at safety improvement. They also increase the effectiveness of transport processes and natural environment protection.

In the ITS, defining the subjects of transport is important. As presented by Wydro [4], they include: (1) direct transport infrastructure users, (2) travellers, pedestrians and passengers, (3) means of transport, (4) roads and their direct environment, (5) institutions and organisations (including, among others, road infrastructure administration, business—infrastructure users, infrastructure construction and maintenance companies), (6) providers of complementary services (e.g. motels, restaurants, vehicle service points), (7) institutions assuring order and safety (e.g. police, border guards, emergency medical services, property protection), (8) public administration.

Overcoming geographic barriers to make integration between all subjects involved in transport possible is one of the tasks of the European Union Cohesion Policy that could be accomplished with the help of ITS. This is also the appropriate direction for a better use of the economic potential of regions.

In Poland, Intelligent Transport Systems (ITS) are usually implemented with the aid of the European Union funds of the Operational Programme Infrastructure and Environment (the subsidy is up to 85 % of the investment project value) and Operational Programme Development of Eastern Poland. Construction of new roads or modernisation of the existing ones is the best moment for implementation of such solutions.

The most frequently applied ITS solutions are: (1) traffic management systems, (2) public transport management systems, (3) freight transport and fleet of vehicles management systems, (4) road events and rescue services management systems, (5) traffic safety management and violation of regulations monitoring systems, (6) information services for travellers, (7) electronic toll collection systems, (8) advanced technologies in vehicles [1, 5].

Within the frameworks of the listed applications of ITS, photovoltaics may play the most important role in expanding the system to include further locations in particular in not urbanised areas: information signs, warning signs and, first of all, the system of variable content signs, which is primarily an invaluable impact on the safety of road users.

2 Material and Methodology of Studies

For the purpose of the paper was study and analysis of literature ITS and practical application of photovoltaic panels. Particular attention was paid to the use of road infrastructure of energy from renewable sources. For this purpose, within the framework of the paper the locations of photovoltaic panels supplying information and warning signs on national roads within the area of Warmińsko-Mazurskie voivodship in north-eastern Poland have been identified. Information concerning use of photovoltaic panels in signage on national roads in the region was obtained from the General Directorate of National Roads and Motorways, branch in Olsztyn administering those roads (data as at September 2013). GIS tools were used for identification of the existing road signs supplied by photovoltaics. The MapInfo Professional application was used for development of the appropriate subject map. For the purpose of precise location of the objects Google Maps and Street View service were used. This work is application in its character. One of the functions of MapInfo professional using to for the identification of photovoltaic panels in the road infrastructure used to geocoding. Geocoding consists in assigning the info about a given location coordinates to visualize on the map. Analysis of the use of photovoltaic panels in road infrastructure was conducted to define whether application of such solutions is justified.

3 Potential of Photovoltaics Use for Road Safety Improvement

Photovoltaics is a scientific discipline dealing with transformation of solar radiation energy into power by applying photovoltaic cells. It is one of the most promising renewable energy sources representing an alternative for traditional not renewable resources.

Solar energy may be transformed into power using photovoltaic cells (PV cells), solar cells converting light directly into power. That process is also possible by

means of concentrating solar power (CSP) where parabolic solar collectors or solar towers concentrate the light for the purpose of warming up a single point generating in that way steam driving the turbine. PV cells based power stations can be connected to storage batteries or to the power grid. Heat from the CSP can be stored for energy generation in case of unavailability of solar light [6]. Solar power, i.e. photovoltaics is considered one of the most environment friendly energy sources given the wide potential for obtaining energetic benefits. Their simple construction, ease of installation compared to other energy sources and availability, i.e. the possibility of installing in difficult to access terrain are the major advantages of PV systems.

Electricity powered cars are the future of transport. According to Moćko et al. [7] the volume of total greenhouse gases emissions produced by a car is very highly dependent on the type of renewable energy in power grid. Solar energy seems to be the most rational solution. However, productivity of photovoltaic panels depends on the year season, hour, location and weather conditions. The advantage of the system is that it can be installed in places with difficult access to power, it does not pollute the air and does not generate noise. It must, however, be appropriately oriented as the highest power generation productivity is possible in case of southern exposure [8, 9].

In different parts of the world solar power is less or more popular. In Poland, so far, thermal energy obtained from solar installations enjoyed interest.

The actual spread of photovoltaics in Poland is quite limited. We observe very high disproportions compared to the other European countries. According to Forowicza [10] German photovoltaic installations offered the capacity of 17,200 MW while in Poland it was just 1.75 MW. According to Romański et al. [11], the volume of energy obtained in our climate is small and highly dependent on the year season. The authors also evaluate efficiency of the devices as very poor—ranging within 6–15 %. The examples of photovoltaics use in other countries, e.g. Germany, that are situated in the climate zone very similar to Poland can be presented as contradicting the opinions presented. In 2013, energy production from renewable sources, mainly photovoltaics, is at the record level. Worldwide, only the United States and Japan are ahead of Germany in total capacity of the installed photovoltaic systems. Photovoltaics market is developing at a surprising rate; new solar power plants are established, but Poland, unfortunately, because of the legal regulations and politics is lagging behind the majority of the European countries.

All the time new solutions for energy from renewable sources are proposed (in ventilation devices, lighting, industrial machines and motors, construction of energy efficient houses) [12].

Sharma and Harinarayana [13] propose energy production with photovoltaic installations forming a roof-type structure along the national roads and motorways. According to the authors, such solutions offer numerous benefits for road traffic participants. They draw particular attention to the effect of shade that causes decrease in energy consumption by air conditioning devices in vehicles, longer life of tyres and significantly lower damages to road surfaces [14]. The advantage of such solution is also making use of the space taken for road belts and decreasing of CO_2 emissions to the environment or creating new jobs [13].

There are also other ways and methods of using photovoltaics technology on the roads, e.g. lighting the road using the LED supplied with solar energy [15]. It is worth mentioning that lighting of roads improves the safety of traffic participants significantly.

Photovoltaic systems are economic and environment friendly solutions both at locations where connection to the existing power grid is impossible and in towns where such connections happen to be costly. Road signs supplied with solar energy provide good visibility even from long distances and during bad weather conditions. They also allow signage of every high risk location on the road [16].

Photovoltaics also has other applications in road infrastructure devices. Increasingly frequently we can see point objects supplied with solar energy i.e.: parking fee collection points, street lamps or lighting of pedestrian crossings. Photovoltaic panels' applications in Poland could be observed the most frequently along national roads and motorways, in most cases in places of roads modernisation or construction, places with particular hindrances to traffic, etc.

Location photovoltaic panels along the public roads can have a huge role in education—will get used to the new billowing RES and persuade and encourage prosumers to install photovoltaic systems in the future.

4 Photovoltaics Use on Roads Administered by GDDKiA Branch in Olsztyn

A study of transport system development and the status of development may and should use the potential of spatial information systems in the areas of both databases and analysis and modelling tools. Within both the first and the second area it is worth to take into consideration both the known base solutions and new, complementary techniques and data sources [17].

Within the area of Warmińsko-Mazurskie voivodship, General Directorate of National Roads and Motorways administers sections of express roads S7, S22 and S61 as well as sections of national roads number: 15, 16, 51, 54, 58, 59, 63 and 65. Currently there are no motorways in the area of the region. On the Governing GDDKiA in Olsztyn total is 1300, 343 km of national roads. The distribution and technical classes of national roads in the region are presented in Fig. 1 and Table 1.

During the recent time, construction works in Warmińsko-Mazurskie voivodship were carried out on 88 km of national roads of which construction of the express roads S7 (61 km) and S51 (6 km) involved 67 km. The works were carried out on two sections: Pasłęk—Miłomłyn with the length of ca. 37 and 31 km section Olsztynek—Nidzica including Olsztynek bypass on the road S51. Those projects were co-financed by the European Union within the framework of the Operational Programme Infrastructure and Environment. Funds of the same Programme are also applied for the 8.2 km section of the national road number 16 from Biskupiec to Borki Wielkie.

Fig. 1 Rough location of points on the national road No. 16 (Gietrzwałd)

Construction of 4.8 km long Ełk bypass in the course of the national roads number 16 and 65 has been completed. The bypass was constructed using the funds of the Operational Programme Development of Eastern Poland.

Another project implemented from the Operational Programme Development of Eastern Poland—Olecko bypass 7.6 km in length in the course of the national road number 65 is nearing completion. During 2012, two bridges on national roads have been commissioned for use. In Iława, a new arch bridge was constructed on the national road number 16 and in Braniewo, on the national road No. 54 the bridge over the Pasłęka river has been rehabilitated.

Based on the information obtained from GDDKiA branch in Olsztynie photovoltaic panels are applied in 95 locations. The specification for individual sections of national roads in the region is presented in Table 2.

In Warmińsko-Mazurskie voivodship, photovoltaic panels are used mainly with warning signs. They are located in areas of open spaces at locations of crossings (narrowing of road belt), pedestrian crossings and viaducts. Analysis of the use of photovoltaics in the region confirms that its application on newly constructed or modernised sections of roads (e.g. Gołdap bypass) is justified.

5 Application of GIS Tools for Identification of Road Infrastructure Elements Supplied with Solar Energy

5.1 Geographic Information Systems (GIS)

GIS is a system of software, hardware, data, personnel operating the system and methods for data development, handling, processing and analysing [18]. The main GIS functionalities include acquiring, verifying, collecting, integrating, processing and sharing of spatial data (information on the geographical space).

Table 1 List of national roads administered by GDDKiA branch in Olsztyn

Number of road	Course of the road in Warmińsko-Mazurskie voivodship	Class of road	
		Section of the class	Class
7	Border voivodship–Elbląg–Ostróda–Olsztynek–Nidzica–border voivodship	Border voivodship–Elbląg	GP
		Elbląg bypass	GP/S
		Elbląg–Kalsk	GP/S
		Kalsk–Miłomłyn	GP
		Miłomłyn bypass	S
		Miłomnyn–Ostróda–Olsztynek–Nidzica–border voivodship	GP
15	Border voivodship–Nowe Miasto Lubawskie–Lubawa–Ostróda	Border voivodship–Nowe Miasto Lubawskie–Lubawa–Ostróda	GP
16	Border voivodship–Kisielice–Iława–Ostróda–Olsztyn–Barczewo–Biskupiec–Mragowo–Mikołajki–Orzysz–Ełk–border voivodship	Border voivodship–Kisielice–Iława–Ostróda–Olsztyn–Barczewo–Biskupiec–Mragowo–Mikołajki–Orzysz–Ełk–border voivodship	GP
22	Border voivodship–Elbląg–Chruściel–Grzechotki–stateborder	Border voivodship–Elbląg	GP
		Elbląg–Chruściel–Grzechotki–state border	S
51	State border–Bezledy–Bartoszyce–Lidzbark Warmiński–Dobre Miasto–Olsztyn–Olsztynek	State border–Bezledy–Bartoszyce–Lidzbark Warmiński–Dobre Miasto–Olsztyn–Olsztynek	GP
53	Olsztyn–Pasym–Szczytno–Rozogi–border voivodship	Olsztyn–Pasym–Szczytno–Rozogi	GP
		Rozogi–border voivodship	G
54	Chruściel–Braniewo–Gronowo–state border	Chruściel–Braniewo–Gronowo–state border	GP
57	Bartoszyce–Bisztynek–Biskupiec–Dźwierzuty–Szczytno–-Wielbark–border voivodship	Bartoszyce–Bisztynek–Biskupiec–Dźwierzuty–Szczytno–Wielbark–border voivodship	G
58	Olsztynek–Zgniłocha–Jedwabno–Szczytno–Babięta–Ruciane Nida–Pisz–Biała Piska–border voivodship	Olsztynek–Zgniłocha–Jedwabno–Szczytno–Babięta–Ruciane Nida–Pisz–Biała Piska–border voivodship	G
59	Giżycko–Ryn–Mrągowo–Piecki–Nawiady–Stare Kiełbonki–Rozogi	Giżycko–Ryn–Mrągowo–Piecki–Nawiady–Stare Kiełbonki–Rozogi	G
63	State border–Węgorzewo–Giżycko–Orzysz–Pisz–border voivodship	State border–Węgorzewo–Giżycko–Orzysz–Pisz–border voivodship	GP
65	State border–Gołdap–Olecko–Ełk–border voivodship	State border–Gołdap–Olecko–Ełk–border voivodship	GP

Table 2 Use of photovoltaic panels for signage on national roads administered by GDDKiA branch in Olsztyn

Number of road	Quantity of locations	Quantity of panels	Location
7	23	27	Junction, viaduct
15	4	4	
16	31	31	Bypass Wój-towo, crossroad
22	–	–	–
51	3	6	Crossroad, crosswalk
53	4	4	Road
54	–	–	–
57	–	–	–
58	1	1	Road
59	7	8	Crossroad
63	–	–	–
65	22	22	Bypass Gołdap

GIS provides the user with the opportunity to merge descriptive data on objects with information on their spatial location, and also allows thematic mapping, performing spatial analyses, and formulating conclusions.

5.2 MapInfo Professional Software

MapInfo Professional is a product of the MapInfo Corporation company, being one of rather commonly used programs supporting geographic information systems in addition to such packages as ArcGIS, GeoMedia, or Quantum GIS. MapInfo is included in the group of programs described as "desktop GIS". It is distinguished by low system requirements, relative user-friendliness and, at the same time, high level of functionality.

Basic tasks to be accomplished using the MapInfo include: (1) creation of spatial databases, management of numerical map layers and tables of descriptive data, (2) making use of external sets of data (of various formats and locations) through ODBC import or connection, (3) searching for and transforming data using SQL, (4) vectorisation and edition of the geometry of object, imaging data input, (5) statistical calculations, measurements, calculations of the location, length and surface of objects, (6) spatial analyses, determining relationships between objects, and syntheses (e.g. regionalisation), (7) geocoding—making use of address information for the localisation of objects and network analyses, (8) editing cartographic presentations, general geographical and thematic maps (choropleth maps, diagram maps, dot map, etc.), (9) creating, publication and printing reports [19].

MapInfo Professional provides functions which allow connecting with the WMS (Web Map Services) and WFS (Web Feature Services) services. Thanks to these

options of the program, it is possible to e.g. make use of the resources of Polish Geoportal, and show of the other phenomena.

5.3 Thematic Maps

The most efficient way to present a given phenomenon in space, and determine the variation of the spatial value, density, or intensity of geographical phenomena, as well as relationships between them, is through thematic maps, which provide the visualisation of specific and socio-economic issues and phenomena. Thematic maps are graphic material supporting decision-making processes of various institutions and organisations implementing socio-economic strategies and programmes. An increased interest in such maps stimulates searching for new contents which they may present [20].

Thematic maps as created in the MapInfo constitute subsequent layers in the database. These were edited on the basis of spatial objects contained in the newly-created elements of road infrastructure database. Descriptive data from multiple tables may be used through SQL queries.

For a given layer, multiple alternative presentations of the same issue may be prepared. A significant feature of thematic overlays is the dynamic refreshing thereof during the edition of attribute values. This allows maintaining the on-going relevance along with the permanent expansion of the RES database.

6 Creating the Spatial Database in MapInfo for Identification of Road Infrastructure Elements

Based on the information obtained from GDDKiA, the database concerning use of photovoltaic panels in signage on national roads administered by the branch in Olsztyn was developed.

In the data obtained from GDDKiA, location of photovoltaic panels is defined by the number of the distance marker. Given that the average distance between the distance markers obtained was 1,000 m, generally available map portals were used to increase the precision of geocoding for the purpose of identification of the location of individual photovoltaic panels. Additionally, using them allowed determination on which side of the road section the photovoltaic panel is situated as geocoding would position the point automatically on the road axis.

The precise location of the object was possible by using the Google Maps and Street View service (Fig. 2).

For the purpose of confirming the object location identification correctness, the nearest distance marker was located and the station value was read.

Data export to the tabulation format allowed automatic presentation of points in MapInfo Professional (Fig. 3).

Fig. 2 Object identification in space on the national road No. 16: point 38 Gietrzwałd (126 + 250 km)

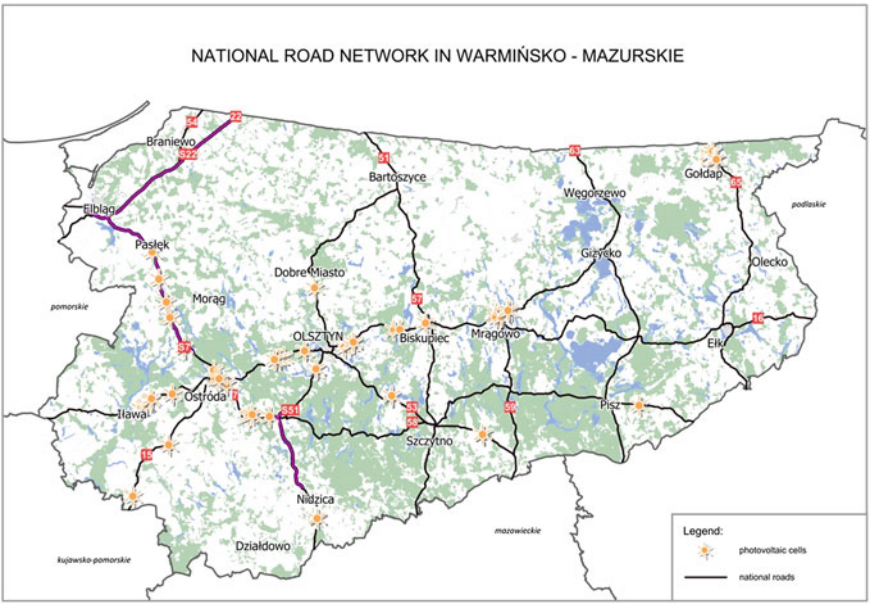

Fig. 3 Distribution of national roads in Warmińsko-Mazurskie voivodship with photovoltaic systems

Very dynamic development of the road network during the recent years and increasingly frequent use of photovoltaic cells in road infrastructure caused that for many sections of roads the presentation (Street View) allowing placement of the cells on the map has not existed yet (e.g. Olecko bypass). According to the data presented in the portal, satellite images used for locating the cells were taken in

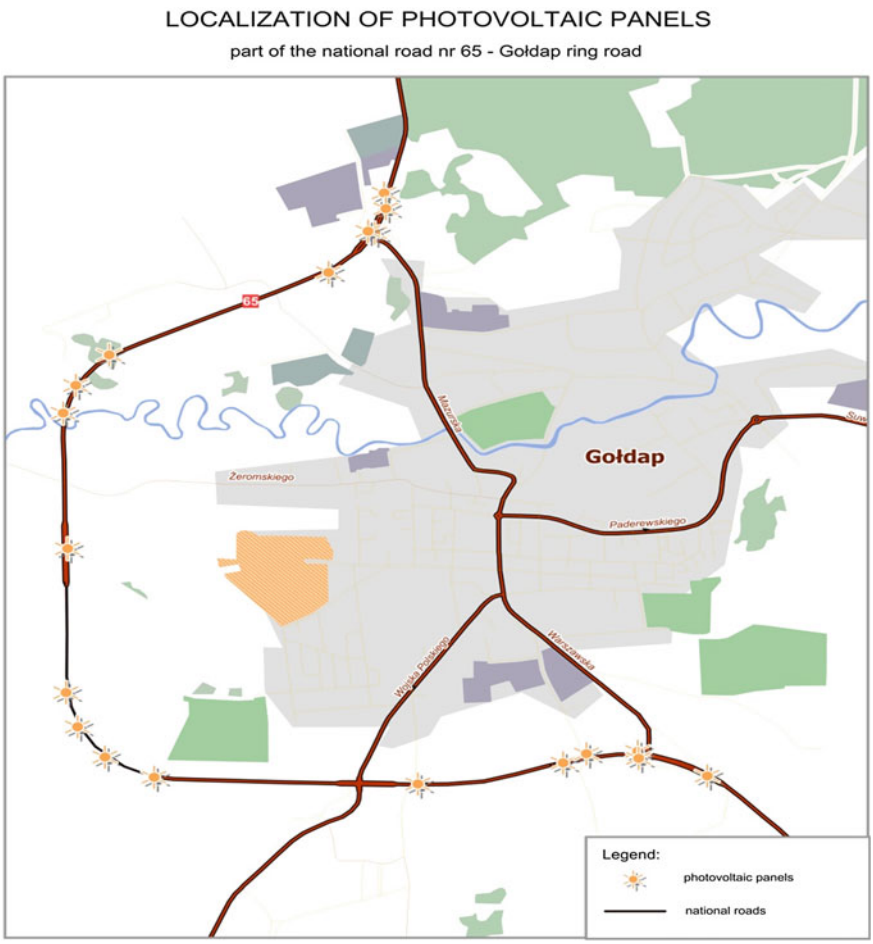

Fig. 4 Location of photovoltaic system on the Gołdap bypass

2013 while the data for Street View was obtained during the period of July–August 2012. Moreover, new photovoltaic cells are installed on the long existing sections of roads (and hence on the resulting map individual panels are missing) (Fig. 4).

7 Conclusions

Transport is one of the most important factors determining socioeconomic development of the country. Modern infrastructure and effective transport system support spreading the economic growth of strong centres over those parts of the country which, because of absence of good territorial access remain stagnant. Warmińsko-Mazurskie voivodship is an example of such a region in Poland. Poorly developed

network of national roads and absence of motorways determine treatment of that region as peripherally located, i.e. a region with limited territorial access. The technical status of the roads is also unsatisfactory. Based on the conducted analyses of photovoltaics use along the roads administered by the General Directorate of National Roads and Motorways in Olsztyn up to date it can be concluded that the potential for applying solar energy is unlimited. Photovoltaic cells have been applied in 95 locations and to a limited extent only, i.e. for lighting the warning and information signs. In the analysed region, so far, photovoltaics has not been used for lighting the variable content signs.

Application of photovoltaic panels in Poland represents a new solution but, as it can be seen, an increasingly popular one. The possibilities of installation allow stating that photovoltaics is the most appropriate renewable energy source for use in road infrastructure. It works excellently in lighting road signs (information and warning). Given the plans for the ITS development, it should also find application in development of the global/mobile transport system supported by the EU. Thanks to the solar energy, the Intelligent Transport System could be implemented wide scale and outside urbanised areas. The system based on power from photovoltaics will allow presenting the current situation on the road in hard to access locations where traditional power grid is absent. General Directorate of National Roads and Motorways conducts monitoring of roads, it checks the weather conditions and provides information on road works. However, the range of services provided and information collected is of local nature while the intelligent transport system should provide at least regional and ultimately global coverage. Wider scale use of photovoltaics would contribute to ITS development. The Directive on … also draws attention to application of new solutions based on renewable energy.

For the future, development of motorisation powered by electricity is projected. It is important that the power should originate from renewable sources. Photovoltaics may play an immense role also in this case—it may be used for construction of fast loading stations in, e.g. traveller service points. Based on the solar energy cameras could be installed for traffic and safety control on roads. The need exists for creating a consistent and efficiently functioning transport system integrated with the European and global system. According to the authors, the European system of information on the current situation on the road using GIS and GSM should be implemented as fast as possible. Photovoltaics as environment friendly renewable energy source easy for installation and working under all conditions should find wider use in road infrastructure, among others in the Intelligent Transport System development.

References

1. Koźlak A (2008) Intelligent transport systems as instrument of improvement in transport's efficiency, Logistyka (2). http://akademor.webd.pl/download/kozlak_inteligentneST.pdf. Accessed 10 July 2013
2. Transport Development Strategy to 2020 (2013) Ministry of transport, construction and maritime economy, Warsaw

3. Directive 2010/40/EU of the European Parliament and of the Council of 7 July 2010 on the framework for the deployment of Intelligent Transport Systems in the field of road transport and for interfaces with other modes of transport
4. Wydro KB (2004) Wymiana informacji w systemie inteligentnego transport lądowego. Telekomunikacja I techniki Informacyjne 1–2:19–30
5. Planning a Modern Transport System (2004) A guide to Intelligent Transport System architecture. European Communities. http://www.frame-online.net/sites/default/files/first-view/further-reading/PlanningGuide.pdf. Accessed 20 Sep 2013
6. Renewable Energy Changes the World (2011) European Union, Luxemburg
7. Moćko W, Wojciechowski A, Staniak P (2012) Application of renewable energy sources in transport. Zeszyty Problemowe—Maszyny Elektryczne 95(2):99–104
8. Mehleri ED, Zervas PL, Sarimveis H, Palyvos JA, Markatos NC (2010) Determination of the optimal tilt angle and orientation for solar photovoltaic arrays. Renew Energy 35(11): 2468–2475
9. Chang TP (2009) Performance analysis of tracked panel according to predicted global radiation. Energy Convers Manag 50(50):2029–2034
10. Forowicz K (2011) Słońce czysty biznes. Środowisko 18(450):17–19
11. Romański L, Bukowski P, Dębowski M (2012) Analysis of using renewable energy in rural farms. Agric Eng Z 2(137):259–268
12. Zweibel K (2010) Should solar photovoltaics be deployed sooner because of long operating life at low, predictable cost? Energy Policy 38(11):7519–7530
13. Sharma P, Harinarayana T (2013) Solar energy generation potential along national highways. Int J Energy Environ Eng 4:16
14. Centre for Urban Forest Research (2007) http://www.fs.fed.us/psw/programs/used/uep/products/cufr_673_WhyShadeStreets_10-06.pdf. Accessed 10 July 2012
15. Wu MS, Huang BJ, Tang CW, Cheng CW (2009) Economic feasibility of solar-powered led roadway lighting. Energy 34(8):1934–1938
16. EKKOM (2013) http://edroga.pl/nowosci-w-branzy/urzadzenia/9184-znaki-drogowe-zasilane-przez-energie-sloneczna. Accessed 29 Sep 2013
17. Brzuchowska J (2010) Proposals of transportation phenomena analysis based on raster maps and GIS tools. Tech Trans 3(1-A):125–138
18. Głowacki T (2005) Projekty GIS. Administracja i użytkowanie, Oficyna Wydawnicza Politechniki Wrocławskiej
19. Kowalski PJ (2005) Podstawy obsługi bazy danych przestrzennych oraz redakcji prezentacji kartograficznych w programie MapInfo Professional, Zakład Kartografii Politechniki Warszawskiej
20. Kryszk H, Kurowska K, Brodziński Z (2013) Identification of Renewable Energy Sources in the Region of Warmia and Mazury with the use of MapInfo Professional software. In: Źróbek R, Kereković D (eds) GIS and its implementations. Zagreb, pp 136–148

Urban Heartbeats (Daily Cycle of Public Transport Intensity)

Ivica Paulovičová, Slavomír Ondoš, Lukáš Belušák and Dagmar Kusendová

Abstract Main focus is put on the daily cycle of public transport intensity. In the city, commuting between places of housing and places of work one of the most important types of recurring organized spatial interactions. This is reflected also on the public transport which has tendency of creating communities as a reaction to demand. This feature of public transport in a city can be clearly identified through network analysis. Network approach recently developed in theoretical physics and related disciplines is still a promising direction of research also in the case of urban transportation studies. We use public transport system in a usual European city, a representative day in Bratislava, to demonstrate that it behaves systematically along the daily cycle in response to changing demand. Even through only basic description of data was calculated, the daytime rhythm, which we call the urban heartbeat, can be clearly recognized in the network structure. Though, the difference between intensity is clearly expressed, only the difference between night and day seems to have bigger statistical difference.

Keywords Public transport · Dynamic network analysis · Community · Bratislava

I. Paulovičová (✉) · S. Ondoš · L. Belušák · D. Kusendová
Department of Human Geography and Demography,
Faculty of Natural Sciences, Comenius University in Bratislava,
Mlynská dolina, 842 15 Bratislava, Slovakia
e-mail: paulovicova@fns.uniba.sk

S. Ondoš
e-mail: ondos@fns.uniba.sk

L. Belušák
e-mail: belusak@fns.uniba.sk

D. Kusendová
e-mail: kusendova@fns.uniba.sk

I. Ivan et al. (eds.), *Geoinformatics for Intelligent Transportation*,
Lecture Notes in Geoinformation and Cartography,
DOI 10.1007/978-3-319-11463-7_14

1 Introduction

Each city lives in motion. Households and firms create and abandon connections between them in different roles as economic actors. Some are seemingly random in appearance, others are predictable. Networks of these connections follow surprising orders of their distribution in space and time. Flows of different kinds, as a result of self-organization in city, emerge and die in a rhythm, which we, rather too poetically, give the name urban heartbeats. Time and space merge within and create a spatial-temporal phenomenon crucially important in understanding how cities live.

Movements of people, things, or mere information employ many researchers over generations. Basic aim of their efforts is a functionally better organized city. Public transportation system may serves us as a useful model of spatial interaction, multidimensional complex web of links varying in intensity and regularity over various frequencies, probably most importantly a daily 24-h long.

One of the prominent types of cyclically organized spatial interactions in the city is commuting between places of housing and places of work. Separation of different functions has been symptomatic over the whole 20th Century urban planning. The notion of order and effective organization of daily life in the city was considered progressive in compare to experienced chaotic mixture of unplanned organic cities. Bratislava is for decades the biggest and the fastest growing city in Slovakia. We assume it has the potential to witness such changes.

Without wanting to go in broad discussion concerning positive and negative sides of modernist urban planning we will remain only concerned with most relevant consequences for urban daily rhythm. Modernist urban plan separating housing from work and services is responsible for creating demand for transportation, increasing and decreasing mostly in synchronicity with daily and weekly economic cycles.

Limiting our attention further it's not really technical details behind commuting behavior modeling, subject of vast economic and technical literature. Cyclical self-organization of spatial interaction networks according to our intentions shall be considered a regularly repeating natural experiment worth attention of researchers.

Each daily cycle in urban life is itself a model of human interaction born and maturing up to morning peak hour, then easing over midday and once again growing before daily peak is reached in the late afternoon. Additionally to changing intensities we also expect asymmetry in speed of variation, probably not independent from further qualities and scale.

The public transport network obviously changes over daily and longer cycles. Connection between different parts of a city is more frequent, possibly also faster in different hours depending on modes of transportation operating. Weekend and nighttime rides can be significantly more difficult, at least requiring more advanced planning for minimizing waiting times.

Besides common observations like these, we try to ask a very simple question, whether topological aspects of complex network of public transportation also significantly change and what kind of change it is. More precisely, we are interested in

the specific dynamics of network structure, represented in the categorical variable representing network communities, identified by appropriate technique.

Public transportation network, as described earlier might be decomposed into nodes, geographically located stops, points of departure and arrival of individual vehicles on individual lines, and arcs connecting subsequent stops. In the basic alternative we can use binomial representation for arcs. But network architecture of usual public transportation systems requires the usage of weighted arcs for capturing changing intensity.

We decide to weight the arcs with integer counts of vehicles, connections aggregated over an appropriate interval of time. However, such weighting remains blind to speed of connection. Fast service lines can be significantly preferred to slow lines. Cheap connections can be preferred to expensive. Comfortable connections can be preferred to crowded lines. For the time being we intentionally forget about these complications and only consider frequency of connection indirectly also indicating typical waiting time after arriving at the stop randomly.

Further organization of our paper is typical. We first review an intersection of literatures discussing basic principles of network research in transportation. We are especially interested in papers providing theoretical understanding for the evolving complex network perspective. We also find similar orientation of medical research in mapping of the functional brain topologies. Next we describe a representative daily cycle empirically in the city of Bratislava according to the Apptives schedule as of July 09, 2013. Network is separated in eight 3-h long samples, which are further decomposed into Louvain network communities. Basic counts are provided concerning internal and external flows relative to full network mobility scale, modified between samples. Last section concludes and suggests questions of further interest.

1.1 Evolving Network Perspective in Literature

Significant progress on the field of network analysis by Watts and Strogatz [1], Barabási and Albert [2] or Albert and Barabási [3] have contributed to the expansion of network analysis in various scientific fields. Many systems take the form of networks, sets of nodes or vertices joined together in pairs by links or edges [4]. Examples include social networks [1, 5], technological networks such as the Internet, the World Wide Web [6] and power grids [7], and biological networks such as neural networks [1], or metabolic networks [8].

During the past few years many studies have focused on different types of transportation network analyses, especially on airport [9, 10], railway [11] or bus networks [12]. Also several public transport systems have been investigated using various concepts of complex networks [13–16].

Most of previous studies have analyzed only specific sub-networks of public transport networks in various urban areas and in different parts of the world. For instance, subway network analysis of Boston by Latora and Marchiori [14, 17] who defined measures of local and global network efficiencies. They notably found that

the small-world behaviors existed in that system. In another study Sen et al. [18] found that India's railway network exhibited small-world properties and predicted that railway networks in other countries would also exhibit small world properties. Similar properties were reported by Seaton and Hackett [11] who calculated the clustering coefficient, path length and average degree vertex of the rail systems in Boston, US and Vienna, Austria.

Also, Musso and Vuchic [19], Vuchic and Musso [20] focused on evolution and characteristics of subway networks. Derrible [21] was interested in network centrality of 28 worldwide metro systems, where he studied the emergence of global trends in the evolution of centrality with network size and examine several individual systems in more detail. Sienkiewicz and Holyst [22] have analyzed the bus and tram networks of Polish cities finding that some systems appeared to show a scale-free behavior, with scaling factors. A very similar analysis was offered by Xu et al. [12] focusing the complexity of several bus networks in China.

However, as far as the bus, subway, or tram sub-networks are not closed systems, the inclusion of additional sub-networks has significant impact on the overall network properties as has been shown for the subway and bus networks of Boston [13, 14]. Latora and Marchiori [13] introduced the related concept of efficiency, which measures how easily information is exchanged over the network. They showed that small-world networks are highly efficient. Soh et al. [16] examined Singapore public transportation system where they focused on the degree, strength, clustering, assortativity and eigenvector centrality characteristics of the transportation networks.

Lu and Shi [23] analyzed the public transport networks in three Chinese cities and they found that the public transportation networks have the characteristics of complex networks. In addition, the urban transportation network parameters all significantly affect the accessibility, convenience, and terrorist security capability of the urban public transportation network. Von Ferber et al. [15, 24] used complex network concepts to analyze the statistical properties of public transport networks of several large cities, looking at all technologies and accounting for the overlapping property of transit systems, notably finding a harness effect. They also attempted to model system based on number of stations and lines.

On the other site we do not register many authors who deal with evolving transport networks, especially public transport networks. Albert and Barabási [3] brought fundamentals of evolving networks. If new nodes and edges appear while some old ones disappear, we can talk about evolving networks. The Barabási–Albert model was the first model to derive the network topology from the way the network was constructed with nodes and links being added over time. From there they were derived many other evolving network models. Evolution models are often used primarily to study social networks for instance Snijders et al. [25], Xu and Hero [26]. Nevertheless we register some examples. Zi-You and Ke-Ping [27] investigated the emergence of scale-free behavior in a traffic system by using the NaSch model to simulate the evolution of traffic flow. Xie and Levinson [28] describe generally evolving transportation networks. In this publication they tried to understand the process of network growth by identifying and quantifying its

determining factors. Zhang and Xu [29] applied the evolution model on China domestic airline network from the year 1950 to 2010. All of the above works examined the evolution of transportation networks in several decades. But evolution of public transport network in short periods, for instance 24 h, has not been elaborately described or dealt with in the existing literatures.

Interesting element of the basic characteristics in the public transport network is an analysis of communities. The property of community structure appears to be common to many networks. Consider for a moment the case of social networks, for instance networks of friendships or other acquaintances between individuals. It is a matter of common experience that such networks seem to have communities in them: subsets of vertices within which vertex–vertex connections are dense, but between which connections are less dense.

The ability to detect community structure in a network could clearly have practical applications [30]. Communities in a social network might represent real social groupings, perhaps by interest or background; communities in a citation network might represent related papers on a single topic; communities on the web might represent pages on related topics [31]. The same can be observed also in public transport networks [24].

We do not register any literature that examines in detail communities either in evolving public transport networks or in transport networks generally. It is unexpected, since having the ability to identify communities (in static or dynamic network) could be helpful in more effective understanding and utilizing of these networks. Figure 1 provides an efficient representation of data used throught our paper.

Nowadays has research of communities still mainly significant application in medicine. Communities are widely used in medical science and neuroscience to understanding and examining the processes occurring in the human brain.

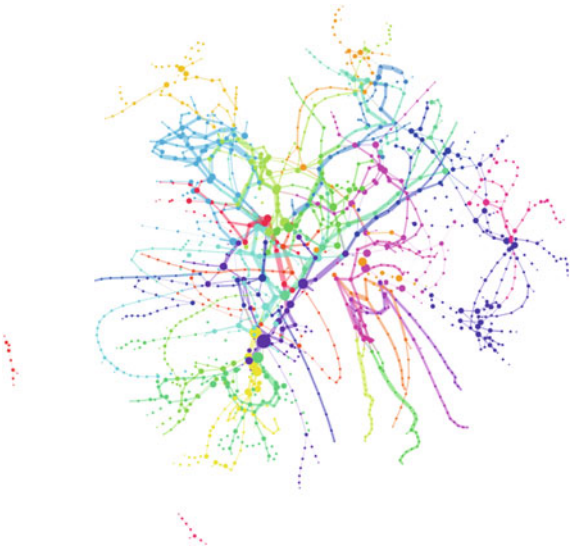

Fig. 1 Louvain network communities identified in pooled 24 h cycle in Bratislava, space is non-geographic for clarity. *Source* July 09, 2013 public transportation schedule by Apptives

Zemanová et al. [32] found that the network of cortical area displays clustered synchronization behavior and the dynamical clusters closely coincide with the topological community structures observed in the anatomical network.

A useful study was elaborated by Wu et al. [33] and it can be used not only in medicine, but also in public transport analyses. The main objective of this study was to reveal an overlapping community structure of the structural brain network in individuals. They demonstrated that 90 brain regions were organized into 5 overlapping communities associated with several well-known brain systems. The overlapped nodes were mainly attributed to brain regions with higher node degrees and nodal efficiency and played a pivotal role in the flow of information through the structural brain network. Similar overlapped nodes exist in communities of public transport network. These nodes (stops) represent the most important places of the public transport network.

There could be also found some parallels between brain network and transportation network research in the recent paper of Crossley et al. [34] which examines community structure of the human brain. They revealed modifications in network structure of dynamic brain network through changes in communities.

2 A Representative Day in Bratislava

We have made first analysis of Bratislava public transport network in our previous paper [35]. Since much information remains hidden in a static network representation, we decided to further elaborate research on the role of time. Data analyzed in this paper are more detailed in respect of temporal dimension. Thus, the analysis is based on the dynamics throughout the day. In our assumption, the nature of public transport changes during day, along with changing demand of its users. This is where our research potentially connects with economic literature.

We obtain detailed time schedules of public network in Bratislava used for iTransit Android client by Apptives. Reference date for the schedule is July 09, 2013, but it consists of alternative daily schedules for ordinary workday, weekend day, and school vacations workday. We proceed by pooling these different schedules into a representative day not existing in reality, but useful as an analytical generalization.

The network under study consists of 584 stations represented as 1,379 station nodes according to their geographical position and total of 94 routes. Because each station node is operated only in one direction, we used directed graph as representation of network. By connecting stations with all routes regardless of vehicle type, we got 1,536 links served by public network. Only some links are operated throughout the whole day. During 24 h cycle we record 463,125 one station rides. For a better comparison, we have split the 24-h day into equal-length samples. Ranges of individual intervals are shown in Table 1.

Table 1 Basic statistics and communities of dynamic public transport network.

Sample	1	2	3	4	5	6	7	8
Duration	00:00–02:59	03:00–05:59	06:00–08:59	09:00–11:59	12:00–14:59	15:00–17:59	18:00–20:59	21:00–23:59
Nodes	661	1,206	1,250	1,177	1,246	1,249	1,220	1,150
Arcs	725	1,699	1,684	1,536	1,677	1,666	1,625	1,543
Rides	8,044	30,137	80,098	70,399	75,474	82,339	69,455	47,179
Rides per arc	11.1	17.7	47.6	45.8	45.0	49.4	42.7	30.6
Communities	28	37	32	34	34	31	31	35
Modularity	0.885	0.864	0.866	0.868	0.867	0.863	0.866	0.868
Average number of nodes per community	23.6	32.6	39.1	34.6	36.6	40.3	39.4	32.9
Rides inside communities	7,490	27,250	72,547	63,980	68,609	74,346	63,254	42,999
Between rides	554	2,887	7,551	6,419	6,865	7,993	6,201	4,180
Share of rides inside (%)	93.1	90.4	90.6	90.9	90.9	90.3	91.1	91.1

Source July 09, 2013 public transportation schedule by Apptives

The physical network described above is transferred to graph in the most typical way, stations to nodes/vertices and links to edges. As Barthélemy [36] have shown, there are many ways of representing public transport system as a network. For the aim of this paper we have chosen the space-of-stops or so called L-space representation. Each station is represented in graph by a node and an arc (oriented edge) between two nodes indicates that these are consecutive stations of at least one route [24].

As the result from previous, neighbors are only those stations that can be reached within single-station trip. As mentioned before, the graph we constructed is directed and thus it better reflects real conditions of selected public transportation network. As weights we used the volume of public traffic between stations for given time.

As expected, there are two modes in the network corresponding with rush hours. The first mode, second and third interval sample, is the sharper one, as during first interval there is only small amount of traffic. Second mode can be detected between 12 and 18 h. The volume of traffic is then slowly declining when approaching midnight. Both nodes are visible on all statistics, but mostly on the flow.

Rides per arc summarize flow intensities in subsequent samples. Minimum of 11.1 rides is found in the first sample. Network grows fast between first (+60 %) and third sample (+168 %). First peak is reached over the morning commuting times over 6–9 AM period when we observe 47.6 rides per arc. High level of mobility is then preserved with slightly falling trend until afternoon (−4 and −2 %). After 3 PM the network rises once again (+10 %) and reaches 24 h culmination at 49.4 rides per arc. Last sample is at the level 30.6 rides to which and beyond the network dies relative slowly (−14, −28, −64 %) in compare to morning rises. Urban heartbeat is regular but not symmetric. Visual representation in graph series in the Fig. 2 supports this observation.

Second panel in the Table 1 summarizes few basic statistics for communities identified on described network [37]. If we compare statistics with previous we can conclude, that with rising amount of traffic, the network is more concentrated. It is also visible from smaller amount of bigger communities in the rush hours. High modularity levels in all samples suggest that the network under observation is composed of surprisingly well defined structural elements. The individual parts of topology are connected rather inside than between. Links between these play the role of bridges. Only about 9 % of rides over 24 h cycle establish these bridges.

We further pay attention to the number of nodes per community as one of possible evaluation criteria. Naturally, nodes have varying position in the network captured by different centrality measures, including the basic degree distribution. But still we may see from the Fig. 3 that we consistently observe about one large community having above 100 departure points. Average number of nodes per community varies between minimum of 24 in the first sample and maximum of 40 in the evening peak sample. The average lies at 35 nodes, which describes a standard network community in Bratislava daily cycle. Larger composition units appear during morning peak 6–9 AM and afternoon/evening 12 AM–9 PM.

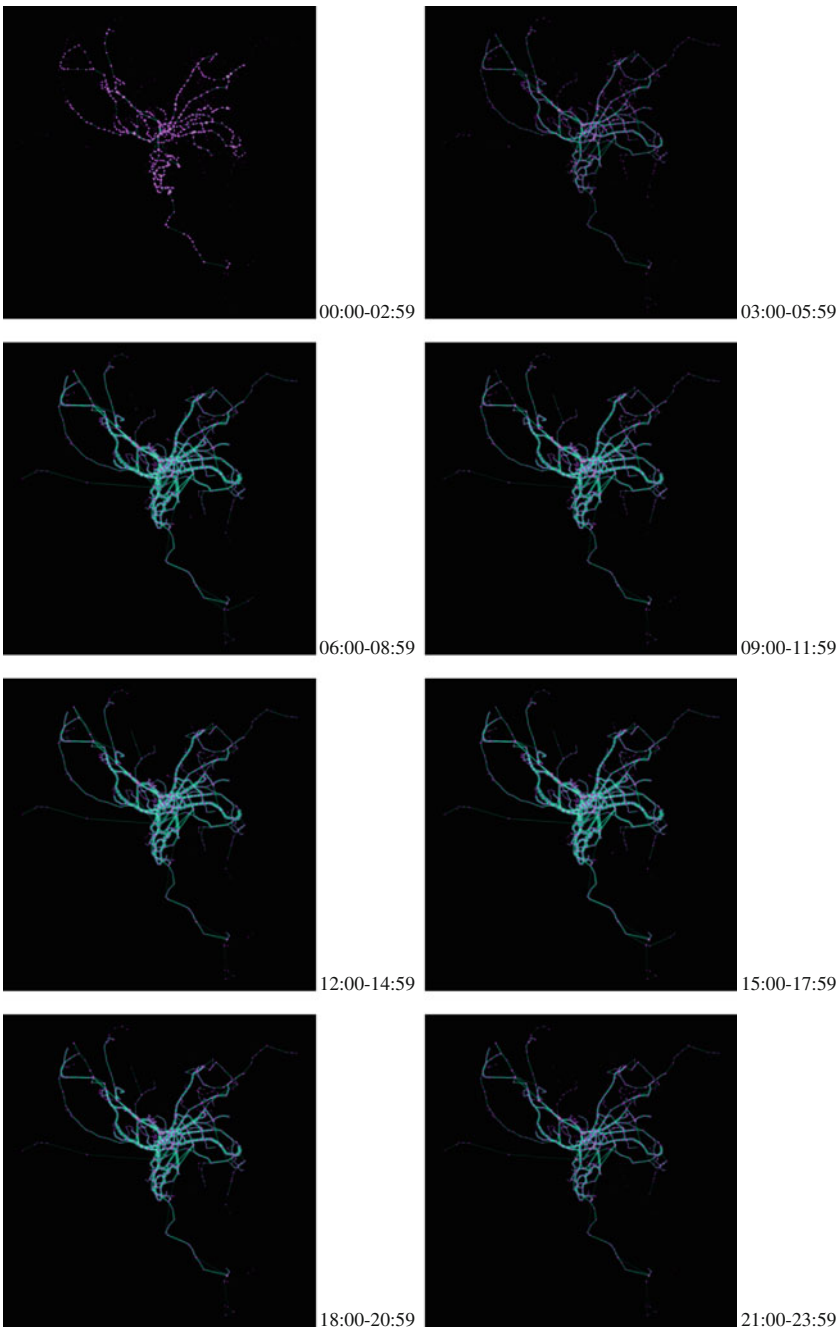

Fig. 2 Eight aggregated samples represent varying degree of connected nodes linked by operating vehicle-count integer weighted links in Bratislava. *Source* July 09, 2013 public transportation schedule by Apptives

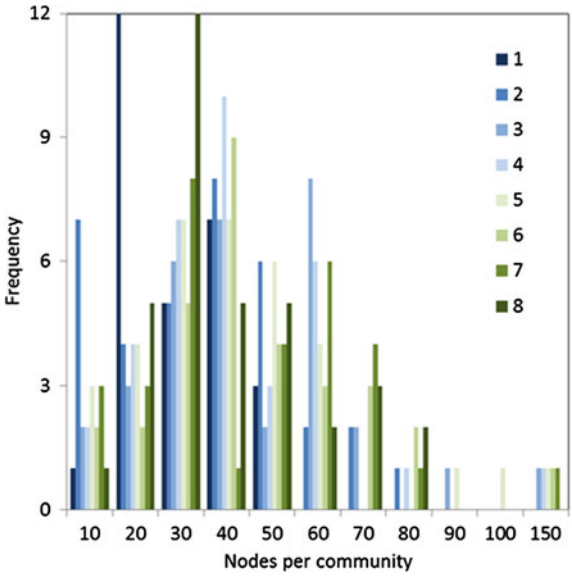

Fig. 3 Size distribution of network communities identified in eight time samples (1–8). *Source* July 09, 2013 public transportation schedule by Apptives

3 Conclusion

Network approach recently developed in theoretical physics and related disciplines continuously proves to be a promising direction of research also in case of urban transportation studies. We use public transport system in a usual European city to demonstrate that it behaves systematically along the daily cycle in response to changing demand from inhabitants and firms in roles of economic actors. Not only overall scale of this network is modified but also structural composition of network topology.

Even the most basic description of data available from schedule demonstrates that daytime rhythm, which we call urban heartbeat, is present in network structure very clearly. Network consists of smaller communities in times of lowest intensities of interaction supplied by public service lines and largest communities in times of highest intensities of interaction over peak hours. Mobility system therefore integrates with scale increase and disintegrates with scale decrease. This finding might be trivial, but it has interesting implications hypothetically beyond the lines of transportation research.

This paper did not even touch details of the subject of precise topology composition. Public transport stops are members of the same community consistently with others, on average, exactly 34 partners, but not over the whole day. From hour to hour de facto barriers within the urban fabric are crossed by the same or different network bridges. Knowing where these are located and possibly explained why exactly there and not in a different place is a suggestion for further developments in this research.

Acknowledgments This research was supported by VEGA grant 1/0562/12 with the name "New demographical analysis and prognosis of the population of Slovakia and its regions by using of progressive geographical applications" and by UK grant UK/221/2013 titled "Analysis and modeling of Bratislava public transport". We also thank Apptives for providing data.

References

1. Watts DJ, Strogatz SH (1998) Collective dynamics of 'small-world' networks. Nature 393 (4):440–442
2. Barabasi AL, Albert R (1999) Emergence of scaling in random networks. Science 286:509–512
3. Albert R, Barabási AL (2002) Statistical mechanics of complex networks. Rev Mod Phys 74:47–97
4. Strogatz SH (2001) Exploring complex networks. Nature 410(6825):268–276
5. Scott J, Carrington PJ et al (2011) The SAGE handbook of social network analysis. SAGE publications, London
6. Choi JH et al (2006) Comparing world city networks: a network analysis of Internet backbone and air transport intercity linkages. Glob Netw 6(1):81–99
7. Amaral LAN et al (2000) Classes of small-world networks. Proc Natl Acad Sci 97 (21):11149–11152
8. Jeong H et al (2000) The large-scale organization of metabolic networks. Nature 407 (6804):651–654
9. Bagler G (2008) Analysis of the airport network of India as a complex weighted network. Phys A Stat Mech Appl 387(12):2972–2980
10. Zhang J et al (2010) Evolution of Chinese airport network. Phys A Stat Mech Appl 389 (18):3922–3931
11. Seaton KA, Hackett LM (2004) Stations, trains and small-world networks. Phys A 339 (3–4):635–644
12. Xu X et al (2007) Scaling and correlations in three bus-transport networks of China. Phys A 374(1):441–448
13. Latora V, Marchiori M (2001) Efficient behavior of small-world networks. Phys Rev Lett 87 (19):198701–198704
14. Latora V, Marchiori M (2002) Is the Boston subway a small-world network? Phys A 314 (1–4):109–113
15. Von Ferber C, Holovatch T, Holovatch Y, Palchykov V (2007) Network harness: metropolis public transport. Phys A 380:585–891
16. Soh H et al (2010) Weighted complex network analysis of travel routes on the Singapore public transportation system. Phys A 389:5852–5863
17. Latora V, Marchiori M (2000) Harmony in the small world. Phys A 285(3–4):539–546
18. Sen P et al (2003) Small-world properties of the Indian railway network. Phys Rev E 67(3), id 036106
19. Musso A, Vuchic VR (1988) Characteristics of metro networks and methodology for their evaluation. Transp Res Rec 1162:22–33
20. Vuchic VR, Musso A (1991) Theory and practice of metro network design. Public Transp Int 40(3):298–325
21. Derrible S (2012) Network centrality of metro systems. PLoS ONE 7(7):e40575
22. Sienkiewicz J, Holyst JA (2005) Statistical analysis of 22 public transport networks in Poland. Phys Rev E 72(4):0461271–04612711
23. Lu H, Shi Y (2007) Complexity of public transport networks. Tsinghua Sci Technol 12 (2):204–213

24. Von Ferber C, Holovatch T, Holovatch Y, Palchykov V (2009) Public transport networks: empirical analysis and modeling. Eur Phys J B 68(2):261–275
25. Snijders T et al (2007) Modeling the co-evolution of networks and behavior. In: van Montfort K, Oud H, Satorra A (eds) Longitudinal models in the behavioral and related sciences. Lawrence Erlbaum, Mahwah, pp 41–71
26. Xu KS, Hero AO (2013) Dynamic stochastic blockmodels: statistical models for time-evolving networks. Available via DIALOG. http://arxiv.org/pdf/1304.5974v1.pdf. Accessed 25 Sep 2013
27. Zi-You GAO, Ke-Ping LI (2005) Evolution of traffic flow with scale-free topology. Chin Phys Lett 22(10):2711
28. Xie F, Levinson DM (2011) Evolving transportation networks, vol 1. Springer, Berlin. ISBN: 978-1-4419-9803-3
29. Zhang W, Xu D (2012) Evolving model for the complex traffic and transportation network considering self-growth situation. Discrete Dyn Nat Soc. doi:10.1155/2012/291965
30. Girvan M, Newman ME (2002) Community structure in social and biological networks. Proc Natl Acad Sci 99(12):7821–7826
31. Fortunato S (2010) Community detection in graphs. Phys Rep 486(3):75–174
32. Zemanová L et al (2008) Complex brain networks: from topological communities to clustered dynamics. Pramana 70(6):1087–1097
33. Wu K et al (2011) The overlapping community structure of structural brain network in young healthy individuals. PLoS ONE 6(5):e19608
34. Crossley NA et al (2013) Cognitive relevance of the community structure of the human brain functional coactivation network. Proc Natl Acad Sci 110(28):11583–11588
35. Ondoš S, Paulovičová I, Belušák L, Kusendová D (2013) The Bratislava public transport in network analysis. GIS Ostrava 2013, Ostrava, VŠB—Technická Univerzita Ostrava. ISBN: 978-80-248-2951-7
36. Barthélemy M (2011) Spatial networks. Phys Rep 499:1–101
37. Blondel DV, Guillaume J-L, Lambiotte R, Lefebvre E (2008) Fast unfolding of communities in large networks. J Stat Mech Theor Exp 10:P1000

Improving Geolocation by Combining GPS with Image Analysis

Fábio Pinho, Alexandre Carvalho and Rui Carreira

Abstract The Global Positioning System (GPS) provides geolocation to a considerable number of applications in domains such as agriculture, commerce, transportation and tourism. Operational factors such as signal noise or the lack of direct vision from the receiver to the satellites, reduce the GPS geolocation accuracy. Urban canyons are a good example of an environment where continuous GPS signal reception may fail. For some applications, the lack of geolocation accuracy, even if happening for a short period of time, may lead to undesired results. For instance, consider the damages caused by the failure of the geolocation system in a city tour-bus transportation that shows location-sensitive data (historical/cultural data, publicity) in its screens as it passes by a location. This work presents an innovative approach for keeping geolocation accurate in mobile systems that rely mostly on GPS, by using computer vision to help providing geolocation data when the GPS signal becomes temporarily low or even unavailable. Captured frames of the landscape surrounding the mobile system are analysed in real-time by a computer vision algorithm, trying to match it with a set of geo-referenced images in a preconfigured database. When a match is found, it is assumed that the mobile system current location is close to the GPS location of the corresponding matched point. We tested this approach several times, in a real world scenario, and the results achieved evidence that geolocation can effectively be improved for scenarios where GPS signal stops being available.

F. Pinho (✉)
Associação Fraunhofer Portugal Research, Rua Alfredo Allen 455,
4200-135 Porto, Portugal
e-mail: fabio.pinho@fraunhofer.pt

A. Carvalho
INESC Porto, Rua Dr. Roberto Frias, 378, 4200-465 Porto, Portugal
e-mail: alexandre.valle@fe.up.pt

R. Carreira
Instituto de Telecomunicações, Departamento de Engenharia Electrotécnica e de Computadores, Faculdade de Engenharia da Universidade do Porto, Rua Dr. Roberto Frias, S/N, 4200-465 Porto, Portugal
e-mail: ruicar@fe.up.pt

I. Ivan et al. (eds.), *Geoinformatics for Intelligent Transportation*,
Lecture Notes in Geoinformation and Cartography,
DOI 10.1007/978-3-319-11463-7_15

Keywords Computer vision · Geolocation · GPS · A-GPS · Image analysis · Pattern recognition

1 Introduction

In recent years, the means used in the calculation of geographic location have evolved, becoming progressively more accurate. Some of the methods and technologies used in geolocation can give an accurate location on the Earth's surface, but not an exact location [1]. In the field of geographic location, currently, there are three main technologies: Global Positioning System (usually known as GPS), Assisted-GPS (usually known as A-GPS) and Cell tower ID. The first, GPS, is based on a set of geostationary satellites and a computation having as input the GPS signal from those satellite and as output a location on the Earth's surface. However, GPS has two main drawbacks: its signal is highly affected by noise and it requires direct vision between the GPS receiver and a set of at least four satellites [2]. To compensate this problems, and accelerate the positioning, the A-GPS technology was developed, combining GPS information with information from the network. As the main characteristic of this technology indicates, it is internet dependant, which means that the major strength of A-GPS does not work everywhere [3]. Finally, the Cell Tower ID, is a GPS-free technology, that uses only cellular network to reference a position. This technology uses cell coverage to determine the position of some device, but it is not much accurate [4].

The geolocation technologies above presented perform well for most of the cases. However, for some situations, GPS and A-GPS may not be able to provide geographic location. For instance, when a vehicle suddenly enters a long urban street cutting through skyscrapers, the GPS signal may be affected by the metal structures of the buildings and the lack of direct vision from the receiver to the satellites.

Our approach tries to overcome this problem by combining computer vision (CV) with GPS, regarding the scope of geolocation, where CV is used to help in the geolocation process when GPS signal is weak or not available.

Computer vision has evolved in the last decade and its applications are becoming more comprehensive. As Bernal stated [5], when we think about computer vision, it is impossible not to think about using features. In CV, many feature descriptors have already been proposed and tested. According to Bernal, feature descriptors can be divided into four main groups: texture descriptors, colour descriptors, shape descriptors and motion descriptors [5]. For the purpose of the current work, a study of several descriptors was previously performed and three main descriptors were selected as being most promising: Scale Invariant Feature Transform (SIFT, [6]), Speeded-up Robust Features (SURF, [7]) and Histogram of oriented gradients (HOG, [8]). The three algorithms present good results, in terms of analysis success rate and response time, but the HOG was slightly inferior to SIFT and SURF.

Besides this fact, both SIFT and SURF are Scale invariant, which means that both can detect features for images captured from different distances (affecting the size of a target, in a picture). The HOG does not provide this important feature. The SIFT algorithm provides another critical feature for our purposes: it is rotation invariant, meaning that it can contour rotation problems. Due to this second invariance feature it takes a little more time to process an image, compared to the SURF algorithm [5].

Our approach relies on a set of characteristic points stored in a reference database. Each point is designated by Point of Interest (POI) and consists of one or more geo-referenced model images of a building, road or monument. In our approach we assume that a mobile system is near the location of a POI if the POI is recognized in one of the captured images assigned to it. Hence, whenever GPS signal fails, the CV system takes over the geolocation data feed process: summarizing, captured frames of the mobile system surrounding landscape are analysed by a CV algorithm, in real-time, trying to recognize POIs (from the database) in the captured frames. To the extent of the test cases, the current work demonstrates that, without GPS signal and with the help of simple computer vision algorithms, it is possible to obtain conclusive answers about a mobile system current location based on the proximity to a well-known (POI) location.

In Chap. 2, the proposed approach is described and explained in more detail and, in Chap. 3, the prototype used for tests is presented. Chapter 4 shows the tests that we conducted in order to validate our prototype and Chap. 5 presents the achieved results. In Chap. 66 the results are discussed and finally Chap. 7 and Chap. 8 present the conclusions and future work perspectives.

2 Improving Geolocation by Combining GPS with Image Analysis

The following method is based on the described approach which combines computer vision with GPS (CV-GPS): conceptually, if we consider that the GPS function is to assign coordinates to a location then, by using an inverse logic, if we see a particular geo-referenced POI, then we can assume that we are near to the GPS coordinates of that POI. In the city sightseeing tour example previously mentioned, the “near” concept to a POI can be the line of sight proximity inside an urban canyon.

2.1 CV-GPS Method

GPS alone cannot provide an accurate positioning in situations where the receiver fails to see the required satellites. Feature recognition through computer vision algorithms cannot be used as a solo geolocation method because it would imply to compare millions of images, trying to identify a feature (with geolocation previously associated). For current microcomputers, such task is not possible to be

performed in real-time. If we want to use computer vision to "geo-reference" a location, it is necessary to reduce the set of images to compare. Both these technologies (feature recognition from CV and GPS) can complement each other, in order to create a valuable new geolocation method, able to compensate the complete or partial lack of positioning information.

The main idea of the CV-GPS method is to use available coordinates sent by the GPS receiver and to start the image analysis process when the GPS signal is weak or absent, being impossible to accurately reference the current location. To achieve it, the image analysis process tries to identify a POI in the current captured images. If one is found, the corresponding GPS location is used. The set of POIs is kept in a database where, for each POI, one or more images can be kept. Furthermore, in the database, each image of the POI has the corresponding GPS coordinates associated.

The operation of this method is depicted in Fig. 1, where X is the limit distance, in meters, from which the image analysis process starts being executed, and Y is the maximum time, in milliseconds, that the system may be absent of GPS data before starting the image analysis process. A system implementing this method receives and uses the GPS data acquired from the GPS receiver for geolocation. If the GPS sensor can determine its own accuracy (value in meters correspondent to the approximate error of the coordinates) then the accuracy information is also used.

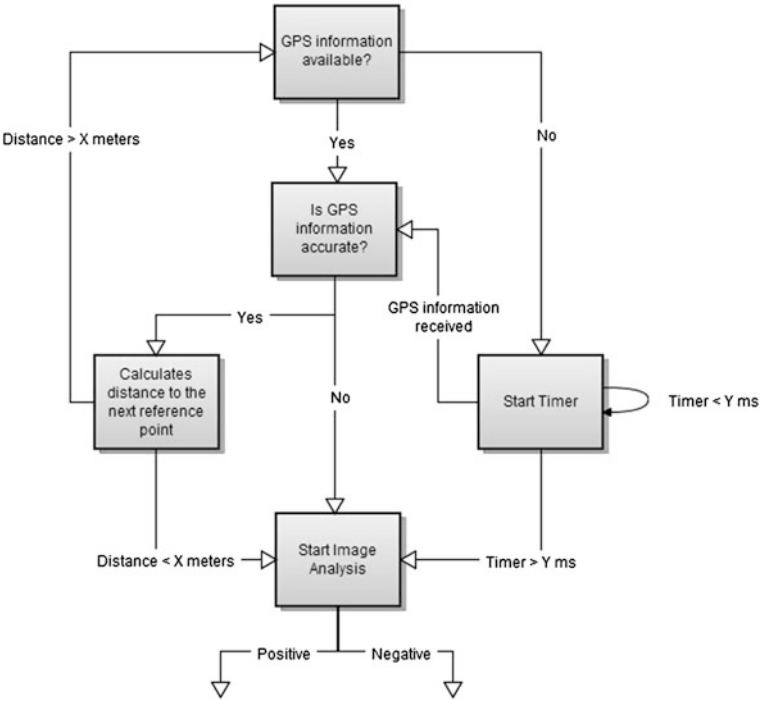

Fig. 1 CV-GPS system operation

In this case, if the GPS information is accurate enough for the geolocation, then the latitude and longitude coordinates may be used to calculate the distance from the current position to the closest set of reference points. This calculation has the purpose of discarding the more distant POIs, reducing the number of valid POIs for image comparison, at any time. If, on the other hand, the received GPS information is not accurate enough to be reliable, then the image analysis is started, to compensate that lack of accurate geolocation information. If the system suddenly stops receiving GPS information, a timer is started. This timer stops either because GPS data is available again or because a maximum time Y is exceeded. In the second situation the image analysis process is started. When this process takes over, if the result of analysis is positive—a POI has been detected in a video frame—the system knows that it is close to the geographic coordinates associated to the matched POI.

2.2 The Image Analysis Component

The image analysis process requests images from two sources: an external camera, placed near the GPS receiver, capturing frames in real-time (observed image) and a database of POIs (model images). From the database, only the images of POIs closer than a threshold X to the actual location are considered. In order to obtain good performances, the number of image comparisons should be the lowest possible, avoiding unnecessary image analysis. To analyse the images, a feature descriptor is used, which detects characteristic elements (features) between two images and compares them trying to find similarities. In our approach, the SURF (Speeded-up Robust Features) algorithm has been used, due to its scale invariance property, which is an important factor to consider when capturing images at distinct distances, affecting the scale of the point to detect [5]. The performance of SURF has also been taken into account, compared to other feature descriptors [9]. The necessary time to analyse each captured frame is an important factor to consider in order to be able to process regions with a higher density of POIs. To guarantee better results, it is important that every reference point has more than one associated reference image, captured from distinct points of view. Ideally, for every POI the database should hold at least three images, one frontal and two lateral, in which case only one match would be necessary to obtain a positive result. This three images allow us to contour the partial lack of rotation invariance of the SURF algorithm. Figure 2 shows outputs generated by the image analysis process.

As it is possible to see in Fig. 2a, the image analysis process found a match, but clearly (red line shape depicts result from algorithm) it does not correspond to a POI, generating a false positive situation. In order to provide better results and discard situations like this, it is important to implement a filter for False Positive discarding. The false positive detection was based in the analysis of the red quadrilateral (more specifically of the four points returned by the algorithm). If the points do not represent a quadrilateral (as depicted in Fig. 2c), the system considers it as a false positive and discards it, because in true positives, the shape resembles a

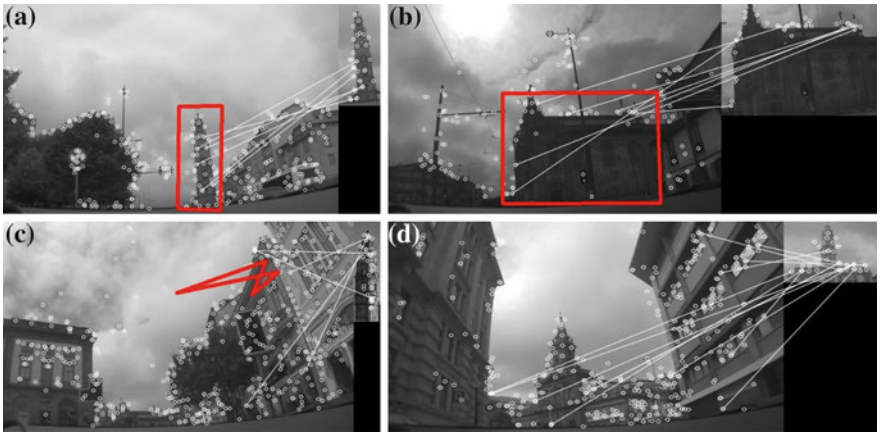

Fig. 2 Image analysis results. **a** and **b** are true positives; **c** is a false positive; **d** similar buildings could generate mistakes but the algorithm performed correctly

quadrilateral (as observed in Fig. 2a, b). In this method context, it is acceptable to discard a true positive, because over a route and for a single POI it is expected several true positive detections, but it is not so good not to discard a false positive, because over a route only one positive is necessary to confirm the geolocation (the method trusts the CV component).

3 Testing Prototype

3.1 Architecture Overview

Conceptually, the proposed method was instantiated through a system architecture composed of three logical modules: media, GPS and server modules. Figure 3 illustrated the three modules as well as the interaction between them.

The Media module is composed by a camera (or set of cameras), properly configured to provide access to one or more video streams (sets of video frames). It is important that these cameras are strategically placed in the vehicle, in order to obtain a clear view of the outside landscape. If this module is composed by only one camera, it should be positioned in the front of the vehicle and pointing forward, so the requested images may display a reference point before passing by it. If this module is composed by more than one camera, then only one of these cameras must be placed as above described, and the others may be placed in order to complement the video capture of the first one. In our prototype, the media module used a video camera Axis M3114-R. The GPS module is composed by a GPS receiver. This receiver must be steady, in order to guarantee that an eventual lack of accuracy of the GPS information is only resultant of the signal reception itself, and not from the

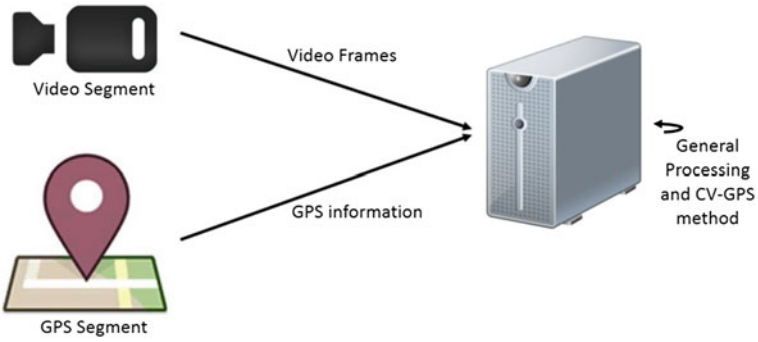

Fig. 3 System architecture

bad adjustment of the receiver. Besides the signal reception, this module must be capable of sending the information to the server module, where it is properly analysed. In the current implementation, an Android Smartphone was used to instantiate the GPS module, running a simple application that captures the GPS coordinates and periodically sends them to the server module. Finally, the server module, implemented as a desktop application, is responsible for most of the processing activity: it receives the video frames from the media module, and the GPS information from the GPS module, and processes the information in order to obtain a valid and accurate positioning of the system. The CV-GPS processing is performed in this module.

This architecture was implemented and tested using a personal vehicle, as illustrated in Fig. 4. In this Figure, it is possible to see the camera and the GPS steady placed over the vehicle's dashboard, and the laptop, running the server application.

Fig. 4 System assembled in the vehicle

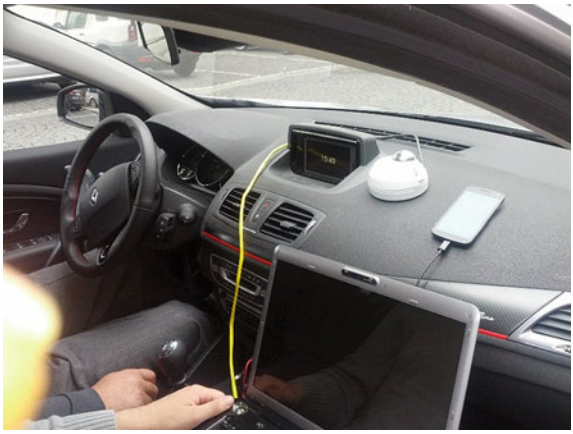

4 Testing and Results

In order to properly evaluate the CV-GPS method, a set of experiments was performed, evaluating if the proposed method can provide geolocation improvements, and if the image analysis system is working as expected in different light conditions (which varies, for instance, with the atmospheric conditions), vehicle velocities or road pavement conditions. It is expected, though, that the system fails in situations where is not possible to get a clear picture of the elements to detect (for instance, under heavy rain). The next sections present the test scenarios used for evaluating the system and the routes and Points of Interest used for performing the experiments. After that, the obtained results are presented and discussed.

4.1 Test Routes and Points of Interest

In the development of the test scenarios three test routes were used, all in the Porto downtown, Portugal. The routes were chosen according with specific characteristics like different distances, road pavements, illumination conditions, and the distance and line of visibility from the road to the Points of Interest expected to be detected.

Also three POIs were used, specifically, POI1 (GPS coordinates 41.145669, –8.614728, two model images associated in the database), the POI2 (GPS coordinates 41.149594, –8.610303, two model images associated in the database) and POI3 (GPS coordinates 41.1475314, –8.6165759, one model image associated in the database). These POIs have distinct shape and textures and as we can see in Fig. 5, their model images were captured under less favourable light conditions (in order to test the system under the worst conditions).

4.2 Experiments

To correctly validate the system, eight experiments were performed, some of them inclusively repeated, in a total of 13 tests. In order to provide enough information to

Fig. 5 Points of Interest used in the detection: **a** POI1; **b** POI2; **c** POI3

replicate the same conditions of these experiments, this tests were performed without rain but with a very cloudy sky (difficult illumination conditions) at 9 of June 2013, between 1 h 30 pm and 4 h 30 pm. In these experiments the CV-GPS method was configured to trigger the image analysis inside a threshold distance of 300 m of the POI (X parameter), or after 2 s without GPS information (Y parameter).

Some of the experiments had similar goals, although performed in different routes and different Points of Interest. This way, the first, second and third experiments had the goal of simply detect the POIs. The first and third experiments were repeated three times (referred as 1.1, 1.2, 1.3 and 3.1, 3.2, 3.3 in the results table). The fourth and fifth experiments targeted the detection of false positives. In the fifth experiment the error was inclusively provoked, by searching for a POI that did not belong to the performed route. The fifth experiment was executed twice (5.1 and 5.2 in results table). The sixth and seventh experiments targeted the simulation of urban canyon situations. To test this situation, we turned off the GPS signal during partial or total time of the route. Finally, the eighth experiment had the purpose of testing a situation where a vehicle is close to a POI, but without seeing it. This happens for instance in single way roads, where the POI is only visible in one way. This way, the vehicle may be passing very close to the POI, but the system only should target it when it is visible (this is not possible by a GPS only solution, because the distance to the POI would probably be the same (or approximately) in both ways of the road, but is possible with the CV-GPS method because the system only returns a valid geolocation when the POI is detected in the image.

5 Results

The execution of the set of experiments described in the previous section allowed us to extract results and take conclusions about the correctness and validity of the CV-GPS system. Table 1 summarizes the results achieved.

The evaluated parameters were the *Duration*, *Number of kilometres* of the route (km), *Average Speed* in which the route was performed (Av. Speed), *Image Analysis Percentage Time* (IAPT) which is the percentage of time in which the image analysis method was running, *Number of Analysed Images* (NAI), *Number of False Positives* (NFP) and finally if the POI was detected in time or not (before the vehicle with the assembled system passes by it). Some of the parameters measured and presented on the table are influenced by the traffic conditions (traffic, semaphores, crosswalks, etc.). All the tests were performed in an urban environment with the limit speed of 50 km/h and with normal traffic conditions. The routes were performed in different average speeds and during an approximated period of 3 h between 1 h 30 pm and 4 h 30 pm. During that period a slightly change of atmospheric conditions occurred, causing a slight increase of the luminosity, but maintaining a very cloudy sky. The (a) label in the `POI detected' column in the test 5.1 refers to the building detected in the false positive, once it was not correspondent to the one we were trying to provoke in this test, but to another building in

Table 1 Experiments results

Test #	Duration (min)	km	Average speed	IAPT (%)	NAI	NP	NFP	POI detected
1.1	3.45	1	25	100	122	6	0	Yes
1.2	3.40	1	35	100	124	7	1	Yes
1.3	3.40	1	40	100	129	6	1	Yes
2	3.25	1	35	100	268	2	0	Yes
3.1	2.15	1.2	30	90	72	5	0	Yes
3.2	2.25	1.2	30	90	76	6	1	Yes
3.3	2.05	1.2	35	90	69	4	0	Yes
4	9.55	2.5	35	18	102	*6*	*0*	Yes
5.1	2.05	1.2	35	90	70	1	1	No[a]
5.2	2.15	1.2	30	90	70	0	0	No
6	9.40	2.5	30	34	187	5	0	Yes
7	3.50	1.2	25	100	107	10	0	Yes
8	3.25	1.2	25	90	76	5	0	Yes

[a] This false positive was not expected

that route (was a regular false positive). This false positive detection was not seen in the other repetition performed in the same route. It is important to refer that the false positives in 1.2, 1.3, 3.2 and 5.1 were detected at a considerable distance of the intended POI (from 180 to 220 m).

6 Discussion

The analysis of the achieved results makes it possible to verify that, for all the performed tests, the target POI was successfully detected in time, and more than once per repetition.

In the first experiment (1.1, 1.2 and 1.3), the POI was detected 6, 7 and 6 times respectively, but also two false positives were found. The false positives were detected with the vehicle stopped at a semaphore, which discards the possibility of being caused by the road conditions or velocity. In the second experiment (2), a single image was available in the database (the POI only had one image associate) for the image analysis matching. For this reason there were performed a lot of more matches than in other experiments. On the other hand, only two positives were detected, because the road where the POI is visible for the camera is only around 50 m long (short time available for detection). In the third experiment (3.1, 3.2 and 3.3), only 90 % of the route was covered by image analysis, because the 10 % remaining were off the analysis maximum distance perimeter. This allowed us to verify that the combination of both technologies was working well, and that the image analysis was being triggered in the right time. Only one false positive was

detected in the third experiment, and it was similar to the one detected in the first experiment. The fourth experiment was performed over a bigger route (2.5 km), but only 18 % of it was covered by image analysis. In this experiment it was possible to verify that the GPS information was properly working together with the image analysis, in order to minimize the detections in places where no POI was available for detection. At the same time, it was possible to verify that no false positives were detected in this route. The fifth experiment had the deliberate objective of mislead the system. By introducing incorrect information in the database it was possible to verify if the image analysis component would mix up the POIs and detect a not existing POI in the image (the POI did not even belonged to that route). This experiment was repeated twice. In the first repetition, 5.1, a false positive was detected, but not where it was expected. The false positive was detected around 180 m of the coordinates of the target POI, which means that the system did not confused the POI1 with POI2, but failed in a common detection as in the false positives detected in the experiments number one and three. In the second repetition, 5.2, the experiment went as expected and no POI was detected. The sixth experiment tried to simulate an urban canyon situation, where suddenly the GPS coordinates stop being available. In order to simulate this, as explained in the previous sections, the GPS was turned off which increased the percentage time of image analysis of this route to 34 %, because the image analysis was started after 2 s without GPS input. The experiment returned positive results, and POI1 was detected in time, without false positives. In the seventh experiment the goal was once again to simulate an urban canyon situation by deactivating the GPS information, but using a different route. The results were as expected and POI2 was detected in time. The eighth and last experiment, evaluated a problematic situation that could not be solved by a GPS only solution. A method using GPS information only would consider that the vehicle was passing by the POI in a situation where the POI would not be visible yet but with this system, the POI was detected in the proper time, and no false positives were detected.

Summarizing, we verified that the system performed as expected in most cases. The light conditions in which the system was tested were not ideal at all, and nevertheless the system responded quite well. With better atmospheric conditions, it is expected that the results are at least this good, because the quality of the captured images would be superior. The false positives detected in tests 1.2, 1.3, 3.2, and 5.1 occurred relatively far from the expected POIs, at variable distances from 180 to 220 m, and can be discarded by simply reducing the threshold distance used to trigger the image analysis (which is clearly too high), or by fixing the problem in the image detection stage, by adding another filter to the results obtained from the image analysis algorithm. This filter would discard the concave quadrilaterals returned in the detection, pattern verified in all the false positives detected. Furthermore, the 300 m distance threshold used in the experiments proved themselves to be an overkill, because in most cases the POIs were not even visible at that distance. Nevertheless, by using that distance was possible to keep the image analysis running for a longer period of time, allowing a better study of the false positive detections and guaranteeing that the number of false positives was already

satisfactory. In future tests, perhaps it would suffice to use the image analysis within a distance threshold of 100–150 m to the POI. Finally, regarding performance of the system, concerning the image descriptor, although the results of the image analysis are very good (considering the number of analysed images and the number of false positives detected) the time that each analysis took might still be improved by using a faster image descriptor. An example of a faster algorithm is ORB (Oriented BRIEF) detector [10]. Theoretically, this new detector can perform more analysis per second, keeping the same success rate than SURF detector.

7 Conclusion

This work presents an innovative approach for keeping geolocation accurate in mobile systems that rely mostly on GPS, by using computer vision to help providing geolocation data when the GPS signal becomes temporarily low or even unavailable. For some applications, for instance, a city tour-bus transportation that shows location-sensitive data in its screens as it passes by a POI, the lack of GPS data, even for a short period of time, may lead to undesired results.

The main contribution of this work is a method that enables geolocation by using feature recognition from computer vision and GPS technology in a complementary fashion. When available, GPS signal is used in order to know the distance from the mobile system where the CV-GPS is assembled, to the nearer POIs. This way, it prevents the CV system from trying to find a match with the entire set of POIs available in the database. When GPS signal is unavailable the CV module (feature recognition) is used to identity POIs in video frames, captured by a video camera placed on a mobile system. If a POI is matched to one of the POIs available in the database containing model images, then it is assumed the mobile transport is known to be near GPS coordinates associated to the matched POI. As soon as GPS data restarts being available, the computer vision system stands by.

To test our method we defined a set of experiments (appropriate variables and test scenarios). The resulting set consisted of eight experiments, some of which were repeated more than once. The experiments targeted different goals: to test the simple detection of POIs, to test false positive situations by forcing these situations, to simulate situations of lack of GPS signal and simulate urban canyon situations (no GPS signal). Three distinct routes and three distinct POIs were used in our experiments, with different characteristics, such as, different road conditions or POIs texture or shape. The atmospheric conditions under which the tests were conducted were not ideal (cloudy day), with less favorable light conditions.

The results achieved were positive for almost every experiment: only few false positives were detected. Good results were achieved with different floor conditions, vehicle velocities and with or without GPS information available, returning only four bad result instances. The four false positive detections are acceptable if we consider that 1,472 images were analyzed. Furthermore, we detected a pattern in the identified false positives (the pattern recognition result returns a concave

quadrilateral), which allows us to hereafter develop a new filter capable of discard a larger set of false positives.

The achieved results allow us to conclude that the proposed method is valid for scenarios similar to those where we conducted our experiences. Other improvements can be performed, which are defined in the next section.

8 Future Work

Future work will address issues related to system performance, POI match outcome and further experiments. Regarding performance, although the SURF algorithm has presented good results, it would be important to test the ORB detector, which theoretically can perform more analysis per second with the same success rate. Regarding POI match outcome, a new filter should be tested that detects the current false positive situations by discarding concave quadrilaterals. Finally, further experiments are recommended with distinct light conditions, for instance, higher luminosity, and a higher density of POIs to detect, in order to verify the system accuracy and performance.

References

1. Wing M, Eklund A (2007) Performance comparison of a low-cost mapping grade global positioning systems (GPS) receiver and consumer grade GPS receiver under dense forest canopy. J For 105:9–14
2. Monico J (2000) Posicionamento pelo NAVSTAR-GPS. Editora UNESP, São Paulo
3. Diggelen F (2009) A-GPS—Assisted GPS, GNSS and SBAS. Artech House, Boston
4. Figueiras J, Frattasi S (2010) Mobile positioning and tracking: from conventional to cooperative techniques. Wiley, London
5. Bernal J, Vilariño F, Sánchez J (2010) Feature detectors and feature descriptors: where we are now. Universitat Autonoma de Barcelona, Barcelona
6. Lowe DG (1999) Object recognition from local scale-invariant features. In: The proceedings of the seventh IEEE international conference on computer vision, 1999, 20–27 Sept 1999, pp 1150–1157
7. Bay H, Tuytelaars T, Van Gool L (2006) SURF: speeded up robust features. In: Computer vision-ECCV, Springer, Graz, 7–13 May 2006, pp 404–417
8. Dalal N, Triggs B (2005) Histograms of oriented gradients for human detection. Computer vision and pattern recognition (CVPR 2005), San Diego, 25 June 2005, pp 886–893
9. Juan L, Gwun O (2009) A comparison of SIFT, PCA-SIFT and SURF. Int J Image Process 3:143–152
10. Rublee E, Rabaud V, Konolige K, Bradski G (2011) ORB: an efficient alternative to SIFT or SURF. International conference on computer vision, Barcelona

The Impact of Data Aggregation on Potential Accessibility Values

Marcin Stępniak and Piotr Rosik

Abstract The paper focuses on an investigation of the Modified Areal Unit Problem (MAUP) in a potential accessibility case study of the Mazovia region. Three different potential accessibility models were prepared based on the same theoretical background and coherent spatial data: a municipal model, a grid model and a population-weighted average travel time model. We concentrated on two main issues: the differences in the results produced by the three different models, and the impact of different methods of calculation of self-potential on these differences. The results show significant differences in accessibility values produced by the three models tested. The municipal model produced underestimated values of potential accessibility indicator in all spatial units. The differences are first of all a consequence of taking into consideration the densely populated peripheral districts of Warsaw that are 'visible' in grid-based models, but 'not visible' (i.e. averaged) in the central-location oriented municipal model. As a consequence, the total travel time between the average (population-weighted) origin-destination grid nodes is shorter than that calculated at the municipal level and the potential accessibility values are higher in both grid-based models. However, in general, the main cause of the differences of accessibility values observed is not the self-potential but rather the complexity of transportation and land use relations between neighbouring municipalities.

Keywords Potential accessibility · Modifiable areal unit problem · Self-potential · Poland

M. Stępniak (✉) · P. Rosik
Polish Academy of Sciences, Institute of Geography and Spatial Organization,
ul. Twarda 51/55, 00-818 Warsaw, Poland
e-mail: stepniak@twarda.pan.pl

P. Rosik
e-mail: rosik@twarda.pan.pl

I. Ivan et al. (eds.), *Geoinformatics for Intelligent Transportation*,
Lecture Notes in Geoinformation and Cartography,
DOI 10.1007/978-3-319-11463-7_16

1 Introduction

Over recent years accessibility has become one of the key questions discussed, not only in the narrow context of transport geography research, but also in a broad range of economic, social or planning studies. The possibilities that have emerged resulted from increased computational capacity and the wide application of GIS-software in accessibility studies and have provoked a growing number of studies dedicated to transport geography issues. These increased possibilities permit the use of more and more detailed geographical data prepared for wider study areas. Nevertheless, there is a significant lack of reflection on the consequences for accessibility analyses of the application of data designed at different spatial resolutions. We still have limited knowledge about how models that are based on highly disaggregated spatial data alter accessibility scale and pattern. The so-called MAUP-effect (*Modifiable Areal Unit Problem*; [1]), broadly discussed in the spatial studies literature [2–5], is still relatively undiscovered in the field of accessibility studies. The existing investigations follow the approach of Townshend and Justice [6], i.e. they concentrate on the selection of the resolution appropriate to the particular analysis focusing on the scale dimension of the MAUP [7, 8]. At the same time, they do not compare results between models that are based on administrative units and grid layers. The paper presented here tries to bridge this gap, following Fotheringham's highlighting of the need for multiscalar spatial analysis [2]. We used an assumption provided by Kwan and Weber [9], that the use of multilevel modelling to explain accessibility offers the opportunity to find geographical variations previously invisible with single level models. Finally, the aim of the paper is not only to provide evidence of the existence of the MAUP in accessibility analysis (which is quite obvious), but also, following Wong [10], to highlight locations that deserve more attention when applying the MAUP approach in potential accessibility analysis.

The MAUP is a consequence of the use of arbitrarily defined boundaries of areal units [11], i.e. the results of spatial analysis depend on the definition of the areal units applied to the analysis [3]. The impact of MAUP can be divided into two components: the scale effect and the zoning effect. The former is related to the level of aggregation of spatial data, while the latter to the redrawing or regrouping of spatial units at a given scale [1]. The difference between the units applied in the study presented (i.e. municipalities and raster-cells) is linked to the scale effect of the MAUP. The results of the accessibility study may be questioned when aggregated data is used (e.g. municipal data), while no such criticism applies to an investigation that is based on disaggregated data [3] or data that represents the continuous space [2]. Herein, the raster layer consisting of 1 km^2 grid cells is used as a proxy of disaggregated data that should be free from the MAUP effect. Due to the smoothing process [3, 10] an accessibility model that uses larger areal units (i.e. municipalities) should provide a more homogenous surface for the spatial accessibility pattern than a model that applies more detailed spatial units (i.e. raster-cells). However, in addition to the scale of spatial units, the spatial aggregation

mechanism is also a key factor that determines the impact of the MAUP [10]. Therefore, our study is trying to provide information concerning the impact of the aggregation mechanisms on the results of potential accessibility analysis.

The paper is divided into five main sections. After the introduction, the potential accessibility approach is outlined. Then, in the third section, a case study area of the Mazovia region is presented, including the network and population data involved in the analysis. The same section covers the data processing procedure and three different potential accessibility models are presented in detail. In the fourth section the empirical results are presented followed by the conclusions in the final section.

2 The Potential Accessibility Approach

In transport studies, several different meanings are ascribed to the term 'accessibility', comprising issues relating to land use policy, infrastructure equipment, quality of transport networks, opportunities for interaction at the society level etc. The potential accessibility approach enables the observer to present one face of the multifaceted phenomenon of accessibility. Potential accessibility studies are focused on one or more of the following main themes:

- Assessment of the scale and pattern of regional accessibility disparities [12–14]
- Examination of the impact of accessibility on regional development, e.g. in terms of the location of manufacturing firms [15] or population distribution [16]
- Evaluation of new transport investments, including their impact on the improvement of overall accessibility [17−19] and/or the degree of territorial cohesion [20–23].

The proposed methodology, which is tested in the research presented here, can be applied in all of the above mentioned types of investigation. Nevertheless, due to the fact that calculations are extremely work-intensive and time-consuming, efforts should be made to provide some limits to the area of study.

Potential accessibility models are based on the distance, travel time or cost between all pairs of origin-destination nodes within the given model assuming a greater impact of larger centres than smaller ones, and a diminishing importance of more distantly located destinations [24, 25]. Its mathematical description presents as follows:

$$A_i = \sum_j g(M_j) f(c_{ij}). \tag{1}$$

where $g(M_j)$ is the function of destination attractiveness, and $f(c_{ij})$ is a distance decay function. In the analysis presented below we use time, calculated as travel time by private car, as a distance decay element. The destination attractiveness (so-called 'mass') is measured as the total population attributed to a given network node (i.e. municipality or grid cell). The distance decay function responds to the

negative correlation between distance and the importance of the interrelation between a given pair of nodes. Although a large body of literature exists which is dedicated to different types of distance decay functions [26, 27], we decided to restrict the tests of our methodology to only one of those most commonly used in accessibility studies: the negative exponential function ([12, 28, 29], among others):

$$f(c_{ij}) = \exp(-\beta c_{ij}) \tag{2}$$

The selection of a particular value of β parameter allows one to estimate the accessibility level in terms of different travel purposes [13]. We chose time as a distance decay element. As the methodology presented is potentially valuable for the local scale of analysis, we decided to select the β parameter of 0.023105, which corresponds to short-distance trips (e.g. commuting), i.e. median travel time is equal to 30 min [23]. The assumed median travel time is in accordance with empirical observations derived from the *Warsaw Traffic Survey* [30].

Taking this further, the incorporation of self-potential is an important factor that leads to the obtaining of proper values of the potential accessibility indicator [31, 32]. The calculation of self-potential is based on the estimation of internal travel time within a given spatial unit that is based on the radius r_i, involving the formula proposed by Rich [33]:

$$t_{ii} = \frac{0.5 * r_i}{\overline{v_{ii}}} \tag{3}$$

using a speed $\overline{v_{ii}}$ equal to 20 km/h as the assumed internal travel time. Similarly, the travel time between each pair of nodes should be increased to take account of the time needed to arrive at the origin and destination node (access and egress time). This is achieved by the application of the same formula as that used for obtaining the internal travel time (separately for both origin and destination units respectively).

3 Study Area and Data Processing

The proposed methodology has been tested on the Mazovia region, the biggest (35,600 km^2) and the most populated (5.2 m inhabitants) *voivodeship* (NUTS-2 unit) in Poland. This region is strongly monocentric, with the dominant role of the capital city, Warsaw, and its metropolitan area. However, it is also highly diverse in terms of population density and settlement structure, as well as in terms of density and the quality of road transport networks. The motorway network is unequally distributed and consists of a relatively well-developed infrastructure in the south-western part of the region, and only a few, short and fragmented motorway sections in the eastern and northern parts of Mazovia.

Apart from its internal diversity, the most significant characteristic of the study area is its central location in Poland. In spatial analysis, distortion of the results can be

observed in peripheral parts of the study area [34]. The so-called 'edge effect' was also observed in accessibility analyses (e.g. [35, 36], among others). In order to account for this problem, potential analysis was carried out based on the study area extended to the whole country, even though the remote destinations have limited impact on potential indicator values. Thus, all municipalities in Poland are included when calculating the potential accessibility indicator, however results are only presented and analysed for those which are located within the Mazovia region (314 units).

The municipal population data for 2012 were collected from the Local Data Bank. Apart from analysis at the very detailed administrative level (LAU-2, the lowest administrative division in Poland), the model has also been developed at the higher resolution of 1 km^2 grid cells. Therefore, the population data in 1 × 1 km grid cells were prepared on the basis of the GEOSTAT 2006 population grid dataset. In order to ensure the comparability of results the GEOSTAT data were updated using 2012 population data at municipality level derived from the Local Data Bank for the estimates. Finally, due to the extremely time-consuming calculations expected, population data is only disaggregated in the case of LAU-2 units located within the Mazovia region. In consequence, municipalities located outside the Mazovia region remain unaffected.

The original, very detailed road network dataset is used in the analysis which corresponds to the road infrastructure in Poland on 1st January 2013. The database consists of approx. 70 thousand edges, divided into different road categories (motorways, express roads, dual-carriageway roads, main (national), secondary (regional) and tertiary (local) roads). Travel times are calculated based on the maximum speeds for a private car derived from the Polish Highway Code and then, adjusted downwards, taking account of impediments to driving, i.e. built-up areas, topography and population density (for details consult: [37]). The node representing a municipality is located in the centre of its main locality. The nodes representing 1-km grids are the centroids of grid cells. The latter are connected to the existing road network using a straight line to the nearest road section. Travel times between municipalities or between grid cells are received based on the shortest travel time algorithm between network nodes that represent the pair of units analysed (grid cells or municipalities).

Taking the assumed aims of the study as the point of departure, three different potential accessibility models were prepared based on the same theoretical background. Nevertheless, due to the different spatial resolution of the data involved and differences in the aggregation procedure, some slight differences can be noticed. In detail, the potential accessibility models developed and used in the research presented can be characterised as follows:

1. **Municipal model (M1)**. In the first model, every municipality is represented by one node, located in the central part of an administrative unit (e.g. main crossroads), with the mass of the unit attributed to one node. Therefore, the value of the potential accessibility indicator for municipality i (A_i) is calculated by using the travel times between node i and any other administrative node

located within the selected case study. The indicator is then calculated according to the formula

$$A_i = M_i \exp(-\beta t_{ii}) + \sum_j M_j \exp(-\beta t_{ij}) + \sum_k M_k \exp(-\beta t_{ik}) \quad (4)$$

where i and j are municipalities located within the Mazovia region, k is any other Polish municipality (outside the Mazovia region), and M_i, M_j and M_k are the populations of municipalities i, j and k, respectively. In consequence, $M_i \exp(-\beta t_{ii})$ is the value of the self-potential of municipality i, and $\sum_j M_j \exp(-\beta t_{ij}) + \sum_k M_k \exp(-\beta t_{ik})$ represents the sum of the potential resulting from the opportunity to access all other Polish municipalities.

2. **Grid model (M2)**. The second model is calculated similarly to the previous one however it uses grid cells in the calculation process instead of the municipalities of the Mazovia region. The indicator values received for particular grid cells are further aggregated to the municipal level using the population weighted average:

$$A_i = \frac{\sum_a \left((M_a \exp(-\beta t_{aa}) + \sum_b (M_b \exp(-\beta t_{ab}) + \sum_c (M_c \exp(-\beta t_{ac}) + \sum_k (M_k \exp(-\beta t_{ak})) * M_a) \right)}{\sum_a M_a} \quad (5)$$

where a and b are grid cells located within a municipality i, c is a grid cell located in municipality j, but outside of the municipality where a and b are located, M_a, M_b and M_c are the population of grid cells a, b and c, respectively, while k and M_k are described as above. The difference between the results received from the first and the second models is a factor of the scale dimension of the MAUP, i.e. it is a consequence of the application of different spatial resolutions.

3. **Population-weighted average travel time model (M3)**. The last accessibility model differs from the second one by the method of data aggregation from grid into municipal resolution. While the previous one aggregates the results of potential accessibility indicator values, in the third model the distance decay function includes the population-weighted average travel times between all pairs of grid-cell-nodes located in the municipalities analysed. As a result, the potential accessibility for administrative unit i is obtained using the following formula:

$$A_i = M_i \exp\left(-\beta \frac{\sum_a \left(\frac{\sum_b (t_{ab} * M_b)}{\sum_b M_b} * M_a \right)}{\sum_a M_a}\right) + \sum_j M_j \exp\left(-\beta \frac{\sum_a \left(\frac{\sum_c (t_{ac} * M_c)}{\sum_c M_c} * M_a \right)}{\sum_a M_a}\right) + \sum_k M_k \exp\left(-\beta \frac{\sum_a \left(\frac{\sum_k (t_{ak} * M_k)}{\sum_k M_k} * M_a \right)}{\sum_a M_a}\right) \quad (6)$$

The indirect consequence of the application of these three potential accessibility models is that they each include self-potential in a different way. The 'municipal model' estimates the self-potential using the radius of a circle equalling the area of the municipality in order to approximate the travel impedance, according to formula 3. In the case of the 'grid model', the potential of municipality i resulting from the interconnections between all grid-cell-nodes located inside i is calculated as a population-weighted average of values of potential accessibility indicator obtained for these nodes. The last model uses the population-weighted average travel times between all pairs of grid-cell-nodes located inside a municipality i to estimate the internal travel time (t_{ii}). The difference in the self-potentials of municipality i between the first and the third model is then related to the different methods of receiving the internal travel time (the area originated vs. population-weighted average travel time).

In the next section the empirical results of potential accessibility analyses are presented. We concentrate on two main issues: the differences in the results obtained from the three different models, and the impact of different methods of calculation of self-potential on these differences.

4 Results

The application of three different models produces some visible differences in potential accessibility values. In general, the grid model (M2) provides higher A_i values—the population weighted average amounts to 1,623 comparing to 1,368 in the case of the municipal model (M1), thus the A_i values are multiplied by 1.19 on average, while the difference between M1 and M3 is slightly lower (on average 1.12). Application of model M1 results leads to the largest amplitude of outliers.

Nevertheless, when standardising the results with the use of the population-weighted regional average (Fig. 1) the accessibility patterns are rather similar. In all variants the dominating position of Warsaw is clearly visible. The dominance of the Polish capital mainly results from its self-potential, although an important role of the densely populated metropolitan area, as well as the relatively good connections to the motorway and express road network in a south-westerly direction, are also

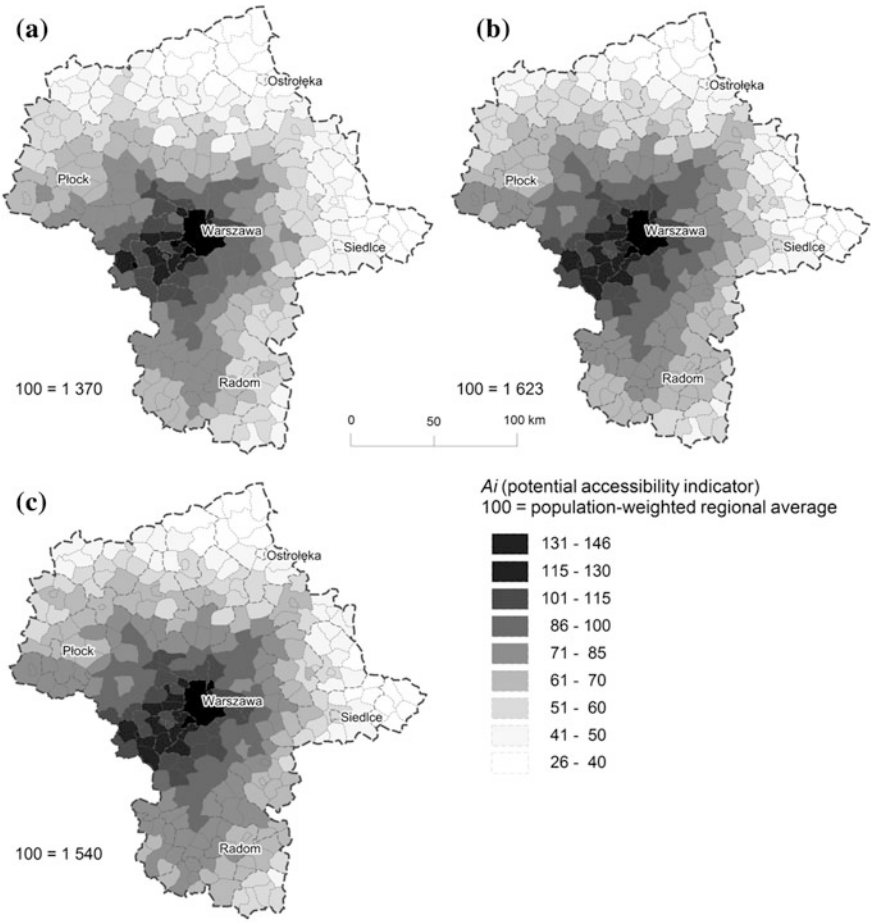

Fig. 1 Potential accessibility values (Ai) in the Mazovia region. **a** Municipal model (M1), **b** grid model (M2), **c** population-weighted average travel time model (M3)

significant factors. Furthermore, the regional disparities in the Mazovia region are mostly influenced by the existence of two connected poles of relatively higher accessibility visible at the national level (cf. [23]) which are located in the central part of Poland, including Warsaw and Łódź metropolitan areas, and the southern part of the country containing Cracow and the Upper Silesia conurbation. The intraregional accessibility disparities are even strengthened by the location of the majority of the high quality infrastructure in the most accessible part of the region linking Warsaw with Łódź and the central part of Poland. As a result, better road accessibility is observed in the south-western part of the Mazovia region, while peripheral areas in the eastern and northern part of the region are clearly less accessible. Nevertheless, there are some exceptions to the above rule resulting from the location of a short section of

express road in the north-eastern environs of Warsaw and a motorway bypass of Minsk Mazowiecki 50 km to the east of Warsaw (Fig. 1).

Comparisons of potential accessibility values resulting from the individual models are presented in Fig. 2. The differences reach a maximum of almost 50 % and mostly affect the environs of Warsaw, which is a direct consequence of the "sprawl" of mass from the city centre (in the M1 model) towards peripheral, residential districts with high population densities (Fig. 2a). As a result, the distance to the highly populated districts of Warsaw from suburban municipalities is smaller and the accessibility values in the M2 model are higher. Moreover, there is a clear positive correlation between increasing distance from Warsaw and diminishing differences in *Ai* values. The differences are also more visible where accessibility

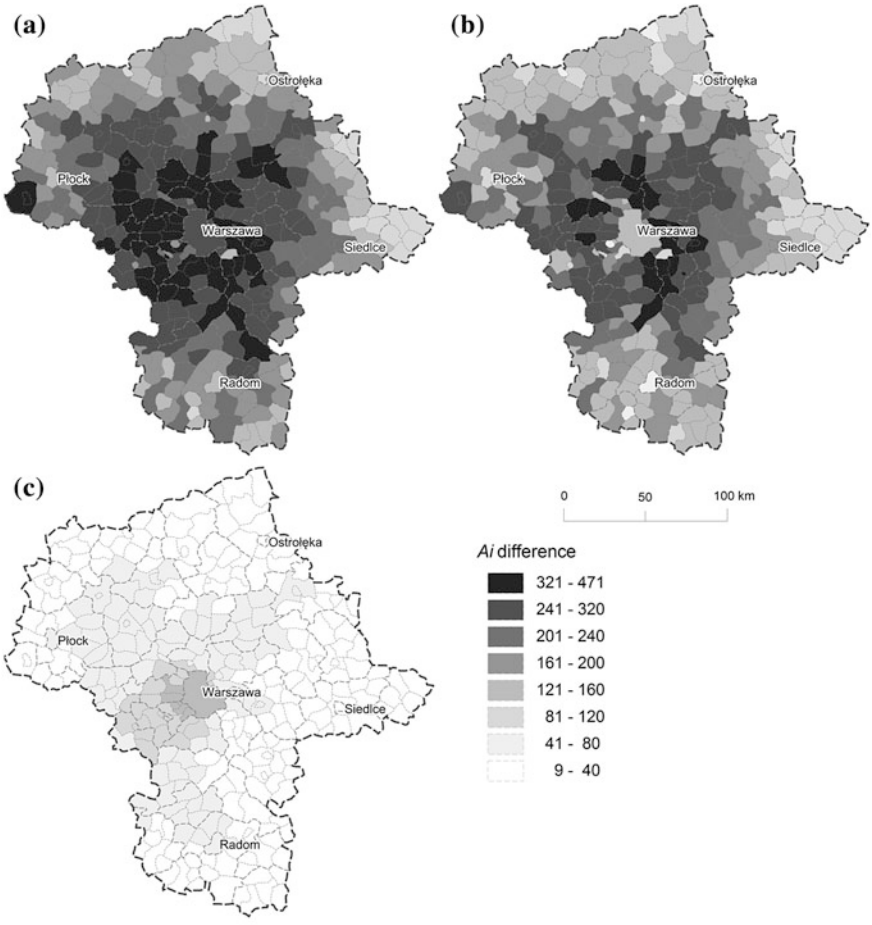

Fig. 2 Differences in potential accessibility values. **a** Ai(M2) − Ai(M1), **b** Ai(M3) − Ai(M1), **c** Ai (M2) − Ai(M3)

values are higher. Consequently, the smallest differences are noticed in the extreme north and east of the Mazovia region. Furthermore, the grid model gives higher accessibility results for municipalities located along rivers and with a high density of forest. This may to some extent be explained by the concentration of population along main roads and the low population density in the peripheral areas.

The differences between models M3 and M1 present quite a similar pattern (Fig. 2b), although the scale of dissimilarities is lower than between models M2 and M1. The grid model (M2) generates higher values than the population-weighted average travel time model (M3) especially in the case of Warsaw and those areas which are located along the transport corridors (Fig. 2c).

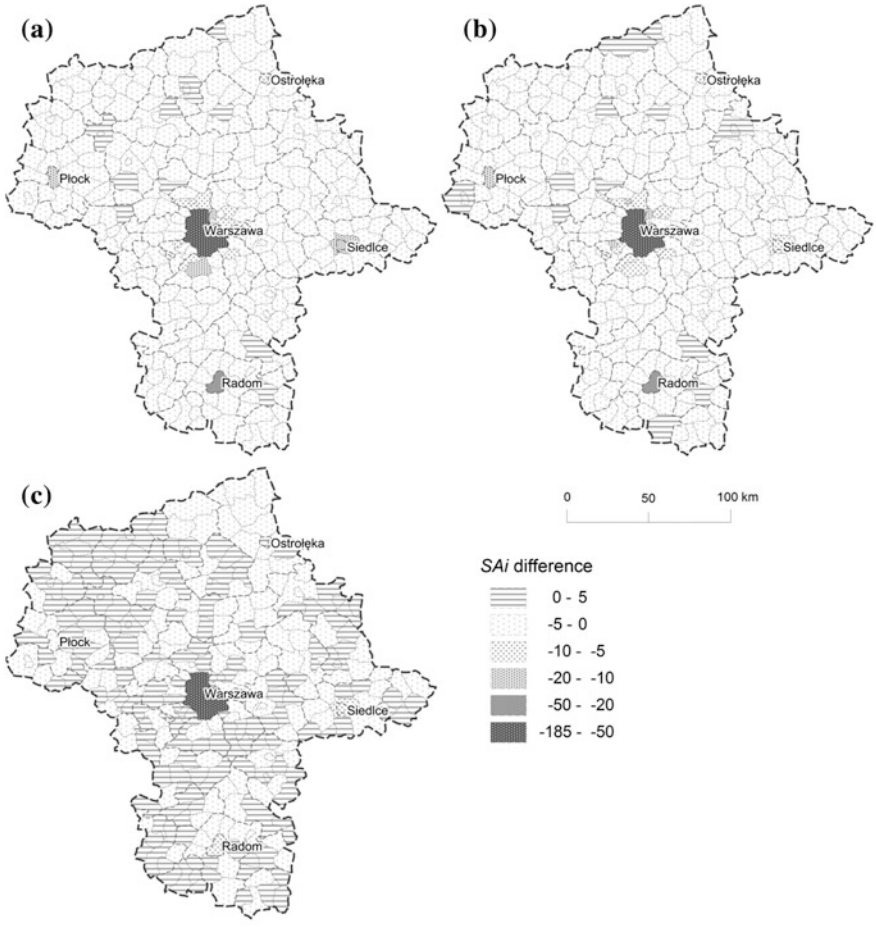

Fig. 3 Differences in self-potential values (SAi). **a** SAi(M2) − SAi(M1), **b** SAi(M3) − SAi(M1), **c** SAi(M2) − SAi(M3)

One of the possible explanations of the differences described above is that they are the consequence of different methods of calculation of self-potential. To test this hypothesis, a comparison of self-potential values calculated within particular models was prepared (Fig. 3). Even a first glance at the maps enables one to disprove the hypothesis. The differences between the values obtained from the models being compared are totally the inverse of that expected with this explanation. In general the self-potential values obtained within the municipal model (M1) are higher than in other models while the potential accessibility values are lower (cf. Figs. 2 and 3). In the case of Warsaw and most other big cities (so-called 'subregional centres') the self-potential values obtained from the municipal model are much higher than those in both grid-based models (and especially those in model M2). In consequence, the method of calculation of travel time between municipalities or data aggregation method should be treated as the main source of the differences of A_i values, rather than the method of calculation of self-potential.

5 Conclusions

The potential accessibility analysis for the Mazovia region shows both significant differences in the accessibility values obtained from the three models tested and a relatively stable spatial pattern when the results are standardised according to the population-weighted average. The latter suggests that the potential accessibility indicator is, to some extent, independent of the aggregation mechanism applied for the investigation. This applies in the case of comparison of differences of accessibility values over space. Nevertheless, the differences are clearly visible when investigating the overall level of potential accessibility. The municipal model (M1) provides comparatively low values of potential accessibility indicator for all spatial units, while the application of the population-weighted average travel time model (M3) and particularly the grid model (M2) result in significantly higher values.

The results are in line with the assumptions made on the basis of the concept of a smoothing process. The application of larger units (municipalities in the model M1), provokes more smoothing than other models, thus the values should be lower. The application of the M3 model causes significantly less smoothing in comparison to the M1 model, but more in comparison to the M2 model, thus the results are in-between the others, closer to the latter than to the former one. Nevertheless, the most important seems to be the fact that the higher number of relatively short-distance trips provides the higher A_i results, even though the mass ascribed to destination nodes is substantially lower. This explains the difference between models M1 and M2. The difference between models M1 and M3 is the consequence of the different method of calculation of travel time between each pair of units. The results show that the (population-weighted) average travel time (M3) is significantly lower than the travel time derived directly from the O-D matrix between nodes that

represent municipalities (M1). Thus, the A_i values in the M3 model are significantly higher than in the M1 model.

The differences between models are a consequence of taking the densely populated peripheral districts of Warsaw into consideration, which do not influence the grid-based models (M2 and M3), but do have an impact on the central-location oriented municipal model (M1). Furthermore, the population is more concentrated in the municipalities which are located along the main transport networks or those where urbanised land constitutes a relatively low percentage of the area (e.g. woodlands, river valleys). In consequence the total travel time between the average (population-weighted) origin-destination grid nodes is shorter than calculated at the municipal level. For that reason the potential accessibility values are higher in both grid-based models.

Second, in case of almost all administrative units, the self-potentials produced by the municipal model are higher than in both of the grid-based models. This effect can either be caused by excessive internal speed impedance or by too short internal distances. However, the internal speed of 20 km/h at the municipal level seems, in general, to even be too low when compared with other accessibility studies that include self-potential values [8]. This speed is also lower than that observed in the Warsaw metropolitan area [30]. Therefore, we conclude that the internal distance used to calculate the self-potential should be increased beyond the length of 0.5 radius proposed by Rich [33] (for detailed discussion concerning the approximation of travel impedance please consult: Frost and Spence [38]).

Third, the differences in accessibility values between municipal and grid-based models are not caused by the distinct method of calculating the self-potential values. Therefore, our hypothesis is that the main cause of the differences of A_i values observed is the complexity of transportation and land use relations between neighbouring municipalities. Nevertheless, the issue of the impact of disaggregation of population data (or even more generally: the mass applied for the potential accessibility model) should be further investigated. Although our analysis provides some empirical results presenting the consequences of the use of different types of spatial data (i.e. administrative units vs. raster cells), the role of the MAUP in accessibility studies is still an open question.

References

1. Openshaw S, Taylor PJ (1981) The modifiable areal unit problem. In: Wrigley N, Bennett RJ (eds) Quantitative geography: a British view. Routledge, London, pp 60–70
2. Fotheringham AS (1989) Scale-independent spatial analysis. In: Goodchild M, Gopa S (eds) The accuracy of spatial databases. Taylor & Francis, London, pp 221–228
3. Fotheringham SA, Brunsdon C, Charlton M (2000) Quantitative geography: perspectives on spatial data analysis. Sage Publications, London
4. Sheppard E, McMaster R (2004) Scale and geographical inquiry: nature, society, and method. Blackwell, Boston

5. Wong DWS, Lasus H, Falk RF (1999) Exploring the variability of segregation index D with scale and zonal systems: an analysis of thirty US cities. Environ Plan A 31(3):507–522
6. Townshend JRG, Justice CO (1988) Selecting the spatial resolution of satellite sensors required for global monitoring of land transformations. Int J Remote Sens 9(2):187–236
7. Boussauw K, Neutens T, Witlox F (2012) Relationship between spatial proximity and travel-to-work distance: the effect of the compact city. Reg Stud 46(6):1–20
8. Kotavaara O, Antikainen H, Marmion M, Rusanen J (2012) Scale in the effect of accessibility on population change: GIS and a statistical approach to road, air and rail accessibility in Finland, 1990–2008. Geogr J 178(4):366–382
9. Kwan M-P, Weber J (2008) Scale and accessibility: implications for the analysis of land use–travel interaction. Appl Geogr 28(2):110–123
10. Wong DWS (2009) The modifiable areal unit problem (MAUP). In: Fotheringham SA, Rogerson PA (eds) The SAGE handbook of spatial analysis. SAGE, London, pp 105–123
11. Heywood DI, Cornelius S, Carver S (2006) An introduction to geographical information systems, 3rd edn. Pearson Prentice Hall, Harlow
12. Schürmann C, Talaat A (2000) Towards a European peripherality index. Final report. Report for General Directorate XVI Regional Policy of the European Commission
13. Spiekermann K, Wegener M, Květoň V, Marada M, Schürmann C, Biosca O, Ulied Segui A, Antikainen H, Kotavaara O, Rusanen J, Bielańska D, Fiorello D, Komornicki T, Rosik P, Stepniak M (2013) TRACC transport accessibility at regional/local scale and patterns in Europe. Draft final report. ESPON applied research
14. Tóth G, Kincses A (2011) New aspects of European road accessibility. Geogr Pol 84(2):33–46
15. Holl A (2004) Manufacturing location and impacts of road transport infrastructure: empirical evidence from Spain. Reg Sci Urban Econ 34(3):341–363
16. Kotavaara O, Antikainen H, Rusanen J (2011) Population change and accessibility by road and rail networks: GIS and statistical approach to Finland 1970–2007. J Transp Geogr 19 (4):926–935
17. Gutiérrez J, Condeço-Melhorado A, López E, Monzón A (2011) Evaluating the European added value of TEN-T projects: a methodological proposal based on spatial spillovers, accessibility and GIS. J Transp Geogr 19(4):840–850
18. Holl A (2007) Twenty years of accessibility improvements. The case of the Spanish motorway building programme. J Transp Geogr 15(4):286–297
19. Spiekermann K, Schürmann C (2007) Update of selected potential accessibility indicators. Final report. Spiekermann & Wegener, urban and regional research (S&W), RRG Spatial Planning and Geoinformation
20. Bröcker J, Korzhenevych A, Schürmann C (2010) Assessing spatial equity and efficiency impacts of transport infrastructure projects. Transp Res Part B Methodol 44(7):795–811
21. López E, Gutiérrez J, Gómez G (2008) Measuring regional cohesion effects of large-scale transport infrastructure investments: an accessibility approach. Eur Plan Stud 16(2):277–301
22. Ortega E, López E, Monzón A (2012) Territorial cohesion impacts of high-speed rail at different planning levels. J Transp Geogr 24:130–141
23. Stepniak M, Rosik P (2013) Accessibility improvement, territorial cohesion and spillovers: a multidimensional evaluation of two motorway sections in Poland. J Transp Geogr 31:154–163
24. Hansen WG (1959) How accessibility shapes land-use. J Am Inst Plan 25:73–76
25. Harris CD (1954) The market as a factor in the localization of industry in the United States. Ann Assoc Am Geogr 44:315–348
26. Kwan M-P (1998) Space-time and integral measures of individual accessibility: a comparative analysis using a point-based framework. Geogr Anal 30(3):191–216
27. Reggiani A, Bucci P, Russo G (2010) Accessibility and impedance forms: empirical applications to the German commuting network. Int Reg Sci Rev 34(2):230–252
28. Fotheringham AS, O'Kelly ME (1989) Spatial interaction models. Kluwer, Dordrecht
29. Neutens T, Schwanen T, Witlox F, De Maeyer P (2010) Evaluating the temporal organization of public service provision using space-time accessibility analysis. Urban Geogr 31(8):1039–1064

30. Warsaw Traffic Survey (2005) BPRW S.A., Warszawa
31. Bröcker J (1989) How to eliminate certain defects of the potential formula. Environ Plan A 21 (6):817–830
32. Bruinsma F, Rietveld P (1998) The accessibility of European cities: theoretical framework and comparison approaches. Environ Plan A 30:499–521
33. Rich DC (1978) Population potential, potential transportation cost and industrial location. Area 10:222–226
34. Anselin L (1988) Spatial econometrics: methods and models. Kluwer Academic, Dordrecht
35. Fortney J, Rost K, Warren J (2000) Comparing alternative methods of measuring geographic access to health services. Health Serv Outcomes Res Methodol 1(2):173–184
36. Vandenbulcke G, Steenberghen T, Thomas I (2009) Mapping accessibility in Belgium: a tool for land-use and transport planning? J Transp Geogr 17(1):39–53
37. Rosik P (2012) Dostępność lądowa przestrzeni Polski w wymiarze europejskim. IGiPZ PAN, Warszawa
38. Frost ME, Spence NA (1995) The rediscovery of accessibility and economic potential: the critical issue of self-potential. Environ Plan A 27(11):1833–1848

The Accuracy of Digital Models for Road Design

Václav Šafář and Zdeněk Šmejkal

Abstract The paper presents majority of current methods for digital terrain models (DTM) measuring and basic requirements of traffic engineers on accuracy in the process of road design and construction. Conventional geodetic surveying methods are described as well as modern non-contact methods of the ground surface measurement, e.g. the laser scanning measurements from cars. When designing new road infrastructure, all the requirements of the environmental impact assessment imposed by the European Union must be taken into account. In connection with the application of Directive 2011/92/EU of the European Parliament saying that all newly constructed multi-lane roads must go through an intense impact on the environment (EIA analysis) and it also includes repairs of existing roads of more than 10 km length. Shortest roads may not require an EIA, but still must be built according to geometrical design standards. Calculations of the horizontal and vertical road centreline determine the three-dimensional physical location of a road considering operational, economic and environmental requirements. The density and accuracy of the DTM determine the final quality and efficiency as the design work, the quality of the geometric structure of the building. The quality and accuracy of the DTM especially determine the financial performance of the road construction. All alternative solutions are then assessed simultaneously with all the environmental and economic criteria. During reviews variants, for a first approximation with the situation, can be used DTM with less accuracy approximately 15 cm. For the design selected variant is required the accuracy of DTM around 2–3 cm. Only high quality DTM will allow us to rightly and accurately calculate the cost of road construction, to determine the exact volume of material moved and make any necessary animations and simulations. Then all simulations of transport

V. Šafář (✉)
Výzkumný ústav geodetický, topografický a kartografický v.v.i.,
Ústecká 98, 250 66 Zdiby, Czech Republic
e-mail: vaclav.safar@vugtk.cz

Z. Šmejkal
Znalecká a realitní kancelář – Ing. Zdeněk Šmejkal,
Škroupova 561, 530 03 Pardubice I, Czech Republic
e-mail: zdenek.smejkal@iol.cz

I. Ivan et al. (eds.), *Geoinformatics for Intelligent Transportation*,
Lecture Notes in Geoinformation and Cartography,
DOI 10.1007/978-3-319-11463-7_17

capacity, fuel consumption and emissions will be of high quality. Only on the basis of high quality three-dimensional data it is possible to determine the horizontal and vertical axis of communication and to optimize the location of the axis, and consider operational, economic and environmental performance.

Keywords EIA · DTM accuracy · Methods of DTM measuring

1 Introduction

Construction of roads is a very complicated process—spatially, financially and organizationally. Preparation, realization and the construction itself will change the neighbouring terrain and the environment related to the construction for a long time. The basic source materials for road preparation, planning and construction are the surveying data obtained by various surveying methods. The geodetic, photogrammetric and laser scanning methods belong to them. Outputs of these methods provide the basic information for all stages of the road construction, from study of the road run up to the construction implementation.

2 Data and Surveying Methods Used During the Road Planning

Data sources must be provided for preparation stage as well as the implementation itself. Majority of the data should be in 3D form. The topicality, accuracy, correctness and suitability of the sources for the planning and implementation itself must be considered. Within preparation of the source materials, data and maps, it is necessary to concentrate on early obtained documents made by state administration bodies, which should be verified for topicality and accuracy. If they do not comply with the required accuracy or topicality, new data must be obtained.

When determining the area for motorways and first class roads in the Czech Republic, the 1:200,000 regional schematic road maps are used. Another map source is usually the Czech Republic (CR) 1:50,000 road map depicting the motorways, roads, grade separations, nodal points of the localization system of the road databank, bridges, underpasses, railway-crossings, tunnels, ferries, curves, risings, passes, etc. Also cadastral maps, which contain points of the point field, planimetry, all real estates, parcel indexes and relevant cadastral territory, are used for designing works. From the Partial Territorial Decision level, the designer requires current cadastral maps in vector form, i.e. the digital cadastral map or digitized cadastral maps.

Geodetic data forms the basis of the special-purpose materials that practically enables to incorporate the construction into the area of interest. The detailed point field serves to that purpose. In the CR, the digital terrain model is used for the study

level in form of 3D contour lines as a part of the Fundamental Base of Geographic Data of the Czech Republic (ZABAGED). Furthermore, the Digital Relief Model (DMR) can be used in DMR1 to DMR5 versions. The latest versions feature utilization of aerial laser scanning. By 2016, a model with regular 5 m grid will be available in the whole CR territory. However the accuracy, because of the RMSE h = 0.18 m [1] will only be suitable for study of the road run and its variants. For subsequent designing works more precise elevation data must be obtained.

The entire documentation of all stages of the road construction is elaborated in the Baltic system after adjustment and in the national S-JTSK datum. The geodetic, photogrammetric and laser scanning serve for obtaining quality input data for designing documentation elaboration. The data enable to incorporate the construction variants into the territory of interest. Required accuracy and size of the territory of interest are the decisive factors for selecting a suitable method for the material elaboration. One of the most important source data, on which quality depends majority of control surveying during the designing works and during the construction itself, are the elevation data in the future construction area as well as in the area of future borrow-pits and other construction manipulation areas. If the natural terrain is not surveyed precisely, the assessment of suggested road variants is very uncertain and simulation of vehicle movement on thus variants is not sufficiently evidential. All subsequent calculations will be uncertain since there would not be a first-quality origin, from which the drawn/thrown up material could be calculated and which would enable to compare the current state with the designed one [2]. Following methods seem to be suitable for sufficiently precise digital terrain model:

(a) Methods of aerial photogrammetry and stereoscopic mapping of aerial photographs. The resulting material for the road variant study as well as for subsequent designing works is a set of digital planimetry and altimetry files of a special-purpose map. The RMSE accuracy of the altimetry derived by photogrammetry-stereoscopic method is h = 0.045 m for the ground sample distance of the aerial photographs equal 0.035 m, see e.g. [3].
(b) Methods of aerial laser scanning for creating a digital model needed for designing activity (after selecting and approving the appropriate variant) enable to obtain (after the flight and primary data processing) very dense and precise digital terrain model. The laser scanning apparatus usually emits one light beam and receives it back (after its reflection from the terrain) divided up to eight so called echoes. Information recorded for the first and last reflection of the beam is used for evaluation of planimetry and altimetry information on the terrain. Such determined Digital Surface Model contains all terrain obstacles. The model is further adjusted with special algorithms and calibrated onto map control points surveyed in the terrain. After subsequent result adjustment and necessary filtrations of the terrain objects, the DTM of the particular area is obtained with density up to 12 points per m^2 (in open terrain) with RMSE h = 0.03 m (Fig. 1).
(c) Methods of terrestrial mobile laser scanning for production of precise 3D digital terrain model utilized during designing works are based on an apparatus

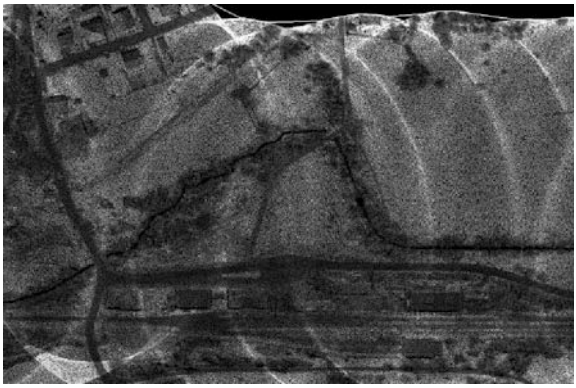

Fig. 1 Data sample of the aerial laser scanning—source material for re-laying the R55 road (*Courtesy* of GEODIS BRNO Ltd)

usually consisting of two integrated units: scanning and navigational. Due to high density, speed and above all the spatial accuracy of obtained point clouds, the method represents one of the most effective methods of obtaining spatial information for precise designing works. By selecting a suitable measurement method, using appropriate vehicles (eventually utilizing terrain three-wheelers or manual walk-survey under hard inaccessible terrain conditions with an apparatus in bag) and subsequent elaboration we can reach results, which we could not reach by other methods. During post-processing, we can use additional information received during scanning each point, especially the sequence of reflections and reflective intensity. The cleared data can serve for generating detailed digital models, depicting cross and longitudinal sections in any position and make other elevation analysis. Such data with RMSW h = 0.015 m—see [4], represent the most accurate source material for designing works. Currently there are various SW platforms, which are ready to work with these data and also enable the 3D designing. In comparison with conventional methods, this one brings relatively high time savings during the designing works and above all the savings during the construction itself (Fig. 2).

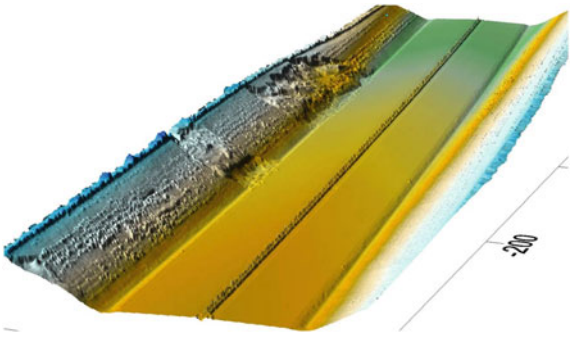

Fig. 2 Sample of detailed 3D digital model of a current road (*Courtesy* GEOVAP Pardubice Ltd)

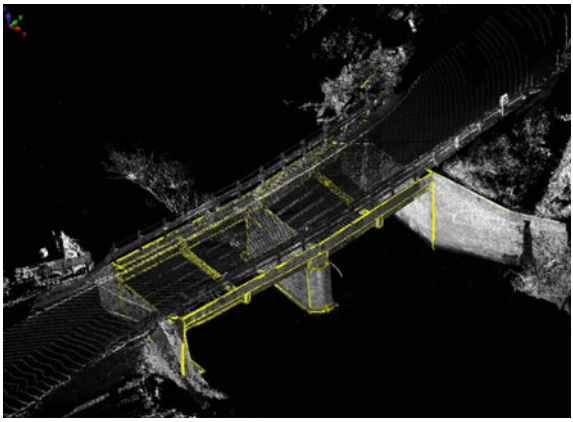

Fig. 3 Sample of a road bridge surveying (*Courtesy* GEOVAP Pardubice Ltd)

(d) Methods of terrestrial static laser scanning represent suitable methods for operative and precise surveying of partial source materials for designing activities of selected transportation objects (e.g. probably crossing of designed construction with existing bridges, tunnels, supporting walls, noise protection barriers). In connection with the aerial and terrestrial mobile laser scanning, the methods enable complex surveying of existing transportation facilities, which are supposed to influence the future construction or to utilize it. The RMSE elevation of these methods is e.g. at the bridge surveying utilizing phase laser scanners with range of 20–50 m, 0.005 m—see [5] (Fig. 3).

3 Results and Discussions

Point clouds received by both correlation methods from stereoscopic photographs (or by direct stereoscopic measuring by an operator) and laser scanning methods (mainly by mobile terrestrial laser scanning) can also be utilized in connection with an orthophotomap with ground sample distance of 2.5 cm for creating various types of visualizations and animations above a real landscape. The data can be used for simulations of various vehicle movements. Such a view and simulation can reveal potential future danger sections and suggest and design with utilizing real data a safe, economically optimal and ecologically acceptable road and thus exploit all features of the digital terrain models, which can currently be utilized by above mentioned methods (Table 1).

Table 1 Financial, time and accuracy characteristics of surveying methods used on 10 km section elaborated in three variants (Parameters of test area—3 strips (variants), long 10 km (each), 0.5 km (width) = 500 ha, 70 % open area, 30 % covered (forest))

Description of method	Vertical accuracy (RMSE) in (cm)	Approximate price for the area 500 ha in Euros	Approximate time of delivery in days
Data DMR 5	18	125	3
Aerial photogrammetry and stereoscopic mapping	4.5	8,800	30
Aerial laser scanning	3.5	11,200	30
Terrestrial mobile laser scanning	1.5	25,600	60
Terrestrial static laser scanning	0.5	58,000	100

4 Conclusion

New requirements on always more superior altimetry map sources for needs of road designing call (within more effective collection of altimetry data and their subsequent elaboration) for suitable selection of the acquisition method. Using above stated methods for acquisition of source materials for designing works and above all their accuracy, 3D character and optimization of the designing works will enable to suggest and create a real work, which will be both economical and ecological one.

References

1. Bělka L (2012) Letecké laserové skenování a tvorba nového vyškopisu Českе republiky. Vojensky geograficky obzor 55(1):19–25. ISSN:1214-3707
2. Fellendorf M (2013) Digital terrain models for road design and traffic simulation. Photogrammetric week ’13, Stuttgart, 9–13 Sep, Wichmann Verlag, pp 309–317. ISBN-13:978-3-87907-531-7
3. Höhle J (2011) DEM generation by means of new digital aerial cameras. In: Conference PIA 2011, international archives of the photogrammetry, remote sensing and spatial information sciences XXXVIII-3/W22, 2011, ISPRS, pp 185–190
4. Lechner J (2013) Zpráva o výsledcích testování mobilních laserových zařízení pro měření na pozemních komunikacích. Technická zpráva (in print), Lechner Jiří, - Zdiby,VÚGTK
5. Kašpar M, Pospíšil J, Štroner M, Křemen T, Tejkal M (2003) Laserové skenovací systémy ve stavebnictví. Vega s.r.o., Hradec Králové. ISBN:80-900860-3-9

GPS Data and Car Drivers' Parking Search Behavior in the City of Turnhout, Belgium

Peter van der Waerden, Harry Timmermans and Lies Van Hove

Abstract This paper describes an exploratory study regarding parking search behavior. Based on GPS tracks of 97 car trips, the temporal and spatial components of parking search behavior are investigated in more detail. The data collection took place in November 2012 in the city of Turnhout, Belgium. The paper presents the way the data collection has been organized, the way the data have been analyzed, and some findings of the study. It appears that GPS tracking can be used to investigate both the temporal and spatial aspects of parking search behavior. The average parking search time found in this study is 1 min and 18 s (approximately 14 % of the total travel time). The use of street segments for parking is influenced by distance to the city center, distance to nearest parking facility, presence of shops, and parking tariffs.

Keywords GPS · Parking search · Behavior · TransCAD · GIS ostrava 2014

1 Introduction

The increase in car use has resulted into an increase in heavily congested streets, especially in and around the central business district and shopping areas. Previous studies have shown that a considerable share of cars in these streets is searching for a free parking space [1, 2]. Due to a decrease in available parking spaces, the

P. van der Waerden (✉) · H. Timmermans
Urban Planning Group, Faculty of the Built Environment, Eindhoven University of Technology, PO Box 513, 5600 MB Eindhoven, The Netherlands
e-mail: p.j.h.j.v.d.waerden@tue.nl

H. Timmermans
e-mail: h.j.p.timmermans@tue.nl

L. Van Hove
Transport Research Group, Hasselt University, PO Box 6, 3590 Hasselt, Belgium
e-mail: liesje_van_hove@hotmail.com

I. Ivan et al. (eds.), *Geoinformatics for Intelligent Transportation*,
Lecture Notes in Geoinformation and Cartography,
DOI 10.1007/978-3-319-11463-7_18

searching for parking will likely increase in the future with several accompanying effects such as a decrease of accessibility and attractiveness of destinations. For transport planners and decision makers, reliable information about parking search behavior is therefore important when assessing the accessibility of destinations and environmental effects of traffic in central business districts and shopping areas.

In the past, most studies focused on the number of cars searching for a free space. To date, little attention has been paid to search time and the kind of streets car drivers use while searching [3]. To the extent attention has been paid to parking search time, the duration of search is mainly based on car drivers' assessment of time [2]. This study aims at getting more detailed insights into both the temporal and spatial aspects of car drivers' parking search behavior based on empirical data. The research is still in the phase of exploration of data collection and analyses methods. The study is an extension of a previous study in which the use of GPS to investigate car drivers' parking search behavior was explored [4].

The remainder of the paper is organized as follows. First, a brief overview is given of existing insights and adopted approaches regarding (modeling of) parking search behavior. Next, the adopted research approach is outlined. This section is followed by a brief description of the data collection process. The findings of the data collection are described in Sect. 4. The paper ends with the conclusions and some recommendations for future research.

2 Parking Search Behavior

When car drivers approach their final destination, they start to look for a free parking place. This last part of a car trip is defined as car drivers' parking search behavior [1]. Basically, parking search behavior consists of two components: a temporal (time used for searching) and a spatial (streets used for searching) component. Both components influence the accessibility and the livability of areas. Especially in dense inner-city areas, the presence of parking search traffic influences the accessibility by car and the livability of visitors and residents negatively. This is one of the reasons that serious attention is paid to the issue of parking search behavior, both by local authorities and researchers. Spitaels et al. [5] give a detailed overview of several behavioral aspects that are related to car drivers' in parking search behavior.

Previous studies could be divided into two groups: studies with a focus on empirical insights and studies with a focus on model development. A recent study regarding empirical insights is presented by Van Ommeren et al. [2]. Based on the Dutch National Travel Survey (MON) for the years 2005–2007, they found that the average cruising time is 36 s per car trip, that cruising time increases with travel and parking duration, and that cruising has a distinctive pattern across the day. The average cruising time is totally different from the times Shoup [1] presented in his work (ranging from 3.5 to 14 min). Waraich et al. [6] already indicated that 'the

parking strategy evaluation procedure of the previous parking search models delivers systematically too high search times'.

The second group of related studies concerns studies in which parking search models are developed (for a literature review see [3, 7, 8]. The studies focus on extensions of network based assignment models [9] or agent-based models [6, 8, 10]. The models aim to investigate:

- The impact of cruising for parking on traffic congestion [9];
- The environmental costs of parking search process [10];
- The generation of distributions of key values like search time, walking distance, and parking costs over different drivers groups [8].

A variety of publications shows that the use of GPS tracking data becomes more popular to collect travel related data [11–13]. The data is easy to collect, accurate, and detailed [14]. Also in the context of parking search behavior, GPS tracking is a useful means of data collection [3, 4]. The experiences with the use of GPS tracking to identify parking search behavior are still limited.

3 Research Approach and Data Collection

To get insight into car drivers' parking search behavior the following research approach has been adopted. First, a city was selected according to requirements defined by Kaplan and Bekhor [3]. Next, participants were recruited who plan to make several trips by car to the centre of the selected city. All participants received a GPS logger and were asked to turn on the logger when driving with their car to the city center of the selected city. In this study the 'i-Blue 747A+GPS recorder' was used. Every 3 s, the recorder stores its (horizontal and vertical) position, the day and time of day, and the number of satellites involved in the registration. For technical details of this recorder see http://blinkgadget.blogspot.com/2010/10/kode-produk-747a.html. The logger is easily to set and the data is easily to retrieve using for example the software 'DataLog' (http://www.datalog.de). The spatial data are stored, analyzed, and presented using the Geographic Information System TransCAD 6.0 (http://www.caliper.com).

In additions, the participants were invited to filled out a small questionnaire consisting of some questions regarding personal characteristics (gender, age, familiarity with the city, and possession of parking card) and for each trip some specific characteristics (type of car used during the trip, orientation on specific parking facility before leaving home, and trip purpose).

The study was carried out in the city of Turnhout, a small city in the North of Belgium (Fig. 1). The city meets the four basic requirements set by Kaplan and Bekhor [3]: (i) area should be characterized by high activity generation and limited parking supply; (ii) area should offer a selection of off-street and on-street parking opportunities; (iii) area should attract both local and non-local visitors, and (iv) area should be bounded by natural and/or street network boundaries.

Fig. 1 Study area: Turnhout, Belgium (*source* Google Maps)

The city's road network consists of 531 street segments (links between two intersections). On 85 % of the street segments on-street parking is allowed. In total, 7 street segments can be used as entrance of a parking facility. The parking tariffs for on-street parking range from 0.00 (Free) to 2.00 euro/h. On almost 50 % of the road segments parking is free. Most streets (approximately 80 %) are two direction streets. Approximately 90 % of the road segments include one or more residences. All these streets are designed as local roads. On almost 15 % of the road segments one or more shops are present.

The data collection took place in November 2012. In total, 15 persons participated in the field study describing 97 trips (Fig. 2). The small number of participants was mainly caused by limited time and money resources. Unfortunately, the respondents are not equally distributed across the included personal characteristic levels: gender (60 % women, 40 % men); age groups (46 % younger than 36 years, 54 % older than 35 years); and familiarity with the city (74 % well to very well, 26 % limited to poor). Regarding the trip purpose, it appears that 36 % of the trips were work related trips, 27 % shopping trips, 19 % leisure trips, and 18 % other (like picking up or dropping of persons).

To determine the 'search' part of a trip the following approach is applied. The approach is based on experiences from previous empirical studies [4]. The best method found until now, starts at the arrival time of the car and includes information concerning average speed (over different observations) and acceleration or deceleration of the car ('speed change'). The search for an optimal average travel

Fig. 2 Presentation of GPS tracking data on the street network of Turnhout, Belgium

speed is done by 'trial and error', minimizing the number of incorrect predictions (compared to real world observations of parking search behavior). The starting point of searching is set when the average speed is below 23 km/h (measured over 5 time periods) and the speed difference is less than 5 km/h as observed in the GPS data.

4 Analyses

The GPS information is stored in a (comma separated value—csv) data file (Table 1) produced by the program DataLog. The program generates a data file with several columns including time period (date and time), position of observation (latitude, longitude, and height), and vertical and horizontal accuracy (PDOP, HDOP, and VDOP, NSAT). The columns 'Latitude', 'Longitude', and 'Speed' are used in this study. In Table 1, the yellow box indicates the start of the search process.

The data were analyzed in two different ways. First, the parking search time was investigated in more detail. Based on the observations of 97 city oriented car trips the following details can be noticed. The average car trip takes almost 14 min (minimum of 1 min and maximum of 60 min. The average parking search time is 1 min and 18 s (minimum of 0 s and maximum of 6 min and 48 s). Figure 3 shows the distribution (in classes) of parking search times over all 97 car trips. Approximately 50 % of the parking search times are between 0 and 60 s. When this search

Table 1 Example of database produced by DataLog

	A	B	C	D	E	F	G	H	I	J	K	L	M	N	O	P	Q
1	INDEX	RCR	DATE	TIME	VALID	LATITUDE	N/S	LONGITUDE	E/W	HEIGHT	SPEED	SPEED/1000	PDOP	HDOP	VDOP	NSAT (USED	DISTANCE
199	198	T	28-8-2012	8:36:48	SPS	51.361.781	N	4.858.652	E	69.094 M	59.118	59,12	1.49	0.90	1.18	9(11)	49.96 M
200	199	T	28-8-2012	8:36:51	SPS	51.361.501	N	4.859.164	E	68.279 M	56.115	56,12	1.49	0.90	1.18	9(11)	47.39 M
201	200	T	28-8-2012	8:36:54	SPS	51.361.237	N	4.859.661	E	68.326 M	53.149	53,15	1.66	0.97	1.35	8(11)	45.38 M
202	201	T	28-8-2012	8:36:57	SPS	51.360.990	N	4.860.108	E	68.556 M	46.689	46,69	1.25	0.96	0.80	8(11)	41.53 M
203	202	T	28-8-2012	8:37:00	SPS	51.360.774	N	4.860.507	E	68.710 M	43.227	43,23	1.49	0.90	1.18	9(11)	36.75 M
204	203	T	28-8-2012	8:37:03	SPS	51.360.567	N	4.860.898	E	69.236 M	44.314	44,31	1.25	0.96	0.80	8(11)	36.39 M
205	204	T	28-8-2012	8:37:06	SPS	51.360.340	N	4.861.300	E	69.135 M	44.934	44,93	1.25	0.96	0.81	8(11)	37.03 M
206	205	T	28-8-2012	8:37:09	SPS	51.360.123	N	4.861.692	E	69.070 M	43.089	43,09	1.66	0.97	1.35	8(11)	36.40 M
207	206	T	28-8-2012	8:37:12	SPS	51.359.931	N	4.862.065	E	69.415 M	38.557	38,56	1.48	0.90	1.18	9(11)	33.66 M
208	207	T	28-8-2012	8:37:15	SPS	51.359.814	N	4.862.459	E	69.497 M	37.446	37,45	1.66	0.97	1.35	8(11)	30.39 M
209	208	T	28-8-2012	8:37:18	SPS	51.359.754	N	4.862.860	E	69.065 M	30.932	30,93	1.48	0.90	1.18	9(11)	28.70 M
210	209	T	28-8-2012	8:37:21	SPS	51.359.703	N	4.863.161	E	68.556 M	23.970	23,97	1.86	1.26	1.37	8(11)	21.72 M
211	210	T	28-8-2012	8:37:24	SPS	51.359.646	N	4.863.305	E	69.869 M	21.846	21,85	1.25	0.96	0.80	8(11)	20.18 M
212	211	T	28-8-2012	8:37:27	SPS	51.359.417	N	4.863.393	E	70.229 M	18.753	18,75	1.34	1.7	0.82	7(11)	15.64 M
213	212	T	28-8-2012	8:37:30	SPS	51.359.288	N	4.863.400	E	69.877 M	14.081	14,08	1.25	0.96	0.80	8(11)	14.37 M
214	213	T	28-8-2012	8:37:33	SPS	51.359.211	N	4.863.404	E	70.400 M	8.802	8,80	1.25	0.96	0.80	8(11)	8.55 M
215	214	T	28-8-2012	8:37:36	SPS	51.359.133	N	4.863.414	E	70.611 M	14.046	14,05	1.66	0.97	1.35	8(11)	8.74 M
216	215	T	28-8-2012	8:37:39	SPS	51.359.025	N	4.863.423	E	70.524 M	13.587	13,59	1.79	1.9	1.42	7(11)	12.03 M
217	216	T	28-8-2012	8:37:42	SPS	51.358.949	N	4.863.428	E	71.099 M	3.171	3,17	2.33	1.69	1.60	6(11)	8.40 M
218	217	T	28-8-2012	8:37:45	SPS	51.358.946	N	4.863.424	E	71.834 M	159	0,16	1.34	1.7	0.82	7(11)	0.86 M
219	218	T	28-8-2012	8:37:48	SPS	51.358.947	N	4.863.425	E	71.771 M	127	0,13	1.75	1.53	0.85	6(11)	0.10 M
220	219	T	28-8-2012	8:37:51	SPS	51.358.943	N	4.863.427	E	71.717 M	4.438	4,44	1.75	1.53	0.85	6(11)	0.41 M
221	220	T	28-8-2012	8:37:54	SPS	51.358.877	N	4.863.440	E	71.640 M	12.269	12,27	1.79	1.9	1.42	7(11)	7.44 M
222	221	T	28-8-2012	8:37:57	SPS	51.358.785	N	4.863.444	E	71.833 M	10.666	10,67	1.75	1.53	0.85	7(11)	10.24 M

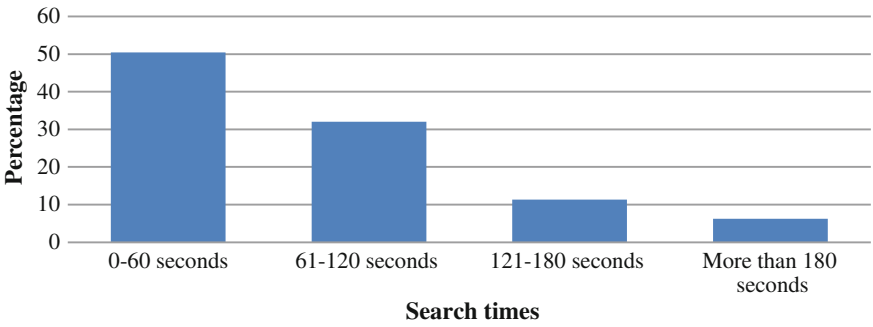

Fig. 3 Distribution of parking search times in Turnhout, Belgium

time is related to the total travel time, it appears that on average 14 % of the total travel time is used for parking search (minimum 0 % and maximum of 49 %).

In the second part of the analyses, parking search routes and included street segments were analyzed in more detail. The GPS data were related to street segments of the urban street network using TransCAD (Fig. 4). After the calculation of the number of times each street segment was used in the various parking search routes, the numbers were related to some street segment characteristics. The use of street segments is related to characteristics of the street segments using multiple regression analyses. The (logarithm of) numbers of times are used as dependent variable; while various street characteristics are used as independent variables (see Table 2).

Figure 5 presents the number of times each street segment is used for parking search. The numbers range from 0 to 237 times. The latter street segment is close to one of the main parking facilities in the center. The figure also shows that car drivers already start to search at a considerable distance from the core of the city center.

Fig. 4 Basic representation of GPS observation

Table 2 List of investigated street segment characteristics

Attribute	Levels
Walking distance between street segment and center	Meters/10
Distance between street segment and closest parking facility	Meters/10
Presence of parking lot	Yes, no
Presence of parking garage	Yes, no
Presence of on-street parking	Yes, no
Presence of houses	Yes, no
Presence of shops	Yes, no
Number of allowed driving directions	One way, two way
Presence of dynamic parking guidance system	Yes, no
Parking tariff	Euros per hour
Street type	Primary, secondary

For planning purposes the individual GPS tracks could be related to characteristics of individual street segments and/or routes (a set of linked street segments). This can be done in various ways as shown in the section about (modeling) parking search behavior. For illustration purpose, in this study the use of street segments is related to attributes of the street segments using regression analyses. In the analyses, the dependent variable is the natural logarithm of the number of times a street segment is used for searching. A variety of street segment attributes are used as independent variables (Table 2). The selection of interesting variables was based on existing literature (see before) and the ease of gathering information regarding the

Fig. 5 Use of street segments for parking search

variables. The following hypotheses were defined regarding the effects of the included variables: a higher usage is expected for street segments.

- Larger distance from the center (final destination);
- Short distance between street segment and parking facility;
- No presence of parking facilities;
- Presence of on-street parking;
- Presence of shops or residences;
- Presence of two-way driving direction;
- Absence of dynamic parking guidance system;
- High parking tariff;
- Secondary streets.

For a first exploration of the relationship between the use of street segments and the characteristics of street a basic linear regression model is estimated (Eq. 1).

$$Ln(F + 0.5) = \sum_i \beta_i \cdot X_i \tag{1}$$

where,

F Number of times a street segment is used for searching
X_i The *i*-th attribute of a street segment
β_i The weight (parameter) of the *i*-th attribute.

After evaluating several regression models, the best performing model only includes four street segment attributes. The other attributes were removed from the analyses because of a high correlation or the absence of a significant effect (Table 3).

Table 3 Parameter estimates of regression analyses

Attributes	Parameters	Significance
Constant	−0.297	0.100
Walking distance between street segment and center	0.047	0.001
Distance between street segment and closest parking facility	−0.010	0.000
Presence of shops	0.365	0.039
Parking tariff	0.649	0.000
Goodness-of-fit		
F-value	25.538 (sign. 0.000)	
R-square	0.163	
Adjusted R-square	0.157	

The performance of the model is poor (based on adjusted R-square value) but still acceptable (based on F-value).

The parameters show the contribution of attributes to the number of car drivers using the street segment. A positive sign means that an increase of the attribute levels results in a higher number of searchers in the street segment, while a negative sign indicates a decrease of searchers when the attribute level increases. The positive sign for the distance indicates that car drivers start to search for a free parking space at some distance from the center (see before). If a car driver approaches a parking facility, he/she stops searching and drives immediately to the parking facility. Streets close to parking facilities are less used for searching. In streets with shops the number of searchers is higher than in streets without shops. Finally, the parameter estimate of parking tariffs shows that the higher the parking tariff the higher the number of searchers in a street.

5 Conclusions

The study described in this paper aims to provide more insight into the temporal and spatial aspects of car drivers' parking search behavior in central business districts and shopping areas. Special attention is paid to the collection of empirical data using GPS loggers. It appears that GPS data could be used for describe car drivers' search behavior both in terms of time and location. The approach provides information regarding search time which can be included in accessibility studies. Also detailed information becomes available regarding the use of street segments that could be used in livability studies. Young [7] summarizes this as follows: *Parking search models provide an ability to investigate long-term commitments to parking expenditure, the impact of parking information on route choice, the time spent in searching for a space, and the choice strategy*.

The temporal and spatial data could be explored in more detail when more data (more trips and more car drivers) were available. The same holds for the modeling

part presented in this paper. More sophisticated analyses could be explored to related search behavior to streets segments.

Future research on car drivers' parking search behavior will focus on:

- Extend the collection of empirical GPS data;
- Validate the identification of parking search behavior based on GPS data;
- Relate parking search behavior to characteristics of street segments (including traffic flows and parking occupation levels).

References

1. Shoup D (2006) Cruising for parking. Transp Policy 13:479–486
2. Van Ommeren JN, Wentink D, Rietveld P (2012) Empirical evidence on cruising for parking. Transp Res A 46:123–130
3. Kaplan S, Bekhor S (2011) Exploring En-route parking search choice: decision making framework and survey design. In: Proceedings of 2nd international choice modeling conference, Oulton Hall, UK
4. Van der Waerden P, Timmermans H, Haberkorn P (2012) Studying car drivers' parking search behavior using GPS trip loggers. In: Proceedings of the 11th international conference on design and decision support systems, Eindhoven, The Netherlands
5. Spitaels K, Maerivoet S, De Ceuster G, Nijs G, Clette V, Lannoy P, Dieussart K, Aerts K, Steenberghen T (2009) Optimizing price and location of parking in cities under a sustainable constraint 'SUSTAPARK'. Science for a Sustainable Development, Brussels
6. Waraich RA, Dobler C, Axhausen KW (2012) Modeling parking search behavior with an agent-based approach. In: 13th International conference on travel research behavior (IATBR), Toronto, Canada
7. Young W (2008) Modeling Parking. In: Hensher D, Button KJ (eds) Handbook of transport modeling, 2nd edn. Elsevier, Oxford, pp 475–487
8. Benenson I, Martens K, Birfir S (2008) PARKAGENT: an agent-based model of parking in the city. Comput Environ Urban Syst 32:431–439
9. Gallo M, D'Acierno L, Montella B (2011) A multilayer model to simulate cruising for parking in urban areas. Transp Policy 18:735–744
10. Guo L, Huang S, Sadek AW (2013) A novel agent-based transportation model of a university campus with application to quantifying the environmental costs of parking search. Transp Res Part A 50:86–104
11. Papinski D, Scott DM, Doherty ST (2009) Exploring the route choice decision-making process: a comparison of planned and observed routes obtained using person-based GPS. Transp Res Part F 12:347–358
12. Gong H, Chen C, Bialostozky E, Lawson CL (2012) A GPS/GIS method for travel mode detection in New York City. Comput Environ Urban Syst 36:131–139
13. Lin M, Hsu W-J (2014) Mining GPS data for mobility patterns: a survey, pervasive and mobile computing, vol 12. pp 1–16
14. Stopher P, FitzGerald C, Zhang J (2008) Search for a global positioning system device to measure person travel. Transp Res Part C 16:350–369

Mobile Application for Acquiring Geodata on Public Transport Network

Lenka Zajíčková

Abstract Following the detected deficiencies in managing geodata on public transport network in the Olomouc Region, potential solutions of the situation were analysed. On the basis of extensive research of global standards in public transport data standardization, a data model of entities and their attributes according to the needs of public transport management and control in the Czech Republic was established. Further, a data warehouse was created on the base of the newly created data model by means of the special software specializing in work with lines and network elements. A mobile application for a tablet to collect field data was designed to supply the warehouse. The concept of public transport geodata collection, management and updating was created in cooperation of Asseco Central Europe, Coordinator of the Integrated Transport System in the Olomouc Region and the Department of Geoinformatics of Palacky University in Olomouc in reaction to the unsuitable data situation in public transport in the Olomouc Region. Current filling of the data warehouse by means of the designed mobile application will later be followed by creating an interactive transport plan and spatial analysis based on the data about the managed area.

Keywords Data model · Data warehouse · Geodata · Mobile application · Public transport

1 Introduction

The issue of collection, management and long-time sustainability of current information about the public transport network in regions is, in conditions of the Czech Republic, dealt with especially by coordinators (organizers) of the integrated

L. Zajíčková (✉)
Faculty of Science, Department of Geoinformatics, Palacky University in Olomouc,
17. listopadu 50, 771 46 Olomouc, Czech Republic
e-mail: lenka.zajickova@upol.cz

I. Ivan et al. (eds.), *Geoinformatics for Intelligent Transportation*,
Lecture Notes in Geoinformation and Cartography,
DOI 10.1007/978-3-319-11463-7_19

transport systems (integrovaný dopravní systém, hereinafter referred to as "IDS"). The majority of the information is—due to the nature of phenomenons which take place in space—related to spatial data; they are therefore predestined to be processed and stored in GIS. With respect to the expanding possibilities to publish and present digital data, there is an ever growing need to deal with currency, accessibility, particularity, good arrangement and accuracy of public transport (hereinafter referred to as "PT") data. Most of the IDS control bodies realize the importance and benefits of quality register of spatial network data in GIS. However, the absence of a unifying standard results in many different approaches, different data quality and incompatibility in case of their exchange. The question of data updating is also often discussed because, though the network is rather stable, there is a great number of objects to register and many of their attributes are subject to frequent changes.

The goal of this text is to introduce the conception and launching of the mobile application for collection of the PT network geodata in the area administered by the Integrated Transport System Coordinator of the Olomouc Region which is widely extensible and applicable in other regions. The partial goal of the text is to introduce the data model of the registered entities established on the basis of global standards accounting for the effort to standardize in the Czech Republic, newly established data warehouse respecting this data model and the updating method of this extensive database.

2 The Scope of Available Public Transport Geodata and the Base of Their Standardization

The quality and scope of the PT network data differs in various regions of the Czech Republic. In some regions, the data are processed in GIS, in others graphic software (e.g. Corel Draw) is used; in regions served by carriers without central administration there are no geodata at all [1]. However, data warehouses of IDS organizers in GIS are often incomplete, the objects are not located correctly, the layers lack a coordinate system and errors like undershoots, overshoots and missing attributes frequently occur. The logical structure is often inappropriate as the data are not based on a quality data model and also the way of data processing is not ideal.

The only present solution to keep the basic information regarding the movement of PT vehicles in national scope is the unified data format (hereinafter referred to as "JDF") defined by the Decree of the Ministry of Transport No. 388/2000 Coll., on Regular Public Transport Timetables, and the Decree No. 175/2000 Coll., on Transport Rules for Public Railway and Road Transport of People [2]. It is a predefined data format designed for regular PT road and railway carriers in order to process the timetables (hereinafter referred to as "JŘ") for the purposes of the National Information System on Timetables (hereinafter referred to as "CIS JŘ"). The carrier processes the timetables in an electronic form, is responsible for them and submits them to the appropriate transport authority for an approval and to be

advanced to CIS JŘ the management of which was delegated to CHAPS Ltd. [3] from 26th October 2001. However, no spatial information is related to the data inserted in the CSV files, attributes to individual entities are insufficiently registered and hardly anyone fills in the voluntary files. For passengers' needs, CHAPS allows not only searching for the appropriate connection but also the possibility of graphic display. It involves coordinate visualization of the stops on the base of a source map and their interconnection by straight lines. From the point of view of GIS, this solution is unsatisfactory and incorrect, however, CHAPS primarily deals with timetable administration and the visualization and spatial information are not the subject of their business.

The first attempt to implement a standard for PT data in the Czech Republic was the project called "The unified public transport data system with respect to a standard form application with the possibility to interconnect the existing systems to a unified software platform" (JSDV). The project was realized in 2011–2013 by the Transport Research Centre (Centrum dopravního výzkumu v.v.i.) in cooperation with CHAPS Ltd. and APEX, Ltd. The ground of the project consisted of the existing situation in public transport information systems, valid Czech and European legislation and first of all the Service Interface for Real-time Information (hereinafter referred to as "SIRI") [4]. The general goal of the project was to support public transport competitiveness by implementing the uniformly arranged telematic system with a standardised interface which should have allowed later integration of other information systems of carriers, integrated transport systems and/or transport route operators/administrators. The partial goal was to create the central data warehouse and to prepare standardised data formats for data exchange. Further, the project should have used the CIS JŘ information to create a national information system in real time (so-called CISReal). The outcomes are the central information system, drafts of the architecture, feasibility study and the methodology for building up the information system. In course of the project, the Czech technical standard ČSN was being formulated [5]. Nevertheless, the involvement in the project outcomes is still self-imposed; no binding duty is implied for the carriers and organizers.

3 Draft of the Solution for Acquiring Complete Data on the PT Network

Asseco Central Europe (hereinafter referred to as Asseco), Coordinator of the Integrated Transport System in the Olomouc Region (hereinafter referred to as KIDSOK) and the Department of Geoinformatics of Palacky University in Olomouc developed a solution to acquire complete GIS data on PT network for the needs of KIDSOK and defined the rules for their updating. The aim was to create a solution for data collection, processing and updating that could easily be repeated in any other region or area, keep the compatibility with the existing exchange formats

and respect international standards in PT data standardization. KIDSOK detected incorrect topology in individual layers, insufficient scope of the attributes and poor structure of the existing data which was based on the analysis of the administered geodata, the scope and nature of the data for the needs of PT management and control. That was why a new data model was drafted for the PT network geodata, a way of supplying the newly established data warehouse was specified and rules for current data sustainability were defined.

4 The Data Model of the Public Transport Network

The drafted data model is based on the extensive Network Exchange (hereinafter referred to as NeTEx) standard which is a new, still developing standard in the PT data standardization [6]. It is based on the Transmodel V5.1 EN [7], on the CEN technical standard "Identification of Fixed Objects in Public Transport" (IFOPT) [8] and on the SIRI standard. The aim of NeTEx is to provide pan-European standard for exchanging data from timetables and related data and information. It is a complex and extensive standard describing statistic elements of the PT network (stops, stations, access areas, equipment etc.) but also operational descriptive elements of the network (e.g. transfers). Only the parts applicable for Czech Republic conditions were selected, adapted and completed from this standard when formulating the data model. Compatibility with the JDF format was also taken into account. The initial concept was completed by code lists from the national level (JDF) and by KIDSOK specific requirements.

The basic element of the data model is a stop as a point feature and also an umbrella term for all other spatial entities (entities with spatial relation to the stop, see Fig. 1).

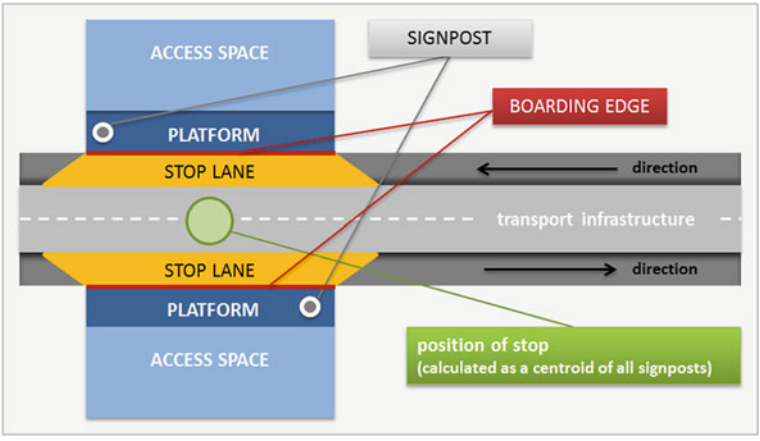

Fig. 1 Stop and its parts (*Source* internal)

The stop is delimited by a boarding edge which is a border part of the platform and is defined as a paved area allowing safe movement of passengers when boarding or leaving a vehicle or waiting for a connection. Most of the stops have two boarding edges (one for each direction); larger transfer hubs can have more than two. Another adjoining entity is a stop lane delineating the area where the PT vehicles stop. Every boarding edge must contain at least one signpost, which is defined as a distinct upright marker designating bus, tram, trolleybus or other stop [9]. The important change comparing to the existing entity registration is the rule for calculating the position of the stop which says that the position of the stop is calculated as a centroid of all signposts of the involved stop. Among outdoor captured spatial entities also belong other spaces and objects related to boarding edges or stops. These include especially the equipment or furniture of stops (e.g. shelters, concourses, waiting areas, benches, ticket machines etc.).

The result of standard research and element analysis of PT network is the data model of static elements respecting strict hierarchy of entities which are mutually interconnected by unique identifiers and which have various mutual relations (Fig. 2). The unequivocal identifier of a stop is the ID from CIS JŘ (e.g. 20580) which corresponds with the unique name of the stop. The code of the boarding edge consists of the stop ID in CIS JŘ + the index of the boarding edge sequence (e.g. NH1) + the orientation of the edge (e.g. N-S). The example of a unique code of the first boarding edge of the 20580 stop with the north-south orientation is 20580/NH1-N-S. The orientation of the boarding edge is derived from the position of the beginning (location of the signpost) and end of the boarding edge (the position where the vehicle enters the stop). If the PT vehicle enters the stop from the south and heads to the north, the orientation of the boarding edge is north-south (i.e. N-S). Possible boarding edge orientations are derived from cardinal points (N-S, S-N, W-E, E-W, SE-NW, NW-SE, NE-SW and SW-NE). Analogically, unique codes for IDs (20580/NH1-N-S/OZ1), stop lanes (20580/NH1-N-S/ZP1), stop equipment (20580/NH1-N-S/V1) and access spaces (20580/NH1-N-S/PP1) related to the boarding edge are derived from the boarding edge code. Tariff zones and parking possibilities are tied to the stop as a whole.

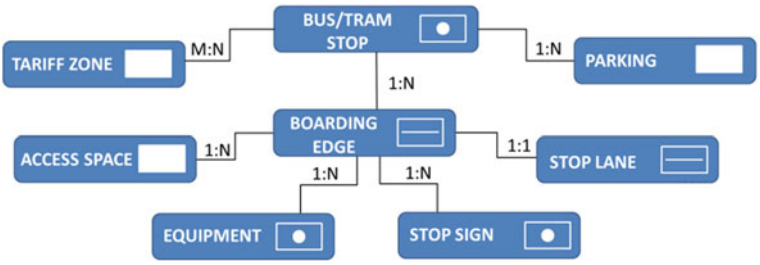

Fig. 2 The outline of proposed data model for data management (*Source* internal)

5 Data Warehouse Lids

The practical solution of the data model of transport network static elements is based on the LIDS geographic information system of BERIT, Brno division of Asseco [10], which offers wide functionality for registering spatial data (especially those related to networks), their maintenance, processing, analyses and evaluation. The GIS software solution of LIDS uses a three-layer architecture utilizing the XML standard. The ground is the Oracle spatial geodatabase where the geometry, semantics and topology of individual network elements are stored. LIDS allows for very effective graphic and non-graphic data management and their storing in a unique central database in compliance with standards of the OpenGIS consortium [11]. The graphic interface is formulated by means of the CAD MicroStation software (or the PowerMap Bentley Systems); the core of the system is the well scalable LIDS data server which supports long-term transactions and replications of the database data [12]. The interconnection with users and third parties' products is provided by the intranet LIDS application server (LAS). The LIDS system is designed as a general system and its specific behaviour is controlled by the data model in the form of system configuration tables unique for the actual application [13]. In this case, the application was based on the newly designed data model for KIDSOK public transport geodata management.

The disadvantage of the GIS solution of LIDS is the pre-defined configuration for a specific data model which is difficult to adapt or extend; the great advantage is the effective management of code lists (set of values may be acquired by the attributes) by means of so-called Codelist Manager (Fig. 3). It is a user-friendly interface where all code lists and their values, which occur in the data model, may be managed. Apart from erasing, other values may be added or the existing values may be modified. The LIDS Codelist Manager for the geodata management data model of the PT network comprises nearly 40 different code lists. Some were

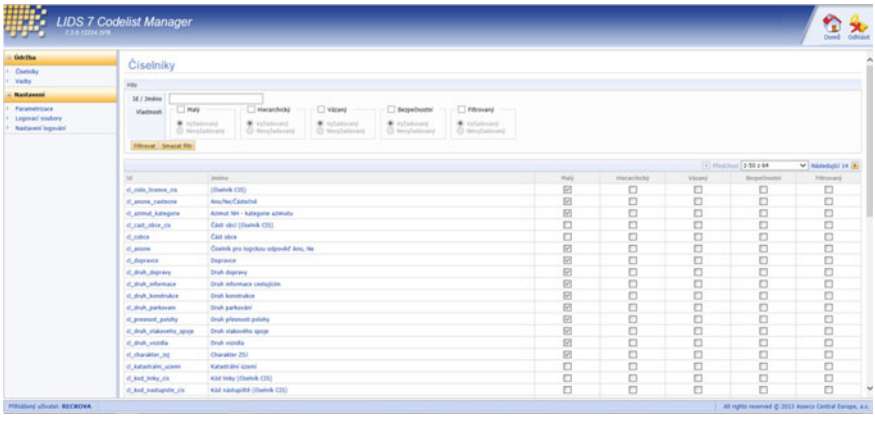

Fig. 3 The Codelist Manager for the management of data model codelists (*Source* internal)

adopted from CIS JŘ, others were adopted and modified from the NeTEx standard and some were newly created for the needs of KIDSOK upon their new requirements or the existing sources. The names of the code lists have strict rules according to their content (C_name_of_codelist); most of them are of text data type with the scope up to 50 characters. The key codelist is the list of complete names of all stops which comprises three codelists from the CIS JŘ—the codelist of town names, the codelist of town parts and local designations and the codelist with stop IDs according to CIS JŘ which makes it easy to keep the up-to-date combination of codelists to identify the stop.

6 The Application for Data Acquisition

In the course of the data model development and the data warehouse implementation, an outline of suitable method for PT network data collection has been compiled. The network geoobjects are rather stable compared to the operation; the problem is, however, the number of registered entities and their attributes. That was the reason why for the static network elements (stops, boarding edges, IDs, stop lanes, equipment and spaces and objects related to the boarding edge or the stop) the most effective way of data collection was looked for. Upon the established data model, specification and KIDSOK requirements, Asseco developed the MAPDD mobile application for field public transport geodata documentation. There were many discussions and analyses whether it is more favourable to develop a field application for a Smartphone or for a tablet. In-depth analysis came to the conclusion that a tablet is definitely a better option for field surveys. The main reason was the size of the screen on which it is much faster, clearer and more comfortable to work with forms. The great advantage of the selected technology is the in-built GPS and navigation, the possibility to connect to WiFi or to take pictures. All these options are used when collecting the data in the PT network. Another plus is the long-life of the battery which can moreover be recharged in the car when moving to the next position.

The MAPDD application is designed for a mobile device (tablet) which meets at least the following technical parameters:

- LCD touch-screen with the resolution min. 1024 × 600,
- 1 GHz processor, 8 GB internal memory,
- camera, WiFi and GPS,
- OS Google Android 4.0 and above.

The MAPDD application communicates with the data warehouse on the basis of the server part of the application in LIDS which contains—apart from the environment required for the LIDS data warehouse management—also the application servers. The basic application environment for the mobile application comprises three server services which must be running when the mobile device communicates with the data warehouse. The first service—OracleServiceXE and OracleXETNSListener—is the

operation of the Oracle XE database and allows for connection to the involved database. LIDS, which is a visualization of the Oracle database, is the data source for the mobile application and concurrently the recipient of the change data from MAPDD. The second service represents the application server for LIDS, so-called JBoss Application Server 4.2.3, which provides authentication of the service for the client mobile application. The third service is the domain1 GlassFish Server which represents the application server for the client mobile operation and provides various application services.

The MAPDD application mostly operates off-line; on-line operation is only used when transferring all the data between the data warehouse and the mobile device during the synchronization at the beginning of the field survey. At the end of the survey, only the data exchange from the mobile device is transferred by synchronization to central data warehouse. The process is provided by a module which recognizes and makes versions of the newly edited data. The name of the field worker passing the batch, date and time of the data change is stored together with each downloaded batch (for process scheme of the application operation see Fig. 4). The user account with the assigned role and therefore also the offered functionality is defined for each MAPDD user. All changes made in the data warehouse within the GIS interface of the data warehouse are stored in the data modification history.

When the field survey is carried out in the Olomouc Region, MAPDD enables to choose from the list of all existing stops in alphabetic order the actual stop for data acquiring or updating manually from the list, through filters by using a partial string from the name or by means of automatic search for stops within the radius of two kilometres from current position of the tablet. When the particular stop is selected, a tree of object types which belong to the actual stop opens in the left-hand part of the basic form. Basic data on the edited stop are shown on the top of the form; the right-hand side includes the attributes of the edited entity (Fig. 5). Each type of entity (boarding edge, ID, stop lane, access space or equipment) can be edited, erased or created as a new one.

MAPDD have the functions to register the position of spatial elements (the position of the beginning and end of the boarding edge, stop lanes, ID position and the position of spaces and objects related to the boarding edges or to the stop in general), take pictures and enter describing attributes to parts of the stop or to the stop in general. Entering of most of the attributes is dealt with by means of codelists

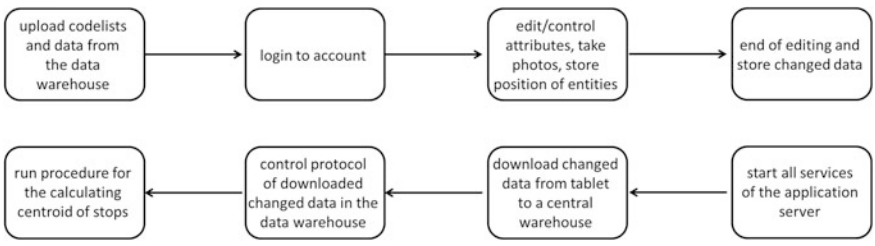

Fig. 4 The process scheme of the application operation (*Source* internal)

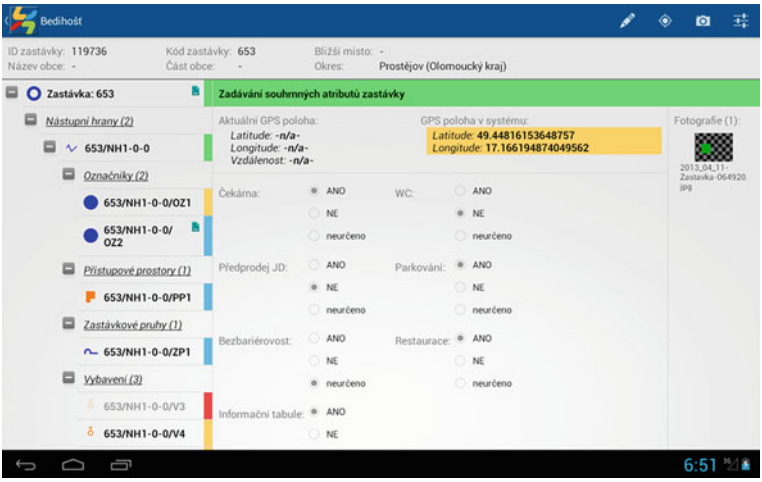

Fig. 5 Example of the MAPDD application form for editing basic data on the Bedihošť stop

in the form of check boxes where only one option can usually be selected. In the field data collecting application, attribute values may be selected from more than 25 codelists; several other codelists work only to allow moves within the entity tree. Entering from the keyboard is minimised to decrease the risk of non-uniform or incorrect entries in the sense of entering various strings for the same aspect. The key codelist is the stop ID codelist from CIS JŘ and derived complete names of all stops comprising codelists for the names of towns, parts of the towns and specific locations which the field worker cannot modify (in other codelists it is possible to add extension of the codelist in comments or select the "other" option). Thanks to this measure, editing of a non-existing stop is avoided. Besides the elimination of logic mistakes, entering of incorrect values resulting from misunderstanding or poor knowledge is dealt with. Help is attached to some attributes or codelists in case the field worker is not sure of the variant of the codelist value or they do not understand the sense of the entered attribute. Apart from texts, the help often contains pictures for clearness.

7 User Aspects of MAPDD

The data will prevailingly be used by the officials who manage the PT network, potentially change the routes or names of the stops, create synoptic maps and provide information reports and notices for general public. So far the KIDSOK staff only worked with a point layer where each record represented a stop with all its compounds in one point. Upon these data, they elaborated synoptic maps for passengers and source materials for internal purposes (negotiations on integrating

Fig. 6 Picture of the boarding edge in-situ (*Source* internal)

routes or lines etc.). As a part of the requirement to increase the attraction and competitiveness of public transport, the demand was expressed to form an interactive transport plan and analyse transport services in the area, define attraction districts of stops and many others. That was the moment when KIDSOK staff realized that the existing data are insufficient and the effort and financial means will have to be invested to acquire correct, up-to-date and first of all complete data. The data will be used by the organiser's officials, later also by passengers and carriers' controller systems because the data model contains attributes important for PT organizers (focused on passenger needs and public transport management and control) but also attributes related to operation. While the passenger is interested in information about wheelchair access, vehicles moving within the network, delays, possible connections between two points and the appearance of the boarding edge (Fig. 6), the carrier needs to know the data concerning the height of the boarding edge, the length and depth of the bay, lighting and other technical parameters of the stop or its parts.

The benefit of the newly established data warehouse of the expertly created data model is the evidence of complete data on PT including all existing attributes, the existence of the expertly elaborated codelists preventing unprofessional interpretation, great positional and topological accuracy of objects, ensuring complete data collection by means of modern technologies (GPS, tablet, GIS) and easy updating of the data.

8 Sustainability of Data Currency

Within the draft of the data model, elaboration of MAPDD and pilot filling of the data warehouse, the concept of PT network data updating was also formulated as it is complicated due to the large number of registered entities and their attributes. Within the KIDSOK operated area, there are more than 2,500 unique stop names and more than 6,000 signposts; similar numbers were reached also with boarding edges and other stop elements which need to be registered. Moreover, many attributes and aspects need to be monitored with respect to providing information for the handicapped. This is the most time consuming part of the work on the data warehouse. The newly created stops, parts of stops and any spatial and organization changes will further be monitored with the participation of several subjects (Fig. 7). At the moment, 20 % of the whole network in the Olomouc Region have undergone MAPDD pilot testing and debugging. The time frame necessary to document one latest, fully equipped stop (including all its parts) is 20 min on average. The rest of the network will be documented in spring 2014; the data warehouse shall be complete by autumn 2014.

Updating of the data from CIS JŘ (codelists of stop names, stop IDs etc.) are contracted with CHAPS Ltd. with the period of 1 month, other up-to-date information is acquired from the Transport Authority of the Olomouc Region (ensured by the Department of Transport and Road Management of the Olomouc Region) or is consulted directly with carriers. The last source of information about transport network is represented by the towns which are usually owners or administrators of the stops and which often provide primary information. MAPDD elaboration, maintenance and technical support is provided by Asseco.

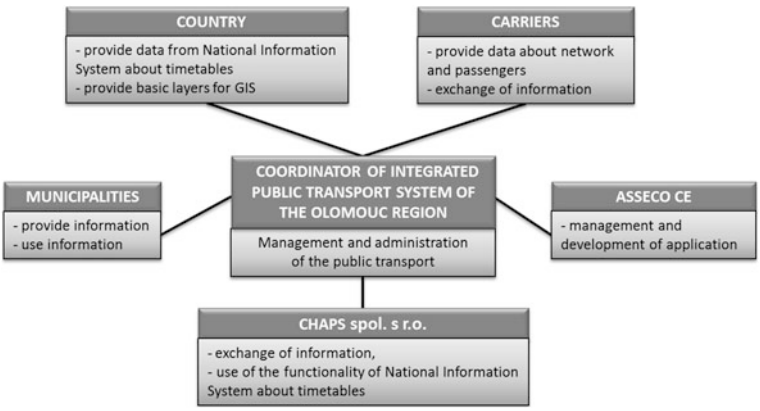

Fig. 7 The organization of the public transport network management

9 Conclusion

Within the draft of the data model, elaboration of MAPDD and pilot filling of the data warehouse, the concept of PT network data updating was also formulated as it is complicated due to the large number of registered entities and their attributes. Regarding time perspective, filling of the data warehouse is the most demanding work. The newly created stops, parts of stops and any spatial and organization changes will further be monitored with the participation of several subjects. In future, the same problem as KIDSOK will be dealt with by most of other PT organizers who can draw inspiration from this solution. Asseco is considering the possibility to offer MAPDD and LIDS as a commercial product for PT network geodata documentation and management in the Czech and Slovak Republics.

At the moment, 20 % of the whole network in the Olomouc Region have undergone MAPDD pilot testing and debugging. The data warehouse shall be complete by autumn 2014. This phase will be followed by elaboration of an interactive transport plan based on the collected data, the possibility to find a connection with a visualization in the map and with the option to provide information concerning on characteristics of the stops (especially the wheelchair access for general public). Concurrently, the managed area will undergo many spatial analyses based on these data (transport services, attraction districts of stops, number of connections and many others). These data will also comprise a base for a controller system.

Acknowledgments The author gratefully acknowledges the support by the Operational Program Education for Competitiveness—European Social Fund (project CZ.1.07/2.3.00/20.0170 of the Ministry of Education, Youth and Sports of the Czech Republic). The author also acknowledges the support of the Internal Grant Agency of Palacky University in Olomouc (Project No. PrF 2013 024).

References

1. Drdla P (2008) IDS in The Czech Republic—comparisons and strangeness (IDS v České republice - srovnání a zvláštnosti). Perner´s Contacts 3(5):69–74. Available via DIALOG. http://pernerscontacts.upce.cz/12_2008/drdla1.pdf
2. CHAPS spol. s r. o. (2005) Popis formátu a struktury dat pro elektronické zpracování drážních jízdních řádů (verze 1.1) CHAPS: Celostátní informační systém o jízdních řádech. Available via DIALOG. http://www.chaps.cz/files/cis/jdf-1.1-v.pdf. Accessed 18 Mar 2013
3. CHAPS spol. s r. o. (2013) Celostátní informační systém o jízdních řádech: Popis systému. CHAPS: Celostátní informační systém o jízdních řádech. Available via DIALOG. http://www.chaps.cz/cs/products/CIS. Accessed 16 Mar 2013
4. CEN/TS 15531:2011 (2011) Service interface for real time information. European Committee for Standardization, Brussels. Available via DIALOG. http://www.kizoom.com/standards/siri
5. Centrum dopravního výzkumu, v. v. i. (2012) Jednotný systém dat ve veřejné dopravě. Available via DIALOG. http://jsdv.cdvinfo.cz/. Accessed 4 Mar 2013
6. PRE/CEN TC 278 WG9 (2012) Network exchange. European Committee for Standardization, Brussels. Available via DIALOG. http://www.kizoom.com/standards/netex/schema/index.htm

7. EN 12896:2006 (2006) Road transport and traffic telematics—public transport—reference data model. European Committee for Standardization, Brussels. Available via DIALOG. http://www.transmodel.org/en/cadre1.html
8. EN 28701:2012 (2012) Intelligent transport systems—public transport—identification of fixed objects in public transport (IFOPT). European Committee for Standardization, Brussels. Available via DIALOG.http://www.dft.gov.uk/naptan/ifopt/ifoptV1.0-36/CENTC278WG3SG6_IFOPT_20081110_36.pdf
9. Zákon č. 111/1994 Sb., o silniční dopravě, v platném znění (1994)
10. Asseco Berit (2012) Solutions for demanding business. ASSECO Berit. Available via DIALOG. http://www.asseco-berit.de/asseco-berit/ueber-asseco-berit/. Accessed 4 Nov 2013
11. Open Geospatial Consortium (2013) OGC standards and supporting documents. Available via DIALOG. http://www.opengeospatial.org/standards. Accessed 7 Oct 2013
12. Bentley Systems (2013) Bentley PowerMap. Available via DIALOG. http://www.bentley.com/cs-CZ/Products/Bentley+Map/PowerMap-Product.htm. Accessed 7 Oct 2013
13. Asseco Berit (2013) Solutions for demanding business: LIDS 7 Geografisches informationssystem (GIS) und Betriebsmittelverwaltung (BIS) aus einem Guss. Available via DIALOG. http://www.asseco-berit.de/produkte/lids/. Accessed 7 Oct 2013

Author Index

A
Andziulis Arūnas, 1

B
Belušák Lukáš, 201
Boori Mukesh, 17

C
Caha Jan, 39
Carreira Rui, 213
Carvalho Alexandre, 213

D
Dobešová Zdena, 51
Dvorský Jiří, 39

E
Eglynas Tomas, 1

F
Feng Tao, 61
Ferraro Ralph, 17
Fojtík David, 93

H
Halounová Lena, 77, 109
Holubec Vladimír, 77
Horák Jiří, 93, 137
Hron Vojtěch, 109
Hübnerová Jitka, 121
Hybner Radek, 51

I
Ivan Igor, 93, 137

J
Jakovlev Sergej, 1
Jánošíková Ľudmila, 149

K
Kietlińska Ewa, 187
Kolisko Pavel, 161
Krempl Michal, 149
Kryszk Hubert, 187
Kurowska Krystyna, 187
Kusendová Dagmar, 201

L
Lenkauskas Tomas, 1

O
Ondoš Slavomír, 201

P
Paulovičová Ivica, 201
Pinho Fábio, 213

R
Rosik Piotr, 227

S
Šafář Václav, 241
Šmejkal Zdeněk, 241
Stępniak Marcin, 227

T
Timmermans Harry J.P., 61, 247

I. Ivan et al. (eds.), *Geoinformatics for Intelligent Transportation*,
Lecture Notes in Geoinformation and Cartography,
DOI 10.1007/978-3-319-11463-7

V
Van der Waerden Peter, 247
Van Hove Lies, 247
Vozňák Miroslav, 1

Z
Zajíčková Lenka, 257